University of Alberta

Mechanism underlying the maturation of AMPA receptors in zebrafish

by

Shunmoogum Aroonassala Patten

A thesis submitted to the Faculty of Graduate Studies and Research
in partial fulfillment of the requirements for the degree of

Doctor of Philosophy

in

Physiology, Cell Biology and Developmental Biology

Department of Biological Sciences

Fall 2009

Edmonton, Alberta

Examining Committee

Declan Ali, Department of Biological Sciences

John Chang, Department of Biological Sciences

John Greer, Department of Physiology

Ted Allison, Department of Biological Sciences

Naweed Syed, Department of Cell Biology and Anatomy, University of Calgary

ABSTRACT

Glutamate AMPA receptors (AMPARs) are major excitatory receptors in the vertebrate CNS. In many biological systems there are changes in the properties of AMPARs during development that are essential for providing an increase in efficiency of information transfer between neurons and a refinement of motor co-ordination and sensory perception and cognition. It is not surprising that improper development or loss of function of AMPARs can lead to many neurological disorders such as epilepsy and amyotrophic lateral sclerosis. Thus, determining the mechanisms by which AMPARs mature is of particular importance. The objectives of my thesis were to characterize the developmental changes in AMPAR-mediated currents in zebrafish Mauthner cells and to determine the mechanisms underlying any changes. The major findings reported in this thesis are that (1) there are developmental changes in the properties of AMPAR-currents as the Mauthner cell matures; (2) the mechanism underlying these changes is a switch in the composition of AMPA receptor subtypes; and (3) PKCγ is necessary for the developmental switch in AMPAR subtypes from slow receptors to fast receptors. These findings provide valuable insights into the mechanism underlying the development of AMPARs. In addition, they provide the first instance of a signalling link (PKCγ) required for the developmental subunit switch and the developmental speeding of AMPAR kinetics.

ACKNOWLEDGEMENTS

First and foremost, I would like to express my gratitude for the years of support, mentorship and encouragement provided to me by my supervisor, Dr. Declan Ali. You introduced me to the world of neuroscience and electrophysiology, for which I am extremely grateful. Your enthusiasm and genuine interest for science has led to interesting discussions, which has made me a better scientist. Your teaching style caters for the development of independent research and is priceless, thank you. It was a great pleasure working with you over the past years. Also, your impressive generosity and friendliness deserve to be mentioned.

Dr. John Chang, thank you for sharing your vast scientific knowledge and for your support and constructive advice in times when Declan was away.

To Dr. Christopher Coutts, a special thank-you for all the time and effort you have contributed to me over the years incredible friend and I have enjoyed the good times we had together and that I truly and for the many scientific discussions we have shared. You have also been an value your friendship. To my fellow graduate students and friends; Nicole Sylvain, Birbickram Roy and Daniel Brewster, I valued the time spent with you all and I wish you all the best for the future.

In addition, I would like to thank the individuals that I have had the opportunity to collaborate with over the years; to Dr. Patrick Hanington, Laura Reaume, Dr.

Andrew Waskiewicz, Dr. Miodrag Belosevic and Dr. James Stafford; I have learned something from you all.

Thank you also Ben Montgomery, Scott Parks, Martin Tresguerres, Tyson MacCormick, Yi Yu, Caleb Grey, Barbara Katzenback, Steven Hitchen, Maria Thistle, Kim Onj, Jaime Gorrell, and Aaron Schaffer for good times and interesting discussions.

All the summer students: Leslie Balt, Rena Sihra, Dinesh Witharana, and Marcus Cunningham, you are all acknowledged for your enthusiasm and great camaraderie. Your presence at the lab made it more joyful to work during the summers.

I would like to thank KAI pharmaceuticals for supplying the peptides γV5-3 and C1. I am also immensely grateful to all the people, at the Department of Biological Sciences, for their support and for creating a friendly and fun atmosphere.

Last, but certainly not least, I would like to thank my parents for their never-ending support and belief in me. Thank you!

TABLE OF CONTENTS

TABLE OF FIGURES

LIST OF ABBREVIATIONS

ABP	AMPAR-binding protein
AMPA	α-methyl-4-isoxazoleproprionic acid
AMPAR	AMPA receptor
APV	D(-)-2-amino-5-phosphonopentanoic acid
BAPTA	1,2-bis(2-aminophenoxy)ethane-N,N,N',N'-tetra-acetic acid
BIS I	Bisindolymaleimide I
BSA	Bovine serum albumin
C	Conserved sequence
CaMK	Calcium/calmodulin dependent kinase family
DAG	Diacylglycerol
DOG	1,2-dioctanoyl-sn-glycerol
dpf	Day post-fertilization
DPP	Depolarizing pulse protocol
EPSC	Excitatory postsynaptic current
EPSP	Excitatory postsynaptic potential
GABA	γ- aminobutyric acid
GluR	AMPA receptor subunit
GRIP	Glutamate receptor-interacting protein
hpf	Hour post-fertilization
iGluR	ionotropic glutamate receptor
IP_3	Inositol-1,4,5-triphophosphate
KYN	Kynurenic acid
LTD	Long-term depression
LTP	Long-term potentiation
MAPK	Mitogen-activated protein kinase
M-cell	Mauthner cell
mEPSC	miniature excitatory postsynaptic current
mGluR	Metabotropic glutamate receptor
NASPM	1-Napthylacetylspermine
NMDA	N-methyl-D-aspartate
NMDAR	NMDA receptor
NR	NMDA receptor subunit
NSF	N-ethylmaleimide-sensitive fusion protein
PB	Pentobarbitol
PBS	Phosphate-buffered solution
PICK1	Protein interacting with C kinase 1
PIP_2	Phosphatidylinositol-1,4,5-triphophosphate
PKA	Protein kinase A
PKC	Protein kinase C
PKCγ-MO	PKCγ morpholino
PMA	Phorbol 12-myristate 13-acetate
PS	Phosphatidylserine
PSD	Postsynaptic density
RT-PCR	reverse transcriptase polymerase chain reaction
S880	Serine site 880
SAP97	Synaptic associated protein 97
TARP	Transmembrane AMPA receptor regulatory protein
TTX	Tetrodotoxin

V	variable region
αCaMKII	α-Calcium/calmodulin-dependent kinase II

Chapter 1 INTRODUCTION AND LITERATURE REVIEW

1.1 Introduction

Fast excitatory synaptic transmission in the vertebrate CNS is mediated predominantly by the α-amino-3-hydroxy-5-methylisoxazole-4-propionic acid (AMPA) ionotropic glutamate receptor. The strength of synaptic transmission at excitatory synapses depends, in part, upon receptor properties such as channel conductance and open/close rates (Ambros-Ingerson and Lynch, 1993; Benke et al., 1998; Lin et al., 2002). The amplitude and time course of the synaptic currents that are mediated by AMPA receptors (AMPARs) are key players of synaptic information efficacy and cell excitability, and changes in the nature of these currents will impact upon cell activity. Developmental alterations in the properties of synaptic currents have been observed at excitatory synapses (Sakmann and Brenner, 1978; Hestrin, 1992b; Wall et al., 2002) and the most prominent change is that the decay kinetics of postsynaptic currents becomes faster during development. This speeding of the current is thought to be essential for the organized motor movements and accurate sensory perception and cognition (Galarreta and Hestrin, 2001; Cathala et al., 2003).

The developmental speeding of synaptic currents was first documented at the rat neuromuscular junction (Sakmann and Brenner,

1978; Fischbach and Schuetze, 1980). Similarly, at glutamatergic excitarory synapses in the CNS, the decay time of NMDA receptor (NMDAR)-mediated excitatory postsynaptic currents (EPSCs) becomes faster as the animal matures. However, information about the developmental changes in AMPAR-EPSC is somewhat contradictory. For instance, in hippocampal pyramidal cells, AMPAR-EPSCs show an increase in decay times with maturation (Seifert et al., 2000), whereas at the majority of excitatory synapses there is a developmental decrease in decay times (Taschenberger and von Gersdorff, 2000; Iwasaki and Takahashi, 2001; Joshi and Wang, 2002; Wall et al., 2002; Yamashita et al., 2003; Rumpel et al., 2004).

The developmental speeding of the synaptic currents mediated by either nicotinic acetylcholine receptors or NMDARs (Mishina et al., 1986; Monyer et al., 1994; Takahashi et al., 1996) depends upon switches of receptor subunits. However, the mechanisms that underlie the developmental changes in AMPAR kinetics are poorly understood and may encompass such events as changes in receptor subunit composition, changes in synaptic morphology and changes in the states of receptor phosphorylation.

1.2 Objectives of thesis

The overall goal of my thesis was to provide detailed information on the developmental changes in AMPAR properties. My research focused on determining the properties of AMPAR-mediated currents in Mauthner cells of developing zebrafish and the reasons underlying these developmental changes. The specific aims of my research were:

(1) to characterize the developmental changes in AMPAR-mediated currents observed in developing Mauthner cells (M-cells).

(2) to determine the mechanisms (such as subunit switching, synaptic morphological changes and phosphorylation by kinases) underlying the developmental changes in the properties of the AMPAR currents

The hypotheses were (1) AMPAR properties would change during zebrafish development; (2) the mechanisms underlying these changes would be an alteration in the transient of glutamate in the synaptic cleft, a switch in AMPAR subunit and/or changes in AMPAR phosphorylation rates.

1.3 Outline of thesis

In the first chapter, I review the current literature with regard to glutamate synapses, AMPARs, protein kinase C and zebrafish development. This chapter primarily focuses on the properties of AMPARs and how the function of these receptors can be altered by phosphorylation by PKC. Chapter 2 contains a detailed description of the Materials and Methods used throughout the thesis. Chapter 3 describes results of the developmental properties of AMPARs in zebrafish M-cells. Specifically, in this chapter, I show that there are major developmental changes in the AMPAR properties between 33 hour post-fertilization (hpf) and 48 hpf of zebrafish development. In Chapter 4, I present the results of studies designed to investigate the mechanisms underlying the developmental changes in AMPAR properties observed in Chapter 3. Chapter 5 demonstrates that AMPAR activity in 48 hpf zebrafish can be increased by PKCγ which induces the trafficking of AMPARs into the plasma membrane. In Chapter 6, I present results of studies designed to investigate the role of AMPAR trafficking in zebrafish neurodevelopment. Finally, in Chapter 7, I present a model of trafficking of AMPARs via activation of PKCγ and conclude that PKCγ is necessary for the developmental changes in AMPAR kinetics in zebrafish Mauthner cells.

1.4 Literature review

1.4.1 Overview

In this section, I summarize the known properties of AMPA receptors, review the dynamics of movement of AMPARs into and out of synaptic membranes, and then present an account of how AMPARs are modulated by protein kinase C. I also review the processes of synaptic development and plasticity. Finally I provide a brief review on zebrafish development and the Mauthner cells.

1.4.2 Synaptic transmission

Synaptic transmission is the transfer of a signal from one neuron to another at synapses, which are specialized contact sites of two neurons, or between a neuron and an effector cell. There are two primary types of synapses: electrical or chemical. Electrical synapses are observed less frequently in the brain than chemical synapses. At electrical synapses, transmission is extremely rapid and occurs by means of direct current flow through gap junctions which connect the cytoplasm of the pre- and postsynaptic cells. At chemical synapses, synaptic transmission is mediated via compounds called neurotransmitters, which are released from the presynaptic cell into the synaptic cleft and bind to receptors on the postsynaptic cell. Common neurotransmitters are glutamate, acetylcholine, glycine and γ-aminobutyric acid (GABA). Glutamate is the primary neurotransmitter mediating excitatory synaptic transmission in the vertebrate central nervous system (CNS). Glutamate activates two types

of glutamate receptors: ionotropic (iGluRs) and metabotropic glutamate receptors (mGluRs) (Nakanishi, 1992). Ionotropic glutamate receptors have been subdivided into AMPA, Kainate and *N*-methyl-D-aspartate (NMDA) receptor subclasses according to their ligand specificity and primary structure. Ionotropic GluRs mediate fast transmission via an intrinsic cation channel, whereas mGluRs are coupled via G proteins and second messenger cascades to ion channels and mediate slower responses to glutamate (Anwyl, 1999). At iGluRs, glutamate binding leads to the opening of the channel and to flow of Na^+ and K^+ ions and sometimes Ca^{2+} down their electrochemical gradients. As a consequence, excitatory postsynaptic potentials (EPSP) are generated, shifting the resting membrane potential towards depolarized values. These local depolarizations of membrane potential in turn lead to the opening of voltage-gated ion channels and promote the generation of a new action potential in the postsynaptic cell.

Once released from the presynaptic terminal, glutamate must be removed from the cleft to prevent receptor desensitization or constant postsynaptic depolarization. Glutamate is removed from the cleft via reuptake of glutamate in glial cells and the presynaptic cell by transporters. After prolonged exposure to glutamate, the receptor can become refractory to subsequent application of glutamate, thus resulting in receptor desensitization.

1.4.3 NMDA receptor

NMDARs are heterotetramers consisting of two NR1 and two NR2 subunits. Four different NR2 subunits have been identified by molecular cloning techniques and have been characterized as NR2A-D (Ishii et al., 1993). Co-assembly between NR1 and various NR2 subunits generates functionally distinct NMDARs. The NR1 subunit consists of 8 splice variants and the incorporation of different NR1 splice variants into NMDAR influences receptor properties such as modulation by zinc, polyamines, PKC, as well as binding to intracellular proteins (Durand et al., 1993; Hollmann et al., 1993; Lin et al., 1998). The NR2 subunit composition, on the other hand, determines the biophysical properties of the receptor such as channel conductance, mean open time and sensitivity to Mg^{2+} (Monyer et al., 1992; Monyer et al., 1994). For instance, receptors formed from NR1/NR2A and NR1/NR2B subunits have higher channel conductances (50 pS) than NR1/NR2C receptors (38 pS) (Stern et al., 1992). NMDARs are expressed throughout the brain. NR1 mRNA is ubiquitously distributed but the four NR2 subunits display distinct regional patterns of expression. NR2A and NR2B are mainly found in the forebrain, NR2C in the cerebellum and NR2D in the brain stem and olfactory bulb (Kutsuwada et al., 1992; Monyer et al., 1992; Cox et al., 2005). In additional, NMDAR subunit, NR3A, has been identified in the mammalian brain (Ciabarra et al., 1995; Sucher et al., 1995). To date, only a few studies have reported

evidence for a functional role of this subunit in the brain (Das et al., 1998; Perez-Otano et al., 2001).

The activation of NMDARs is both ligand- and voltage-dependent. To enter an open state, it first requires the binding of glutamate to the NR1 subunits and of glycine to the NR2 subunits, as well as the removal of a voltage-dependent block by Mg^{2+} (Nowak et al., 1984). The removal of the Mg^{2+} block is achieved by a depolarization of the postsynaptic membrane. Once activated, NMDARs allow the influx of both Na^{+} and Ca^{2+} ions (Ascher and Nowak, 1988). NMDARs are highly Ca^{2+} permeable and their activation leads to long-lasting synaptic currents of about 100 ms or more. The ability to conduct Ca^{2+} is essential for the role of NMDARs in synaptic plasticity and neurotoxicity (Bliss and Collingridge, 1993; Malenka and Nicoll, 1993; Perkel et al., 1993).

1.4.4 AMPA receptor

1.4.4.1 Structure and composition

AMPARs consist of four closely related genes that encode the four subunits GluR1-GluR4. These subunits combine in different stoichiometries to form receptors with distinct functional properties (Hollmann and Heinemann, 1994). The subunits consist of an extracellular N-terminus, three transmembrane domains and an intracellular C-terminus (Bredt and Nicoll, 2003) (Figure 1.1). The AMPAR subunits have very

similar N-terminus and transmembrane domains, but vary in their intracellular C-terminus. The latter determines the binding of the subunit to specific interacting proteins, as well as the modes of regulation of the receptors by protein kinases (Song and Huganir, 2002). All four AMPAR subunits may also undergo alternative splicing, resulting in either a flip or a flop version which exhibit partly different characteristics. For example, the flip isoforms desensitize with slower kinetics than the flop isoforms (Sommer et al., 1990; Mosbacher et al., 1994). AMPARs are also regulated by RNA editing. In the pore region of the GluR2 subunit, glutamine is edited to an arginine (Q/R editing) and this regulates the calcium permeability and channel rectification. GluR2 containing AMPARs are impermeable to calcium and exhibit a linear or outward rectification (Geiger et al., 1995; Seeburg, 1996; Liu and Cull-Candy, 2000; Cull-Candy et al., 2006) while receptors lacking the GluR2 subunit exhibit calcium permeability and an inward rectification (Seeburg, 1996; Cull-Candy et al., 2006; Isaac et al., 2007). The Q/R editing and alternative splicing of AMPARs are both developmentally regulated such that the edited form of GluR2 and the flop isoforms are expressed in adult brains (Kung et al., 2001). During development, the Q/R editing operates before the flip/flop.

The subunit composition of AMPARs varies between brain regions and critically affects the functional properties of AMPA receptors (Derkach et al., 2007; Shepherd and Huganir, 2007).

1.4.4.2 Physiology

AMPARs are the main mediators of rapid excitatory transmission in the CNS and the activation of AMPARs is responsible for the depolarization of the cell, resulting in the activation of voltage-gated ion channels and NMDARs. AMPAR activation occurs with sub-milliseconds time constant, whereas deactivation occurs in the time scale of a few milliseconds (Jonas and Sakmann, 1992). The rate of deactivation of AMPARs is typically fast, in the range of 0.5 – 3 ms (Colquhoun and Hawkes, 1982; Hestrin, 1992a, , 1993; Edmonds et al., 1995; Silver et al., 1996b). For example, AMPARs of hippocampal neurons have a deactivation time course (τ) of ~3ms (Colquhoun and Hawkes, 1982; Tang et al., 1991). In cerebellar granule cells, τ is ~ 0.6 ms (Wyllie and Cull-Candy, 1994). The single channel conductance of AMPARs is reported to be between 7 and 30 pS (Vyklicky et al., 1991; Yamada and Tang, 1993; Swanson et al., 1997). For instance, AMPARs at pyramidal neurons in the rat visual cortex have been shown to exhibit a small unitary conductance of 9 pS (Hestrin, 1992a). AMPARs of 8 pS, 29 pS and 35 pS have been reported at the hippocampus (Tang et al., 1991; Raman and Trussell, 1992). In cerebellar granule cells, AMPARs have a single channel conductance of 30 pS (Silver et al., 1996a). The single channel conductance of an AMPAR is dependent on its subunit composition; therefore cells have different AMPAR conductances due to different assemblies of AMPAR subunits. Differential expression of AMPAR

subunits will not only influence the activity of AMPAR in cells but also affect the trafficking of these receptors.

1.4.4.3 Trafficking

AMPARs undergo constant trafficking between the plasma membrane and the cytoplasm. The trafficking of AMPARs is microtubule-dependent, and transport is an active process involving motor proteins such as myosin, dynein and kinesin (Hirokawa and Takemura, 2005; Lise et al., 2006). AMPAR can be first inserted into the plasma membrane in the soma at extrasynaptic sites and then travel out into dendrites via lateral diffusion in the membrane to the synaptic sites (Adesnik et al., 2005). Several studies have also shown that AMPARs are trafficked intracellularly via cytoskeletal motor proteins and then directly inserted at synaptic sites via SNARE-dependent exocytosis (Lu et al., 2001; Shepherd and Huganir, 2007). However, it is still unclear whether AMPARs are first inserted into the extrasynaptic plasma membrane or directly into synapses. Most likely a combination of all these processes occurs, depending on the subunit composition of the receptors.

The insertion of AMPARs in plasma membrane is regulated by the subunit composition of the receptor. The insertion of GluR1 and GluR4 in the plasma membranes occurs slowly while the insertion of GluR2 is rapid (Hayashi et al., 2000; Passafaro et al., 2001; Shi et al., 2001). Insertion of AMPARs occurs under basal conditions (the constitutive pathway) and is

stimulated by neuronal activity and NMDAR activation (the regulated pathway) (Hayashi et al., 2000). In the constitutive pathway, GluR2-GluR3 receptors continuously cycle in and out of synapses under basal conditions without the need for synaptic activity, whereas in the regulated pathway, GluR1-GluR2 receptors are added into synapses in an activity-dependent manner during synaptic plasticity (Malinow et al., 2000). The constitutive pathway preserves the total number of synaptic AMPARs and may maintain basal synaptic strength and transmission. On the other hand, the regulated pathway may act transiently to enhance synaptic strength and transmission. Recent studies suggest that newly inserted AMPARs at synapses come from recycling AMPAR-containing endosomes (Park et al., 2004; Park et al., 2006). Activation of NMDA receptors can regulate the kinetics of recycling and significantly affect the relative amount of receptors that are maintained intracellularly versus on the membrane surface (Park et al., 2004). However, how NMDA activity regulates recycling still remains unclear.

Trafficking of AMPAR subunits requires the interaction of their C-terminus with intracellular scaffolding proteins. For instance, interaction of AMPA receptor interacting proteins such as synaptic associated protein 97 (SAP97) and 4.1N with cytoplamic tail of GluR1 can mediate endocytosis or exocytosis (Chung et al., 2000; Lee et al., 2003; Man et al., 2007). The GluR2 C-terminus binds to N-ethylmaleide-sensitive fusion protein (NSF) (Nishimune et al., 1998; Song et al., 1998) and this site seems to regulate

the rapid insertion of GluR2 at synaptic sites via exocytosis (Beretta et al., 2005). GluR2 can also bind to glutamate receptor-interacting protein (GRIP), AMPAR-binding protein (ABP) and protein interacting with C kinase 1 (PICK1). PICK1 binds to intracellular pools of GluR2 and provides a ready source of receptors for rapid membrane insertion (Steinberg et al., 2004; Gardner et al., 2005; Liu and Cull-Candy, 2005). NSF binding may dissociate the GluR2-PICK1 complex thus allowing membrane insertion (Hanley et al., 2002). On the other hand, interaction of GluR2 with GRIP/ABP leads to the stabilization of AMPARs in intracellular vesicles. It is believed that interaction of AMPARs with GRIP and PICK1 may play some role in the regulation of receptor recycling to modulate the level of synaptic receptors. The C-terminus of GluR4 consists of binding sites for actin interacting proteins: α-actinin-1 and IQGAP1. GluR4 interacts with both α-actinin-1 and IQGAP. If α-actinin-1 is present, GluR4 is retained in the cytosol; however, if this interaction is disrupted trafficking of AMPARs into the plasma membrane occurs (Nuriya et al., 2005). Endocytosis of AMPARs occurs via clathrin-coated pits and requires dynamin (Carroll et al., 1999b; Wang and Linden, 2000). Recent studies have also indicated that the specific postsynaptic proteins GPG2 and Arc, mediate both constitutive and activity-dependent AMPARs internalization (Steward and Worley, 2001; Cottrell et al., 2004; Rial Verde et al., 2006).

All these processes involved in AMPAR tafficking require the association of AMPAR with different intracellular proteins and this interaction has been shown to be highly dependent on the phosphorylation of AMPARs by protein kinases (Song and Huganir, 2002).

1.4.5 Protein Kinases and AMPA receptor

Protein kinases are enzymes that phosphorylate numerous substrates such as receptor subunits, and phosphoproteins. Protein kinases have been shown to be involved in diverse cellular processes such as synaptic plasticity (Hu et al., 1987; Malenka et al., 1989; Abeliovich et al., 1993b; Abeliovich et al., 1993a; Duffy et al., 2001; Patterson et al., 2001), development (Ohno and Nishizuka, 2002) and apoptosis (Whelan and Parker, 1998; Thiam et al., 1999; Slatter et al., 2005). All AMPAR subunits have several identified phosphorylation sites on their cytoplasmic tails (Song and Huganir, 2002). Changes in the phosphorylation state of the AMPAR subunits can increase single channel conductance and/or lead to a change in the number of AMPARs in the postsynaptic membrane via membrane trafficking mechanisms (Song and Huganir, 2002). AMPAR phosphorylation also seems to play a role in mediating various forms of synaptic plasticity. The protein kinase families that have been studied most intensively in relation to AMPAR function and synaptic plasticity are the calcium/calmodulin-dependent kinase family (CaMK family), cyclic adenosine 3’5’ monophosphate-dependent protein kinase (PKA) family, the mitogen-activated protein kinase (MAPK) family

and the protein kinase C (PKC) family. The role of the PKC family will be discussed in paragraph 1.4.5.1- 1.4.5.3.

1.4.5.1 Protein Kinase C Biochemistry

PKC is one of the key elements in the signal transduction pathway that regulates many cellular processes. It is a serine/threonine kinase that was first characterized on the basis of its activation, *in vitro*, by Ca^{2+}, phospholipid and diacylglycerol (DAG) (Nishizuka, 1992). PKC is composed of approximately 11 different isoforms that have been categorized into three groups based on their mode of activation (Hug and Sarre, 1993; Dekker and Parker, 1994; Ohno and Nishizuka, 2002). The first group of isoforms consists of 4 classical or conventional PKCs (cPKC): α, βI, βII and γ, and requires Ca^{2+}, phosphatidylserine (PS) and diacylglycerol (DAG) for optimal activation. The second group of isoforms consists of 4 novel PKCs (nPKC): δ, ε,θ, and η; and these are dependent on PS and DAG, but not Ca^{2+} for activation. The third group are the atypical PKCs (aPKC: ζ and ι/λ) and they require PS but neither DAG nor Ca^{2+} for stimulation.

The classical PKCs have 4 regions of highly conserved sequences (Cl to C4) interspersed with 5 variable regions (VI to V5) (Hug and Sarre, 1993). The Cl region contains a tandem repeat of 2 cysteine-rich zinc finger structures; the first structure binds DAG and phorbol esters while the second structure is thought to be the binding site for phospholipids

(Shearman et al., 1989). The C2 region contains the calcium binding site and also the binding site for receptors for activated C-kinase (RACKs), which are intracellular PKC receptors that influence the activation by inducing the translocation of PKC from the cytosol to the membrane (Mochly-Rosen et al., 1992; Ron and Mochly-Rosen, 1995; Schechtman and Mochly-Rosen, 2001). The C3 region contains a conserved ATP-binding domain. C4 contains the substrate docking domain. Part of the Cl region contains a stretch of amino acid sequence known as the pseudosubstrate sequence that resembles a PKC substrate but contains alanine and not any serine or threonine residues that can be phosphorylated. This pseudosubstrate region, by binding to the substrate docking region of the C4 domain, is important in keeping PKC in its inactive form. The Cl and C2 regions make up the regulatory domain of PKC while the C3 and C4 regions form the protein kinase domain. The novel PKC isoforms lack the calcium-binding C2 region while atypical PKCs, lack the C2 region, and they have only one cysteine-rich zinc finger-motif, leading to a loss of responsiveness to DAG and phorbol esters.

PKC is activated in the cell by signal transduction cascades that produce IP_3 (inositol-1,4,5-triphosphate) and DAG. Upon appropriate ligand-receptor interaction at the cell surface, and through the mediation of G proteins signal transducers, phospholipase C catalyses the breakdown

of PIP_2 (phosphatidylinositol 4,5-bisphosphate) into IP_3 and DAG (Berridge and Irvine, 1984). IP_3 mobilizes Ca^{2+} from internal stores and the binding of Ca^{2+} to the C2 region and with the help of RACKs, results in translocation of PKC from the cytosol to the cell membrane. At the cell membrane, DAG generated by PIP_2 turnover, and PS, which is constitutively present in the cell membrane, bind to the Cl region. The presence of each of the co-factors increases the affinity of one another for binding to the PKC molecule. Active PKC is believed to consist of 4 molecules of PS, 1 molecule of DAG, and at least 1 Ca^{2+} ion (Hannun and Bell, 1988). In the absence of activating co-factors (Ca^{2+}, PS or DAG), the pseudosubstrate motif at the Cl domain of the regulatory region interacts with the substrate docking site of the C4 domain of the catalytic region and thus prevents access of substrates to the catalytic site (Soderling, 1990).

1.4.5.2 Distribution

PKC isoforms are widely distributed in vertebrate tissues and some isoforms are localized to specific tissues and cell types. The conventional PKCγ isoform is expressed solely in the central nervous system, while PKCα and β are more ubiquitous (Huang and Huang, 1986; Huang et al., 1987). PKCα and β are differentially localized in the brain, spinal cord (Coussens et al., 1987; Patten et al., 2007) and in a variety of other tissues (Kosaka et al., 1988). PKCα is generally associated with presynaptic neurons and neuronal growth cone structures (Shearman et

al., 1989; Igarashi and Komiya, 1991). PKCβ and PKCγ appear to be exclusively localized to the postsynaptic region of neurons (Kose et al., 1990; Tanaka and Nishizuka, 1994). Specifically, PKCγ has been found in dendrites and dendritic spines by eletron microscopy (Saito et al., 1994). The two types of PKCβ (βI and II) are differentially distributed. PKCβI is found mainly in the brain stem with subcellular localization in cytoplasmic clusters near the cell membrane (Saito, 1994). In contrast, PKCβII is localized to the golgi (Saito et al., 1994), synapses (Tanaka et al., 1991) and skeletal muscles (Patten et al., 2007). The atypical PKC isoforms (PKC ζ and ι/λ) are widely expressed in different tissues including brain, spinal cord, lung, kidney, testis and liver (Wetsel et al., 1992; Goldberg and Steinberg, 1996; Patten et al., 2007). Similar to PKCγ, PKCζ has been localized to dendrites (Muslimov et al., 2004). Its expression has also been exclusively associated with the inner segments of the photoreceptors (Osborne et al., 1994). However, the tissue distribution of PKC ι/λ is not as well characterized but has been found to be broadly expressed in the brain (Oster et al., 2004), fetal heart (Rybin et al., 1997) and thymus (Soloff et al., 2004). The expression of the novel PKC isoforms (δ, ε, θ, and η) have been found in the brain, heart, lung, liver and kidney (Mosbacher et al., 1994; Ohno and Nishizuka, 2002). PKCε is found presynaptically in primary sensory neurons, the forebrain, skeletal muscle and the spinal cord (Osada et al., 1992; Saito, 1994; Patten et al., 2007). In the retina, PKCε is expressed in the bipolar cells, and PKCδ in Müller cells and a

subpopulation of ganglion cells (Osborne et al., 1994). PKC isoforms have differential cell and tissue expression. This is likely due to the fact that some PKC isoforms can only modulate the function of some proteins and not other and they are known differ in their function (Saito, 1994).

1.4.5.3 PKC and AMPAR

One way to alter the function of AMPARs is by changing phosphorylation of its subunits. PKC can phosphorylate all AMPAR subunits at serine sites located on the cytoplasmic tails of the subunits. PKC phosphorylation can either increase the single channel conductance of the receptors (Raymond et al., 1993; Tavalin, 2008) or alter the interaction of the subunits with PDZ domain-containing proteins. The latter leads to an increase in clustering and synaptic delivery of AMPARs (Chung et al., 2000; Hirai, 2001; Sacktor, 2008; Zheng and Keifer, 2008).

GluR1 has three identified phosphorylation sites, serines 818 (S818) (Boehm et al., 2006), 831 (S831) and 845 (S845) (Roche et al., 1996). S831 is phosphorylated by CaMKII and PKC, S845 is a PKA substrate (Roche et al., 1996; Barria et al., 1997; Mammen et al., 1997), while S818 is phosphorylated by PKC (Boehm et al., 2006). Phosphorylation of S831 by PKC increases the single channel conductance (Tavalin, 2008). Phosphorylation of S818 by PKC drives GluR1 into synapses (Boehm et al., 2006), however the underlying mechanism is unknown. It is likely that phosphorylation of GluR1 S818

might alter its interaction with SAP97 leading to receptor trafficking. Phosphorylation of GluR2 subunit at serine-880 (S880) has been implicated in synaptic plasticity (Chung et al., 2000; Daw et al., 2000; Matsuda et al., 2000; Kim et al., 2001). The serine site S880 of GluR2 is phosphorylated by PKC (McDonald et al., 2001). When unphosphorylated at S880, GluR2 can interact with PDZ domains of GRIP/ABP but upon phosphorylation of S880, GluR2 preferentially binds to PICK1 (Matsuda et al., 1999; Chung et al., 2000). Interaction between GRIP/ABP and GluR2 has been shown to retain GluR2 in intracellular pools or stabilize AMPARs at synaptic locations (Song et al., 1998; Daw et al., 2000; Braithwaite et al., 2002; Rial Verde et al., 2006). On the other hand, when PICK1 interacts with GluR2, it either promotes endocytosis of the receptors (Chung et al., 2000; Terashima et al., 2004; Lu and Ziff, 2005) or allows insertion of receptors into the plasma membrane (Daw et al., 2000; Gardner et al., 2005; Rial Verde et al., 2006). GluR3 displays sequence homology to GluR2, including the site that binds GRIP/ABP and PICK1, suggesting that phosphorylation of GluR3 may regulate AMPAR trafficking. However, to date there is no indication of the involvement of GluR3 phosphorylation in receptor trafficking. PKC phosphorylates GluR4 at S842 (Rial Verde et al., 2006; Gomes et al., 2007) and increases its surface expression (Gomes et al., 2007). α-Actinin-1 and IQGAP1 are actin-binding proteins and they bind to the C-terminus of GluR4 at the region containing the S842 phosphorylation site. Phosphorylation of GluR4

disrupts its interaction with α-actinin-1, while the interaction with IQGAP-1 is preserved. Binding of GluR4 with α-actinin-1 retains AMPARs in intracellular vesicles, and upon phosphorylation, this interaction is disrupted and GluR4 is inserted into synapse membranes (Nuriya et al., 2005).

1.4.6 Synaptic plasticity

The ability of a synapse to respond to changes in its activity with an increased (potentiation) or decreased (depression) synaptic efficacy is called synaptic plasticity. It is common at most excitatory synapses in the brain and can occur either during development or throughout adult life. Synaptic plasticity is classified as short-term or long-term. Short-term plasticity is the modulation of synaptic strength following repetitive synaptic activity that covers a time scale of ms up to a few minutes (Zucker and Regehr, 2002). Long-term plasticity is the activity-dependent change in the efficacy of the synapse that can last for minutes up to months, may be years (Bliss and Collingridge, 1993).

Long-term potentiation (LTP) of synaptic strength has been widely studied since this phenomenon is thought to be involved in many brain functions, including the mechanisms underlying learning and memory. The induction of this potentiation requires Ca^{2+} influx through NMDARs (Collingridge et al., 1983). The activation of NMDARs requires depolarization of the postsynaptic cell, which is usually accomplished

experimentally by high-frequency stimulation of a large population of presynatic axons synapses, by chemical (high K^+ medium) depolarization of the synapses (Makhinson et al., 1999; Kolarow et al., 2007) or by directly depolarizing the cell (Vincent et al., 1992; Baxter and Wyllie, 2006). LTP has been extensively studied in the hippocampus, a brain region in mammals known to be important for the formation of new memories. Three separate phases of LTP can be distinguished; induction, expression and maintenance (Duffy et al., 2001). One much studied form of LTP can be generated by a brief (1s) high-frequency (100 Hz) stimulation of presynaptic hippocampal CA3 pyramidal cells, and recorded from postsynaptic pyramidal neurons in the CA1 region. After this induction, the excitatory postsynaptic response (EPSPs) of CA1 cells is increased to a constantly maintained level following the stimulus. LTP increases the AMPAR-mediated current to a greater extent than the NMDAR current (Kauer et al., 1988), thus the enhanced synaptic currents in the expression phase of LTP is likely due to an increase in the number of synaptic AMPARs (Malinow and Malenka, 2002). However, other expression mechanisms such as increases in AMPAR channel conductance or increased presynaptic release probability, have also been suggested (Bliss and Collingridge, 1993; Carroll et al., 1999b). Synapses can also undergo a long-lasting weakening of synaptic strength, termed long-term depression (LTD). LTD, discovered in the hippocampal CA1 region in the early 1990s (Mulkey and Malenka, 1992; Dudek and Bear,

1993), is typically induced by a low-frequency stimulation protocol and its induction relies on activation of NMDARs or on mGluRs (Kemp and Bashir, 2001). The expression of LTD may involve both pre- and postsynaptic mechanisms. As with LTP, AMPARs are also thought to be involved in LTD. The decrease in synaptic transmission during LTD is thought to be a result of reduction in the AMPA receptor number in the postsynaptic membrane. This could be explained by a dephosphorylation of AMPA receptors and their retrieval from the synaptic plasma membrane, both of which have been shown to occur during LTD (Lee et al., 1998; Carroll et al., 1999b).

Protein kinases have been suggested to be key components of the molecular machinery of LTP. Pharmacological inhibition of CaMKII, as well as genetic knockout experiments, provide strong evidence for a key role of CaMKII in LTP. PKC may play a role analogous to CaMKII in the induction of LTP, but experimental evidence for PKC (as well as other kinases) is considerably weaker (Malinow and Malenka, 2002). It has been shown that PKC is activated during the induction of LTP (Klann et al., 1993; Sacktor et al., 1993) and the selective inhibition of regulated PKC activity blocks LTP induction (Malinow et al., 1988; Malenka et al., 1989; Malinow et al., 1989; Wang and Feng, 1992). In contrast, selective inhibition of the PKC kinase domain blocks the maintenance of LTP (Malinow et al., 1988; Hrabetova and Sacktor, 1996). LTP-induced increases in channel conductance may be a result of PKC or CaMKII phosphorylation of

AMPARs (Tingley et al., 1993; Derkach et al., 2007). Strong evidence of the role of PKC in postsynaptic LTP comes from intracellular injection of the PKC pseudosubstrate-like inhibitor. This peptide inhibitor prevented the induction of LTP in postsynaptic neurons (Malinow et al., 1989). Interestingly, in PKCγ knockout mice, the induction of LTP is significantly reduced (Abeliovich et al., 1993b). However, after the induction of LTD, these PKCγ null mutants display normal LTP (Abeliovich et al., 1993b). The differential expression of LTP suggests different stimulation protocols have different signal transduction requirements. Thus, it has been suggested that PKC activation does not directly cause LTP but rather PKC signalling modulates this form of plasticity. LTP and LTD were shown to reversibly modify the phosphorylation state of the AMPA receptor GluR1 subunit. LTP induction in naive synapses and depressed synapses increases phosphorylation of the GluR1 subunit by PKC/CaMKII at S831 and by PKA at S845. In contrast, LTD induction in naive synapses dephosphorylates the PKA site, whereas the major PKC/CaMKII site was dephosphorylated in potentiated synapses (Rial Verde et al., 2006). Although its precise role still remains unclear, the importance of PKC activation in modulating aspects of neuronal changes during plasticity is becoming more and more evident.

1.4.7 Development of the glutamate synapse

Development of glutamate synapses can be divided into two stages: (1) the formation of the synapse, and (2) synaptic maturation. Both

stages involve the synthesis and recruitment of a variety of pre- and postsynaptic proteins, the stabilization of initiated synaptic sites and strengthening or weakening, and removal of inappropriate contacts.

1.4.7.1 Formation and maturation of the synapse

For a synapse to form, dendritic filopodia are guided by molecular cues to axons, where they make contacts and induce formation of a presynaptic terminal along the axon (Garner et al., 2002). The formation of the presynaptic bouton includes clustering of synaptic vesicles and the formation of an active zone, where the transmitter-containing vesicles dock and fuse with the cell membrane. On the other hand, at the postsynaptic membrane, receptors and other molecules become clustered and localized to the postsynaptic membrane at sites called postsynaptic densities (PSD). The initial formation of synaptic connections depends on genetic programming and on cell-to-cell contact rather than on neural activity. For instance, mice lacking munc-18, a protein important for synaptic transmitter release developed normally until birth, even though they lacked synaptic activity in their nervous system (Verhage et al., 2000). The formation of the synaptic connections is followed by the maturation of synaptic circuits.

Synaptic maturation involves the reorganization and refinement of the developing connections and this process is largely governed by neural activity (Ben-Ari, 2001; Groc et al., 2002; Ge et al., 2006). A distinct

feature of glutamate synaptic maturation is an increase in the ratio of current mediated by AMPARs relative to NMDARs (Crair and Malenka, 1995; Ye et al., 2000). Maturation of the synapse can be divided into collective maturation and individual maturation. Collective maturation encompasses changes in the behaviour of a synaptic population such as changes in subunit composition of postsynaptic receptors and/or in release probability. During development, several changes occur in the composition of the glutamate receptors. At many synapses, synaptic maturation is marked by an increased in the incorporation of GluR2 subunits in the membrane (Washburn et al., 1997; Das et al., 1998; Migues et al., 2007). For instance, at the pyramidal neurons, the number of GluR2 subunits is greatly increased after postnatal day 16 (Das et al., 1998) where there is an increase in the ratio of GluR2/1 and GluR2/4. Similarly, in cultured hippocampal neurons, there was an increase in GluR2 expression after 2 weeks in culture (Pickard et al., 2000).

Individual synaptic maturation is the selective strengthening of some synapses and the elimination of other synapses to develop functional neural networks. Elimination of synapses is observed during cerebellar development where there is a transition from multiple to single innervations of the Purkinje cells by climbing fibres (Kano et al., 1995). Strengthening of synapses during maturation occurs primarily by incorporation of AMPARs at silent synapses (reviewed in the section

below). However, the molecular and cellular events occurring at collective or individual synaptic maturation are not mutually exclusive.

1.4.7.2 AMPA silent synapses

One of the most striking features of the developing brain is that many glutamate synapses are functionally silent, that is they do not display any evoked transmission at the resting membrane potential. Silent synapses express only NMDARs and would be functionally silent at hyperpolarized membrane potentials (because of the voltage-dependent Mg^{2+} block) and would exhibit NMDAR-mediated responses and no AMPAR responses upon depolarization. These synapses are therefore referred to as AMPA silent synapses (Durand et al., 1993; Isaac et al., 1995; Song et al., 1998). It is well established that silent synapses occur due to an absence of AMPARs (Malinow and Malenka, 2002), however a very low probability of glutamate release has also been forwarded as an alternative explanation for silent synapses (Choi et al., 2000; Gasparini et al., 2000) . In the developing brain, the majority of glutamate synapses are functionally silent. For instance, in the neonatal rat hippocampus AMPA silent synapses constitute at least 50% of the population of glutamate synapses (Durand et al., 1993; Song et al., 1998). In developing zebrafish, about 50 % of synapses in the reticulospinal and motor neurons are functionally silent (Ali et al., 2000b). The relative amount of silent synapses decreases throughout development. The rat visual cortex is composed of about 55 % of silent synapses (postnatal day 3) and as

development proceeds the percentage of silent synapses drops to about 15 % (postnatal day 11) (Rumpel et al., 2004). Similar decrease in the incidence of silent synapses during postnatal development occurs at the neonatal somatosensory cortex (Isaac et al., 1997) and neonatal hippocampus (Durand et al., 1993).

AMPA silent synapses can be converted into AMPA signalling synapses by correlated pre and postsynaptic activity (Durand et al., 1993; Isaac et al., 1995; Song et al., 1998). The unmasking of the AMPA silent synapses towards functionally mature synapses is an LTP based phenomena (Ambros-Ingerson et al., 1993; Isaac et al., 1995; Song et al., 1998). The activation of NMDARs during cellular depolarization and the consequent calcium influx leads to the increase of AMPAR expression at synapses (Sucher et al., 1995). The most likely expression mechanism behind unmasking of AMPA silent synapses, via NMDAR activation and an elevation in the postsynaptic [Ca^{2+}], is a fast trafficking of AMPARs to the synapse (Malinow and Malenka, 2002). The conversion of AMPA silent synapses to functional synapses can be seen as both collective and individual maturation, since the relative number of silent synapses decreases with age in the population and since the switch is activity-dependent and occurs in the individual synapse.

1.4.7.3 Synaptic plasticity at developing synapses

The activity- and experience-dependent refinement of neural circuitry that occurs during development shares features with processes of learning and memory, and thus a role for LTP in this process has been proposed (Bear et al., 1987). It was long held that LTP could not be induced at developing synapses (Park et al., 2006). But, it has been shown that under sufficient postsynaptic depolarization, LTP can be induced in neonatal animals (Song et al., 1998). Interestingly, one key aspect that appears to be common for LTP in developing and mature synapses is the requirement for NMDAR activation for their inductions (Durand et al., 1993; Song et al., 1998). As with LTP at mature synapses, developmental LTP also relies on mechanisms such as AMPAR trafficking (Hayashi et al., 2000; Plant et al., 2006), increases in release probability (Bolshakov and Siegelbaum, 1995; Palmer et al., 2004) and increases in the channel conductance of AMPARs (Benke et al., 1998; Palmer et al., 2004).

The conversion of AMPA silent synapses into AMPA signalling synapses, via receptor trafficking, has been proposed as an important mechanism explaining developmental LTP (Malinow and Malenka, 2002). However, even though the LTP that occurs during development resembles the adult LTP in some respects, important differences between the two have been discovered. For instance, with respect to AMPAR trafficking and LTP there seems to be a shift in the importance of different AMPAR

subunits during development. The GluR1 subunit appears to have a central role in the expression of adult hippocampal LTP since GluR1 subunits are delivered to the synapse during LTP (Hayashi et al., 2000; Plant et al., 2006) and adult GluR1-/- mice are deficient in LTP in the CA3-CA1 synapse (Zamanillo et al., 1999). However, this mouse still exhibits developmental LTP. In the hippocampus, conversion of silent synapses into functional synapses is due to the delivery of receptors containing the GluR2 subunits (Kolleker et al., 2003) and GluR4 (Zhu et al., 2000). GluR2 can be inserted into the synapse by spontaneous synaptic activity or by LTP induction and when this insertion was blocked in neonatal GluR1-/- mice, LTP was abolished (Kolleker et al., 2003). Another important difference between developmental and mature LTP is that developmental LTP requires activation of PKC and PKA, whereas mature LTP requires activation of αCaMKII (Yasuda et al., 2003). For example, αCaMKII activation is not required for synaptic delivery of the GluR4 subunit (Zhu et al., 2000). Moreover, at the end of the second postnatal week (in rats), simultaneous application of αCaMKII blockers and blockers of PKC is required to fully inhibit LTP, whereas, when applied alone, the inhibitors have no effect (Wikstrom et al., 2003). In line with this finding, pharmacological inhibition of αCaMKII did not affect the level of LTP at the end of the first postnatal week, whereas this LTP was abolished by blocking the activity of PKA. The molecular composition of synapses changes during development and that different signalling proteins and

structural interactions mark mature and immature synapses (Lee et al., 2003; Yasuda et al., 2003). It is believed that the mechanisms underlying AMPAR insertion at developing synapses are likely to be distinct from those that govern AMPAR trafficking at mature synapses (Hall and Ghosh, 2008). However, to date, there is no evidence of whether these changes lead to distinct AMPAR trafficking mechanisms during development. In my thesis work, I address this issue by investigating the mechanisms underlying AMPAR trafficking during development.

AMPARs mediate fast excitatory synaptic transmission in the vertebrate CNS. During development, the functional properties of these receptors change and more receptors are inserted into the membrane. However, the mechanisms underlying the of AMPARs maturation are poorly understood. We must understand the intricacies of AMPAR-containing synapses if we are to comprehend how networks of neurons are set in place to operate collectively and effectively; and how locomotion and learning and memory are embedded in such networks. The reasons for our gap in understanding the maturation of AMPAR owe their existence to the complexity of the mammalian brain. Neuronal development and the basic function of the brain are common to all vertebrates and I have opted to use a simple model-zebrafish, because it offers several important advantages (see Section 1.4.8) over other systems.

1.4.8 Zebrafish

Zebrafish (*Danio rerio*) is native to the Ganges river in East India, Pakistan, Bangladesh, Nepal and Burma, where they live in most types of water ranging from streams to stagnant ponds and rice fields. Zebrafish have become a common aquarium fish throughout the world and can now be found in waters of USA, Australia and Columbia. They belong to the cyprinid family of teleost fish. In 1981, George Streisinger introduced zebrafish as a genetic model to study vertebrate development. Zebrafish offer numerous advantages such as their high fecundity (mature females lay several hundred eggs at weekly intervals), short generation time (3-4 months), rapid development, external fertilization, translucent embryos and easy maintenance. These advantages make zebrafish a good research model in many aspects of embryonic development, physiology and disease.

1.4.8.1 Development and behaviour

All developmental stages, including organogenesis, are clearly visible within the embryo and have been described in detail ((Kimmel et al., 1995)). Zebrafish development is divided into 8 periods of embryogenesis – the zygote, cleavage, blastula, gastrula, segmentation, pharyngula, hatching and early larva periods (Figure 1.2). The newly fertilized egg is in the zygote period (0- ¾ h) until the first cleavage occurs. During the cleavage (¾ - 2¼ h) and blastula (2¼ -5¼ h) periods, several characteristic processes occur, including epiboly, involution and

convergent extension. These processes start with the migration of the cells over the yolk followed by extensive rearrangements. Subsequently, in the next three hours, the three primary embryonic germ layers are formed through cell movements, a process called gastrulation (5 ¼ -10 h). During the segmentation period (10-24 h), the basic vertebrate body plan has developed and it marks the beginning of primary organogenesis and somitogenesis. At the pharyngula phase (24 h), the body axis straightens from its curvature about the yolk and the fin starts to develop. At 24 hpf, a heartbeat and associated blood flow can be recognized. At 48 hpf (hatching period), there is the completion of morphogenesis and organogenesis, cartilage development in the head and pectoral fin, and hatching occurs asynchronously. At 72 hpf, the early larval period, the swim bladder inflates and the larvae are able to swim and search for food. During development zebrafish also undergo a series of characteristic behaviours. For instance, at 17-19 hpf, they start to show spontaneous contraction of their trunk and at 21-24 hpf, they exhibit coiling behaviours (Saint-Amant and Drapeau, 1998). The frequency of the coil behaviour accelerates during development and it reaches a maximum speed of contraction just before hatching (48 hpf). At around 30-36 hpf, embryos acquire a touch/startle response and at 48 hpf, they start to hatch out of the chorion, at which point they swim away from a touch stimuli (Kimmel et al., 1974). At 72 hpf, vigorously react to touch stimuli and can actively swim (Kimmel et al., 1974).

1.4.8.2 Expression of AMPARs in developing zebrafish.

All AMPAR transcripts can be detected at approximately the same level by the time of fertilization at the one-cell stage (0 hpf) and the amount of AMPA transcripts increases significantly after neurulation at 24 hpf (Rial Verde et al., 2006). The increase in the expression of GluR1 only becomes significant after hatching (Rial Verde et al., 2006; Hoppmann et al., 2008). The expression of GluR2 gradually increases between 4 and 16 hpf, however, relative to the amount detected at 16 hpf, the increase in GluR2 expression becomes significant after 30 hpf. Starting from 30 hpf, the amount of GluR2 transcripts clearly exceeds the total amount of GluR1, GluR3 and GluR4 transcripts. The amount of GluR3 and GluR4 also increases gradually after 12 hpf but their expression levels are at least 10-fold lower than GluR1 and GluR2 at 72 hpf. GluR2 in adult zebrafish is edited at the Q/R site (Kung et al., 2001) and GluR2 mRNA Q/R editing actually occurs before 24 hpf. The C-terminal alternative splicing is established after 48 hpf; however, there is no change in the ratio of the flip and flop splice variants during the zebrafish development.

The NSF, 4.1 N, GRIP and PICK1 protein-protein interaction motifs within the C-teminal domains are highly conserved in the zebrafish (Rial Verde et al., 2006). However, the SAP97-interacting sequence on the GluR1 subunit is absent. This finding suggests that many common mechanisms regulating trafficking and activity of GluR2-AMPARs are conserved from mammals to zebrafish.

1.4.8.3 Mauthner cells

In 1859, Mauthner discovered the two strikingly giant axons in the teleost spinal cord which now bear his name. These paired giant axons belong to cells in the fish hindbrain called Mauthner cells (M-cells). M-cells are the largest reticulospinal neurons (100 μM) in the teleost CNS and are key players in the initiation of the fast escape response (C-start) to an abrupt stimulus (Zottoli, 1978; Kimmel et al., 1981; Metcalfe et al., 1986) (Figure 1.3). They are also believed to play a role in the hatching process where their activity produces a robust tail-flip that allows the rupture of the egg casing (Eaton and Nissanov, 1985).

M-cells receive sensory inputs from afferents of the somatosensory neurons, the visual, acousto-vestibular and lateral line system. The Mauthner axons cross to the opposite side of the brain to descend the length of the spinal cord and as they do so, they issue axon collaterals that synapse with spinal motor neurons to activate the spinal motor system (Figure 1.3). The M-cell has two large crescent shaped dendrites: the lateral dendrite and the ventral dendrite, and the sensory inputs to the M-cell are segregated to separate dendrites. For instance, inputs from the auditory hair cells, vestibular otoliths and lateral line are localized to regions of the lateral dendrite (Faber and Korn, 1975), while the ventral dendrite receives inputs from the visual system and spinal cord (Chang et al., 1987). These sensory inputs terminate as electrical, chemical or mixed

synaptic contacts on the dendrites. In developing zebrafish, the earliest synapses on M-cells are established by around 24 hpf (Kimmel et al., 1990). Between 2 and 6 dpf, chemical synapses predominate over electrical synapses and mixed synapses are the least frequent (Kimmel et al., 1981). Gap junctions are found mostly on the ventral dendrites and ventral M-cell perikaryon while chemical synaptic contacts are in large numbers on the dorsal surface of the M-cell and the lateral dendrites (Kimmel et al., 1981). The M-cell receives excitatory glutamatergic inputs (AMPA and NMDA) (Ali et al., 2000b) and GABA- and glycinergic inhibition (Legendre, 1997; Triller et al., 1997; Ali et al., 2000a).

The M-cell has been a valuable preparation for the study of cellular processes underlying behaviour (Liu and Fetcho, 1999; Eaton et al., 2001) and for the elucidation of basic mechanisms of synaptic transmission (Ali et al., 2000b; Korn and Faber, 2005). M-cell research provides a potential model for future studies to understand synaptic plasticity by neuromodulators and how they shape the output of neural networks underlying the fish escape response.

My thesis focuses on the development of excitatory synapses on M-cells in zebrafish embryos. The importance of this work lies in the fact that AMPARs are involved in the majority of synaptic excitation in the vertebrate CNS and as such, improper development or loss of function (e.g. during neurotrauma) can have catastrophic effects on behaviour,

health and well-being. For instance, impaired AMPAR function has been implicated in diseases such as Alzheimer's, amyotrophic lateral sclerosis and epilepsy. Therefore, understanding the mechanisms of AMPAR development is not only important for our basic knowledge of synaptic maturation but also for the production of treatments for neurological disorders affecting excitatory synaptic transmission, and for regeneration following neurotrauma.

Figure 1.1 Structure of the AMPAR tetrameric channel and the subunits**.** The channel consists of four subunits (GluR1-4), which are usually two dimmers. The dimmers are two different subunits , such as GluR1- and -2 (illustrated in the figure) or GluR 2- and -3. The individual subunits are composed of three transmembrane domains (TM). The N-terminus is extracellular and the C-terminus is intracellular. Splice variation is within the flip/flop region. The GluR2 subunit undergoes RNA editing at the Q/R site.

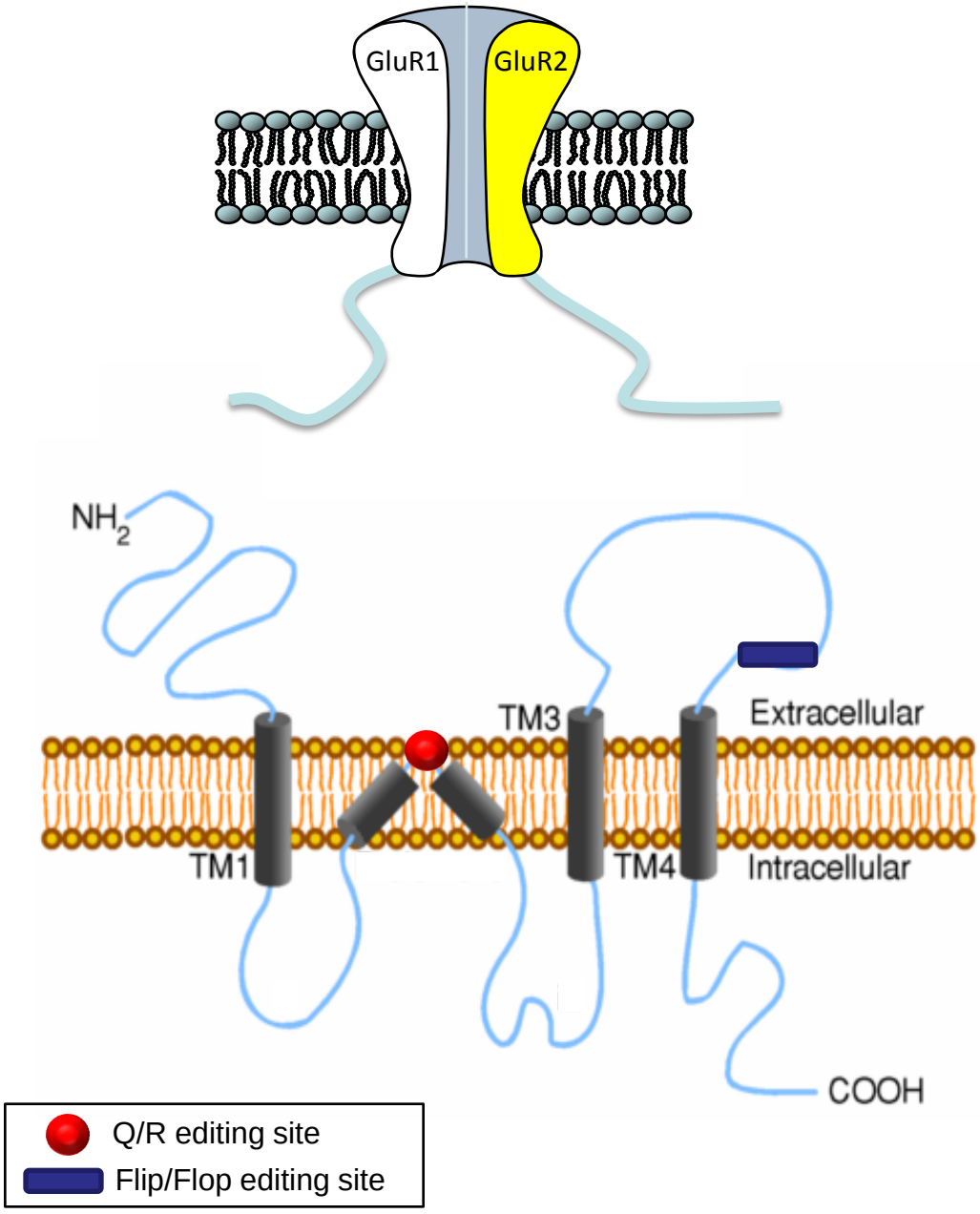
GluR1
GluR2
NH2
TM3
Extracellular
TM1
TM4
Intracellular
COOH
Q/R editing site
Flip/Flop editing site

Figure 1.2 Stages of embryonic development of the zebrafish. Face view photographs (from Cedar-Thomas's webpage) of embryos during the zygote, cleavage, blastula, gastrula, segmentation, pharyngula, hatching and early larva periods.

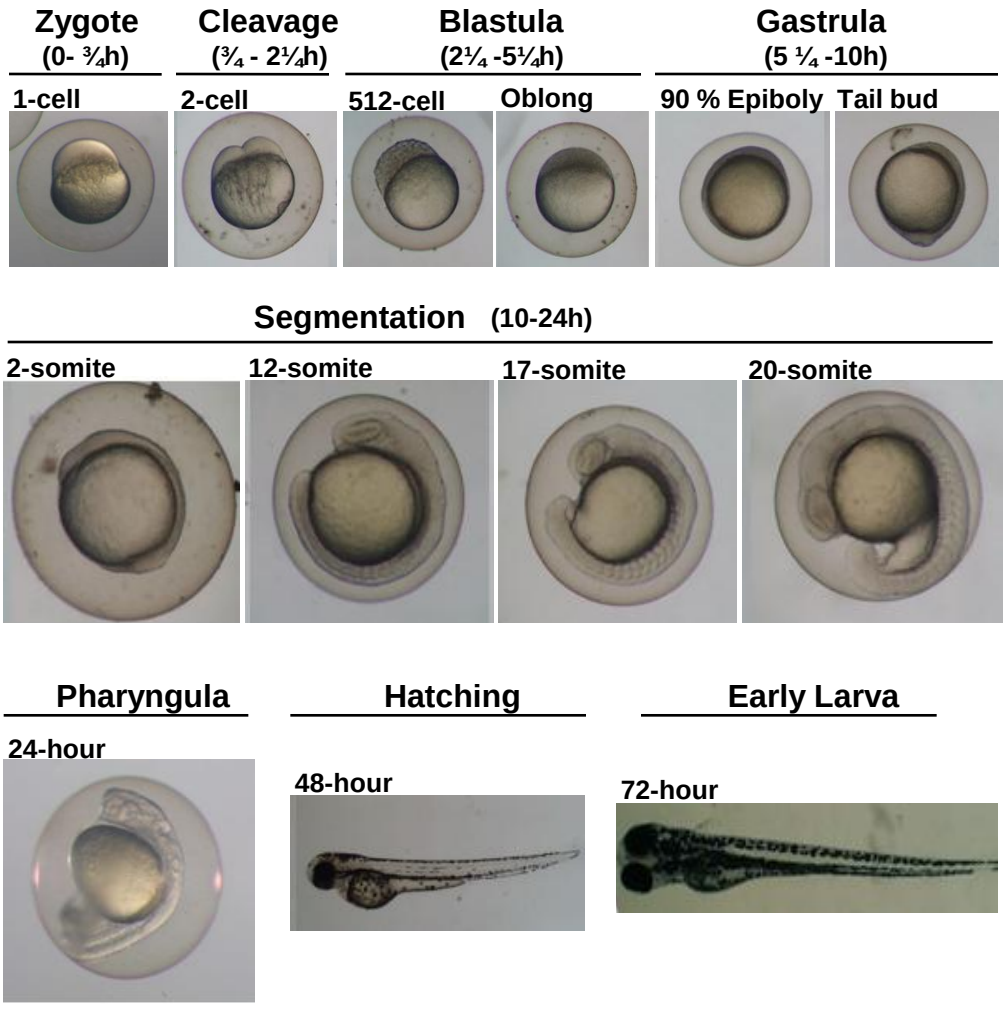
Zygote
(0- ¾h)
Cleavage
(¾ - 2¼h)
Blastula
(2¼ -5¼h)
Gastrula
(5 ¼ -10h)
1-cell
2-cell
512-cell
Oblong
90 % Epiboly
Tail bud
Segmentation (10-24h)
2-somite
12-somite
17-somite
20-somite
Pharyngula
Hatching
Early Larva
24-hour
48-hour
72-hour

Figure 1.3 Zebrafish Mauthner cells. **A**: Zebrafish (dorsal view) possess a pair of Mauthner cells that are located in the hindbrain. Each Mauthner cell has two large dendrites: the lateral dendrite and the ventral dendrite. Excitatory transmission is mediated by glutamate while inhibitory transmission is mediated by Glycine/GABA. **B**: Mauthner cells receive sensory inputs. Their axon cross to the opposite side of the brain to descend the length of the spinal cord and as they do so, they issue axon collaterals that synapse with motor neurons to activate muscles (lateral view). **C**: Dorsal view of the sequential body orientations of a fish engaging in an escape behaviour (Adapted from (Eaton et al., 1977a).

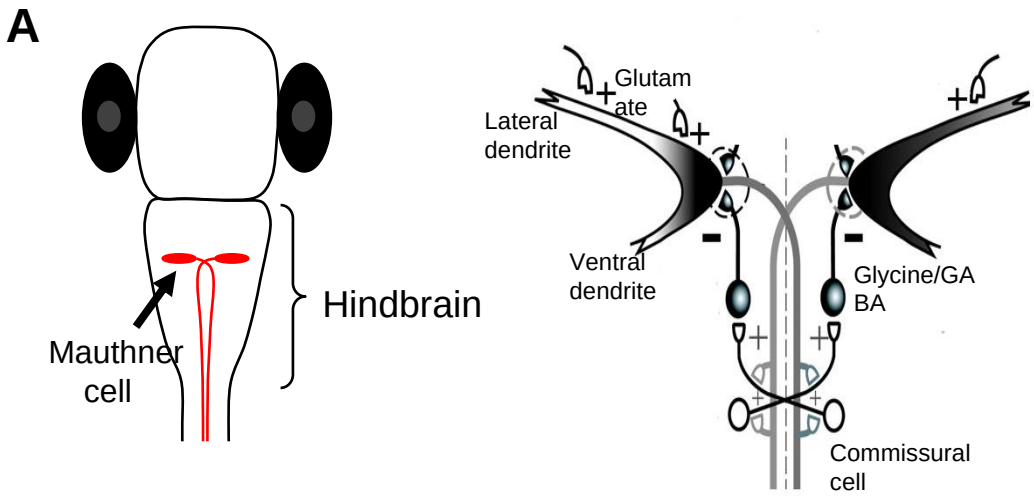
A
Hindbrain
Mauthner cell
Glutam ate
Lateral dendrite
Ventral dendrite
Glycine/GA BA
Commissural cell

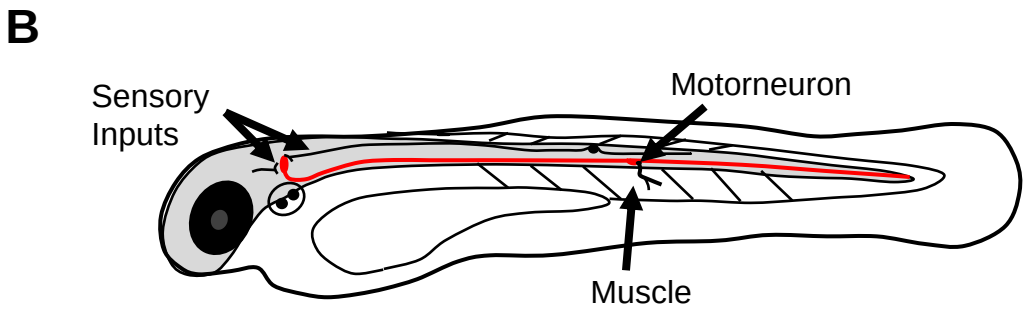
B
Sensory Inputs
Motorneuron
Muscle

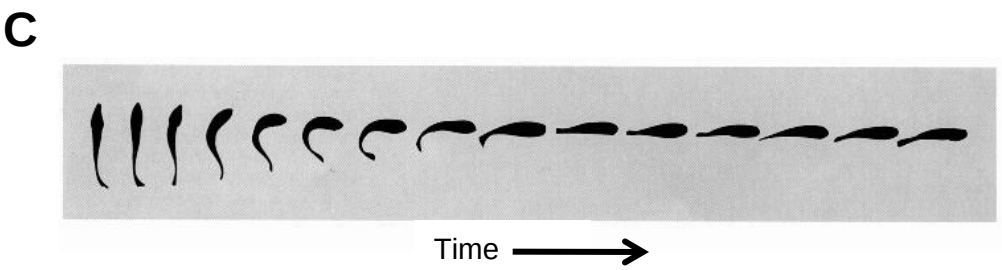
C
Time

Chapter 2 MATERIALS AND METHODS

2.1 Zebrafish preparation

2.1.1 Dissection

Wild-type Zebrafish (*Danio rerio*) embryos were raised at 28.5°C, and collected and staged as previously described (Kimmel et al., 1995; Westerfield, 2000). All procedures were carried out in compliance with the guidelines stipulated by the Canadian Council for Animal Care and University of Alberta. Embryos and newly hatched larvae were anaesthetized in 0.02% tricaine (MS-222) (Sigma, St. Louis, MO) and dissected as described by (Drapeau et al., 1999). Briefly, the entire hindbrain was exposed after removing the forebrain and rostral structures, but leaving the spinal cord intact.

2.1.2 Identification of the Mauthner cell

Mauthner cells are located in rhombomere 4 of the hindbrain and were easily identified under Nomarski Differential Interference Contrast (DIC) optics based on their morphology and location (Eaton and Farley, 1973). To further confirm their identity, the cells were filled with Lucifer Yellow (0.1 %), during the recordings.

2.2 Electrophysiology

2.2.1 AMPA mEPSC recordings

The preparations were moved to the recording set-up and the chamber was continuously perfused at room temperature (20-24^{o}C) with an aerated recording solution that lacked tricaine but contained 15 μM D-tubocurarine (Sigma) to paralyze the preparations. The miniature excitatory postsynaptic current (mEPSC) recording solution contained (in mM) 134 NaCl, 2.9 KCl, 2.1 $CaCl_2$, 1.2 $MgCl_2$, 10 HEPES, 10 glucose and 0.001 Tetrodotoxin (TTX), with the osmolarity adjusted to 280 mOsm, pH 7.8. In addition, blockers for glycine and GABA receptors (5 μM Strychnine and 100 μM picrotoxin, respectively) were added to the bath during all recordings. Patch-clamp electrodes were pulled from borosilicate glass and when filled with a Cs-gluconate solution and had resistances of 3.5-5 MΩ. The Cs-gluconate intracellular solution was composed of (in mM) 115 Cs-gluconate, 15 CsCl, 2 $MgCl_2$, 10 HEPES, 10 EGTA, and 4 Na_2ATP, osmolarity adjusted to 280-290 mOsm, pH 7.2.

Whole-cell currents were recorded using an Axopatch 200B amplifier (MDS Analytical Technologies, Sunnyvale,CA) and were low-pass filtered at 10 kHz (-3 dB) and digitized at 50 kHz. Synaptic currents were recorded at a holding potential of -60 mV. Immediately after establishment of the whole-cell recording mode, series resistance was compensated by 70-85%, using the amplifier's compensation circuitry.

Series resistance was monitored throughout the recording, which was abandoned if the resistance changed by >15%.

For establishment of current-voltage (I-V) relationships, sampling was repeated at a series of membrane command potentials in steps of 20 mV increments from -80 mV to +80 mV. The potential was stepped to a new, constant value before the start of sampling (2-4 s) in order to allow the membrane current to relax to a plateau level. During these recordings, the NMDA blocker, 2-amino-5-phosphonovaleric acid (APV), was included in the extracellular solution.

2.2.2 Pharmacology: PKC modulation of AMPA mEPSCs and AMPA receptor trafficking

To activate PKC, phorbol 12-myristate 13-acetate (PMA) and 1, 2-dioctanoyl-sn-glycerol (DOG) were bath applied to the preparation for 5 min after the initial recording and a second recording was then performed. To test the effects of blocking PKC activity, the PKC inhibitor Bisindolymaleimide I (BIS-I) was applied in the patch pipette for ~2 min before obtaining a recording. Then PKC activators (PMA and DOG) were applied to the patch for 5 min before performing a second recording on that same cell.

All peptides (pep2m, pep4c, pep2-EVKI, pep2-SVKI and Tetanus toxin) used to interfere with AMPA receptor trafficking were applied to the

Mauthner cell cytosol via the patch pipette prior to bath application of PMA.

2.2.3 Neuronal depolarization induced by a 5 mM K^+ medium and a depolarization pulse protocol

Chemical depolarization of the Mauthner cell was induced by a 10 min bath application of a 5 mM K^+ depolarizing medium that contained (in mM):130 NaCl, 5 KCl, 2.1 $CaCl_2$, 0.3 $MgCl_2$, 10 HEPES, 10 glucose, and 1 Tetraethylammonium (TEA), osmolarity adjusted to 280 mOsm, pH 7.8. Postsynaptic depolarization of the Mauthner cell was induced by applying a series of 10 voltage steps from -80 to +20 mV, lasting 3 s, given at an interpulse interval of 6 s (Baxter and Wyllie, 2006).

2.3 Analysis of mEPSCs

Synaptic activity was monitored using pClamp 8.1 software (MDS Analytical Technologies,Sunnyvale, CA). The software detected all events that could be recognized visually. All events were then inspected visually, and those with uneven baselines or overlaying events (<5%) were discarded. The decay time course was analyzed over the first 30 ms and was fit with a sum of exponential curves in Axopraph X. Averages of these events were best fit with one exponential curve. The rise times were defined as the time from 20 to 80% of the mEPSC amplitude. The rectification index was defined as peak current amplitude at a holding potential of +40 mV divided by that at -60 mV.

2.4 Non-stationary fluctuation analysis

In order to estimate the single-channel current (i) and the available number of channels (N), a non-stationary fluctuation analyis (NSFA; (Sigworth, 1980) was performed on the mEPSC recordings. The mEPSCs were aligned on their rise time and events with obvious artifacts were manually discarded. Non-stationary analysis was performed on the deactivation phase of the responses. The averaged current and variance over time were computerized using Axograph 4.6 software (MDS Analytical Technologies,Sunnyvale, CA). Between 40 and 100 traces per patch were obtained for analysis.

The variance (σ^2) was plotted against the mean current (I) and the data points were fitted with the following parabolic function (Sigworth, 1980).

$$\sigma^2 (I)= i\, I – I^2/N+ \sigma_b^2$$

where i is the elementary current of the receptor channel, N is the total number of available AMPARs at the synapse and σ_b^2 is the variance of the background noise. The conductance value (γ) for each channel was then calculated by the equation $i/(V_m – E_{rev})$, with V_m = -60 mV and E_{rev} = 0 mV. In some cases, the parabolic function did not fit the data points of variance versus mean plot accurately, and thus these results were analysed by performing a linear fit to the initial part of the curve (10–15% of the

response range) where the slope factor corresponds to the single-channel current (i) (Benke et al., 1998).

2.5 Immunohistochemistry

2.5.1 Antibody labelling

Zebrafish 2 dpf embryos were fixed in 2% paraformaldehyde for 1–2 h. Tissues were washed several times in phosphate-buffered solution (PBS; 137 mM NaCl, 2.7 mM KCl, 4.3 mM Na_2HPO_4, 1.47 mM $KHPO_4$, pH= 7.4) and permeabilized for 30 min in 4% Triton-X 100 containing 2% bovine serum albumin (BSA) and 10% goat serum. Following blocking, tissues were incubated in the primary antibodies 3A10 (Developmental Studies Hybridoma Bank, University of IOWA ,IOWA,1:250), anti-PKCα, -βII or -γ (Santa Cruz Biotechnology, Santa Cruz, CA; 1:500) for 48 h at 4°C on a shaker. Tissues were washed several times in PBS over a 24 h period, and then incubated in the secondary antibodies conjugated with Cy3 or Alexa 488 (Molecular Probes, Carlsbad, CA, 1:2000) for 4–6 h at room temperature. Animals were washed in PBS several times, de-yolked, cleared in 70% glycerol and mounted.

Negative controls were performed whereby the primary antibody was preincubated with a blocking peptide specific for that antibody in a ratio of 1:5 antibody:blocking peptide (Santa Cruz Biotechnology) overnight. This incubation mixture was then used as the primary antibody to detect PKC in the immunohistochemistry experiments.

2.5.2 Photography and microscopy

Preparations were mounted in glycerol and Z-stack images were photographed using a Zeiss LSM 510 confocal microscope under a 20x objective. The images were then compiled using Zeiss LSM Image Browser software.

2.6 Western blotting

2.6.1 Species cross reactivity

Zebrafish brains were rapidly dissected in ice-cold physiological saline, placed in Tissue-PE LB buffer (G Biosciences, St. Louis, MO, USA) containing protease inhibitors (3 mM Phenylmethylphonyl fluoride (PMSF), 40 μM leupeptin, 4μM pepstatin A, 0.4 mg/ml aprotinin) and immediately placed on dry ice. Mouse cortexes were obtained from Dr. P. Nyugen's lab (University of Alberta) and they were treated similarly as the zebrafish brains. The brains were then homogenized by hand with a Dounce tissue homogenizer and centrifuged at 13,000 x g for 5 min. The supernatant was removed to quantify the protein content and the pellet was discarded. Protein quantification was performed using the Lowry Protein Assay (Bio-Rad, Hercules, CA), and 20 μg of the homogenate was loaded per lane. Samples were subjected to SDS-PAGE (10%) and transferred to nitrocellulose membranes using a semi-dry transfer apparatus (Bio-Rad). Membranes were blocked in blocking buffer (5% skim milk powder, 0.1% Tween-20 in Tris-buffered saline (TBS) for 1 h at room temperature and

incubated in anti-PKCα, βII or γ primary antibody (Santa Cruz Biotechnology, Santa Cruz, CA; 1:1000) overnight at 4°C. Membranes were washed several times in TBS-T (TBS and 0.1% Tween) and incubated in secondary antibody coupled to horse radish peroxidase (HRP; 1:50,000 goat anti rabbit IgG, Santa Cruz Biotechnology) for 1 h at room temperature on a shaker. Signals were detected with enhanced chemiluminescence (SuperSignal® West Pico, Pierce, Rockford, IL) and developed on X-ray film.

Negative controls were performed whereby the primary antibody was preincubated with a blocking peptide specific for that antibody in a ratio of 1:5 antibody:blocking peptide (Santa Cruz Biotechnology) overnight. This incubation mixture was then used as the primary antibody to detect PKC in the immunoblots.

2.6.2 PKCγ membrane translocation study

Zebrafish brains were incubated with or without the PKCγ inhibitor peptide (γV5-3) (1 μM in 200 μL PBS for 10 minutes), followed by 5-minute incubation with or without 5 nM PMA. The incubation was stopped by snap freezing the samples on dry ice. Samples were then homogenized in a homogenization buffer (in mM: sucrose, 250; EDTA, 1; Tris, 30, pH 7.4) containing protease inhibitors (3 mM PMSF, 40 μM leupeptin, 4 μM pepstatin A, 0.4 mg/ml aprotinin) and centrifuged at 1,000 x g at 4°C for 15 min. Supernatants were collected and centrifuged at 10,000 x g at 4°C for

15 min. Then the supernatants were collected, and pellets were re-suspended in homogenization buffer supplemented with 1% SDS (V/V), incubated on ice for 30 min, and spun at 100,000 x g at 4°C for 30 min. The supernatants were removed to quantify the protein content and the pellets were discarded. Protein quantification was performed using the BCA protein assay kit (Pierce, Rockford, IL, USA) and 10 μg of zebrafish homogenate was loaded per lane. Samples were subjected to SDS-PAGE (10%) and transferred to nitrocellulose membranes using a semi-dry transfer apparatus (Bio-Rad, Hercules, CA). Membranes were blocked in blocking buffer (5% skim milk powder, 0.1% Tween-20 in TBS) for 1 h at room temperature and incubated in primary antibodies anti-PKCγ (Santa Cruz Biotechnology, Santa Cruz, CA; 1:1000) and anti-acetylated tubulin (Sigma-Aldrich, St-Louis, MO; 1:20,000) overnight at 4°C. Membranes were washed several times in TBS-T and incubated in secondary antibodies coupled to horse radish peroxidase (HRP; 1:40,000 goat anti-rabbit IgG and HRP; 1:100,000 goat anti-mouse IgG, Santa Cruz Biotechnology) for 1 h at room temperature on a shaker. Signals were detected with enhanced chemiluminescence (SuperSignal® West Pico, Pierce, Rockford, IL) and developed on X-ray film. Immunoreactive bands were quantified densitometry (Adobe Photoshop).

2.7 Generation and analysis of zebrafish PKCγ Morpholino

To reduce PKCγ protein levels, an antisense morpholino oligonucleotide (PKCγ-MO) was used to disrupt the translation of PKCγ transcripts (The translation-blocking morpholino , 5'-TGGACTGAGCGGGACACCCTGAAGA-3', was synthesized by Gene Tools (Philomath, OR). The morpholino was injected into single-cell stage zebrafish embryos at concentrations of 2.5 ng/nl, in volumes of approximately 5 nl. Injected and uninjected embryos were then incubated in embryo media at 28.5 °C for 24 h, after which they were assessed for viability. Two day old PKCγ-MO injected and uninjected embryos were then used for immunohistochemical analysis, behavioural testing and electrophysiological recordings.

2.8 Rescue of PKCγ morphant phenotype

Rescue of the PKCγ morpholino-induced phenotype was achieved by injecting synthetic zebrafish PKCγ mRNA (GenBank accession number: XM_001921680) into the single cell embryo immediately prior to injection of the PKCγ-MO. The PKCγ mRNA was synthesized as follows: the full open reading frame (ORF) of zebrafish PKCγ, linked to a Kozak consensus sequence to permit ribosomal binding, was amplified from zebrafish brain cDNA with forward 5'-GCCACCATGGCCACACCGGTGTCTCCGTCTCC-3' and reverse 5'-TCAGACAGCAGTGAGGGGTGAAGGG-3' primers using 0.4 U of

Phusion High-Fidelity DNA polymerase (Finnzymes) in 20 μL reactions. Cycling parameters were as follows; 40 s at 98^{o}C, 30 cycles of 98^{o}C for 20 s, 64^{o}C for 25 s, 72^{o}C for 30 s, and a final extension step for 7 min at 72^{o}C. Products from each polymerase chain reaction (PCR) were separated on a 1.0% Tris-acetate-ethylenediamine tetraacetic acid(TAE)-agarose gel, visualized by staining with ethidium bromide solution (50 μg/L), and the DNA was then excised, gel purified (Qiagen Gel Extraction Kit) and cloned into pJET1.2/blunt using the blunt-end protocol (Fermentas). pJET1.2/blunt-zebrafish PKCγ plasmids were column purified from an overnight bacterial culture using the Qiagen miniprep kit and then sequenced at the molecular biology services unit in the Department of Biological Sciences, University of Alberta, on an ABI 3730 DNA sequencer. Two micrograms of pJET1.2/blunt- PKCγ plasmid was linearized with 20 U of EcoRV (Fermentas) for 4 h at 37^{o}C and then purified by phenol/chloroform extraction followed by precipitation with 3 M sodium acetate at -20^{o}C for 1 h in ethanol. Template DNA was re-suspended in DEPC-treated water and 1 μg used for the generation of mRNA using the TranscriptAid T7 High Yield Transcription Kit (Fermentas) according to manufacturer's instructions. Synthesized RNA transcripts were then phenol/chloroform extracted, precipitated, and re-suspended in DEPC-treated water. Three hundred picograms of the synthetic mRNA was then injected into embryos at the one-cell stage. Rescued embryos were visualized and counted using a Leica MZ95 stereoscope. At 48 hpf,

they were used for behavioural testing and electrophysiological recordings.

2.9 Behavioural assays

Zebrafish larvae were assessed for their ability to respond to touch by a tap to their head or tail. PKCγ-MO injected embryos were removed from their chorion immediately before the assay. Fish were placed in ~1% methylcellulose and their response to touch was visualized and captured (1 frame/42 ms) using an Olympus SZX12 stereoscope with a Qimaging micropublisher camera.

2.10 Drugs and blocking peptides

Strychnine (5 μM), picrotoxin (100 μM), APV (50 μM), Pentobarbital (100 μM), 1-Napthylacetylspermine (NASPM; 10 μM) and BAPTA (5 mM) were obtained from Sigma-Aldrich (St-Louis, MO). Phorbol 12-myristate 13-acetate (PMA; 100 nM) was obtained from Alexis Biochemical (San Diego, CA). 1, 2-dioctanoyl-sn-glycerol (DOG), Bisindolymaleimide I (BIS I; 500 nM) and Latrunculin B (5 μM) were purchased from Calbiochem (Gibbstown,NJ). Tetrodotoxin (TTX; 1 μM) and the peptides pep2m, pep4c, pep2-EVKI and pep2-SVKE were purchased from Tocris (Avonmouth, UK). The PKCγ inhibitor, γV5-3 (10 nM) and its control peptide (C1; 10 nM) were gifts from KAI pharmaceuticals (Stanford, CA).

The peptide competes with activated PKCγ for binding to the isozyme-specific docking proteins, receptors for activated C kinase (RACK). This strategy prevents PKC isozyme translocation and functioning in an isozyme-specific manner (MochlyRosen et al., 1991) Active PKCγ (10 ng/μl) was obtained from Millipore (Billerica, MA). Tetanus toxin light chain (TeTx; 200 nM) was purchased from List Biological Laboratories (Campbell, CA).

2.11 Statistical analysis

All data values are given as means ± SEM. Correlations were calculated with the use of a least-squares linear regression analysis. The term “significant” denotes a relationship with $p < 0.05$ or $p < 0.001$ determined using one-way ANOVA and Fisher LSD for normally distributed, equal variance data, unpaired and paired t-test. Kruskal-Wallis ANOVA and Dunn’s method of comparison were used for non-normal distributions.

Chapter 3 [*]PROPERTIES OF AMPA RECEPTORS AT DEVELOPING SYNAPSES IN THE ZEBRAFISH MAUTHNER NEURON

3.1 Introduction

AMPARs mediate fast excitatory synaptic transmission in the vertebrate CNS and their properties change during development. However, information about developmental changes in AMPAR-mediated currents is somewhat contradictory. For example, in hippocampal pyramidal cells, AMPAR-mediated currents show an increase in decay times with maturation (Seifert et al., 2000), whereas most other studies report a developmental decrease in decay time constants (Taschenberger and von Gersdorff, 2000; Iwasaki and Takahashi, 2001; Joshi and Wang, 2002; Wall et al., 2002; Yamashita et al., 2003; Rumpel et al., 2004). The earliest synapses on M-cells are established by around 24 hpf (Kimmel et al., 1990) with functional inputs occurring around 26-27 hpf (Grunwald et al., 1988; Ali et al., 2000a). Some characteristics of GluRs on developing M-cells have already been investigated (Ali et al., 2000b), but the developmental profile of AMPAR properties still remain unknown.

Therefore, I have undertaken this study to fully examine the developmental properties of AMPAR-mediated currents *in vivo*, on zebrafish M-cells. The main objectives of the experiments reported in this

[*]A version of this chapter has been published: Patten and Ali 2007. *Journal of Physiology*, 581(Pt 3):1043-56.

chapter are: 1) to isolate non-NMDA mediated mEPSCs recordings; and 2) to characterize the developmental properties of AMPARs. The hypothesis is that the properties of AMPARs undergo changes during zebrafish development.

3.2 Results

In this study, I examined the properties of AMPAR-mediated currents in Mauthner cells of zebrafish ranging in age from 30 hpf to 72 hpf. Recordings were limited to these ages due to the difficulty of obtaining sufficiently clean dissections before 30 hpf, and the difficulty of recording from large, improperly clamped M-cells in animals older than 72 hpf. Recordings taken from 30 hpf to 36 hpf fish were pooled and are referred to as 33 hpf throughout my work. Recordings taken at 2 dpf were more accurately staged as 48 ± 3 hpf, while recordings at 3 days of age were 72 ± 3 hpf. In the remainder of the thesis, these periods are referred to as 48 hpf and 72 hpf. The cell capacitance (C_m) values ranged from 17 ± 2 pF (33 hpf) to 28 ± 1 pF in 48 hpf fish, and finally to 32 ± 2 pF in 72 hpf fish. Values for the membrane resistance (R_m) were 902 ± 36 MΩ (33 hpf), 253 ± 48 MΩ (48 hpf) and 87 ± 19 MΩ (72 hpf) while the resting membrane potentials were -54 ± 1 mV (33 hpf), -58 ± 2 mV (48 hpf) and -61 ± 2 mV (72 hpf).

3.2.1 Isolation of non-NMDA mediated mEPSCs

Mauthner cells were identified in *vivo* based upon the location of their large cell bodies adjacent to the otic vesicles in the hindbrain. Cells were filled with Lucifer yellow to confirm their identity (Figure 3.1A).

Miniature excitatory postsynaptic currents (mEPSCs), unlike evoked currents, allow accuracy in determining the properties of postsynaptic receptors because their decay kinetics in particular are not influenced by developmental changes in the synchrony of vesicular release or release probability (Silver et al., 1996a; Wall et al., 2002; Cathala et al., 2003). Therefore, I focused my analysis on mEPSCs to determine the developmental changes in the properties of postsynaptic receptors.

A high level of synaptic activity was observed when I recorded from the M-cells in normal physiological saline (Figure 3.1B). The M-cells were clamped at a holding potential of -60 mV, where all inhibitory currents were small and inward. To differentiate inward, excitatory currents from inhibitory currents, blockers for glycine and GABA receptors (5 μM Strychnine and 100 μM picrotoxin, respectively) were added to the bath during all recordings. In these initial experiments, 50 μM APV was added to the bath to block all NMDA receptor activity (Figure 3.1C), but I found that isolated non-NMDA mEPSCs were identical in all aspects when

recorded in the presence or absence of APV. Therefore, I omitted APV for all further recordings at -60 mV, but included it when recording at potentials more positive than -60 mV. Miniature EPSCs were recorded in the presence of 1μM TTX (Figure 3.1C). The remaining mEPSCs were completely blocked by the Non-NMDA antagonist CNQX (10 μM; Figure 3.1C). Individual mEPSCs (~300-1000) from a recording were averaged and all analyses were performed on averaged mEPSCs (Figure 3.1D).

3.2.2 Developmental profile of Non-NMDA mEPSCs

Because it is difficult to properly clamp cells with large and extensive dendrites, whole cell recordings are often subject to the problem of inadequate space clamp (Rall, 1969). Accurate control of dendritic potential from a point voltage source is difficult and synaptic events that are generated at more distal locations may be filtered leading to attenuation and widening. Thus, these events will appear to have longer rise times, smaller peak amplitudes and longer decays (Rall, 1969). Therefore, the correlation between the rise time and peak amplitude of events at 33 hpf, 48 hpf and 72 hpf (Figure 3.2) were examined for all recordings to determine if cells were properly space clamped. The lack of a correlation at all ages ($r=0.02$ at 33 hpf; $r< 0.01$ at 48 hpf; $r=0.04$ at 72 hpf), suggests that the M-cells remained electrically compact over the ages examined, and that space clamping errors were not a major issue in our study. The mEPSC amplitude distribution at all ages remained

unimodal (Figure 3.3), with the average peak amplitude increasing significantly between 33 and 48 hpf (33 hpf: 23.9 ± 2.0, n=10; 48 hpf: 30.0 ± 1.5, n=9 and 72 hpf: 29.4 ± 0.9, n=8; $p < 0.05$) (Figure 3.3B). Amplitude histograms from representative experiments are shown in Figure 3.3A. The tight, normal distributions suggest that there was virtually little or no variation in quantal size.

I observed a significant increase in the mEPSC frequency during development, from 0.7 ± 0.3 Hz in 33 hpf embryos to 2.8 ± 0.4 Hz in 72 hpf larva (Figure 3.4A; $p < 0.05$). The rise times, defined as the time from 20 to 80% of the mEPSC amplitude, were fast, averaging 0.13 ± 0.02 ms at 33 hpf, 0.11 ± 0.01 ms at 48 hpf and 0.11 ± 0.01 ms at 72 hpf, and were not significantly different over the developmental stages examined (Figure 3.4B). Average mEPSC traces were well fit with a single exponential decay curve which decreased during development. The decay kinetics were significantly slower at 33 hpf (0.75 ± 0.09 ms) when compared with that of older animals (48 hpf: 0.47 ± 0.03 ms and 72 hpf: 0.48 ± 0.02) (Figure 3.4C, D; $p < 0.01$). This finding is consistent with other studies that demonstrate a speeding in the time course of AMPAR-mediated EPSCs during CNS maturation (Bellingham et al., 1998; Das et al., 1998; Taschenberger and von Gersdorff, 2000; Brenowitz and Trussell, 2001; Wall et al., 2002; Cathala et al., 2003).

3.2.3 Non-NMDA mEPSCs are only mediated by AMPA receptors

To determine if the mEPSCs were mediated by AMPA or Kainate receptors, I examined the effect of the selective AMPAR antagonist (GYKI; 50 μM), and the selective kainate desensitizing agent SYM (10 μM) on mEPSCs. I found that GYKI completely blocked all mEPSCs (Figure 3.5A) and that SYM had no significant effect on the mEPSC frequency (Figure 3.5B), amplitude (Figure 3.5C), rise time (Figure 3.5D) or the decay time constant (Fig 3.5E) ($p > 0.05$). These results suggest that the mEPSCs were due solely to the activation of AMPA receptors and lacked a kainate component at all ages.

3.3 Summary

In summary, I have characterized several of developmental changes in AMPAR-mediated synaptic currents in Mauthner cells. These developmental changes occur between 33 hpf and 48 hpf and involve an increase in the mEPSC amplitude and frequency and a decrease in the mEPSC decay time constant. My findings are similar to those of previous reports that show a developmental speeding of AMPA mEPSC kinetics (Das et al., 1998; Taschenberger and von Gersdorff, 2000; Brenowitz and Trussell, 2001; Wall et al., 2002).

Figure 3.1 Spontaneous synaptic activity in Mauthner cells. **A**:Differential interference contrast image of a M-cell in a hindbrain preparation. Arrow points to the cell body (*left panel*). The same M-cell as in "*the right panel*" filled with Lucifer Yellow (0.1%) during a typical experiment. Arrowhead points to the axon descending into the spinal cord. Scale bar: 15 μm in the *left panel* and the *middle panel*, and 30 μm in the *right panel*. **B**: Spontaneous activity in a M-cell recorded in normal extracellular saline solution. **C**: Miniature postsynaptic currents (mEPSCs) recorded in the presence of 1 μM TTX, 5 μM Strychnine, 100 μM picrotoxin and 50 μM APV. All mEPSCs were completely blocked after bath application of the non-NMDA receptor antagonist CNQX (10 μM). **D**: Individual mEPSCs were acquired (top) and averaged (bottom). Holding potential was -60 mV.

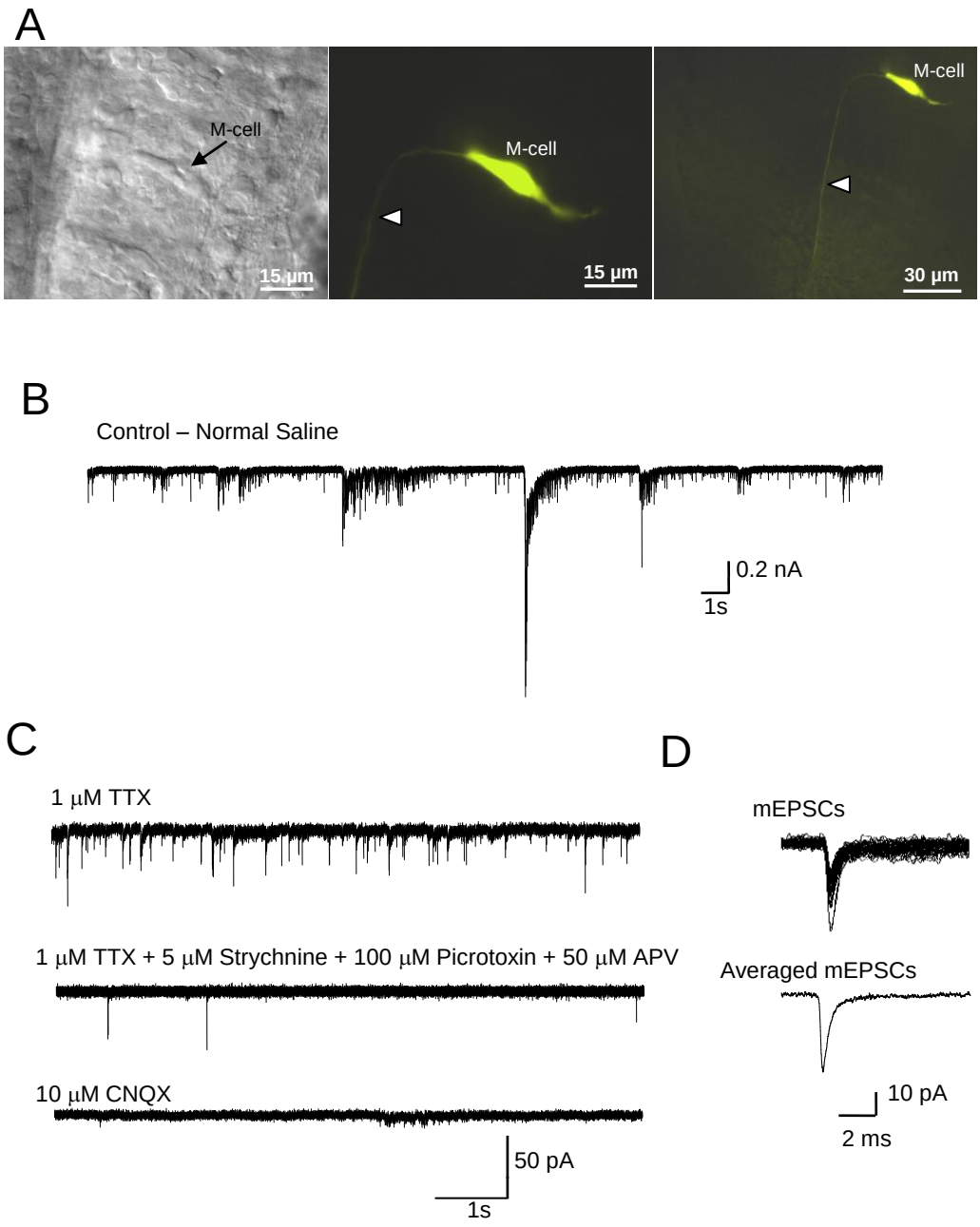
A
M-cell
15 µm
M-cell
15 µm
M-cell
30 µm
B
Control – Normal Saline
0.2 nA
1s
C
1 µM TTX
1 µM TTX + 5 µM Strychnine + 100 µM Picrotoxin + 50 µM APV
10 µM CNQX
50 pA
1s
D
mEPSCs
Averaged mEPSCs
10 pA
2 ms

Figure 3.2 Isolated non-NMDA mEPSCs from M-cells are properly space-clamped. Scatter plots of rise time vs. amplitude of events recorded from a 33 hpf preparation ($r=0.02$; $n=158$ events), 48 hpf preparation ($r<0.01$; $n=218$ events), and a 72 hpf preparation ($r=0.04$; $n=249$ events).

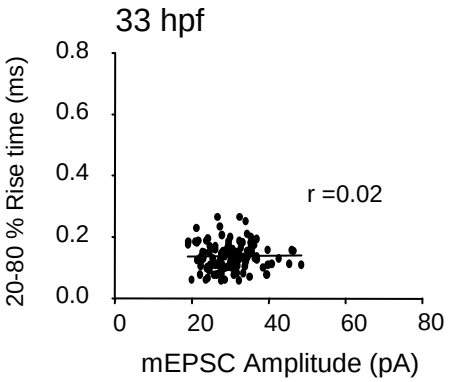
33 hpf
20-80 % Rise time (ms)
0.8
0.6
0.4
0.2
0.0
r =0.02
0
20
40
60
80
mEPSC Amplitude (pA)

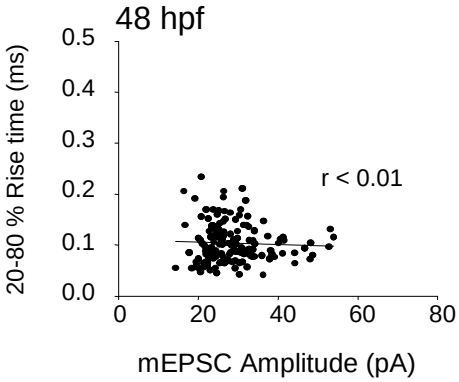
48 hpf
20-80 % Rise time (ms)
0.5
0.4
0.3
0.2
0.1
0.0
r < 0.01
0
20
40
60
80
mEPSC Amplitude (pA)

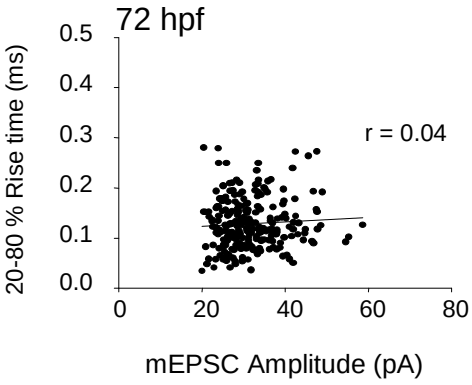
72 hpf
20-80 % Rise time (ms)
0.5
0.4
0.3
0.2
0.1
0.0
r = 0.04
0
20
40
60
80
mEPSC Amplitude (pA)

Figure 3.3 The mEPSC amplitude increases during development. **A**: Amplitude histogram of mEPSCs from a M-cell recorded at 33 hpf, 48 hpf and 72 hpf in the presence of 1 μM TTX, 5 μM Strychnine, 100 μM picrotoxin (binwidth = 2 pA; n=109 (33 hpf); n=278 (48 hpf); n=251 (72 hpf). **B**: Peak amplitude of non-NMDA mEPSCs recorded in the presence of 1 μM TTX, 5 μM Strychnine, and 100 μM picrotoxin. (33 hpf: 24 ± 2.0 pA, n=10; 48 hpf: 30 ± 2 pA, n=9 and 72 hpf: 30 ± 1 pA, n=8). * denotes significantly different from 33 hpf, $p < 0.05$.

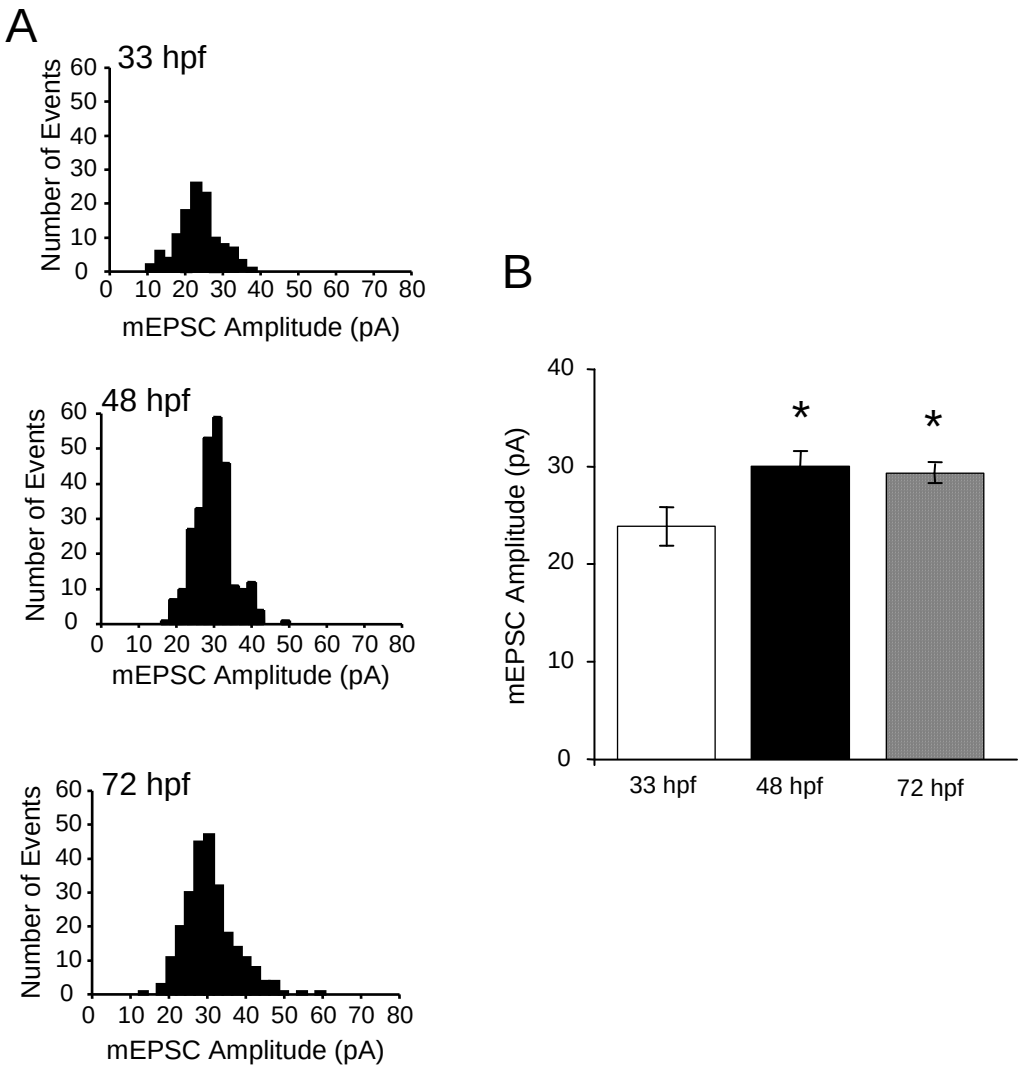
A
33 hpf
Number of Events
60
50
40
30
20
10
0
0 10 20 30 40 50 60 70 80
mEPSC Amplitude (pA)
48 hpf
Number of Events
60
50
40
30
20
10
0
0 10 20 30 40 50 60 70 80
mEPSC Amplitude (pA)
72 hpf
Number of Events
60
50
40
30
20
10
0
0 10 20 30 40 50 60 70 80
mEPSC Amplitude (pA)
B
mEPSC Amplitude (pA)
40
30
20
10
0
*
*
33 hpf
48 hpf
72 hpf

Figure 3.4 Developmental changes in the mEPSC frequency, rise time and decay kinetics of non-NMDA mEPSCs. **A**: Frequency bar graph of the mEPSCs recorded at different ages. **B**: 20-80 % rise time was 0.13 ± 0.02 at 33 hpf (n=10); 0.11 ± 0.01 at 48 hpf (n=9) and 0.11 ± 0.01 at 72 hpf (n=8). **C**: Bar graph of the decay time constant which was fitted with a single exponential function. τ was 0.75 ± 0.09 at 33 hpf (n=10), 0.50 ± 0.03 at 48 hpf (n=9) and 0.49 ± 0.03 at 72 hpf (n=8). **D**: Superimposed averaged mEPSC at 33 hpf, 48 hpf and 72 hpf. Note the slower decay at 33 hpf. * denotes significantly different from 33 hpf $p < 0.05$. ** denotes significantly different from 33 hpf $p < 0.01$.

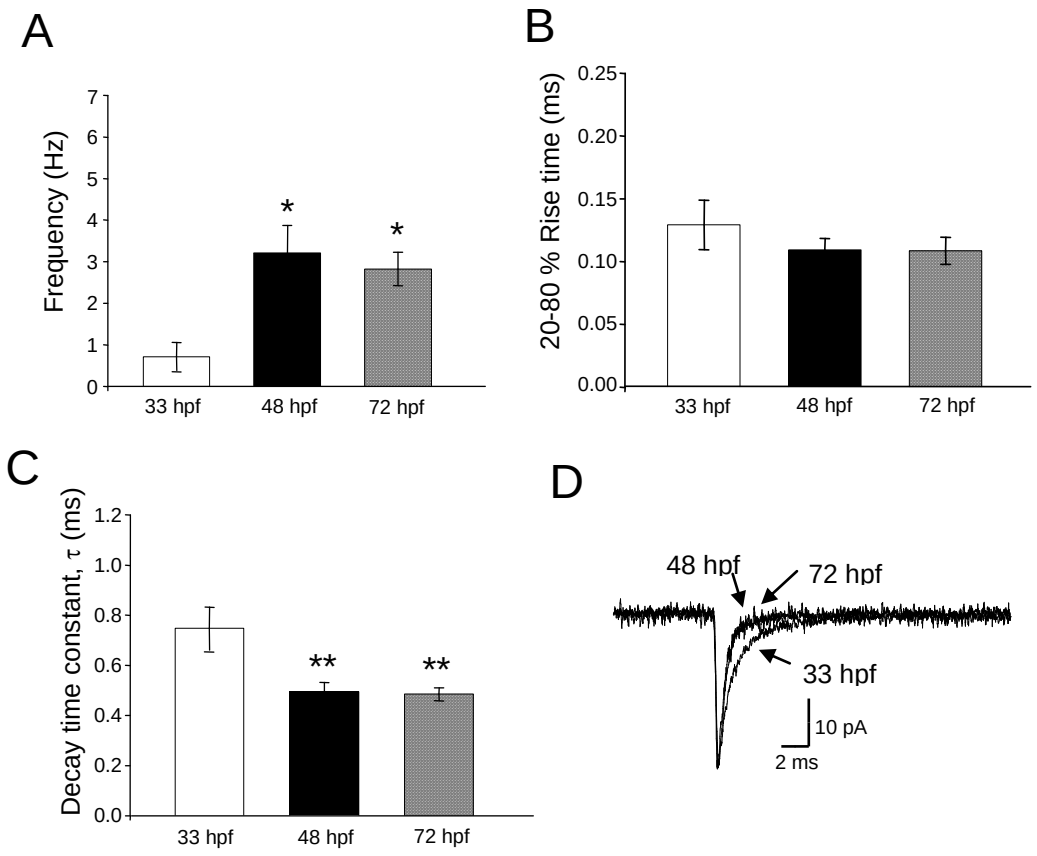
A
Frequency (Hz)
0
1
2
3
4
5
6
7
*
*
33 hpf
48 hpf
72 hpf
B
20-80 % Rise time (ms)
0.00
0.05
0.10
0.15
0.20
0.25
33 hpf
48 hpf
72 hpf
C
Decay time constant, τ (ms)
0.0
0.2
0.4
0.6
0.8
1.0
1.2
**
**
33 hpf
48 hpf
72 hpf
D
48 hpf
72 hpf
33 hpf
10 pA
2 ms

Figure 3.5 Non-NMDA mEPSCs are mediated by AMPA. **A**: mEPSCs recorded in the presence of 1 μM TTX, 5 μM Strychnine, and 100 μM picrotoxin. All mEPSCs were completely blocked after bath application of the specific AMPAR antagonist, GYKI (50 μM) and reappeared after washout of GYKI. **B**: Frequency bar graph of the miniature events recorded at 33 hpf and 48 hpf in the absence (Control; □) and presence (■) of the kainate desensitizing agent, SYM (10 μM). **C**: mEPSC peak amplitude recorded in the absence (□) and presence (■) of 10 μM SYM at 33 hpf (n=3), 48 hpf (n=5) and 72 hpf (n=4). **D**: 20-80% rise time bar graph of the miniature events recorded in the absence (□) and presence (■) of 10 μM SYM at 33 hpf (n=3), 48 hpf (n=5) and 72 hpf (n=4). **E**: Bar graph of the decay time constant, τ, at 33 hpf (n= 3), 48 hpf (n=5) and 72 hpf (n=4) recorded in the absence (□) and presence (■) of 10 μM SYM.

.

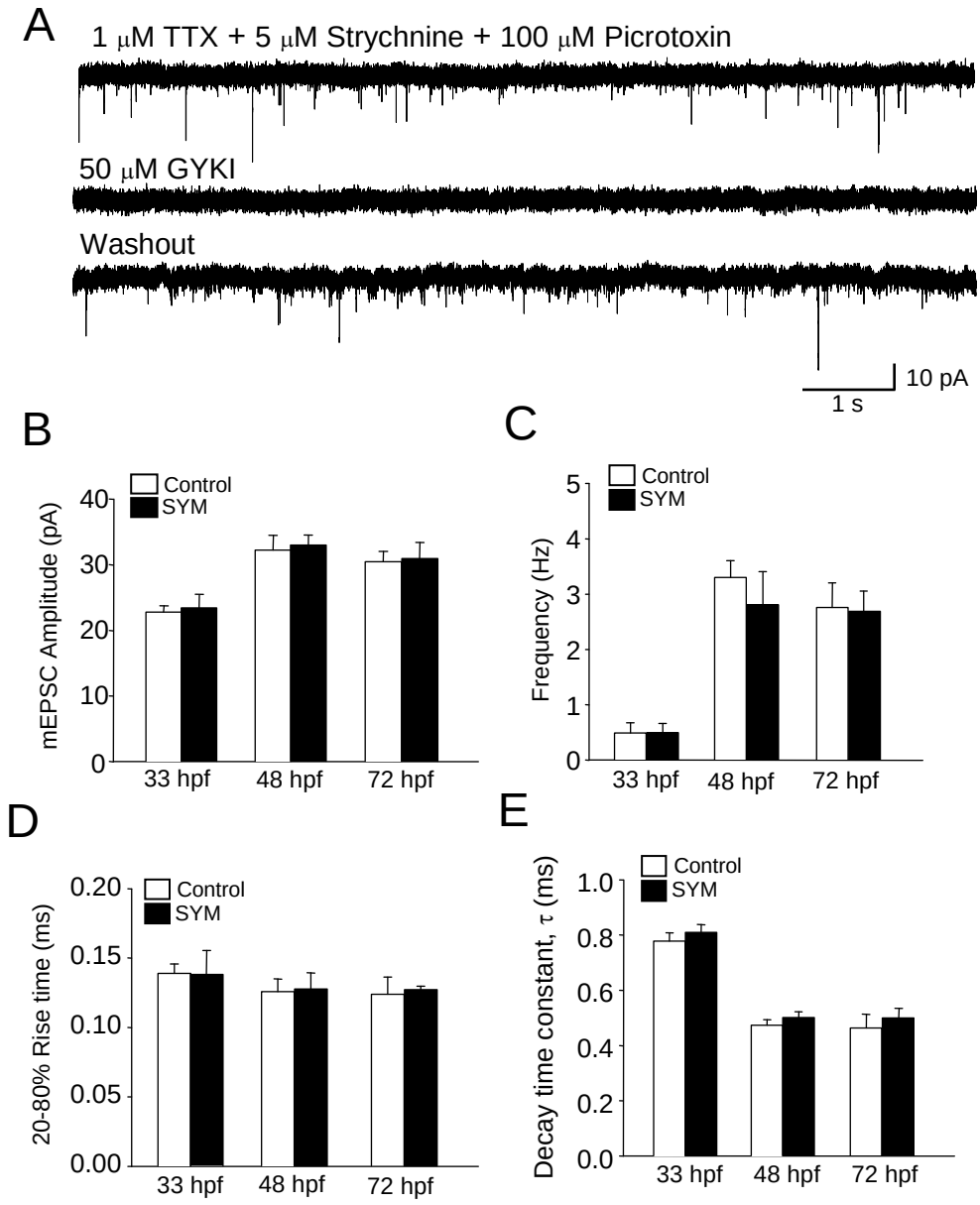
A
1 μM TTX + 5 μM Strychnine + 100 μM Picrotoxin
50 μM GYKI
Washout
10 pA
1 s
B
mEPSC Amplitude (pA)
Control
SYM
33 hpf
48 hpf
72 hpf
C
Frequency (Hz)
D
20-80% Rise time (ms)
E
Decay time constant, τ (ms)

Chapter 4 [†]MECHANISMS UNDERLYING THE DEVELOPMENTAL CHANGES IN AMPA RECEPTOR PROPERTIES

4.1 Introduction

The time course of AMPA-EPSC becomes faster during development and this has been shown to be a crucial determinant for information processing in the CNS (Cathala et al., 2005). However, the factors underlying the developmental speeding of AMPAR kinetics are still poorly understood. The time course of synaptic currents depends upon factors such as receptor affinity (Sucher et al., 1995), desensitization (Sucher et al., 1995), glutamate dynamics in the synaptic cleft (e.g. release, clearance) and synaptic morphology (Cathala et al., 2003). For AMPAR-mediated currents, there are at least two mechanisms that underlie the developmental speeding of the time course of the currents. The first postulates that there is a change in receptor subunit composition (Das et al., 1998; Lawrence and Trussell, 2000), while the second proposes that there is a change in synaptic morphology (Cathala et al., 2003). In Chapter 3, I showed that there is a developmental speeding in AMPAR kinetics in zebrafish that occurs between 33 hpf and 48 hpf. However, the underlying mechanism for this developmental speeding remains unknown.

[†] A version of this chapter has been published: Patten and Ali 2007. *Journal of Physiology*, 581(Pt 3):1043-56.

Therefore, I have undertaken this study to investigate the mechanism underlying the developmental changes observed in AMPAR-mediated mEPSC kinetics in zebrafish M-cells, between 33 hpf and 48 hpf. The hypothesis is that the developmental changes in AMPAR properties may be due to a switch in AMPAR subunits or due to changes in the synaptic morphology. To test the hypothesis, I investigated: (1) any alterations in the glutamate transients in the synaptic cleft between 33 hpf and 48 hpf as an indicative of changes in synaptic morphology and (2) changes in AMPAR-mEPSC properties that are dependent of AMPAR subunit composition.

4.2 Results

4.2.1 Effect of glutamate uptake in shaping the mEPSC

During development, the time course of glutamate in the synaptic cleft changes due to changes in synaptic morphology (Lee and Sheng, 2000). These changes have been shown to lead to increased glutamate clearance from the cleft (Otis et al., 1996; Otis and Trussell, 1996; Diamond and Jahr, 1997) in more mature animals, which might lead to a faster mEPSC decay time constant. Therefore, I first examined if the developmental changes in the mEPSC kinetics are due to a change in the glutamate transient in the cleft during development. I recorded AMPAR-mEPSCs in the presence and absence of the glutamate transporter blocker DL-TBOA, reasoning that the uptake of glutamate would play a greater role in older animals. I found that DL-TBOA did not affect the

mEPSC amplitude (Figure 4.1A), rise time (Figure 4.1C) and decay time constant (Figure 4.1D) ($p > 0.05$) at either 33 or 48 hpf. The lack of effect of DL-TBOA indicates that glutamate uptake does not play a major role in shaping the AMPAR-mESPC in developing zebrafish.

Developmental changes in AMPAR-mEPSC kinetics might be due to an increased concentration of glutamate in the synaptic cleft. Kynurenic acid (KYN) is a glutamate receptor antagonist and can be used to detect changes in the glutamate concentration in the synaptic cleft (Diamond and Jahr, 1997; Yamashita et al., 2003). For instance, the effect of KYN would be weaker if the glutamate concentration in the synaptic cleft is higher. Application of KYN resulted in a reduction in the mEPSC peak amplitude (Figure 4.2A-C) at both 33 hpf and 48 hpf, however the reductions were similar at both ages (Figure 4.2D; $p > 0.05$). KYN caused neither a change in the rise time (Figure 4.2E) nor in the decay time constant (Figure 4.2F) ($p > 0.05$). These data suggest that the glutamate concentration in the synaptic cleft does not change between 33 hpf and 48 hpf and therefore probably does not contribute to the observed developmental changes in the AMPAR-mEPSC kinetics.

4.2.2 Voltage dependence of AMPAR-mediated mEPSCs

The results indicate that changes in the time course of glutamate do not contribute to the changes in AMPAR-mEPSC kinetics during M-cell

maturation. So, I next investigated whether the developmental changes in the AMPAR-mEPSC kinetics are due to alterations in the postsynaptic receptor properties. Because the I/V relationship of AMPARs is known to be subunit dependent (Geiger et al., 1995; Sah and Lopez De Armentia, 2003), I examined the voltage dependence of the mEPSCs by varying the membrane holding potential in steps of 20 mV increments from -80 mV to +80 mV. In order to analyze the current-voltage (I-V) relationship quantitatively, I averaged isolated AMPAR-mEPSCs occurring during 30-60 s periods (n=4-9) at each holding potential and plotted the peak amplitude of each averaged mEPSC against the holding potential (Figure 4.3A, B). I found that the I-V relationship at 33 hpf was linear (Figure 4.3A) while at 48 hpf, it displayed outward rectification. Notably, I found that the time course of the decay phase of the mEPSC was voltage dependent, with a slower decay at more positive potentials. When cells were depolarized from -60 mV to +80 mV, the 33 hpf decay time constant increased by 20 ± 3 % (n=4), while the 48 hpf decay time constant increased by 55 ± 5% (Figure 4.4A,B; n=4, p=0.004). The difference in the % increase in τ with depolarization suggests that the receptors themselves may be different. To confirm that the EPSC decay kinetics were not affected by dendritic filtering when the cells were clamped at positive potentials. I analyzed the change in rise time with depolarization at both age groups. The mEPSC rise time did not change in depolarized cells at

either age (Figure 4.4C), suggesting that at positive potentials the M-cells were indeed properly clamped.

4.2.3 Estimates of synaptic channel conductance

Because the data suggested that the receptors at the two ages may indeed be different, I determined the single channel conductance of the AMPARs at 33 hpf and 48 hpf. In order to do this, I performed NSFA on AMPAR-mEPSCs. Estimates of AMPAR unitary conductance (γ) and numbers of active channels (N) can be obtained from analyses of miniature synaptic events, which examine the variance of fluctuations in the decay phase of synaptic events (Traynelis et al., 1993; Benke et al., 1998). This analysis is based on the assumption that the opening and closing of individual channel are independent events. Thus, the event-to-event fluctuations in synaptic currents will be smallest at the peak and end portion of the event and largest during the decay phase, as determined by single channel conductance and the number of functional channels. Variance - current plots were constructed at both ages and estimates of γ and N were derived from fitted functions (see Chapter 2). I found a significant difference in γ between the two ages (33 hpf: 9.6 ± 0.52 pS and 48 hpf: 15.2 ± 1.17; n=6; p=0.002; Figure 4.5) suggesting that the AMPARs at 33 hpf and at 48 hpf are truly different. There was no significant change in the mean number of active channels at a synapse during development. Specifically, I found that at 33 hpf the number of

active channels was 28 ± 2 and at 48 hpf, it was 33 ± 5 (n=5 at 33 hpf and n=6 at 48 hpf; p=0.38; Figure 4.5D).

4.2.4 Cyclothiazide modulation of AMPAR-mEPSCs kinetics

I then examined the effect of cyclothiazide (CTZ) on AMPA mEPSCs. CTZ suppresses the desensitization of AMPA receptors (Partin et al., 1993; Lise et al., 2006), but does so to a greater degree on the flip splice variants and on heteromeric receptors (Partin et al., 1994; Cotton and Partin, 2000). Therefore, differential effects of CTZ imply the presence of different subunits. I used a low concentration (10 μM) of CTZ to discern between flip and flop forms of the subunits (Partin et al., 1994; Cathala et al., 2003). CTZ had no effect on the mEPSC frequency, amplitude or rise time ($p > 0.05$; Figure 4.6C); however, the decay time at both ages was significantly increased (33 hpf, p=0.011; 48 hpf p=0.012). Importantly, CTZ showed a stronger potentiation of the decay time constant in the older animals (a 4 fold increase in τ at 48 hpf) compared with the younger ones (1.5 fold increase in τ at 33 hpf; Figure 4.6D; p=0.025). These observations suggest that AMPARs at 33 hpf are composed of subunits that are different from those at 48 hpf.

4.2.5 Pharmacological analysis of the GluR2-containing and GluR2-lacking AMPARs

To determine the subunit composition of the AMPARs between 33 hpf and 48 hpf, I tested the ability of the GluR2 blocker, pentobarbital (PB), and the non-GluR2 blocker, NASPM, to block mEPSC amplitude. Pentobarbital (100 μM) blocked 64 ± 3% (n = 5) of the mEPSC amplitude in 33 hpf embryos, and had a significantly greater effect on the amplitude in 48 hpf fish (79 ± 4%; n= 6, $p<0.001$ at 48 hpf (Figure 4.7), indicating that the population of AMPARs at 48 hpf contained a greater proportion of GluR2-containing receptors compared with the existing population. Application of the non-GluR2 blocker, NASPM (10 μM), gave complementary results and blocked the mEPSC amplitude by 32 ± 3 % (n= 5) at 33 hpf and by 13 ± 3% at 48 hpf (n=5; Figure 4.7).

4.3 Summary

The present results suggest that the developmental changes in the properties of AMPAR-mediated mEPSCs are not due to an alteration in the glutamate transient in the synaptic cleft but rather due to the expression of different receptor subtypes. The results also suggest that the AMPARs at the ages examined contain at least one GluR2 subunit, but that the overall receptor subunit assembly changes between 33 and 48 hpf to contain more GluR2 subunits.

Figure 4.1 Glutamate uptake inhibitor DL-TBOA has no effect on AMPAR-mEPSC. Events recorded in the presence of DL-TBOA were normalized to their controls recorded in the absence of DL-TBOA. **A**: Bar graph showing the effect of DL-TBOA (100 μM) on mEPSC frequency at 33 hpf (n=5; □) and 48 hpf (n=5; ■). **B**: mEPSC peak amplitude in the presence of DL-TBOA (100 μM) on the frequency at 33 hpf (n=5; □) and 48 hpf (n=5; ■) **C**: Bar graph showing the effect of DL-TBOA (100 μM) on the 20 – 80% rise time at 33 hpf (n=5; □) and 48 hpf (n=5; ■). **D**: Bar graph showing the effect of DL-TBOA (100 μM) on the decay time constant, τ, at 33 hpf (n=5; □) and 48 hpf (n=5; ■). **E**: Average mEPSCs recorded at 48 hpf under control conditions (*left trace*) and in the presence of 100 μM DL-TBOA (*middle trace*). The waveforms of superimposed normalized responses shown on the right are identical.

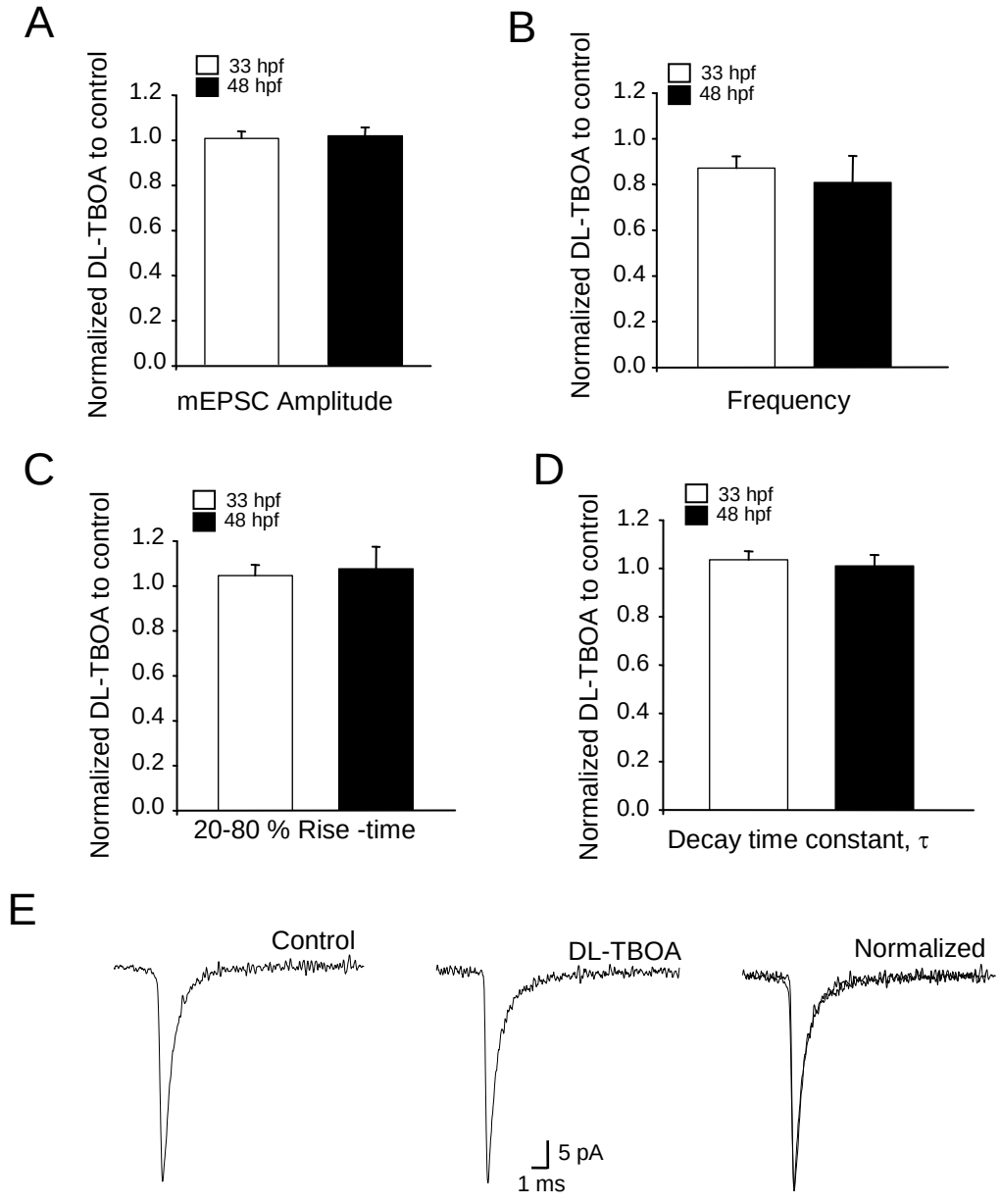
A
33 hpf
48 hpf
Normalized DL-TBOA to control
1.2
1.0
0.8
0.6
0.4
0.2
0.0
mEPSC Amplitude
B
33 hpf
48 hpf
Normalized DL-TBOA to control
1.2
1.0
0.8
0.6
0.4
0.2
0.0
Frequency
C
33 hpf
48 hpf
Normalized DL-TBOA to control
1.2
1.0
0.8
0.6
0.4
0.2
0.0
20-80 % Rise -time
D
33 hpf
48 hpf
Normalized DL-TBOA to control
1.2
1.0
0.8
0.6
0.4
0.2
0.0
Decay time constant, τ
E
Control
DL-TBOA
Normalized
5 pA
1 ms

Figure 4.2 Effect of the glutamate receptor antagonist kynurenic acid (KYN) on AMPAR-mEPSC. **A**: Superimposed (top) and normalized (bottom) mEPSCs recorded from 33 hpf M-cells in the absence and presence of 50 μM KYN (n=4) **B**: Superimposed (top) and normalized (bottom) mEPSCs recorded from 48 hpf M-cells in the absence (control) and presence of 50 μM KYN (n=5). **C**: mEPSC peak amplitude recorded in the absence (control, □) and presence (■) of 50 μM KYN at 33 hpf (n=4) and 48 hpf (n=5). **D**: Bar graph showing percentage inhibition of peak amplitude induced by 50 μM KYN at 33 hpf and 48 hpf. **E**: 20-80 % rise time bar graph of the mEPSCs recorded in the absence (control, □) and presence (■) of 50 μM KYN at 33 hpf (n=4) and 48 hpf (n=5) **F**: Bar graph of the decay time constant, τ at 33 hpf (n= 4) and 48 hpf (n=5) recorded in the absence (control, □) and presence (■) of 50 μM KYN. * denotes significantly different from control, $p< 0.05$.

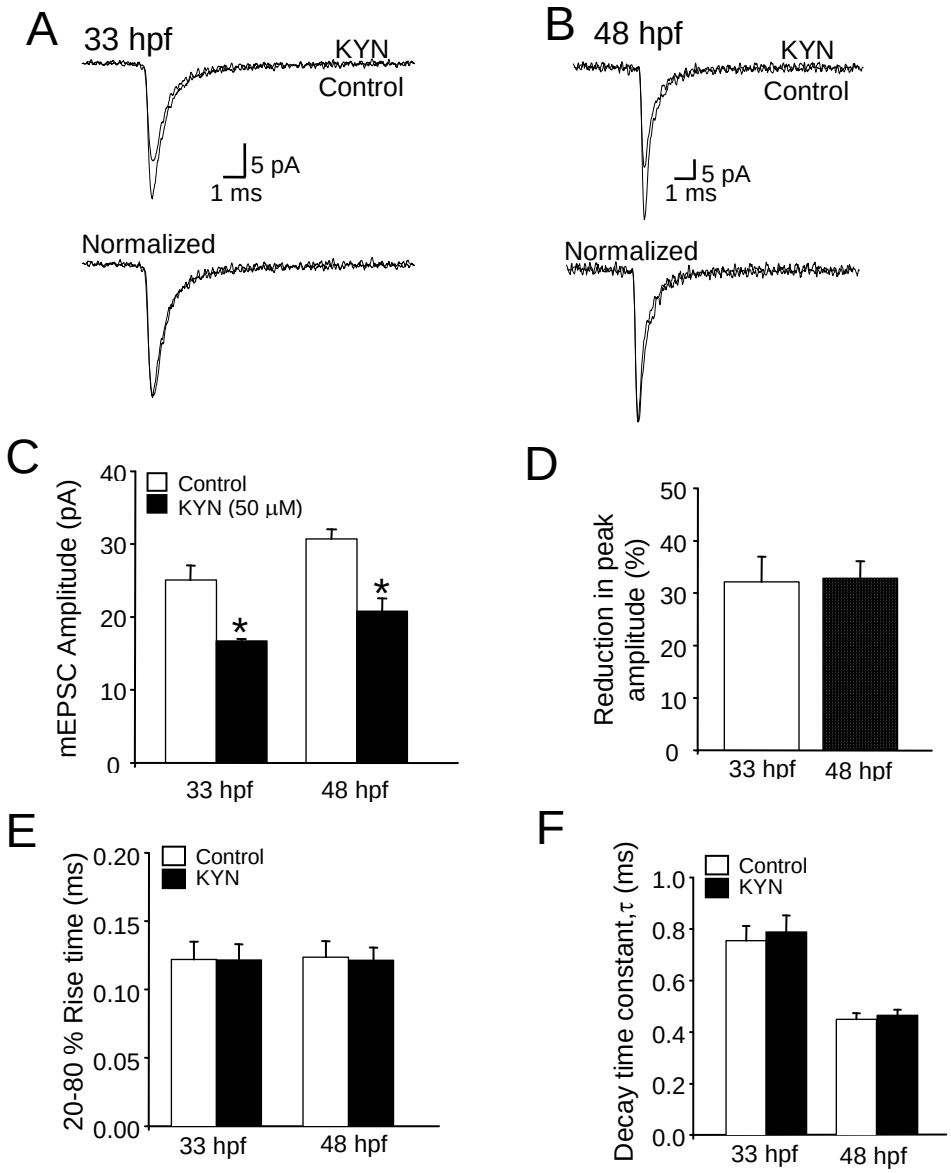
A
33 hpf
KYN
Control
5 pA
1 ms
Normalized
B
48 hpf
KYN
Control
5 pA
1 ms
Normalized
C
mEPSC Amplitude (pA)
Control
KYN (50 μM)
33 hpf
48 hpf
D
Reduction in peak amplitude (%)
33 hpf
48 hpf
E
20-80 % Rise time (ms)
Control
KYN
33 hpf
48 hpf
F
Decay time constant,τ (ms)
Control
KYN
33 hpf
48 hpf

Figure 4.3 Voltage dependence of AMPAR-mEPSC. All events were recorded in the presence of strychnine (5 μM), picrotoxin (100 μM), APV (50 μM) and TTX (1 μM) to isolate AMPA mEPSCs at all holding potentials. **A**: I-V relationship of averaged mEPSCs at 33 hpf (n=4-10) at different holding potentials ranging from -80 mV to +80 mV in 20 mV increments; *right* I/V plot of pooled data was linear **B**: Averaged mEPSC I-V relationship at 48 hpf (n=4-9); *right* I/V plot of pooled data at different holding potentials from -80 mV to +80 mV, was outwardly rectified. AMPA mEPSCs at +20 mV in 48 hpf fish are omitted because they were small in amplitude and were difficult to isolate above background noise.

A

33 hpf

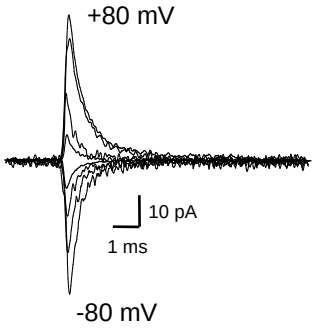

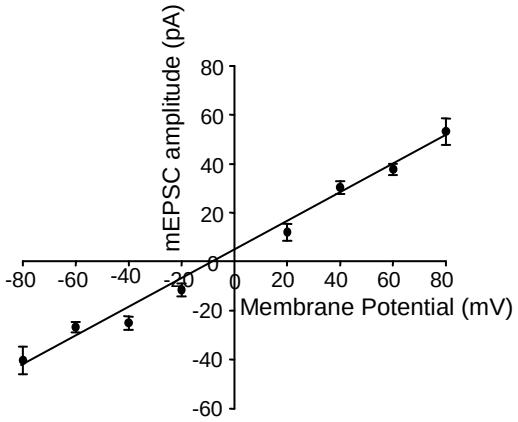

B

48 hpf

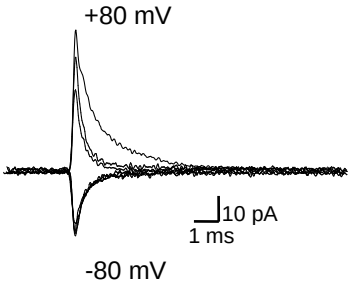

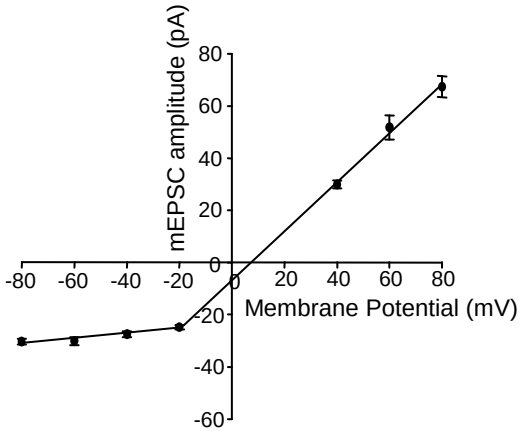

Figure 4.4 Voltage dependence of AMPAR-mEPSC decay time constant. **A**: Plot of mEPSC decay time constant at -60 mV and +80 mV at 33 hpf (n=4, open circle and solid line) and at 48 hpf (n=4, filled circle and broken line). **B**: Bar graph showing the % change in τ from -60 mV to +80 mV. **C**: Plot of 20-80 % rise time at -60 mV and +80 mV. * Denotes significance at $p<0.05$ and ** denotes significance at $p < 0.01$.

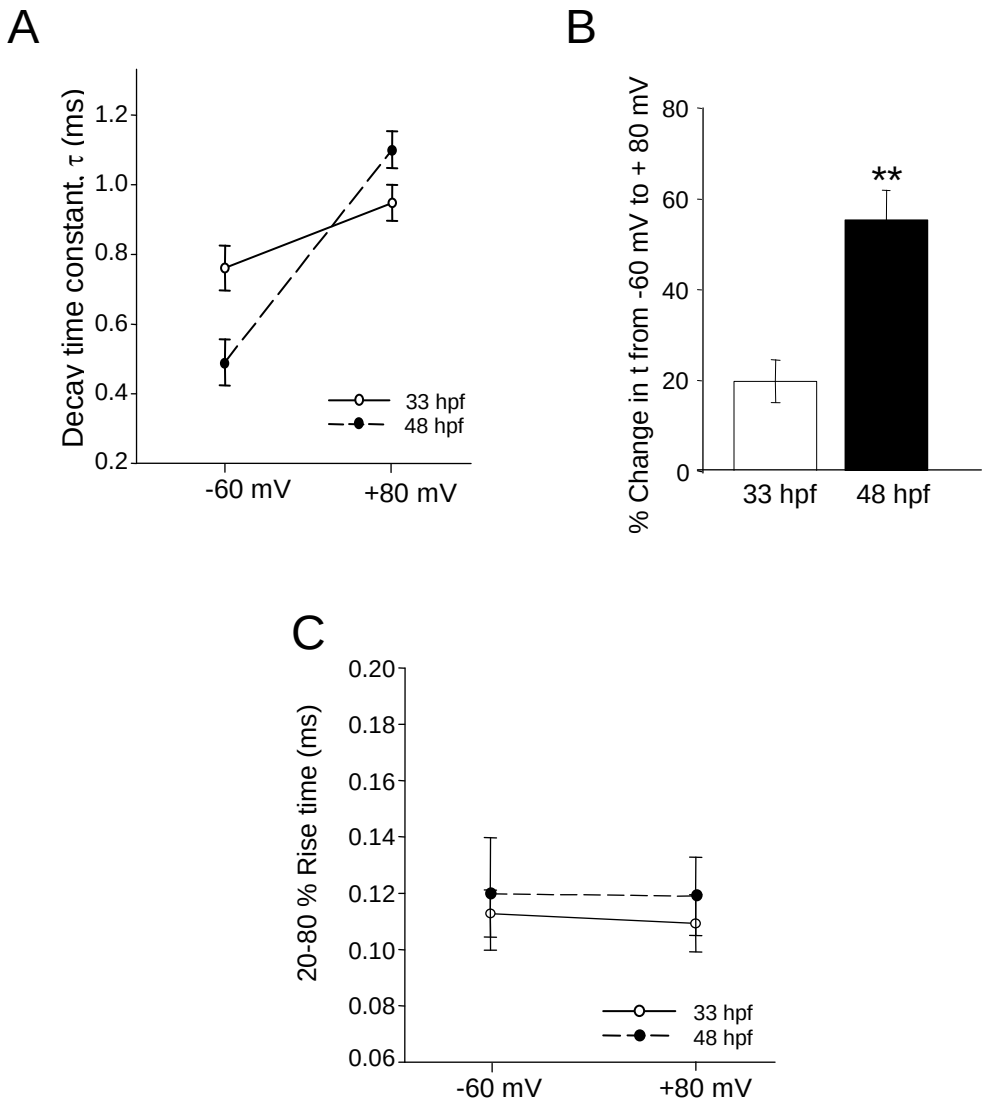
A
Decav time constant. τ (ms)
1.2
1.0
0.8
0.6
0.4
0.2
-60 mV
+80 mV
33 hpf
48 hpf
B
% Change in t from -60 mV to + 80 mV
80
60
40
20
0
**
33 hpf
48 hpf
C
20-80 % Rise time (ms)
0.20
0.18
0.16
0.14
0.12
0.10
0.08
0.06
-60 mV
+80 mV
33 hpf
48 hpf

Figure 4.5 Estimates of synaptic conductance and the number of available AMPARs underlying mEPSCs. **A**: Plot of variance versus mean current amplitude of mEPSCs at 33 hpf. B: Plot of variance versus mean current amplitude of mEPSCs at 48 hpf. The line (**A, B**) indicates the fit to the initial portion of the plot to the theoretical equation (see methods) and it gives an estimate of the elementary current (i) generated by the activation of one receptor. The conductance (γ) was calculated from the eq. $\gamma = i/ V_H$ (V_H = -60 mV). In the experiments shown, γ= 9.4 pS at 33 and 15.9 pS at 48 hpf. **C**: Bar graph of the conductance at 33 hpf (9.6 ± 0.5 pS, n=5) and 48 hpf (15.2 ± 1.2 pS, n= 6). **D**: Bar graph of the number of the available AMPARs, N, at 33 hpf (27 ± 2) and 48 hpf (33 ± 5). * Denotes significance at $p < 0.05$ and ** denotes significance at $p < 0.01$.

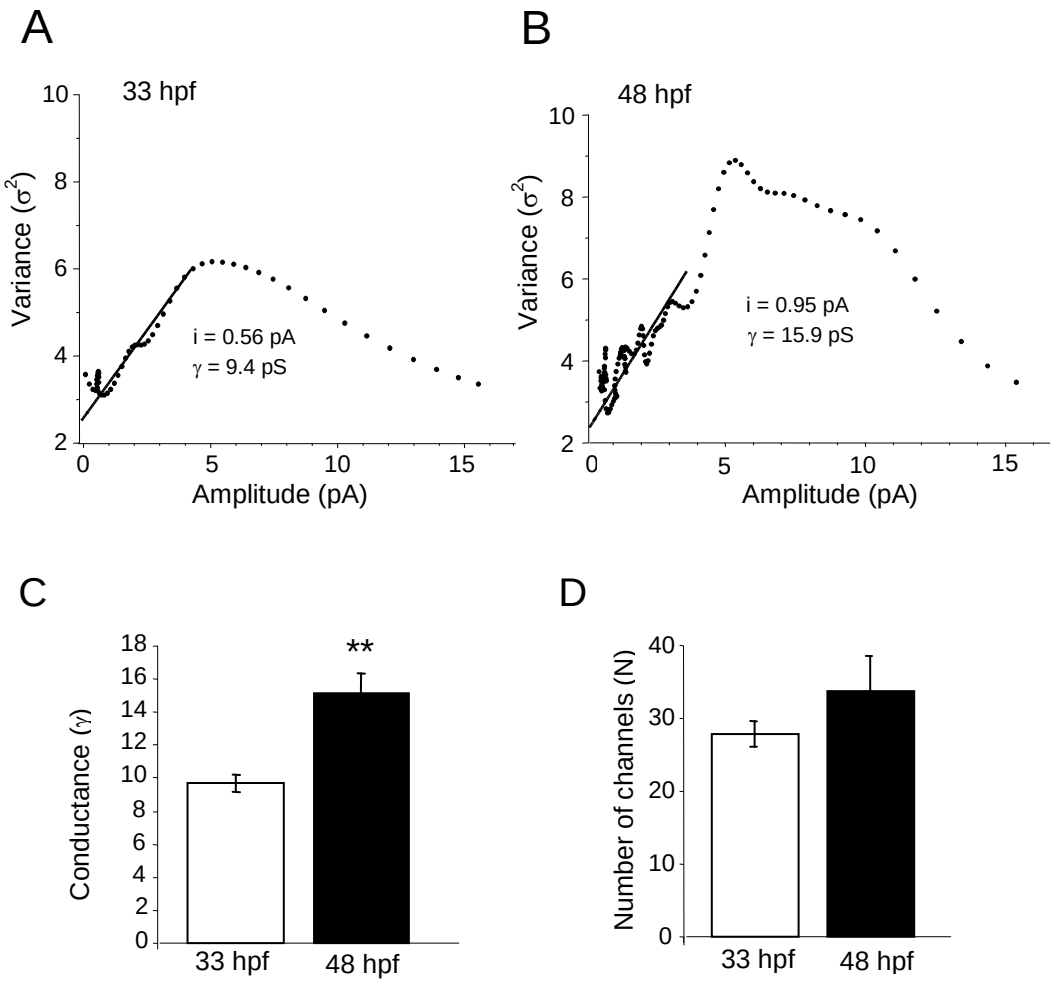
A
33 hpf
Variance (σ²)
Amplitude (pA)
i = 0.56 pA
γ = 9.4 pS
B
48 hpf
Variance (σ²)
Amplitude (pA)
i = 0.95 pA
γ = 15.9 pS
C
Conductance (γ)
**
33 hpf
48 hpf
D
Number of channels (N)
33 hpf
48 hpf

Figure 4.6 Effects of CTZ on AMPAR-mEPSCs. **A**: Average mEPSCs recorded from 33 hpf M-cells in the absence (control) and presence of 10 μM CTZ (n=3, V_H= -60 mV). **B**: Average mEPSCs recorded from 48 hpf M-cells in the absence (control) and presence of 10 μM CTZ (n=4). Events recorded in the presence of CTZ were normalized to their controls recorded in the absence of CTZ. **C**: Bar graphs showing the effect of CTZ on the frequency, peak amplitude and 20−80% rise time at 33 hpf (□) and 48 hpf (■). **D**: The decay time constant (τ) of averaged mEPSCs at 33 hpf and 48 hpf in the presence of 10 μM CTZ. **E**: Bar graph showing of mEPSCs recorded in 10 μM CTZ normalized to control mEPSCs recorded in the absence of CTZ, illustrating the effect of CTZ on the decay time constant of the mEPSCs at 33 hpf and 48 hpf. *denotes significantly different from the age group 33 hpf $p < 0.05$. # denotes significantly different from control $p < 0.05$.

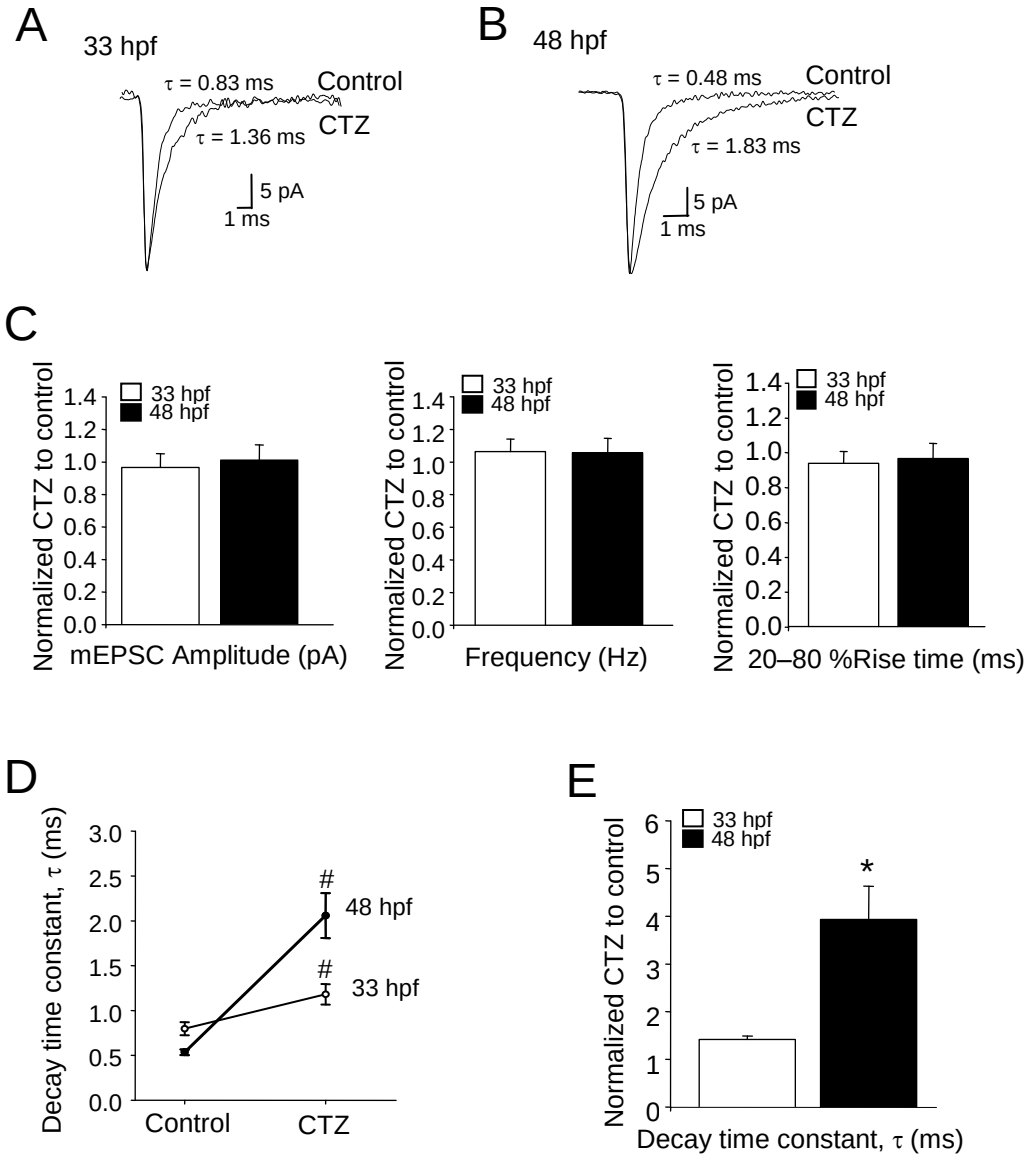
A
33 hpf
τ = 0.83 ms
Control
CTZ
τ = 1.36 ms
5 pA
1 ms
B
48 hpf
τ = 0.48 ms
Control
CTZ
τ = 1.83 ms
5 pA
1 ms
C
Normalized CTZ to control
33 hpf
48 hpf
mEPSC Amplitude (pA)
Frequency (Hz)
20–80 %Rise time (ms)
D
Decay time constant, τ (ms)
48 hpf
33 hpf
Control
CTZ
E
Normalized CTZ to control
Decay time constant, τ (ms)

Figure 4.7 Developmental increases in GluR2 containing AMPARs. Application of the GluR2 blocker, pentobarbital (PB, 100 μM) has a significantly greater effect on mEPSC amplitude at 48 hpf ($p<0.001$). The non-GluR2 blocker, NASPM (10 μM) had a significantly smaller effect on mEPSC amplitude at 48 hpf ($n=5$; $p < 0.001$). *** Significantly different, $p < 0.001$.

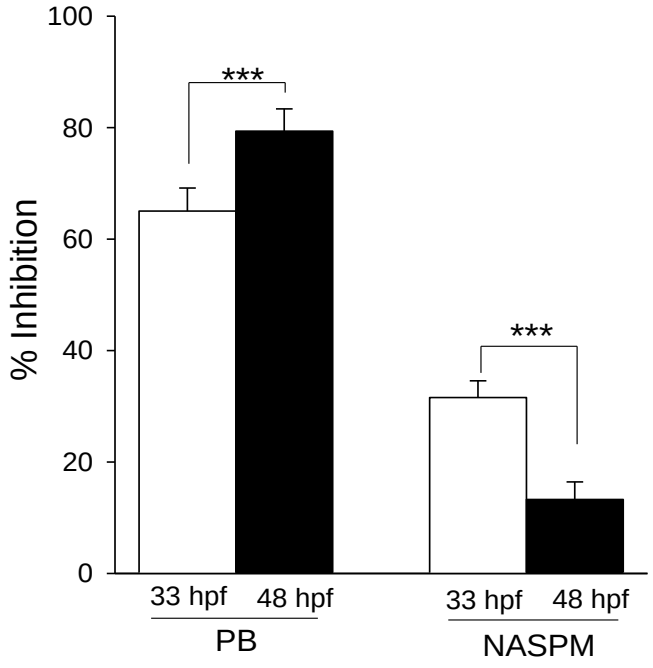
100
80
60
40
20
0
% Inhibition
***
***
33 hpf
48 hpf
33 hpf
48 hpf
PB
NASPM

Chapter 5 ‡MODULATION OF AMPA RECEPTOR ACTIVITY BY PKCγ

5.1 Introduction

Modulation of synaptic transmission plays a crucial role in the development of the nervous system, learning and memory, and pathological states (Bliss and Collingridge, 1993). Protein kinases are well-known to alter the strength of synaptic transmission (Smart, 1997). At excitatory synapses, they modulate synaptic transmission by controlling the function of glutamate receptors. PKA, PKC, CAMKII and tyrosine kinases have all been shown to modulate the function of AMPAR at mature synapses. For instance, phosphorylation of GluR1 by PKA and CaMKII has been shown to enhance synaptic responses (Fang et al., 2003; Lee et al., 2003). Activators of PKC have been shown to potentiate AMPA currents by altering AMPAR channel conductances or by increasing AMPAR surface expression (Daw et al., 2000; Ling et al., 2006; Rial Verde et al., 2006; Tavalin, 2008; Yao et al., 2008). Protein phosphorylation can also affect the speeding of the decay time constant of AMPARs. However, much less is known regarding the modulation of AMPARs by protein kinases at developing synapses.

‡ A version of this chapter has been published: Patten and Ali 2009. *Proceedings of the National Academy of Sciences of the United States of America*,106 (16):6796-801

It was previously shown that zebrafish Mauthner cells express relatively high levels of PKC from early developmental stages (Slatter et al., 2005; Patten et al., 2007). Therefore, I investigated whether PKC might modulate AMPAR function in embryonic zebrafish. The hypothesis is that activation of PKC will affect AMPAR-mediated synaptic activity.

5.2 Results

5.2.1 Effects of PKC activators on AMPA mEPSCs

To determine whether activation of PKC resulted in modulation of AMPAR activity in embryonic (2 dpf) zebrafish, I recorded AMPA mEPSCs in the presence of the PKC activator PMA and found that both the amplitude and frequency increased significantly over control levels (amplitude, from 32.0 ± 1.5 to 54.1 ± 3.3 pA; frequency, from 2.6 ± 1.2 to 8.5 ± 1.0 Hz; $n=7$, $p < 0.001$) (Figure 5.1). There was a shift towards higher amplitude events (Figure 5.1C), but the kinetics of the AMPA currents were not affected (Figure 5.2A). To confirm that PMA activated PKC, I included the specific PKC blocker, BIS I in the pipette, which prevented the increase in amplitude ($n=6$, $p=0.676$), but which had no effect on the frequency ($n=6$, $p < 0.001$) (Figure 5.1A,C). These results were consistent with a presynaptic effect of PMA on mEPSC frequency, and a postsynaptic effect on amplitude. To make sure that the observed enhancement of mEPSC amplitude was not due to a decrease in dendritic filtering, I examined the correlation between mEPSC rise time and

amplitude (Figure 5.2B). The lack of correlation between mEPSC rise time and amplitude suggests that the potentiation of AMPA currents after application of PMA is not due to alterations in dendritic filtering.

To confirm the signalling cascade associated with PKC activation, I activated the PKC signalling pathway through an alternative way via the use of the DAG analog, DOG. Application of DOG resulted in an increase in mEPSC amplitude (from 29.1 ± 1.3 to 42.9 ± 2.2 pA) and frequency (from 3.2 ± 0.3 to 8.3 ± 0.8 Hz) (n=5, $p < 0.001$) (Figure 5.3A), but there was no effect on mEPSC kinetics (Figure 5.3B).

5.2.2 The increase in mEPSC amplitude by PKC is Ca^{2+}-dependent

I next investigated whether the effects of PKC on AMPA mEPSCs were Ca^{2+}-dependent. Intracellular application of the calcium-chelating agent 1,2-bis(2-aminophenoxy)ethane-*N*,*N*,*N*′,*N*′-tetra-acetic acid (BAPTA), blocked the effect of PMA (Figure 5.4A) and DOG (Figure 5.4B) on amplitude (n=6 and n=5, respectively, p=0.783 and p=0.864, respectively), but not frequency. These results suggest that activation of a DAG and Ca^{2+}-dependent PKC isoform may be necessary for the increase in AMPA mEPSC amplitude and therefore implicated a conventional PKC isoform in the effect.

I then sought to investigate which conventional PKC isoform might be responsible for mediating the increase in mEPSC amplitude. I performed immunohistochemistry on whole larvae with antibodies directed against PKCα, βII, and γ, and used the anti-3A10 antibody, a neurofilament marker that identifies M-cells, as a positive control. The results indicated that M-cells express PKCγ, but not PKCα or βII (n=5) (Figure 5.5A). Because all of the antibodies produced against PKC were generated in rabbits against either human, mouse or rat isoforms of the enzyme (Santa Cruz), therefore, to be confident that the antibodies were detecting PKC in zebrafish, I confirmed the specificity of the antibodies by performing SDS PAGE and immunoblots of zebrafish CNS. All negative controls were performed by preabsorbing the primary antibody with a peptide corresponding to the antigenic site on the PKC isoform of interest. This mixture was then used as the primary antibody to detect PKC. Immunoblots of CNS tissue with anti-PKCα and anti-PKCγ resulted in single protein bands (Figure 5.5B). No protein bands were ever detected in any of the preabsorption controls (immunoblots performed in the presence of the blocking peptide). Immunoblotting of CNS tissue with anti-PKC βII did not show protein bands and this finding is supported by the fact that PKCβII is not localized to any neurons or regions in the zebrafish CNS (Patten et al., 2007). However, positive anti-PKC βII staining was associated with muscle tissue (Patten et al., 2007), suggesting that the anti-PKC βII antibody did work on zebrafish tissue. Anti-PKCα detected

one protein band approximately 78–80 kDa in size (n=4) and anti-PKCγ detected a 70–72 kDa protein (n=5) which are identical in size to the mammalian isoforms (Parker et al., 1986; Ohanian et al., 1996).

5.2.4 Effect of PKCγ on AMPA mEPSCs

I then attempted to mimic the effect of PMA by applying active PKCγ directly to the cytosol of the M-cell. A 10-min application of active PKCγ via the recording pipette resulted in a gradual increase in mEPSC amplitude, from 29.3 ± 1.1 to 50.9 ± 1.2 pA (n=5, $p < 0.001$) (Figure 5.6A), but there was no effect on mEPSC frequency and kinetics (Figure 5.6B-D). Application of heat-inactivated PKCγ had no effect on mEPSC amplitude or kinetics (n=4, p=0.227) (Figure 5.6A). Next, I applied a specific PKCγ inhibiting peptide (γV5-3) to the M-cell cytosol before PMA application, and found that γV5-3 completely blocked the PMA-induced increase in amplitude (n= 6, $p < 0.001$), whereas the control peptide (C1) had no effect (Figure 5.7) (n=4, p=0.667). Application of γV5-3 or C1 alone had no effect on basal mEPSC amplitude. To confirm that the blocking peptide prevented the activation and translocation of PKCγ to the membrane, I immunoblotted zebrafish CNS tissue with anti-PKCγ in the presence and absence of γV5-3 and PMA. Inactive PKCγ was largely limited to the cytosol, and activation by PMA led to the movement of PKCγ from the cytosol to the membrane, as expected (n=4, $p < 0.001$) (Figure 5.8).

Addition of γV5-3 completely blocked the translocation of PKCγ from the cytosol to the membrane. Together, our results suggest that PKCγ is responsible for the increase in mEPSC amplitude.

5.2.5 Mechanism underlying the effect of PKCγ on mEPSC amplitude

I then sought to determine the mechanism whereby activation of PKCγ led to a postsynaptic increase in AMPAR mEPSCs amplitude. PKCγ may directly alter the AMPAR conductance, or it may increase the number of functional AMPA receptors at the synapse. To address these possibilities, I performed NSFA on AMPA mEPSCs to determine whether the single channel conductance increased, or whether the number of synaptic AMPARs changed after application of PMA. NSFA indicated that the channel conductance of AMPARs did not change after bath application of PMA (n=7, p=0.865) (Figure 5.9A,B). However, there was a significant increase in the number of synaptic AMPA receptors, from 33.7 ± 1.3 to 63.3 ± 4.6 (n=7, $p < 0.001$), which was prevented by including BIS I in the recording pipette (p=0.788, n=6) (Figure 5.9B). This data suggested that the PMA-induced increase in mEPSC amplitude was probably due to receptor trafficking rather than an increase in channel conductance. Therefore, I tested this hypothesis by bath applying a general actin polymerization blocker, latrunculin B (5 μM), which is known to prevent receptor trafficking (Korkotian and Segal, 2007). I found that latrunculin B

completely inhibited the PMA-induced increase in amplitude (n=5, $p < 0.001$) (Figure 5.10), which is consistent with a trafficking mechanism.

5.2.7 Activation of PKCγ leads to the trafficking of GluR2-containing AMPA receptor subunits

M-cells at 2 dpf express GluR2 subunits (Chapter 4). To determine the subunit composition of the AMPARs being trafficked upon activation of PKC, I tested the ability of the GluR2 blocker, pentobarbital (PB), and the non-GluR2 blocker, NASPM, to block mEPSC amplitude before and after PMA application. PB (100 μM) blocked mEPSC amplitude by 79 ± 4% in control recordings (data from Chapter 4), and by 92 ± 3% after PMA application (n=6, $p < 0.05$) (Figure 5.11A). The non-GluR2 blocker, NASPM (10 μM) blocked the mEPSC amplitude by 13 ± 3% in control recordings (data taken from Chapter 4), and by 6 ± 3% after addition of PMA (n=5, $p < 0.05$) (Figure 5.11A). The presence of GluR2 subunits may be inferred from a linear or outward rectification of AMPA currents (Liu and Cull-Candy, 2002). Therefore, I also examined the mEPSC rectification index ($I_{+40\ mV}/I_{-60\ mV}$) before and after addition of PMA, and found there to be no difference (0.99 ± 0.03 before vs. 1.01 ± 0.04 after application of PMA; n=6; Figure 5.11B). Together, these data suggest that zebrafish M-cells express, and up-regulate, GluR2 containing AMPARs via PKCγ-dependent receptor trafficking.

5.2.8 Trafficking mechanism of GluR2-containing AMPA receptor

To gain more insight into the mechanism of AMPAR trafficking, I tested whether a peptide (pep2m), which interferes with the interaction between NSF and the GluR2 subunit (Figure 5.12), would prevent the effect of PMA. Pep2m is a 10 amino acid sequence that targets the NSF-binding motif on the GluR2 subunit, so I hypothesized that if trafficking of AMPARs required an interaction of the GluR2 subunit with NSF (reviewed in Chapter 1), then application of the pep2m peptide should prevent AMPAR trafficking. Pep2m (200 μM) completely prevented the PMA-induced increase in mEPSC amplitude ($n=4$, $p < 0.001$) (Figure 5.12), whereas the inactive control peptide, pep4c, had no effect ($n=4$, $p= 0.173$) (Figure 5.12). The AMPAR interacting protein PICK1 is also known to regulate the surface expression of GluR2-containing AMPARs (Chung et al., 2000; Daw et al., 2000; Terashima et al., 2004). Therefore, I blocked the interaction between PICK1 and GluR2 with the peptide pep2-EVKI (200 μM), and found that it prevented the effect of PMA ($n=4$, $p < 0.001$). The control peptide, pep2-SVKE (200 μM), had no effect ($n=4$, $p= 0.378$) (Figure 5.13). Together, these results suggest that the effect of PKCγ can be fully accounted for via trafficking of GluR2-containing AMPARs to the synapse in a NSF and PICK1-dependent manner. To further examine if exocytosis of internal receptors was a potential source of new receptors, I determined the sensitivity of PMA-induced increase in mEPSC amplitude to application of tetanus toxin (TeTx). This toxin selectively cleaves

vesicle-associated membrane protein (VAMP), prevents presynaptic exocytosis (Hua and Charlton, 1999), and prevents the Ca^{2+}-evoked exocytosis of postsynaptic vesicles thought to contain new AMPA receptors (Maletic-Savatic and Malinow, 1998). I applied the tetanus toxin (TeTx) light chain to the M-cell cytosol before PMA application. TeTx (200 nM) completely prevented the increase in mEPSC amplitude ($n=6$, $p < 0.001$) (Figure 5.14). Miniature EPSC amplitude during the TeTx wash, before application of PMA (100 nM), was not significantly different from control recordings (Figure 5.1B). Application of heat-inactivated TeTx had no significant effect on the mEPSC amplitude ($n=3$, $p=0.474$) (Figure 5.14). These results suggest that the PKCγ-induced trafficking of AMPARs in developing zebrafish is dependent upon an interaction with NSF, PICK1, and SNARE proteins.

5.2.9 Activation of endogenous PKCγ via physiological mechanisms

Last, to determine whether endogenous PKCγ can induce the trafficking of AMPARs via a more physiological mechanism, I mimicked depolarization of the M-cells via 2 separate methods. First, I bath applied a 5 mM K^+ medium for 10 min to depolarize the cell and its synaptic afferents. Second, I induced a direct depolarization of the M-cell using a depolarization pulse protocol (DPP) (Baxter and Wyllie, 2006). The 5 mM K^+ treatment caused an enhancement in mEPSC amplitude (from 29.3 ±

1.0 to 51.3 ± 1.4 pA) and frequency that was similar to that of PMA (100 nM) (n=6, $p < 0.001$) (Figure 5.15A-C) but had no effects on the mEPSC kinetics (Figure 5.15D). However, direct depolarization of the M-cell using the DPP had no effect on mEPSC amplitude (n=5, $p = 0.675$; Figure 5.16A), frequency (Figure 5.16B) and kinetics (Figure 5.16C). Together, these results suggest that depolarization of the afferents onto M-cells leads to an increase in AMPA mEPSC amplitude.

I then examined if the 5 mM K^+ solution and PKCγ enhance the mEPSC amplitude through the same mechanism by testing the occlusion of the 5 mM K^+ -induced changes by prior stimulation with PKCγ. Active PKCγ was applied to the cytosol of the M-cell for 10 mins prior to washing on the 5 mM K^+ solution. I found that the PKCγ-mediated increase in mEPSC amplitude completely occluded the 5 mM K^+ (Figure 5.17). Further, to determine whether PKCγ was activated after 5 mM K^+ treatment, I applied the PKCγ blocking peptide γV5-3, which blocked the 5 mM K^+-induced increase in amplitude(n= 5, $p < 0.001$), whereas the control peptide (C1) had no effect (n=5, $p = 0.219$) (Figure 5.18A). These results strongly suggest that that depolarization of the M-cell by the 5 mM K^+ activates endogenous PKCγ and once PKCγ activated it potentiates the mEPSC amplitude.

I then tested whether trafficking mechanisms were involved in the 5 mM K^+ effect by applying pep2m to the cytosol of the M-cell before

application of the 5 mM K^+ medium. We found that pep2m prevented the enhancement of mEPSC amplitude (n=5, $p < 0.001$), whereas the control peptide pep4c had no effect (n=5, $p = 0.089$) (Figure 5.18B). Both γV5-3 and pep2m had no effect on mEPSC frequency. Together, these results suggest that depolarization of the afferents onto M-cells leads to activation of endogenous PKCγ and the subsequent trafficking of GluR2-containing AMPARs to the synapse via a NSF-dependent mechanism.

5.2.10 Is the AMPA receptor trafficking dependent on NMDAR activation?

How is PKCγ activated following an increase in cellular activity? The biochemical components upstream of PKCγ are as yet unknown, but the simultaneous activation of NMDA and metabotropic receptors is thought to be partially responsible for PKC activation (Codazzi et al., 2006) in other systems. Therefore, I tested whether the trafficking process was NMDA-dependent by blocking NMDA receptor activation with 2-amino-5-phosphonovaleric acid (APV; 50 μM). We found that APV abolished the 5 mM K^+ induced increase in mEPSC amplitude (n=7, $p < 0.001$) (Figure 5.19).

5.3 Summary

In summary, I show that activation of PKCγ enhances AMPAR-mEPSC amplitude in an embryonic organism by inducing the insertion of GluR2-containing AMPA receptors into synaptic membranes. In addition, the trafficking mechanism requires AMPARs to associate with the scaffolding proteins NSF and PICK1, and occurs through a SNARE-dependent process (Figure 5.20). Finally, the insertion of AMPARs into the synaptic membrane is Ca^{2+}- and NMDA-dependent.

Figure 5.1 Activation of PKC enhances the amplitude and frequency of AMPA mEPSCs. **A**: Representative recordings of mEPSCs in an embryonic zebrafish Mauthner-cell before and after application of PMA (100 nM) and BIS I (500 nM). **B**: PMA increased the mean mEPSC amplitude and frequency (**D**) (n=7, $p < 0.001$). Intracellular application of BIS I (n=6), prior to PMA application, blocked the increase in amplitude (n=7, p=0.668) but had no effect on the frequency. **C** PMA significantly shifts the cumulative probability plot of the mEPSCs amplitude. *** Significantly different, $p < 0.001$.

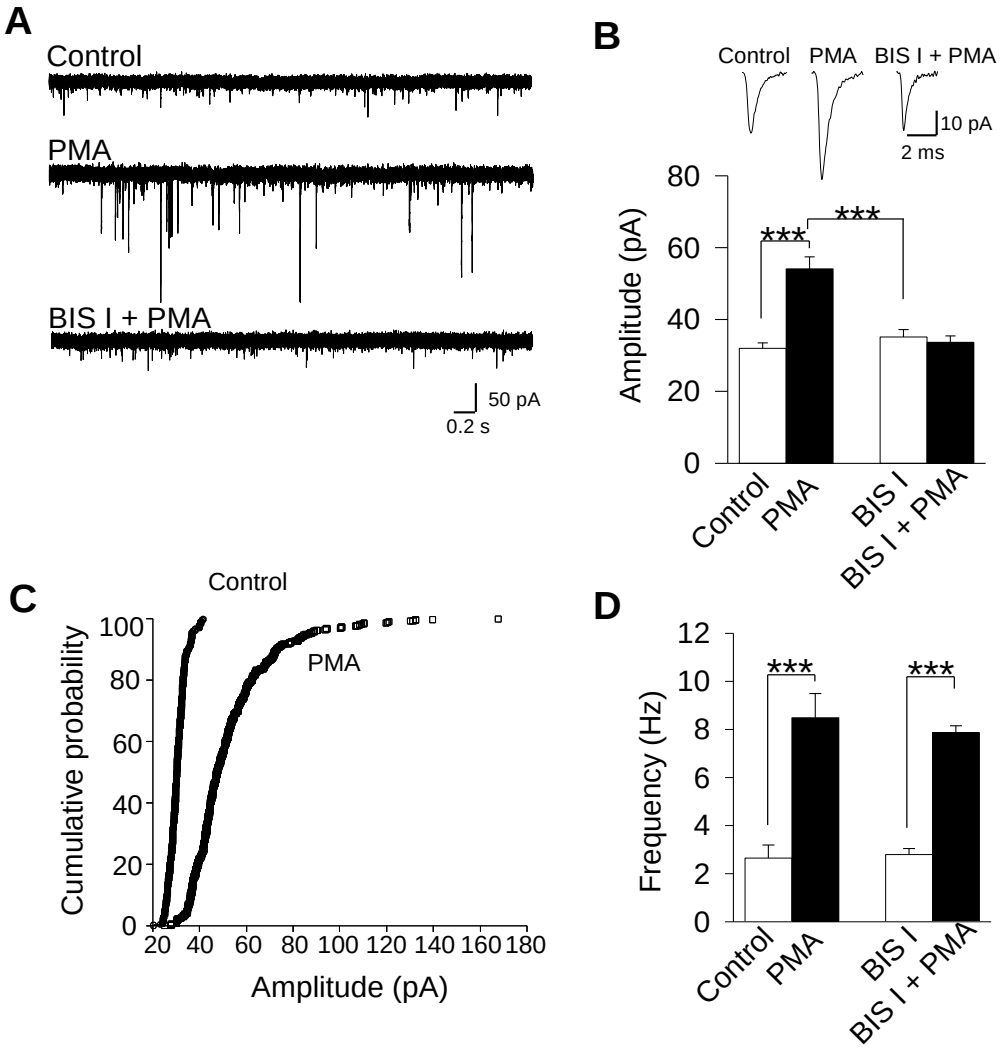
A
Control
PMA
BIS I + PMA
50 pA
0.2 s
B
Control
PMA
BIS I + PMA
10 pA
2 ms
Amplitude (pA)
***
***
Control
PMA
BIS I
BIS I + PMA
C
Control
PMA
Cumulative probability
Amplitude (pA)
D
Frequency (Hz)
***
***
Control
PMA
BIS I
BIS I + PMA

Figure 5.2 PMA-induced increase in mEPSC amplitude is not due to changes in kinetics or dendritic filtering. **A**: Representative traces of mEPSCs (*left* – control; *center* – PMA) from the same cell before and after PMA application. When scaled and superimposed (*right*), the traces do not differ in their time courses and kinetics. Bar graphs of the 20-80% rise time and the decay time constants of the mEPSC indicate that there is no change in kinetics following application of PMA. Error bars indicate mean ± SEM. **B**: Scatter plot of rise time vs. amplitude of events recorded before and after application of PMA. There was no correlation between these parameters before or after PMA application (*left*, control: r = 0.07; *right* PMA-enhanced mEPSCs: r = 0.09).

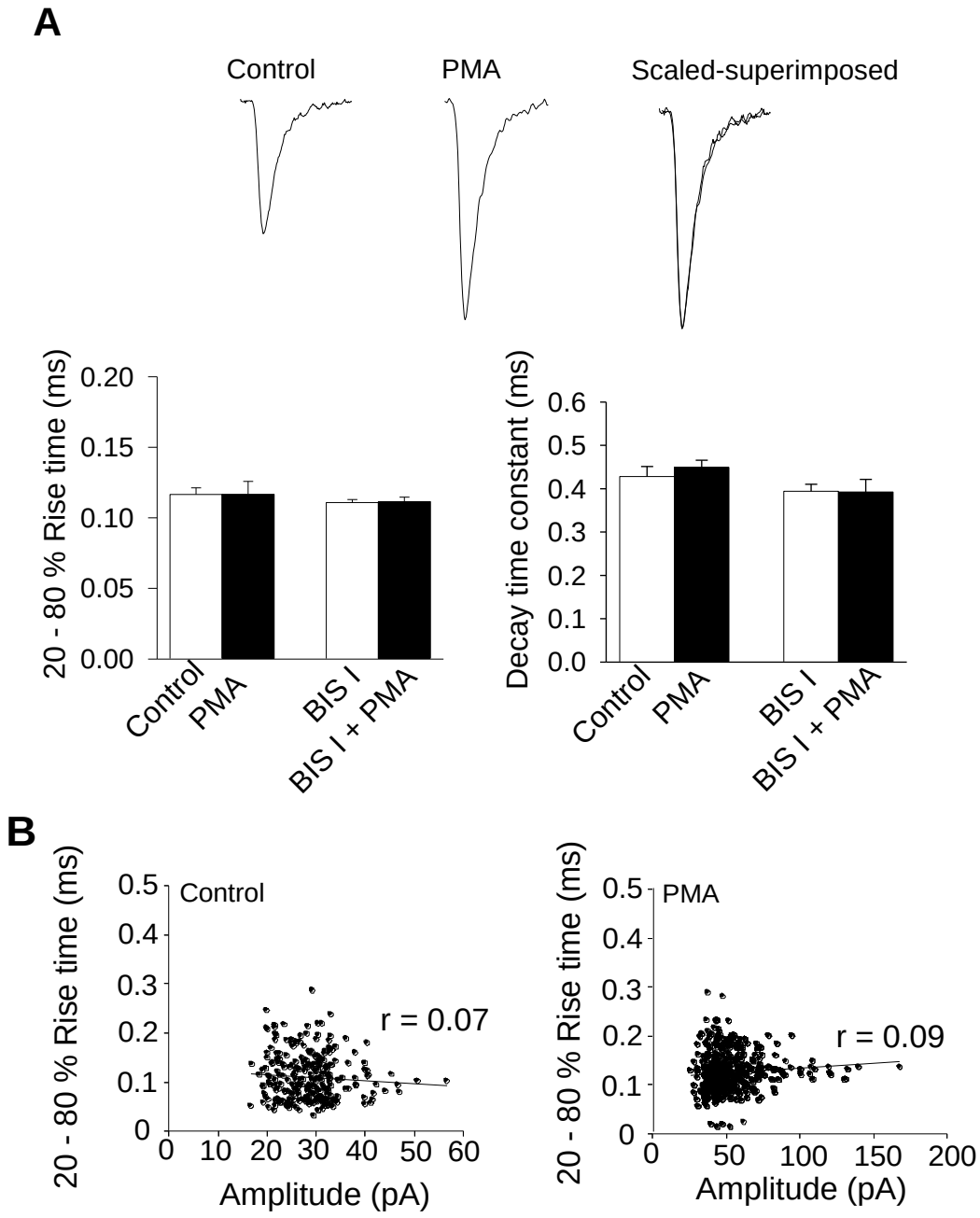
A
Control
PMA
Scaled-superimposed
20 - 80 % Rise time (ms)
0.20
0.15
0.10
0.05
0.00
Control
PMA
BIS I
BIS I + PMA
Decay time constant (ms)
0.6
0.5
0.4
0.3
0.2
0.1
0.0
Control
PMA
BIS I
BIS I + PMA
B
20 - 80 % Rise time (ms)
Control
r = 0.07
0.5
0.4
0.3
0.2
0.1
0
0 10 20 30 40 50 60
Amplitude (pA)
20 - 80 % Rise time (ms)
PMA
r = 0.09
0.5
0.4
0.3
0.2
0.1
0
0 50 100 150 200
Amplitude (pA)

Figure 5.3 DOG-induced increase in mEPSC amplitude and frequency. **A**: Bath application of the DAG analog 1,2-dioctanoylglycerol (DOG, 50 μM) increased the mean mEPSC amplitude and frequency (n=5, $p < 0.001$). Intracellular application of BIS I (500 nM; n=5), prior to DOG application, blocked the increase in amplitude but did not affect the mean mEPSC frequency. **B**: Bar graphs of the 20-80% rise time and the decay time constants of the mEPSC indicate that there is no change in kinetics following application of DOG. *** Significantly different, $p < 0.001$.

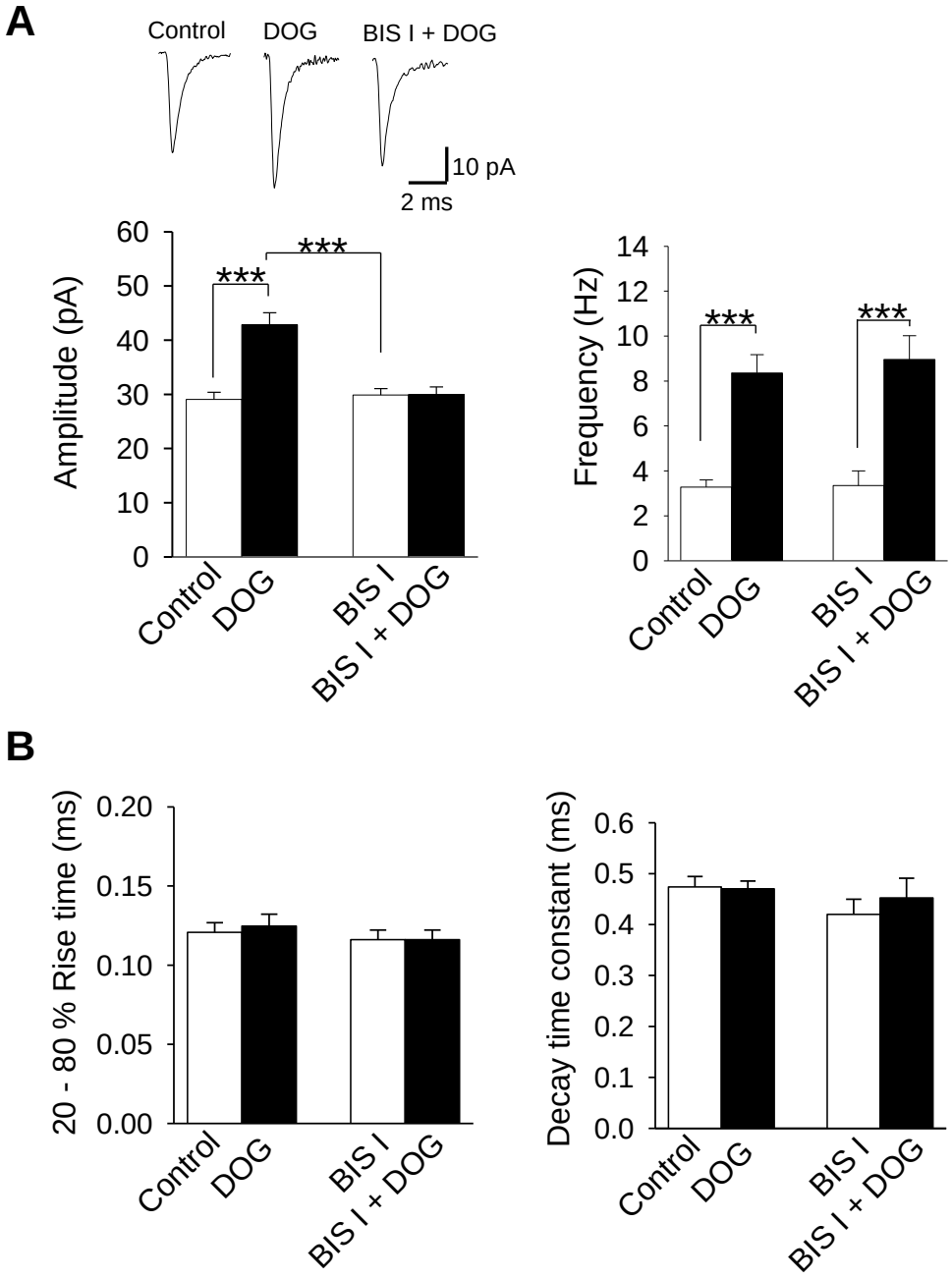
A
Control
DOG
BIS I + DOG
10 pA
2 ms
Amplitude (pA)
60
50
40
30
20
10
0
***
***
Control
DOG
BIS I
BIS I + DOG
Frequency (Hz)
14
12
10
8
6
4
2
0
***
***
Control
DOG
BIS I
BIS I + DOG
B
20 - 80 % Rise time (ms)
0.20
0.15
0.10
0.05
0.00
Control
DOG
BIS I
BIS I + DOG
Decay time constant (ms)
0.6
0.5
0.4
0.3
0.2
0.1
0.0
Control
DOG
BIS I
BIS I + DOG

Figure 5.4 PKC-induced increase in mEPSC amplitude is Ca^{2+}-dependent. **A**: Inclusion of the Ca^{2+}-chelating agent, BAPTA (5 mM), in the patch pipette blocked the PMA-induced (100 nM) increase in amplitude ($n=4$, $p<0.001$), but had no effect on the mEPSC frequency. **B**: Preventing the rise in intracellular Ca^{2+} by including BAPTA (5 mM) in the patch pipette blocked the DOG-induced increase in amplitude ($n=5$, $p<0.001$) but had no effect on the mEPSC frequency. *** Significantly different, $p < 0.001$.

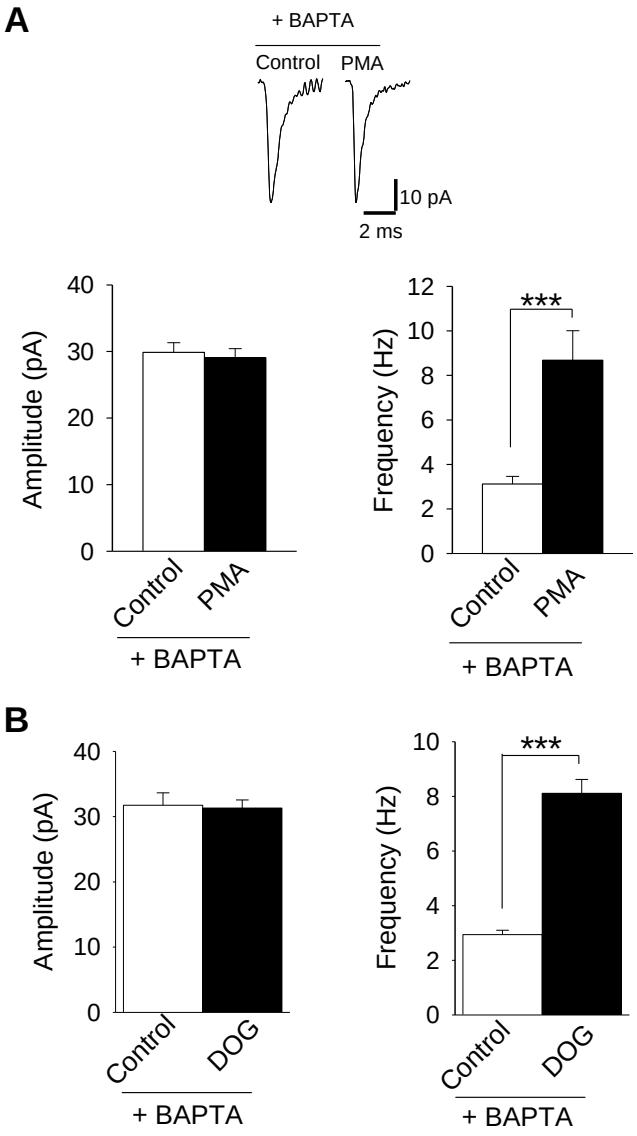
A
+ BAPTA
Control
PMA
10 pA
2 ms
Amplitude (pA)
Frequency (Hz)
***
Control
PMA
+ BAPTA
B
Amplitude (pA)
Frequency (Hz)
***
Control
DOG
+ BAPTA

Figure 5.5 PKCγ is expressed in the Mauthner cell. PKCγ is expressed in the Mauthner cell. **A**: Anti-3A10, anti-PKCα, -βII and -γ immunoreactivity in zebrafish (n=5). Only anti-PKCγ labels the Mauthner cell. Scale bar = 50 μm. **B**: Immunoblots of zebrafish CNS to confirm the specificity of anti-PKCα (n=4), γ (n=5). Proteins were transferred to nitrocellulose membranes and incubated in either anti-PKC or anti-PKC preabsorbed with blocking peptide at a ratio of 1:5 (anti-PKC:blocking peptide).

A

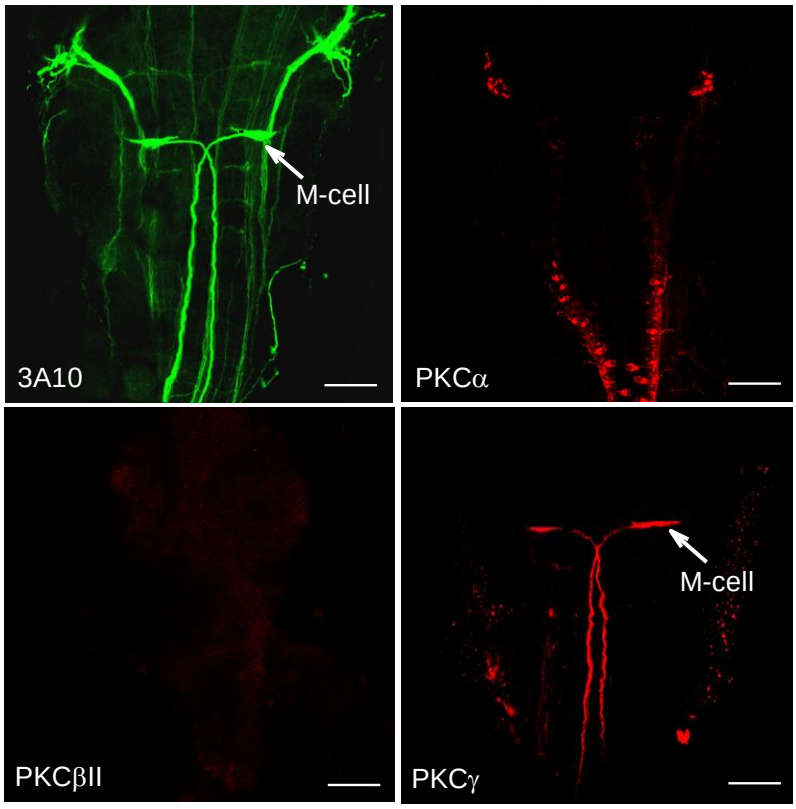
M-cell
3A10
PKCα
PKCβII
M-cell
PKCγ

B

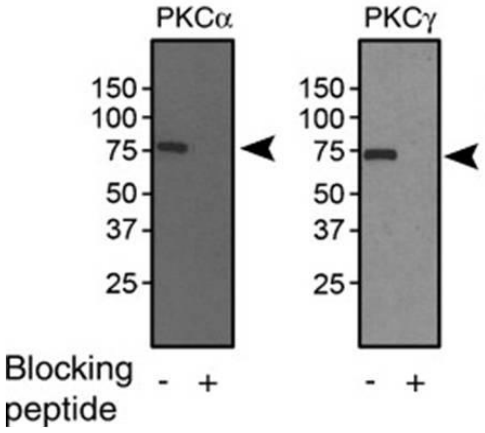
PKCα
PKCγ
150
100
75
50
37
25
150
100
75
50
37
25
Blocking peptide
- +
- +

Figure 5.6 PKCγ leads to an increase in mEPSC. **A**: 10-minute application of the active form of PKCγ to the M-cell cytosol caused an increase mEPSC amplitude (n=5, $p < 0.001$). 10-minute application of heat inactivated PKCγ had no effect (n=4). Controls represent a recording of AMPA mEPSCs at the 10 min time point in normal intra- and extra-cellular solutions. **B-D**: Application of active and heat inactivated PKCγ had no effect on the mEPSC frequency, 20-80% rise time or decay time constant. *** Significantly different, $p < 0.001$.

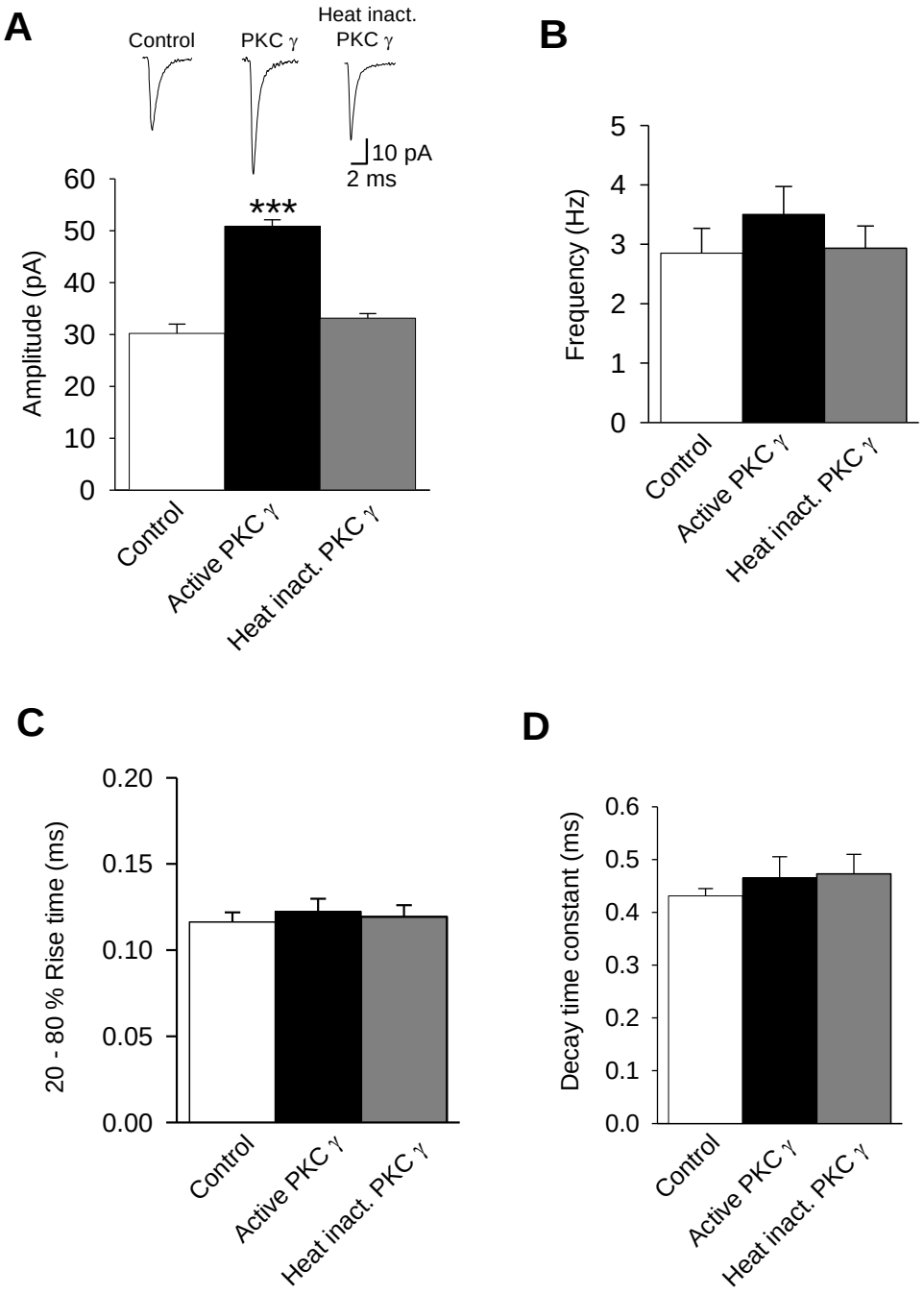
A
Control
PKC γ
Heat inact. PKC γ
10 pA
2 ms
***
Amplitude (pA)
60
50
40
30
20
10
0
Control
Active PKC γ
Heat inact. PKC γ
B
Frequency (Hz)
5
4
3
2
1
0
Control
Active PKC γ
Heat inact. PKC γ
C
20 - 80 % Rise time (ms)
0.20
0.15
0.10
0.05
0.00
Control
Active PKC γ
Heat inact. PKC γ
D
Decay time constant (ms)
0.6
0.5
0.4
0.3
0.2
0.1
0.0
Control
Active PKC γ
Heat inact. PKC γ

Figure 5.7 Activation of PKCγ leads to an increase in mEPSC. Intracellular application of γV5-3 (10 nM) blocked the PMA-induced (100 nM) increase in the amplitude (n=6) whereas the control peptide (C1; 10 nM) had no effect (n=4). *** Significantly different, $p < 0.001$.

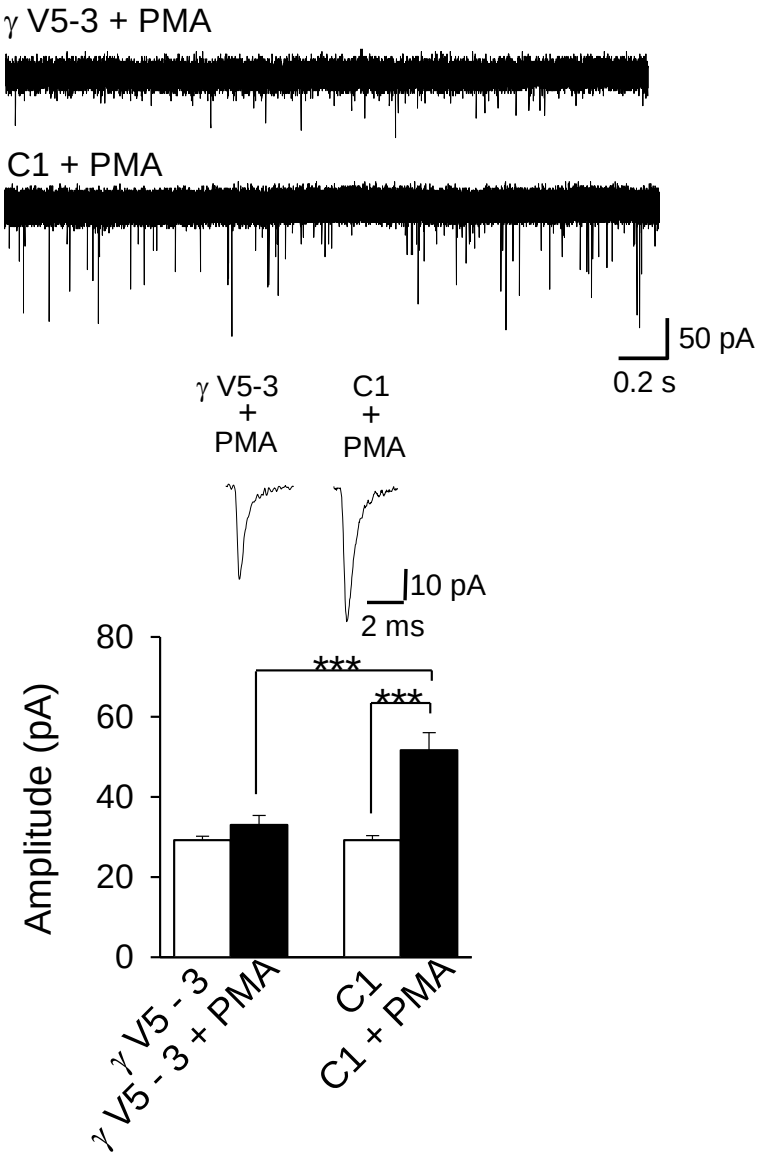
γ V5-3 + PMA
C1 + PMA
50 pA
0.2 s
γ V5-3 + PMA
C1 + PMA
10 pA
2 ms
Amplitude (pA)
80
60
40
20
0
***
***
γ V5 - 3
γ V5 - 3 + PMA
C1
C1 + PMA

Figure 5.8 Specificity of the PKCγ inhibitory peptide. Immunoblot analysis of cytosolic and membrane fractions from zebrafish brain following incubation with or without γV5-3 and PMA (5 nM). An example western blot is shown in the upper panel ans pooled results from replicate experiments shown in the bottom panel. γV5-3 inhibited the PMA-induced loss of PKCγ from the cytosolic fraction (n=4, $p < 0.001$). *** Significantly different, $p<0.001$.

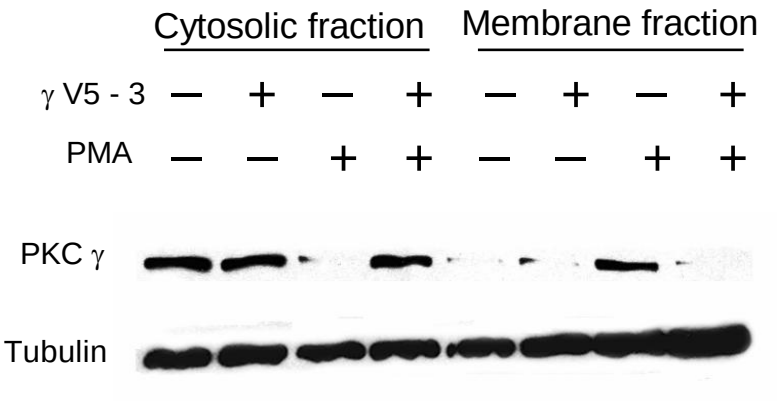
Cytosolic fraction
Membrane fraction
γ V5 - 3 — + — + — + — +
PMA — — + + — — + +
PKC γ
Tubulin

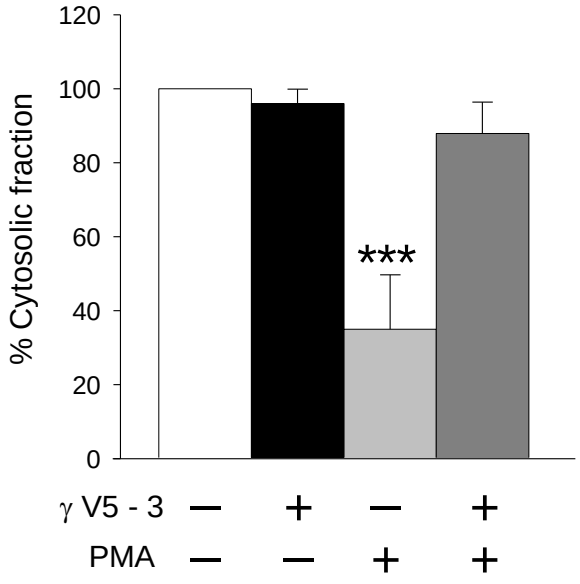
120
100
80
60
40
20
0
% Cytosolic fraction
***
γ V5 - 3 — + — +
PMA — — + +

Figure 5.9 NSFA indicates that the PMA-induced increase in mEPSC amplitude is due to an increase in the number of postsynaptic receptors. **A**: Plot of variance versus mean current of mEPSCs before (open circles) and after application of PMA (solid circles). The parabolic curves exhibited overlap over the initial linear portion and large increases in the variance. **B**: PMA did not change the unit conductance (n=7) but it increased the number of functional postsynaptic AMPARs (n=7, $p < 0.001$). Intracellular application of BIS I (500 nM) blocked the effect of PMA. *** Significantly different, $p < 0.001$.

A

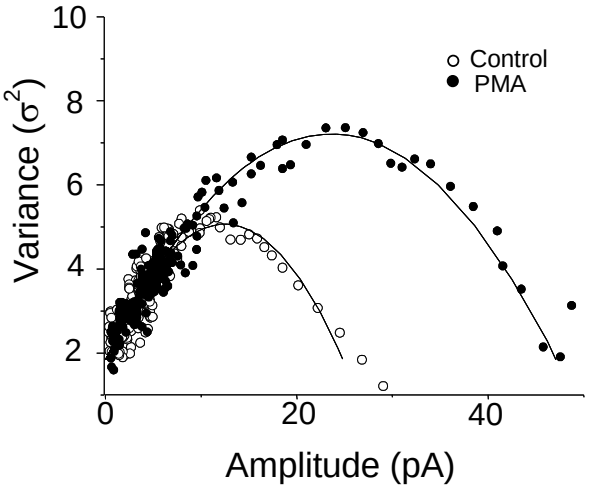
Control
PMA
Variance (σ^2)
Amplitude (pA)
10
8
6
4
2
0
20
40

B

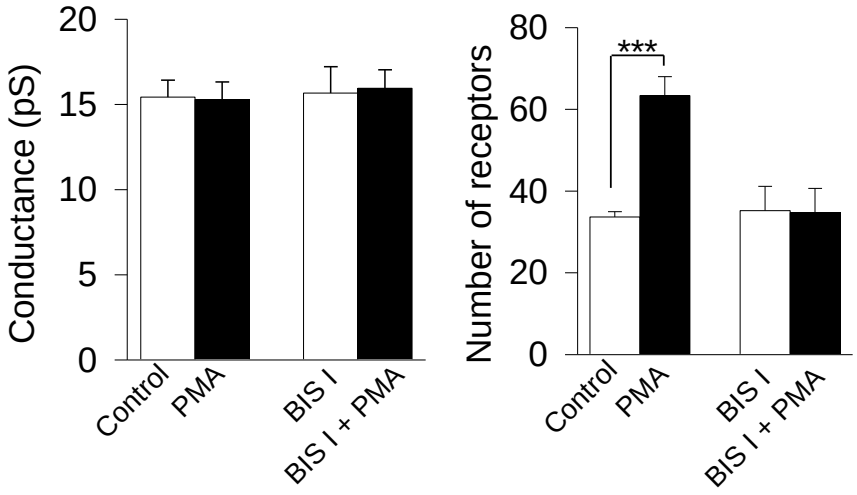
Conductance (pS)
20
15
10
5
0
Control
PMA
BIS I
BIS I + PMA
Number of receptors
80
60
40
20
0
***
Control
PMA
BIS I
BIS I + PMA

Figure 5.10 Latrunculin B blocks the PMA-induced increase in mEPSC amplitude. Effect of latrunculin B (Lat B, 5 mM) on mEPSCs recorded before and after application of PMA (100 nM). Lat B significantly blocked the effect of PMA on the amplitude (n=4). *** Significantly different, $p < 0.001$.

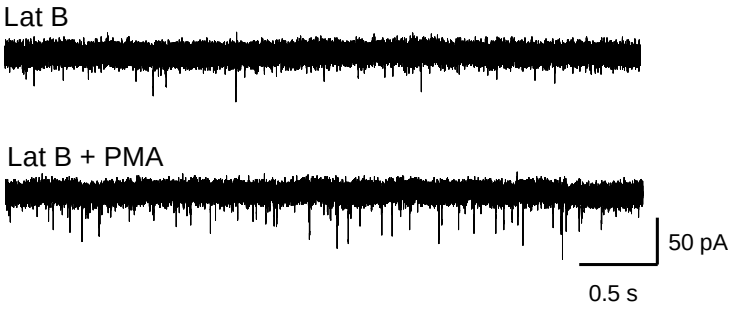
Lat B
Lat B + PMA
50 pA
0.5 s

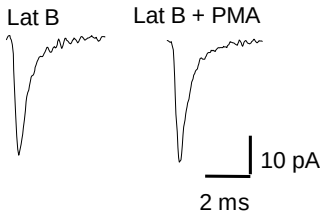
Lat B
Lat B + PMA
10 pA
2 ms

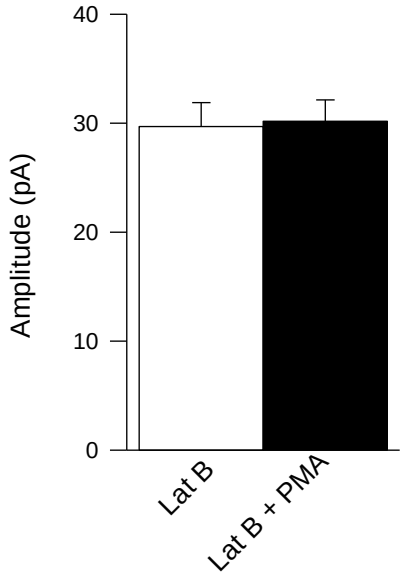
40
30
20
10
0
Amplitude (pA)
Lat B
Lat B + PMA

Figure 5.11 Increase inhibition of GluR2-containing AMPAR-mediated mEPSC amplitude after application of PMA. **A**: Application of the GluR2 blocker, PB (100 μM, n=6) reduces the mEPSC amplitude in the absence and presence of PMA (100 nM), whereas the non-GluR2 blocker, NASPM (10 μM, n=5) had little effect. The data set for the % inhibition of mEPSC amplitude in the presence of PB and NASPM (Chapter 4, Figure 4.7) were used as controls (absence of PMA) in this figure. **B**: The mEPSC rectification index ($I_{+40\ mV}/I_{-60\ mV}$) did not change on the application of PMA (n=6). * Significantly different, $p < 0.05$.

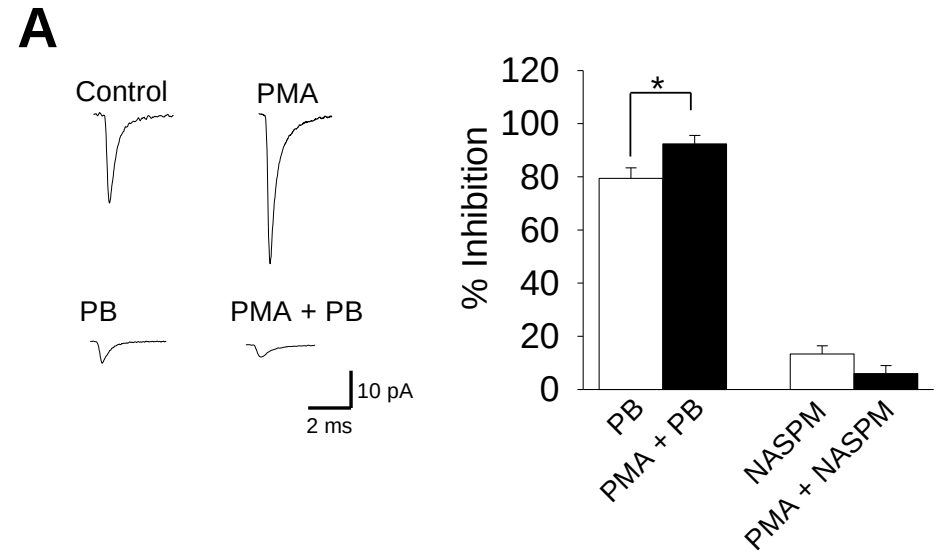
A
Control
PMA
PB
PMA + PB
10 pA
2 ms
% Inhibition
120
100
80
60
40
20
0
*
PB
PMA + PB
NASPM
PMA + NASPM

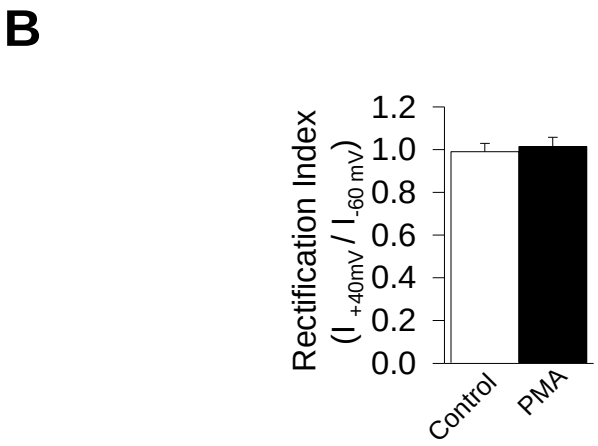
B
Rectification Index
(I +40mV / I -60 mV)
1.2
1.0
0.8
0.6
0.4
0.2
0.0
Control
PMA

Figure 5.12 AMPAR trafficking is dependent upon NSF. Intracellular application of the 10 amino acid peptide that targets the NSF binding motif on GluR2, pep2m, (200 μM, n=4) blocked the effect of PMA (100 nM) on amplitude. The inactive control peptide, pep4c (200 μM, n=4) did not affect the PMA-induced increase in mEPSC amplitude. *** Significantly different, $p < 0.001$.

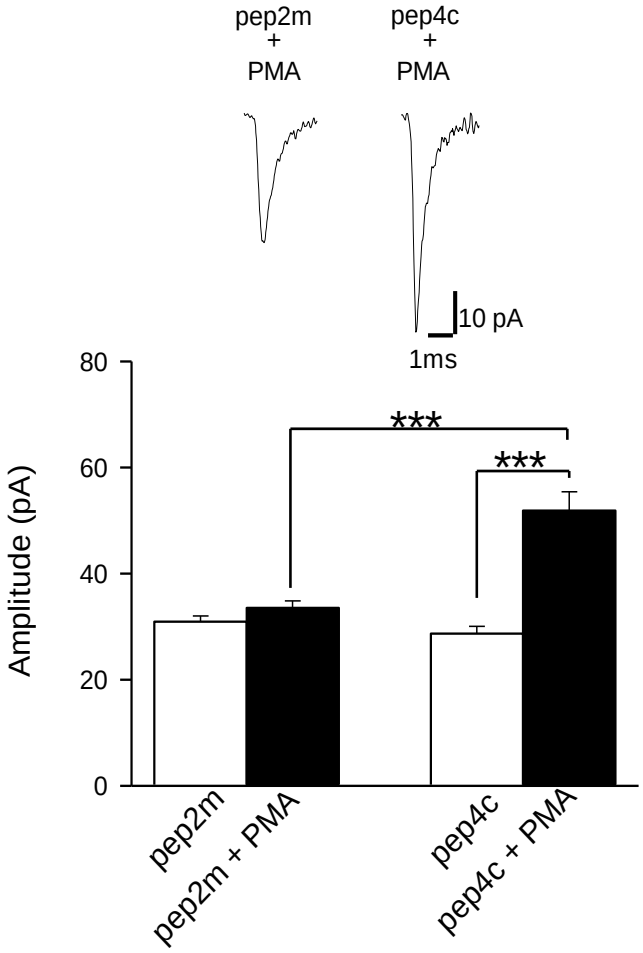
pep2m
+
PMA
pep4c
+
PMA
10 pA
1ms
80
60
40
20
0
Amplitude (pA)
***
***
pep2m
pep2m + PMA
pep4c
pep4c + PMA

Figure 5.13 AMPAR trafficking is dependent upon PICK1. Inclusion of the peptide that targets the PICK1 and binding motif on GluR2, pep2-EVKI (200 μM, n=4) in the patch pipette prevented the PMA-induced (100nM) increase in mEPSC amplitude, whereas the control peptide pep2-SVKE (200 μM, n=4) had no effect. *** Significantly different, $p < 0.001$.

.

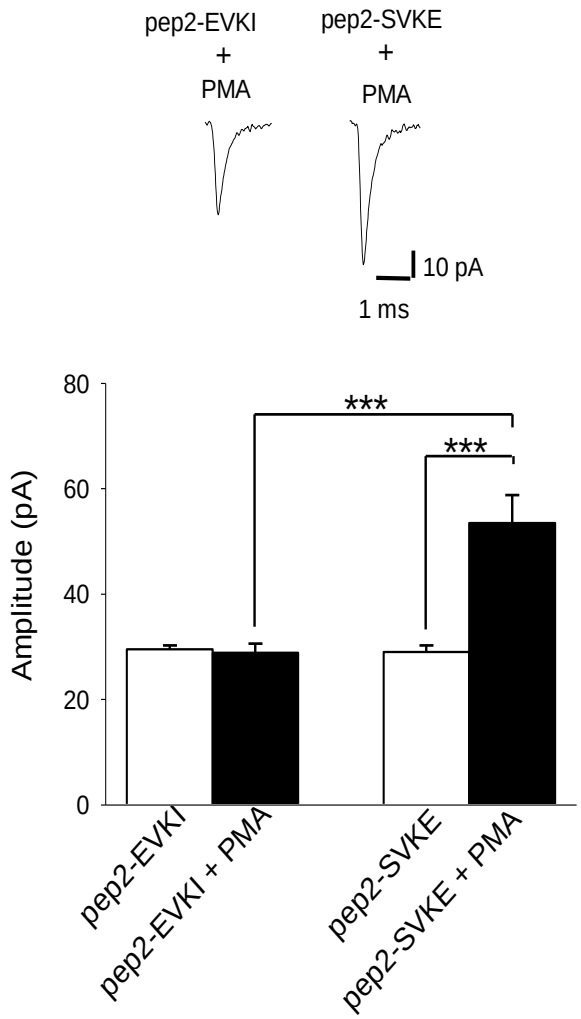
pep2-EVKI
+
PMA
pep2-SVKE
+
PMA
10 pA
1 ms
Amplitude (pA)
80
60
40
20
0
***
***
pep2-EVKI
pep2-EVKI + PMA
pep2-SVKE
pep2-SVKE + PMA

Figure 5.14 AMPAR trafficking requires assembly of the SNARE complex. Intracellular application of TeTx (200 nM; n=6) prevented the PMA-induced (100 nM) increase in mEPSCs, while application of heat-inactived TeTx (n=4) had no effect. *** Significantly different, $p < 0.001$.

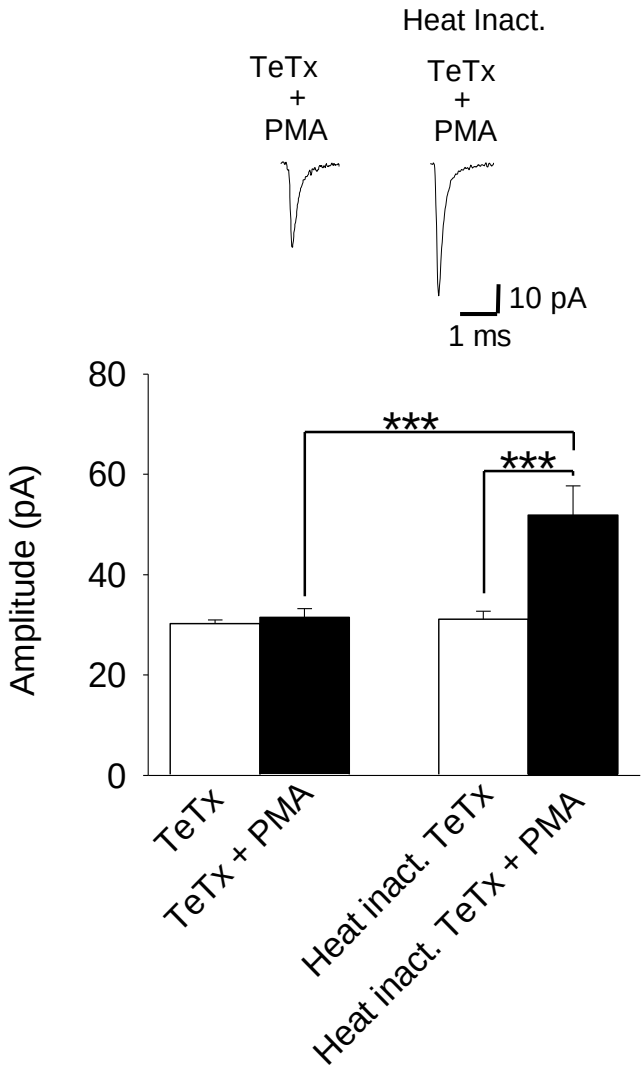
Heat Inact.
TeTx
+
PMA
TeTx
+
PMA
10 pA
1 ms
80
60
40
20
0
Amplitude (pA)
***
***
TeTx
TeTx + PMA
Heat inact. TeTx
Heat inact. TeTx + PMA

Figure 5.15 Chemical depolarization of M-cell and its afferents at 48 hpf. **A**: Representative recordings of mEPSC before and after application of 5 mM K^+. **B**: Application of the 5 mM K^+ solution for 10 min significantly increased mEPSC amplitude (n=5) and frequency (**C**) but had no effect on the mEPSC kinetics (**D**). *** Significantly different, $p < 0.001$.

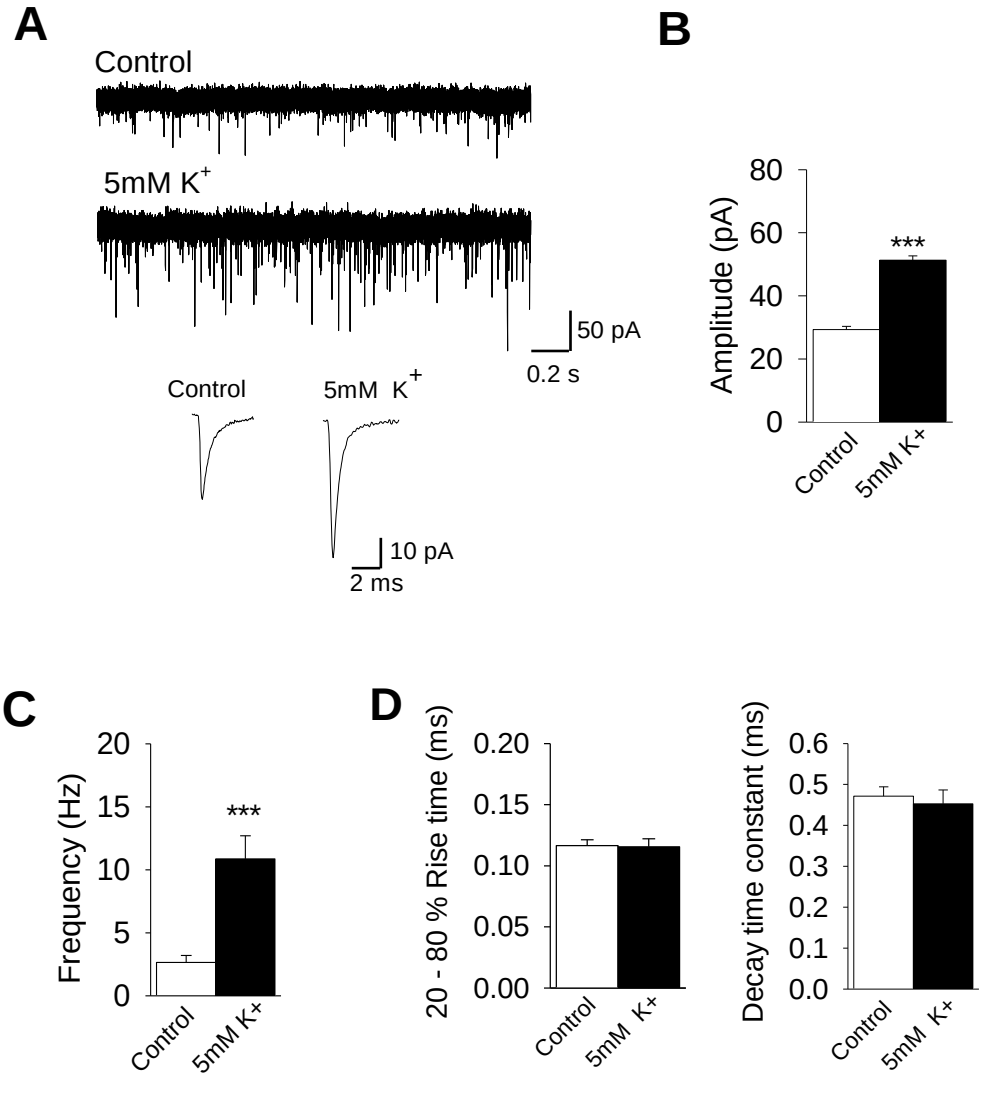
A
Control
5mM K+
50 pA
0.2 s
Control
5mM K+
10 pA
2 ms
B
Amplitude (pA)
80
60
40
20
0
***
Control
5mM K+
C
Frequency (Hz)
20
15
10
5
0
***
Control
5mM K+
D
20 - 80 % Rise time (ms)
0.20
0.15
0.10
0.05
0.00
Control
5mM K+
Decay time constant (ms)
0.6
0.5
0.4
0.3
0.2
0.1
0.0
Control
5mM K+

Figure 5.16 Postsynaptic depolarization of M-cell. **A**: Representative recordings of mEPSC before and after the induction of the M-cell via a depolarizing pulse protocol (DPP). **A**: DPP did not affect the amplitude of the mEPSCs. **B**: After induction of M-cell depolarization via the DPP protocol, the mEPSC frequency was still similar to control recordings. **C-D**: DPP did not alter the kinetics of the mEPSCs.

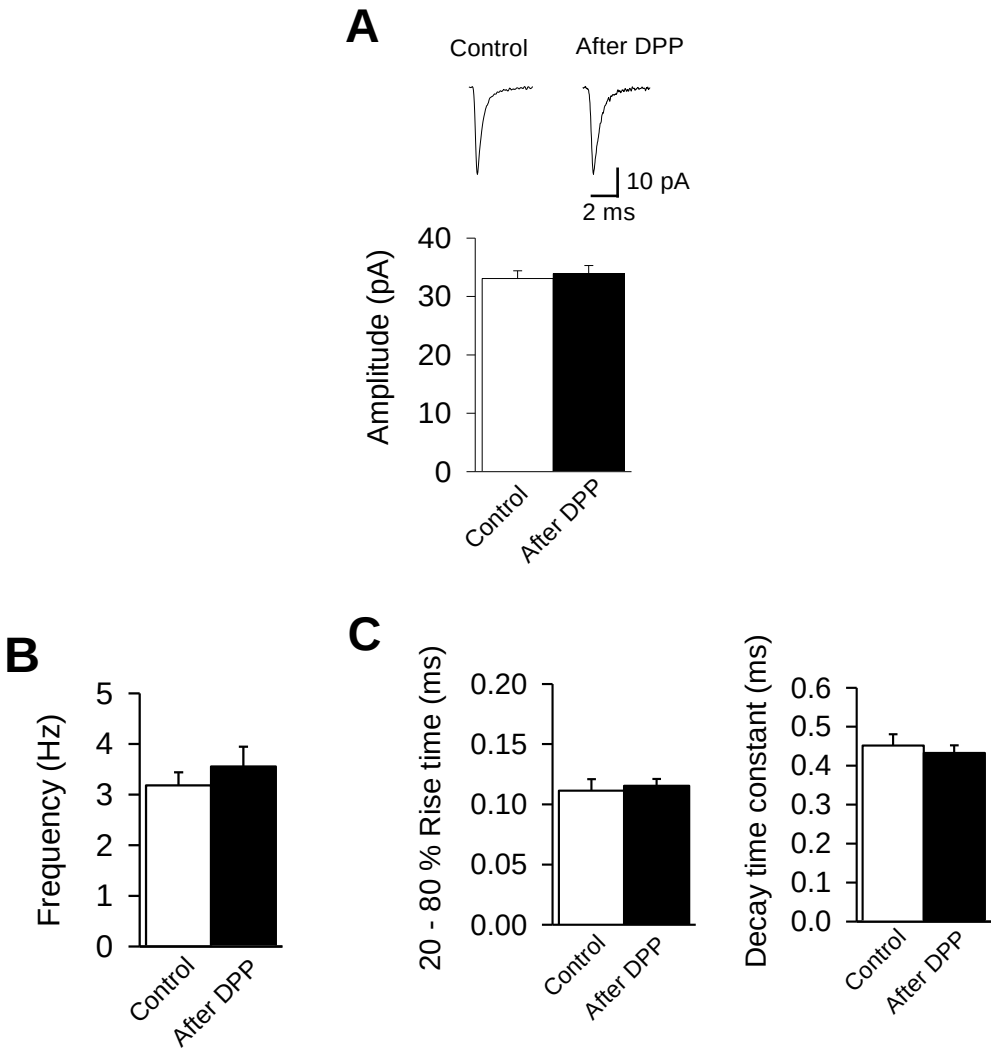
A
Control
After DPP
10 pA
2 ms
Amplitude (pA)
40
30
20
10
0
Control
After DPP
B
Frequency (Hz)
5
4
3
2
1
0
Control
After DPP
C
20 - 80 % Rise time (ms)
0.20
0.15
0.10
0.05
0.00
Control
After DPP
Decay time constant (ms)
0.6
0.5
0.4
0.3
0.2
0.1
0.0
Control
After DPP

Figure 5.17 PKCγ occluded the effect of 5 mM K^+ on the mEPSC amplitude. Application of the active form of PKCγ to the M-cell cytosol increased the mEPSC amplitude. No further increased in the amplitude was observed upon perfusion of the preparation with 5 mM K^+**.**

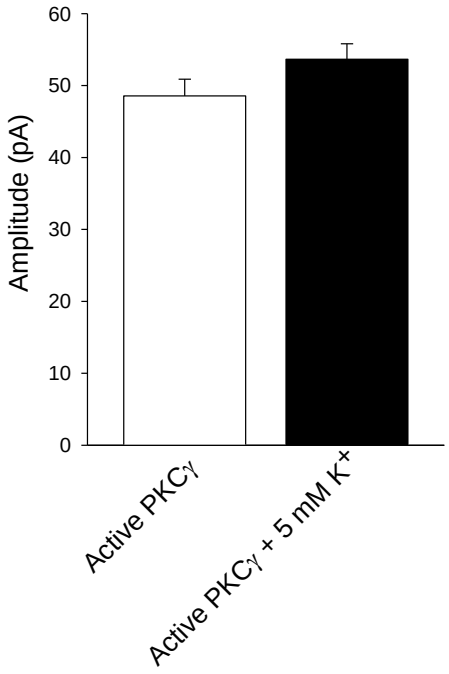
60
50
40
30
20
10
0
Amplitude (pA)
Active PKCγ
Active PKCγ + 5 mM K+

Figure 5.18 Activity-induced trafficking of AMPAR requires activation of PKCγ. **A**: Intracellular application of the PKCγ inhibitory peptide γV5-3 (10 nM) prevented the potentiation in amplitude following the 5 mM K^+ bath (n=5), whereas the control peptide (C1; 10 nM) had no effect (n=5). **B**: Inclusion of the peptide that targets the NSF binding motif on GluR2, pep2m, (200 μM, n=4) in the recording solution completely prevented the 5 mM K^+ induced increase in mEPSC amplitude, whereas the control peptide, pep4c (200 μM, n=4) had no effect. *** Significantly different, $p < 0.001$.

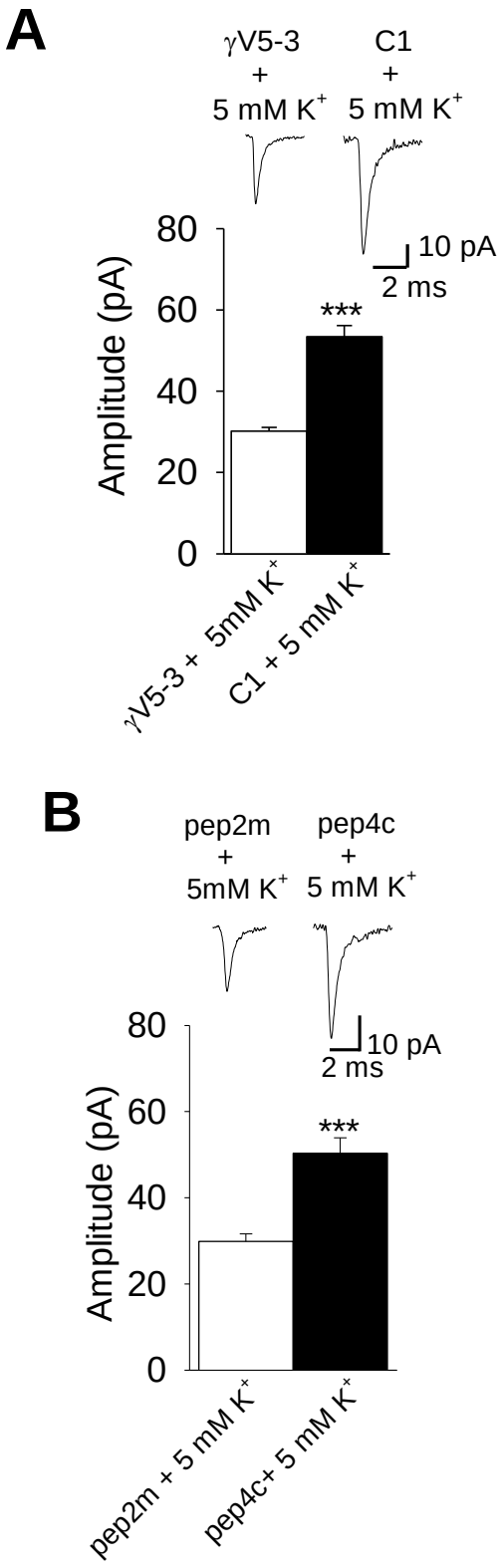
A
γV5-3
+
5 mM K+
C1
+
5 mM K+
10 pA
2 ms
***
Amplitude (pA)
80
60
40
20
0
γV5-3 + 5mM K+
C1 + 5 mM K+
B
pep2m
+
5mM K+
pep4c
+
5 mM K+
10 pA
2 ms
***
Amplitude (pA)
80
60
40
20
0
pep2m + 5 mM K+
pep4c+ 5 mM K+

Figure 5.19 The trafficking of AMPARs is NMDA-dependent. Application of APV (50 μM, n=7) completely blocked the 5 mM K^+ induced increase in mEPSC amplitude. *** Significantly different, $p < 0.001$.

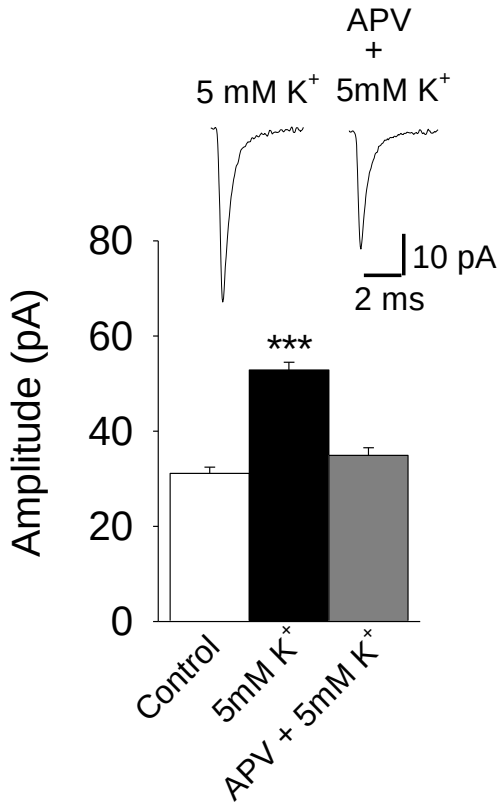
APV
+
5 mM K+
5mM K+
10 pA
2 ms
Amplitude (pA)
80
60
40
20
0
***
Control
5mM K+
APV + 5mM K+

Figure 5.20 Proposed model for trafficking of AMPAR in 48 hpf zebrafish M-cell. An increase in NMDA-dependent cellular activity leads to the activation of PKCγ, which recruits PICK1 to the C-terminus of the GluR2 subunit. AMPARs are trafficked to the membrane where association with NSF and SNARE proteins lead to their insertion into the membrane.

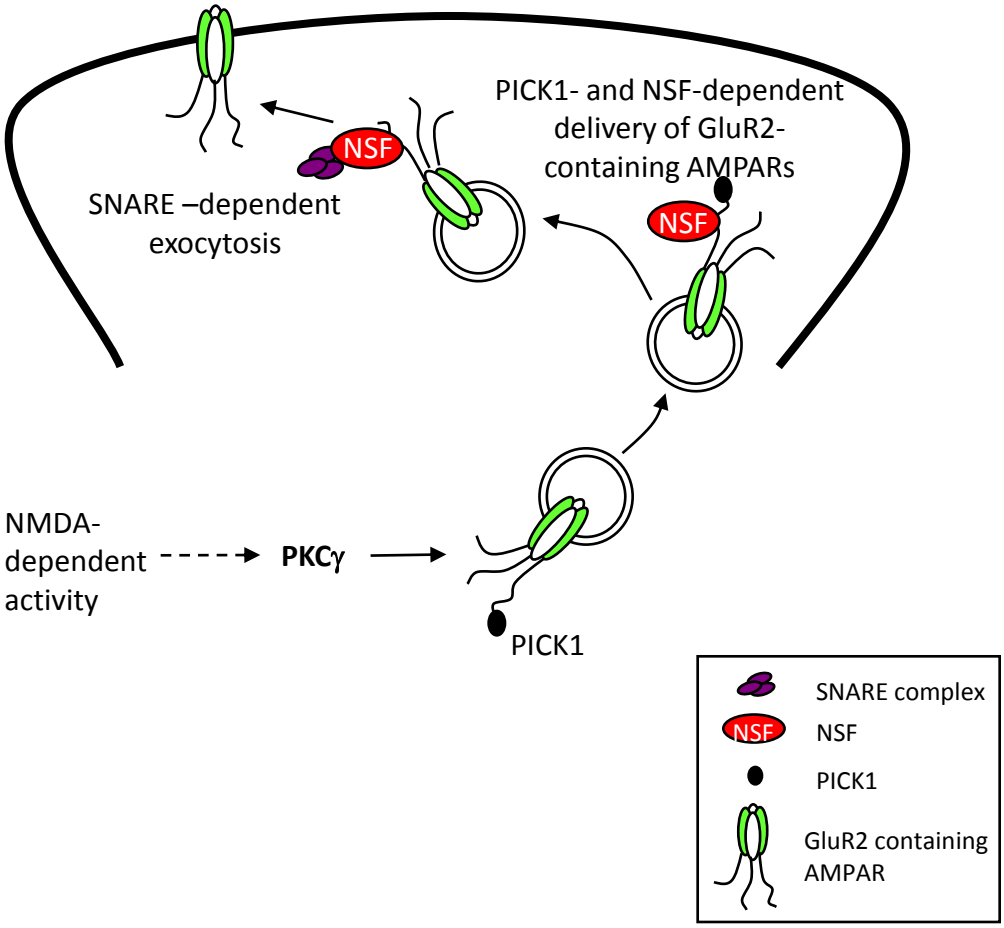
NSF
SNARE –dependent
exocytosis
PICK1- and NSF-dependent
delivery of GluR2-
containing AMPARs
NSF
NMDA-
dependent
activity
PKCγ
PICK1
SNARE complex
NSF
PICK1
GluR2 containing
AMPAR

Chapter 6 ROLE OF AMPA RECEPTOR TRAFFICKING IN ZEBRAFISH NEURODEVELOPMENT

6.1 Introduction

Recent evidence indicates that PKC plays a central role in neuroplasticity and development (Hu et al., 1987; Malenka et al., 1989; Abeliovich et al., 1993b; Perez-Otano et al., 2001). For instance, PKCα is expressed in dendritic spines of hippocampal neurons along with GluR2-containing AMPARs, and its activation induces a reduction in surface expression of AMPARs (Perez-Otano et al., 2001). The constitutively active PKMζ is capable of maintaining long-term potentiation in CA1 hippocampus via a NSF-GluR2 trafficking mechanism (Yao et al., 2008). Early studies reported that PKCγ knockout mice were impaired in motor coordination tasks but exhibited normal cerebellar LTD (Abeliovich et al., 1993a). In Chapter 5, I found that activation of conventional PKCγ was necessary for the rapid trafficking of AMPARs to the synaptic membranes of embryonic zebrafish M-cells via a NSF-, PICK1- and NMDA-dependent mechanism. The insertion or removal of AMPARs from synaptic membranes underlies neuroplasticity phenomena such as long-term potentiation, long-term depression, and development (Nasevicius and Ekker, 2000). However, the physiological significance of the trafficking of AMPARs in embryonic

zebrafish remains unknown. In this section, I set out to examine the role of AMPAR trafficking in zebrafish synaptic development.

6.2 Results

6.2.1 Zebrafish PKCγ morpholino

PKCγ is necessary for the movement and insertion of AMPARs into synaptic membranes of 48 hpf zebrafish. As a first step to investigate the role of AMPARs trafficking in embryonic development in zebrafish, I reduced the expression of PKCγ by injecting embryos with an antisense morpholino oligonucleotide targeted against the PKCγ gene (PKCγ -MO; Figure 6.1), which prevents protein expression by binding to mRNA and temporarily inhibiting protein translation (Carroll et al., 1999a). First I confirmed that PKCγ was knocked down, by performing PKCγ immunohistochemistry on PKCγ -MO injected and uninjected fish (Figure 6.2A; n=4) and used 3A10 to confirm that M-cells were still present in the PKCγ -MO injected fish. Then, I tested for the presence of PKCγ by applying 100 nM PMA or 5 mM K^+, which I had previously shown to be capable of increasing AMPA mEPSC amplitude via activating endogenous PKCγ (Chapter 5). I found that PMA or 5 mM K^+ had no effect on the mEPSC amplitude recorded from morpholino-injected fish (Figure 6.2B,C; n=5). Together these findings were consistent with a reduction in the expression of PKCγ levels.

To confirm the specificity of the morpholino injections, I rescued the PKCγ-MO injected fish with two experimental approaches. First, I included PKCγ in the patch pipette and found that this led to an increase in mEPSC amplitude (Figure 6.3A; n=5; $p < 0.001$), indicating that all of the machinery necessary for AMPAR trafficking is present within the cell. Second, I injected PKCγ mRNA into fertilized eggs immediately prior to the PKCγ-MO injections. The M-cells from these fish responded to 100 nM PMA by increasing AMPA mEPSC amplitude (Figure 6.3B; n=5, $p < 0.001$). Taken together, these findings suggested that the PKCγ-MO was specific for PKCγ and that other proteins were largely unaffected by the procedure.

6.2.2 PKCγ Morpholino fish: Morphology and behaviour

Zebrafish embryos normally hatch out of the chorion between 48 hpf and 72 hpf, however, the PKCγ-MO injected embryos failed to hatch out of the chorion (Figure 6.4A,B; n=8 ,$p < 0.001$) and died by 6 days. When PKCγ-MO injected embryos were manually removed from the chorion at 48 hpf, they responded very poorly to a touch to the head (Figure 6.5A,C; n=8, $p < 0.001$) or trunk (Figure 6.5B,D; n=8, $p < 0.001$) compared with controls. Injection of PKCγ mRNA (XM_001921680) rescued the morpholino phenotypes and resulted in embryos that hatched at 48 hpf (Figure 6.5) and also responded to touch (Figure 6.5).These data

suggest that PKCγ activity might be crucial for the proper network that regulates behavioural development of zebrafish.

6.2.3 AMPAR properties in PKCγ Morpholino fish

Interestingly, I found that the mean mEPSC amplitude in the morpholino-injected fish at 48 hpf (25.7 ± 1.4 pA; n=8) was similar to that in 33 hpf embryos (25.2 ± 0.7 pA; n=6), but was significantly smaller than in normal 48 hpf fish (32.0 ± 1.5 pA; n=7; $p < 0.001$; Figure 6.6A). The mEPSC frequency in the mutants was higher than that at 33 hpf, but less than at 48 hpf (Figure 6.6B) and the decay time constant τ, was similar to that in normal 33 hpf embryos (Figure 6.6C). Thus, overall the mEPSC properties in PKCγ-MO injected embryos were similar to those in the younger fish, suggesting that the synaptic maturation process may require PKCγ. The effect of the morpholinos on mEPSC frequency suggested that there may be a postsynaptic component to AMPA-R synaptic development such as the unmasking of silent synapses.

In zebrafish, AMPA mEPSCs naturally increase in amplitude and frequency, and speed up their decay kinetics between the ages of 33 and 48 hpf (Chapter 3). This shift in properties is likely due to the appearance of a mature receptor isoform, composed of subunits that are different from the immature receptors. I then speculated that if PKCγ is involved in the maturation of AMPARs, then the properties of the mEPSCs at 33 hpf should be modulated by PKCγ.

6.2.4 Modulation of AMPA mEPSC by PKCγ in 33 hpf zebrafish

To determine if PKCγ was capable of modulating AMPAR properties in 33 hpf embryos, I activated endogenous PKCγ in normal embryos by bath applying 100 nM PMA. This treatment significantly increased mEPSC amplitude (from 24.4 ± 1.4 to 42.6 ± 1.9 pA; n=6, $p < 0.001$; Figure 6.7A,B) and frequency (from 0.7 ± 0.1 to 1.7 ± 0.1 Hz; n=6, $p < 0.001$; Figure 6.7C) and decreased the decay time (from 0.9 ± 0.03 to 0.6 ± 0.04 ms; n=6, $p < 0.001$; Figure 6.7D). The effects of PMA were completely blocked by the PKC inhibitor BIS I (500 nM) (Figure 6.7A-D). PMA had no effect on the 20-80% rise time (n=6, p=0.316). Application of DOG (50 μM) also significantly increased mEPSC amplitude (from 23.8 ± 0.8 to 37.9 ± 3.8 pA; n=6; $p < 0.001$; Figure 6.8A) and frequency (from 0.9 ± 0.1 to 1.9 ± 0.3 Hz; n=6; $p < 0.001$; Figure 6.8B) and decreased the decay time (from 0.79 ± 0.08 to 0.60 ± 0.04 ms; n=6; $p < 0.001$; Figure 6.8D) but had no effect on the 20-80% rise time (n=6, p=0.686; Figure 6.8C). The effects of DOG were completely blocked by the PKC inhibitor BIS I (Figure 6.8A-D). These results were intriguing because they showed that activation of PKCγ led to a rapid speeding of AMPAR kinetics (in 33 hpf embryos), and that the increase in mEPSC frequency was a postsynaptic phenomena rather than a presynaptic effect as it was in the 48 hpf embryos (Chapter 5).

To confirm that these effects were specifically due to PKCγ, I first applied active PKCγ directly to the M-cell cytoplasm of the 33 hpf embryos by including it in the patch pipette and found that it too induced an increase in mEPSC amplitude (from 24.2 ± 1.0 to 38.0 ± 1.6 pA; n=6, $p < 0.001$; Figure 6.9A) and frequency (from 0.9 ± 0.1 to 2.8 ± 0.3 Hz; n=6, $p < 0.001$; Figure 6.9B) and a decrease in the decay time constant (from 0.86 ± 0.03 to 0.56 ± 0.04 ms; n=6, $p < 0.001$; Figure 6.9C). Application of the heat-inactivated PKCγ had no effect on the mEPSC amplitude, frequency or kinetics (n=5; Figure 6.9). I then applied the specific PKCγ inhibiting peptide (γV5-3; 10 nM) to the M-cell cytosol before PMA application, and found that γV5-3 completely blocked the PMA-induced increase in amplitude and frequency, and the decrease in the decay time constant (n=6, $p < 0.001$; Figure 6.10), whereas the control peptide (C1) had no effect (Figure 6.10) (n=5). Application of γV5-3 or C1 alone had no effect on basal mEPSC amplitude.

6.2.4 Trafficking mechanism of AMPA receptors at 33 hpf

To further explore the speeding of the AMPAR kinetics by PKCγ, I analyzed the decay time distributions of AMPA mEPSCs obtained from a variety of experimental procedures. The distributions clearly indicate the appearance of a second (faster) population of events in 33 hpf fish following PMA application (Figure 6.11A), that was similar to the

population at 48 hpf. Furthermore, the faster population upon application of active PKCγ (at 33 hpf) (Figure 6.11B). The events with faster kinetics are absent in the PKCγ-MO injected embryos (at 48 hpf), but can be rescued by injection of PKCγ mRNA rescue (Figure 6.11C). These results suggest that between 33 hpf and 48 hpf there is the appearance of a second subtype of AMPAR. I previously reported that the majority of AMPARs in 48 hpf embryos contained a higher proportion of the GluR2 subunit (Chapter 4). Therefore, I used the specific GluR2 blocker, pentobarbital, and the non-GluR2 blocker, NASPM, to determine if the immature, slower subtype of receptor and the newly inserted faster receptor were different with regard to their GluR2 composition. Pentobarbital (100 μM) reduced the mEPSC amplitude in control recordings of 33 hpf embryos by 64 ± 3% (data from Chapter 4), and by 87 ± 2% (n=5, $p<0.001$) after application of PMA (Figure 6.12). Application of the non-GluR2 blocker, NASPM, (to 33 hpf embryos) gave complementary results; and reduced the mEPSC amplitude by 32 ± 3% in the controls (data taken from Chapter 4), and 11 ± 3% (n=5) after PMA application (Figure 6.12). To confirm that these effects were due to receptor trafficking, I applied the actin-polymerization blocker, latrunculin B (5 μM), and found that it prevented the effects of 100 nM PMA on mEPSC amplitude, frequency and decay time constant (Figure 6.13A-C). Finally, the peptide pep2m, which prevents an interaction between NSF and GluR2, also blocked the effects of PMA mEPSC amplitude, frequency and

decay time constant (n=5, $p < 0.001$; Figure 6.13D-F).The inactive control peptide, pep4c, had no effect (n=5). Together, these findings indicated that a population of AMPARs with faster decay kinetics, and composed of a greater proportion of GluR2-containing receptors, was trafficked to the membrane upon activation of PKCγ.

6.2.5 Activity-dependent speeding of the AMPA kinetics

In Chapter 5, I showed that the trafficking of GluR2-containing AMPARs in 48 hpf embryos was Ca^{2+}- and NMDA-dependent. At 33hpf, intracellular application of the calcium-chelating agent BAPTA (5 mM) blocked the effect of both PMA (100 nM) and DOG (50 μM) on amplitude, frequency and decay time constant (Figure 6.14). I then asked if the insertion of AMPARs at 33 hpf depends upon synaptic activity, and specifically NMDA receptor activity. To address this question, I increased synaptic activation of NMDA receptors by adjusting the extracellular K^+ concentration to a level that significantly depolarized presynaptic terminals. While bath application of 5 mM K^+ may have a number of effects on the preparation, I previously showed that direct depolarization of the M-cell via elevated K^+ did not directly lead to AMPA-R trafficking (Chapter 5). Therefore I was confident that the effects of 5 mM K^+ were due to an increase in synaptic activity. I found that bath application of 5 mM K^+ induced a significant rise in mEPSC amplitude (from 25.5 ± 0.6 to 36.5 ± 2 pA; n=5, $p < 0.001$; Figure 6.15A,B) and frequency (from 0.8 ± 0.1 to 1.7 ± 0.1 Hz; n=5, $p < 0.001$; Figure 6.15C), and a decrease in the

decay time constant (from 0.8 ± 0.06 to 0.5 ± 0.05 ms; n=5, $p < 0.001$; Figure 6.15D), that were prevented by the NMDA receptor blocker, APV (50 μM; Figure 6.15E-G;n=5, $p < 0.001$). Moreover, direct activation of NMDA receptors via bath application of 100 μM NMDA also resulted in an increase in mEPSC amplitude (from 23.0 ± 0.9 to 31.3 ± 1.2 pA,; n=5, $p < 0.001$; Figure 6.16A-C) and frequency (from 0.9 ± 0.07 to 2.4 ± 0.3Hz; n=5, $p < 0.001$; Figure 6.16D) and a decrease in the decay time constant (from 0.85 ± 0.07 to 0.54 ± 0.03 ms; n=5, $p < 0.001$; Figure 6.16E). These effects of NMDA were blocked by inclusion of γV5-3 (10 nM) in the pipette (Figure 6.16). I questioned whether the application of NMDA increased mEPSC frequency by acting pre- or postsynaptically, but the ability of intracellularly administered γV5-3 to completely block the effects of NMDA were consistent with the postsynaptic activation of NMDA receptors located directly on the M-cell.

6.3 Summary

In summary, PKCγ -MO injected embryos are incapable of trafficking AMPARs after application of PMA or intracellular administration of PKCγ. The PKCγ antisense morpholino injected embryos are incapable of hatching and do not exhibit the C-start escape response. Increasing synaptic activity in 33 hpf embryos, via application of an elevated K^+ medium or direct application of NMDA, induces a rapid PKCγ-dependent

trafficking of fast kinetic AMPARs to the synaptic membrane. Taken together, these results suggest that activation of PKCγ is required for the normal developmental switch from slow to fast AMPA receptors in embryonic zebrafish M-cells. Furthermore, this change can be driven by an increase in NMDA receptor activity and may be related to developmental events such as hatching and proper development of the escape response.

Figure 6.1 Generation of the PKCγ morpholino. An antisense morpholino against PKCγ was generated to disrupt the translation of PKCγ transcripts. The morpholino was designed to target 25 bases in the 5' untranslated region (UTR) just upstream of the open reading frame (ORF) of the PKCγ mRNA. PKCγ-MO was injected at the one- to two-cell stage under the blastomeres into the yolk sac.

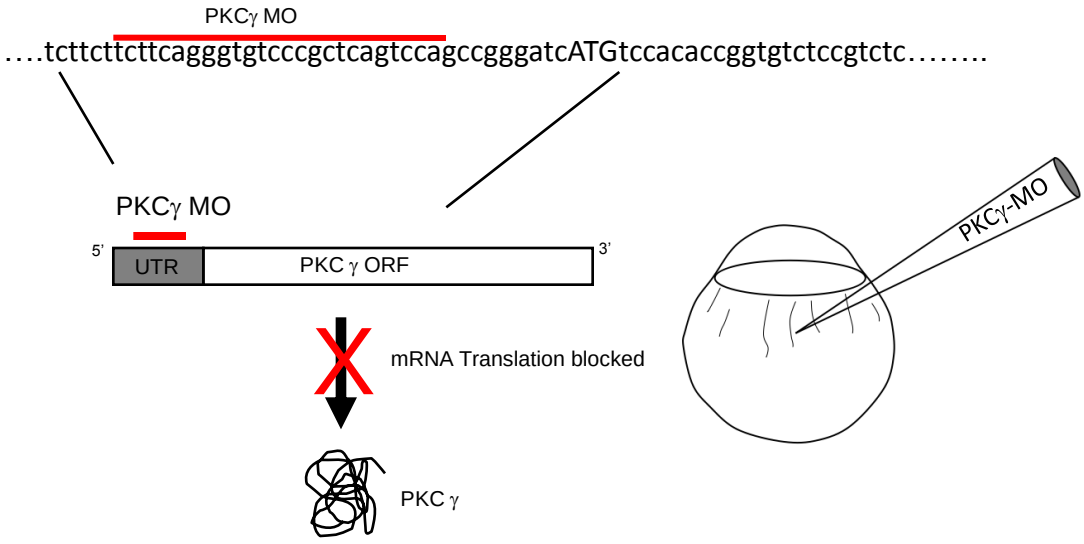
PKCγ MO
….tcttcttcttcagggtgtcccgctcagtccagccgggatcATGtccacaccggtgtctccgtctc……..
PKCγ MO
5'
UTR
PKC γ ORF
3'
mRNA Translation blocked
PKC γ
PKCγ-MO

Figure 6.2 Morpholino knockdown of PKCγ. **A**: Anti-3A10 and anti-PKCγ immunoreactivity in control and PKCγ-MO zebrafish (n=4; an example image is shown). Scale bar = 30 μm. **B**: 100 nM PMA had no effect on the mEPSC amplitude in the PKCγ-MO zebrafish (n=5; $p > 0.001$). **C**: Application of a 5 mM K^+ solution had no significant effect on the mEPSC amplitude (n=5; $p > 0.001$).

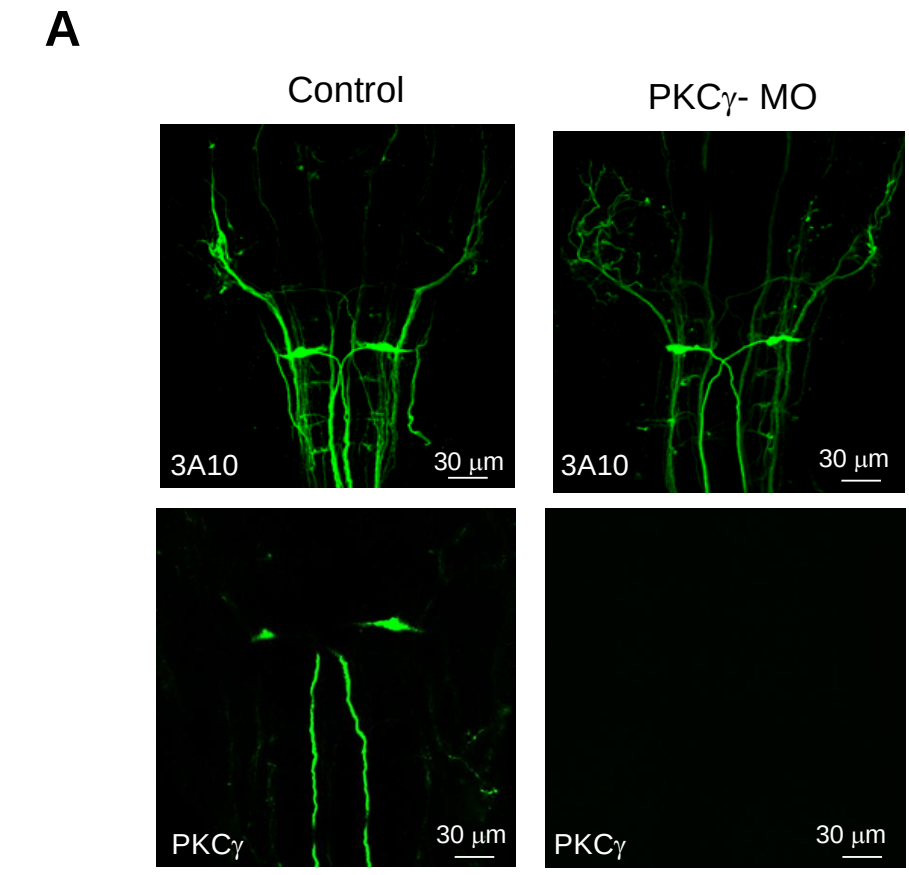
A
Control
PKCγ- MO
3A10
30 μm
3A10
30 μm
PKCγ
30 μm
PKCγ
30 μm

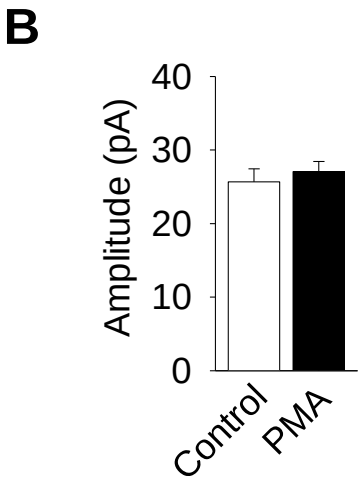
B
Amplitude (pA)
40
30
20
10
0
Control
PMA

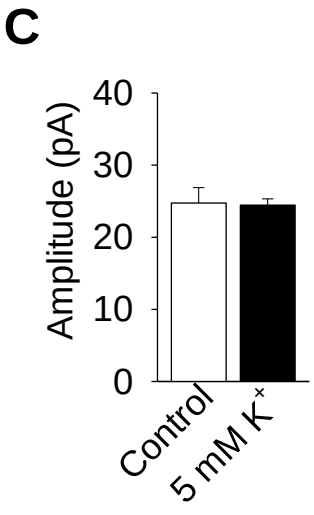
C
Amplitude (pA)
40
30
20
10
0
Control
5 mM K+

Figure 6.3 Specificity of the PKCγ-MO. **A**: Intracellular application of active PKCγ increased the mEPSC amplitude (n=5; $p < 0.001$). **B**: Application of PMA in mRNA rescue zebrafish increased the mEPSC amplitude (n=5; $p < 0.001$). *** Significantly different, $p < 0.001$.

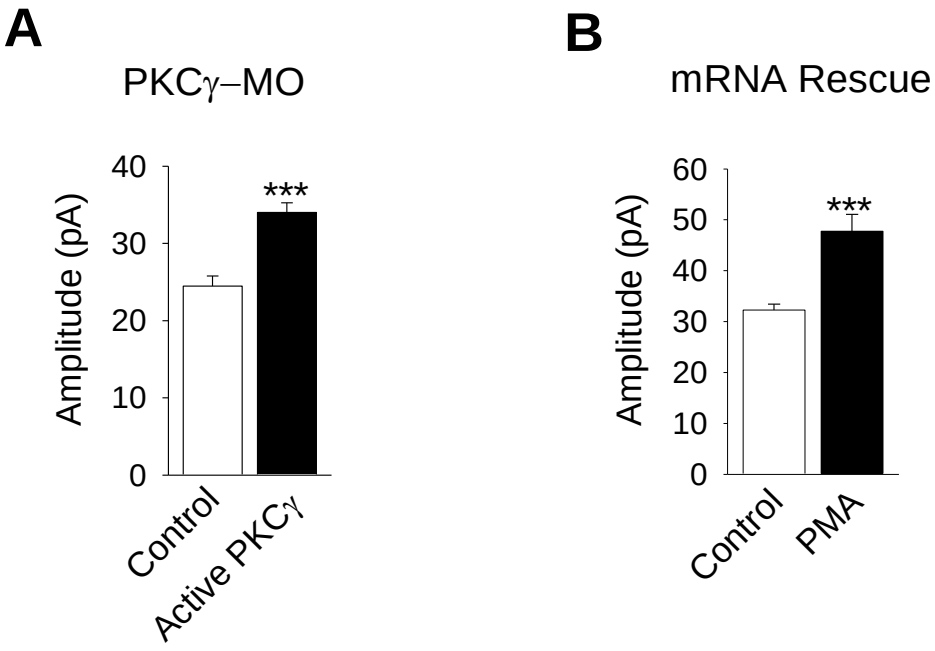
A
PKCγ–MO
Amplitude (pA)
40
30
20
10
0
***
Control
Active PKCγ
B
mRNA Rescue
Amplitude (pA)
60
50
40
30
20
10
0
***
Control
PMA

Figure 6.4 Hatching of PKCγ-MO zebrafish. **A**: Control, PKCγ-MO and mRNA rescue embryos and larvae at different developmental stages. Notice that the PKCγ-MO fish never hatch out of their egg case. **B**: PKCγ-MO injected fish had reduced hatching abilities (n=8; $p < 0.001$) compared with control fish (n=8) and this phenotype was completely rescued in mRNA injected fish (n=8). Scale bar = 15 μm *** Significantly different, $p < 0.001$.

A

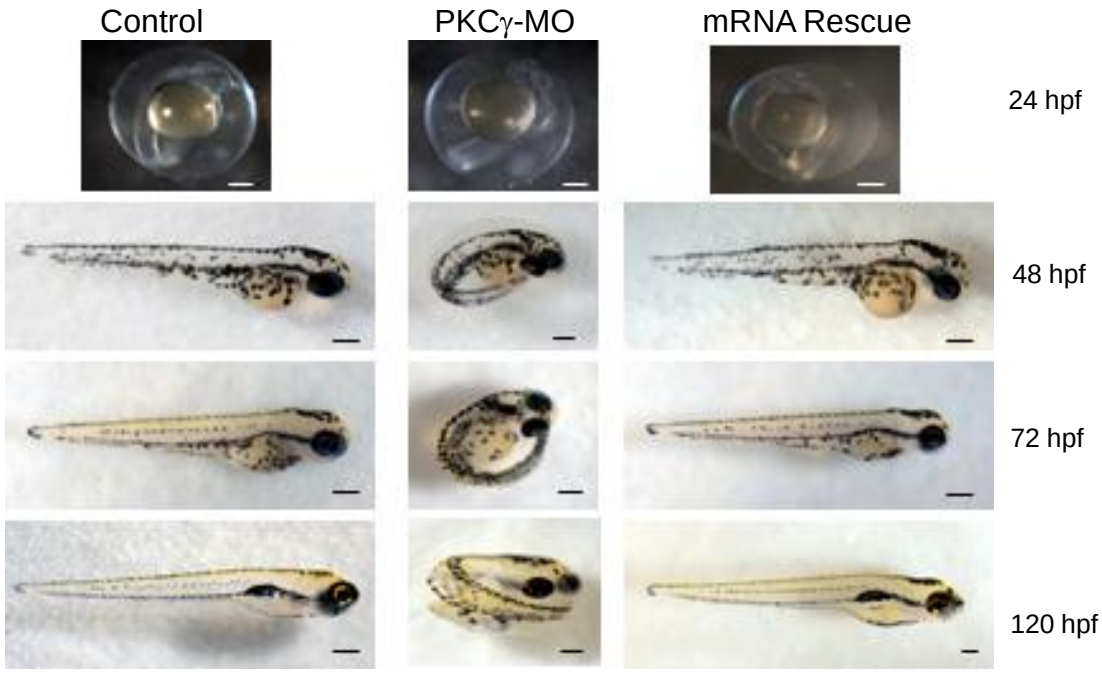
Control
PKCγ-MO
mRNA Rescue
24 hpf
48 hpf
72 hpf
120 hpf

B

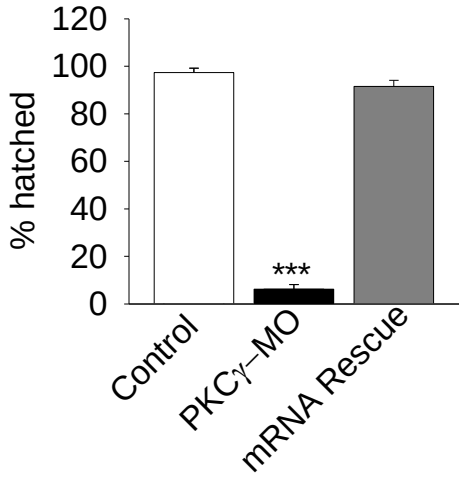
120
100
80
60
40
20
0
% hatched
***
Control
PKCγ–MO
mRNA Rescue

Figure 6.5 Behaviour of PKCγ-MO zebrafish. **A**: Touch responses of control, PKCγ-MO and mRNA rescue fish to a head and tail. (**B**) tap. PKCγ-MO injected fish showed significant reduction in their responses to a head tap (**C**; n=8; $p < 0.001$) or a tail tap (**D**; n=8; $p < 0.001$). Error bars indicate mean ± SEM. *** Significantly different, $p < 0.001$.

A

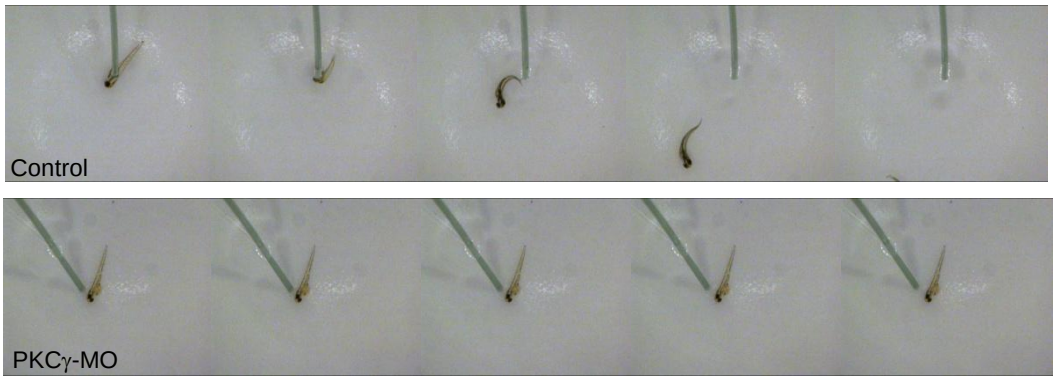
Control
PKCγ-MO

B


Control
PKCγ-MO

C

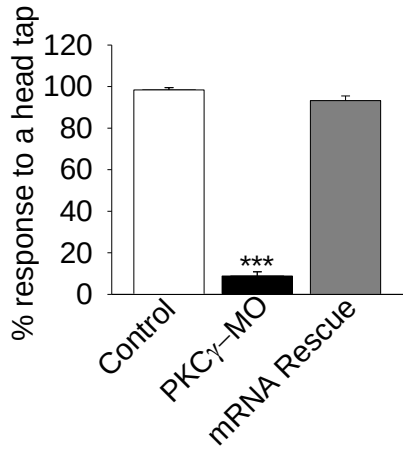
% response to a head tap
120
100
80
60
40
20
0
***
Control
PKCγ–MO
mRNA Rescue

D

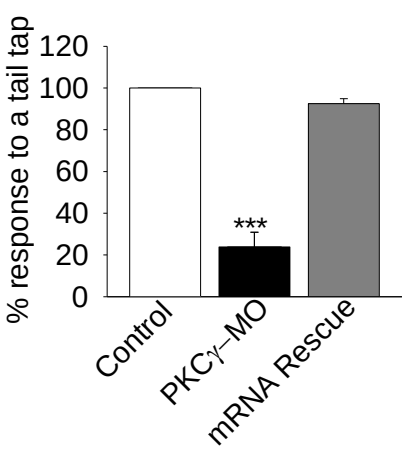
% response to a tail tap
120
100
80
60
40
20
0
***
Control
PKCγ–MO
mRNA Rescue

Figure 6.6 PKCγ-MO fish display immature AMPAR properties. **A**: Averaged mEPSC traces from M-cell recordings in 33 hpf, 48 hpf and 48 hpf PKCγ-MO zebrafish (*upper*). Bar graph of the mEPSC amplitude at 33hpf, 48 hpf and 48 hpf in PKCγ-MO fish (*lower*). **B**: Frequency bar graph of the mEPSCs recorded at 33hpf, 48 hpf and 48 hpf in PKCγ-MO fish. **C**: Superimposed averaged mEPSC (l*eft*). The 48 hpf PKCγ-MO fish display a slower decay time constant than normal 48 hpf fish ($p < 0.001$; *right*; n=6 for 33 hpf . n=8 for 48 hpf and n=8 for 48hpf in PKCγ-MO fish). *** Significantly different, $p < 0.001$.

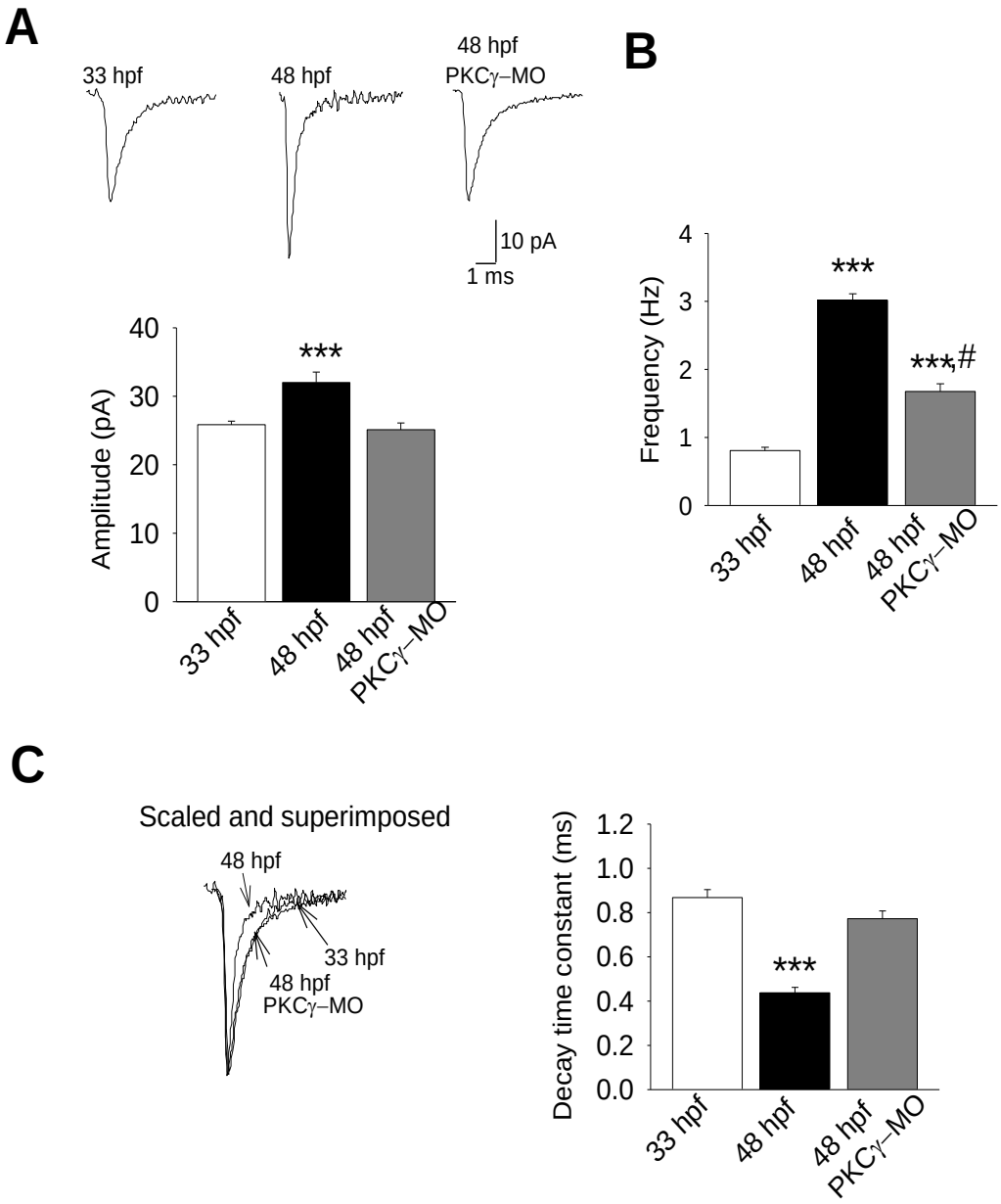
A
33 hpf
48 hpf
48 hpf
PKCγ–MO
10 pA
1 ms
Amplitude (pA)
40
30
20
10
0
***
33 hpf
48 hpf
48 hpf
PKCγ–MO
B
Frequency (Hz)
4
3
2
1
0
***
***,#
33 hpf
48 hpf
48 hpf
PKCγ–MO
C
Scaled and superimposed
48 hpf
33 hpf
48 hpf
PKCγ–MO
Decay time constant (ms)
1.2
1.0
0.8
0.6
0.4
0.2
0.0
***
33 hpf
48 hpf
48 hpf
PKCγ–MO

Figure 6.7 Activation of PKC enhances the amplitude, frequency of and decreases the decay time constant of AMPA mEPSCs. **A**: Representative recordings of mEPSCs in a 33 hpf zebrafish M-cell before and after application of PMA (100 nM) and BIS I (500 nM). Example traces of averaged mEPSC from control (*left*), PMA (*center*) and BIS I + PMA (*right*) recordings. **B**: PMA increased the mean mEPSC amplitude (n=6; $p < 0.001$). **C**: PMA significantly increased the mean mEPSC frequency (n=6; $p < 0.001$). Intracellular application of BIS I (500 nM; n=5), prior to PMA application, blocked the effects of PMA on AMPA mEPSC frequency. **D**: Superimposed traces of the above averaged mEPSC. Note the faster decay time constant in presence of PMA. Application of PMA decreased the decay time constant of the mEPSC (n=6; $p < 0.001$). *** Significantly different, $p < 0.001$.

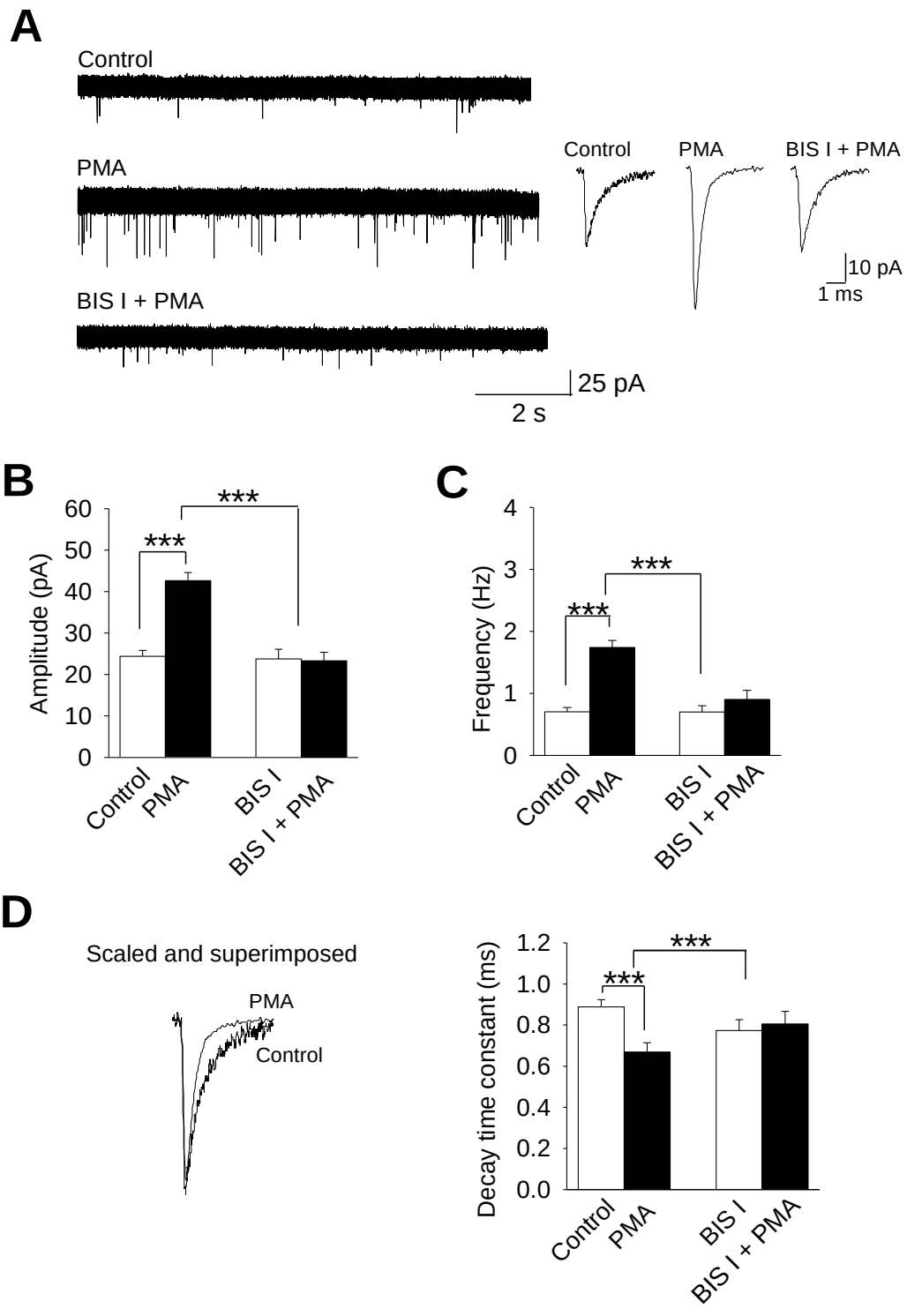
A
Control
PMA
BIS I + PMA
25 pA
2 s
Control
PMA
BIS I + PMA
10 pA
1 ms
B
Amplitude (pA)
60
50
40
30
20
10
0
***
***
Control
PMA
BIS I
BIS I + PMA
C
Frequency (Hz)
4
3
2
1
0
***
***
Control
PMA
BIS I
BIS I + PMA
D
Scaled and superimposed
PMA
Control
Decay time constant (ms)
1.2
1.0
0.8
0.6
0.4
0.2
0.0
***
***
Control
PMA
BIS I
BIS I + PMA

Figure 6.8 Effect of DOG on AMPAR mEPSCs. **A**: Bath application of the DAG analog, DOG (50 μM) increased the mean mEPSC amplitude (n=6; $p < 0.001$). Intracellular application of BIS I (500 nM; n=6), prior to DOG application, blocked the increase in amplitude. **B**: Bath application of the DOG increased the mean mEPSC frequency (n=6; $p < 0.001$) and this effect was completely blocked by BIS I (500 nM; n=6). **C**: There is no change in the 20-80% rise time kinetics following application of DOG (n=6; $p > 0.001$). **D**: DOG decreased the decay time constants of the mEPSC (n=6; $p < 0.001$). *** Significantly different, $p<0.001$.

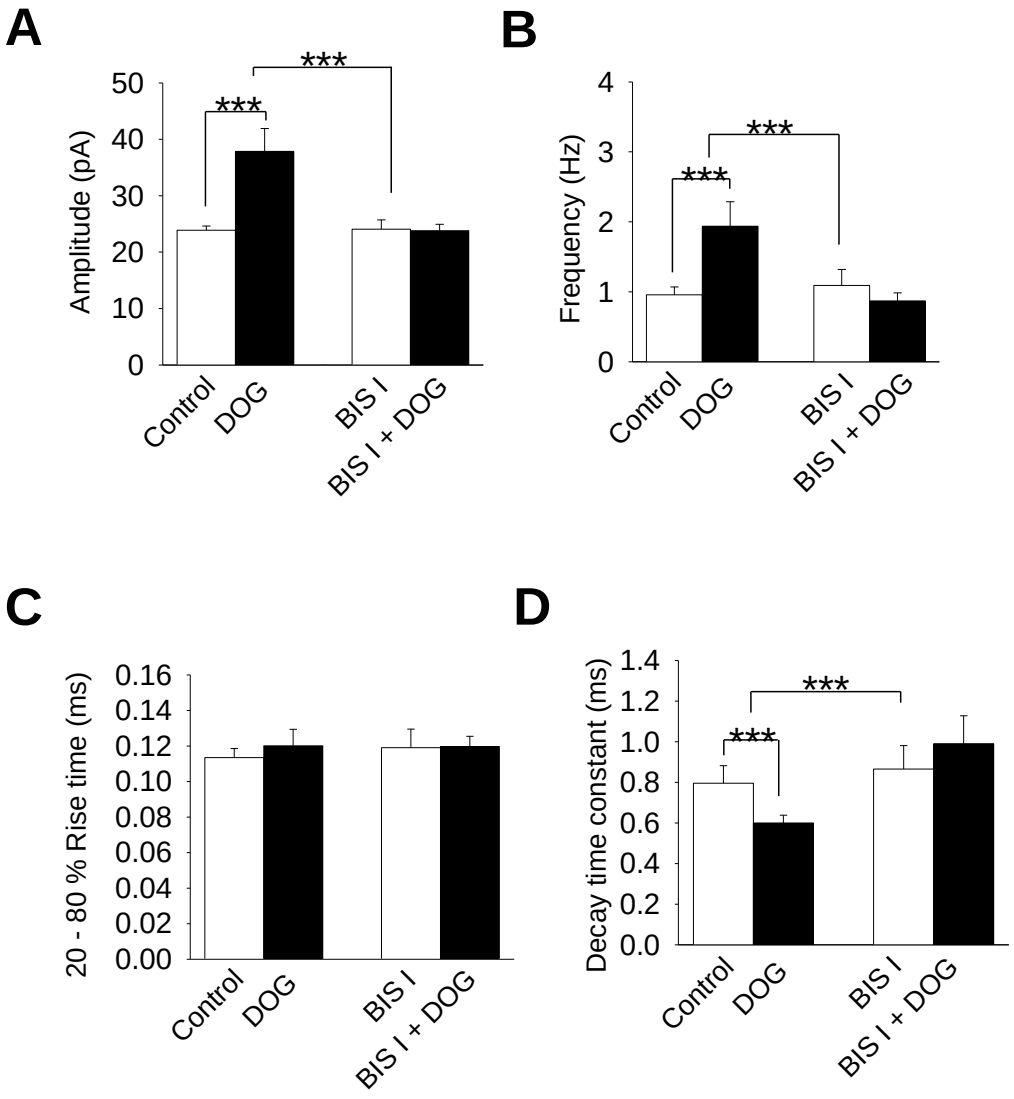
A
B
C
D
Amplitude (pA)
Frequency (Hz)
20 - 80 % Rise time (ms)
Decay time constant (ms)
***
Control
DOG
BIS I
BIS I + DOG

Figure 6.9 Effect of active PKCγ on AMPAR mEPSCs. **A**: Application of active PKCγ (10 ng/μl) increased the mEPSC amplitude (n=6; $p < 0.001$), while the heat-inactivated PKCγ had no effect (n=5; $p > 0.001$). **B**: Active PKCγ increased the mEPSC frequency (n=6; $p < 0.001$), while the heat-inactivated PKCγ had no effect. **C**: Active PKCγ significantly decreased the decay time constant of the mEPSC (n=6; $p < 0.001$), while the heat inactivated PKCγ had no effect (n=5; $p > 0.001$) *** Significantly different, $p < 0.001$.

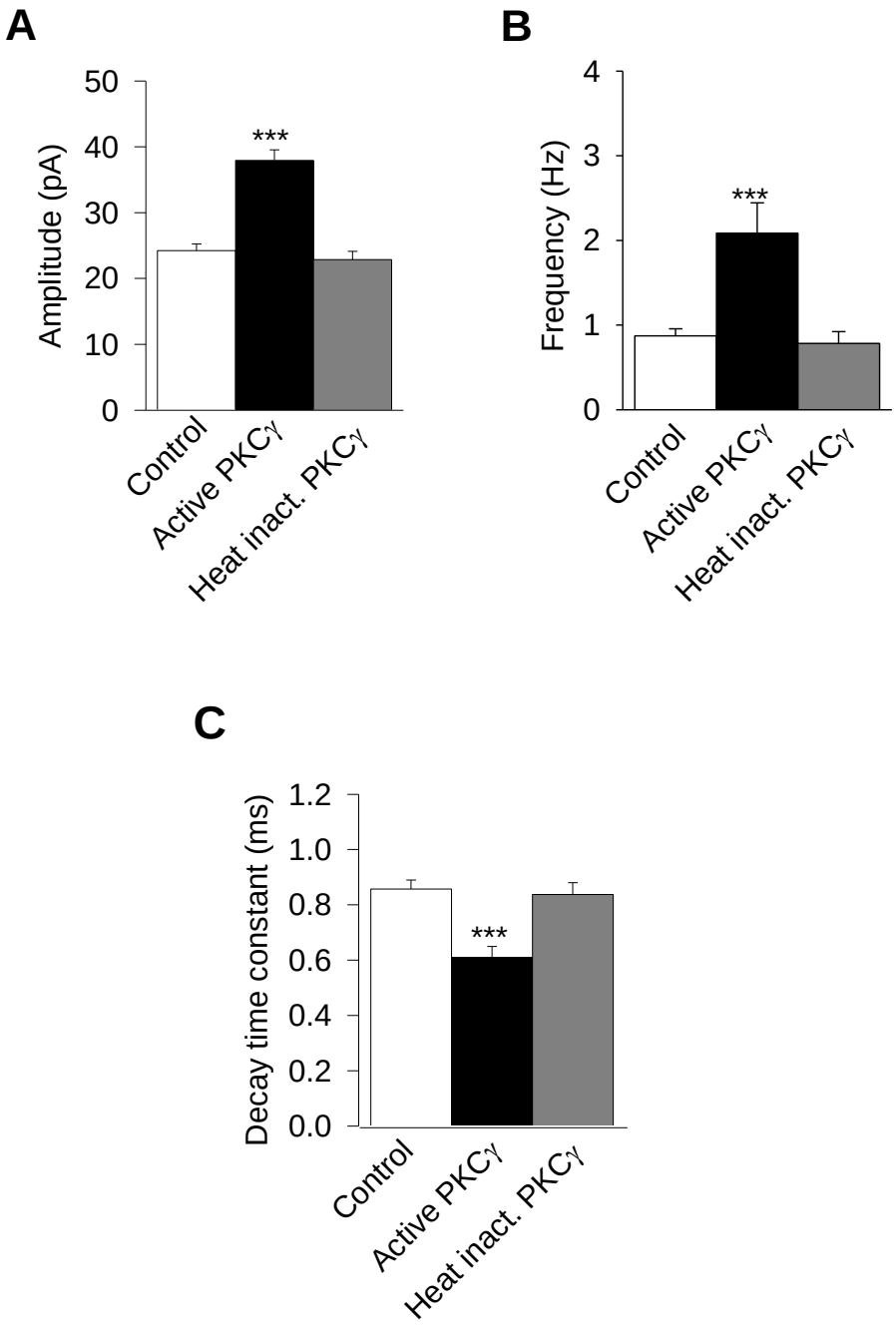
A
B
C
Amplitude (pA)
Frequency (Hz)
Decay time constant (ms)
***
Control
Active PKCγ
Heat inact. PKCγ

Figure 6.10 Inhibiting the activation of PKCγ with γV5-3 blocked the effect of PMA on the mEPSCs. **A**: Intracellular application of γV5-3 (10 nM) blocked the PMA-induced (100 nM) increase in the amplitude (n=6) whereas the control peptide (C1; 10 nM) had no effect (n=5). **B**: Application of γV5-3 (10 nM) blocked the PMA-induced increase in the frequency (n=6) whereas the control peptide (C1; 10 nM) had no effect (n=5).**C**: Application of γV5-3 (10 nM) blocked the PMA-induced decrease in the decay time constant (n=6) whereas the control peptide (C1; 10 nM) had no effect (n=5).*** Significantly different, $p < 0.001$.

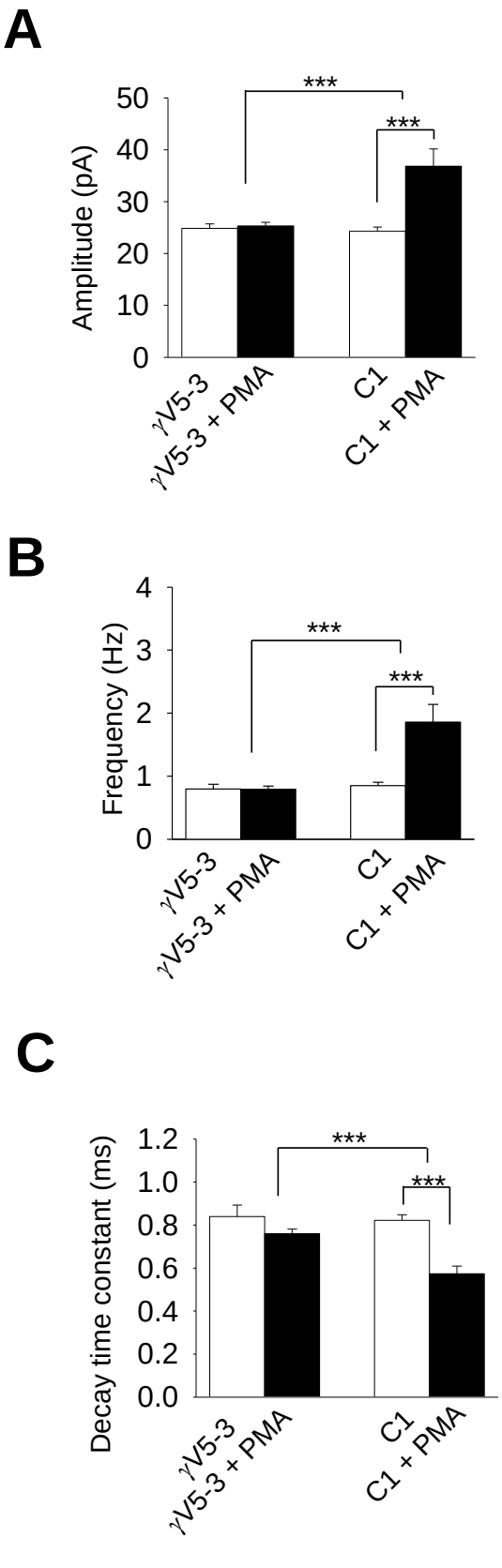
A
***
***
50
40
30
20
10
0
Amplitude (pA)
γV5-3
γV5-3 + PMA
C1
C1 + PMA
B
***
***
4
3
2
1
0
Frequency (Hz)
γV5-3
γV5-3 + PMA
C1
C1 + PMA
C
***
***
1.2
1.0
0.8
0.6
0.4
0.2
0.0
Decay time constant (ms)
γV5-3
γV5-3 + PMA
C1
C1 + PMA

Figure 6.11 Decay time distributions of AMPA mEPSCs. **A**: mEPSCs were obtained from 33 hpf embryos in the presence and absence of PMA (100 nM), and obtained from 48 hpf embryos. **B**: Histogram distributions of the decay time constants of mEPSCs obtained from 33 hpf embryos in the presence of active PKCγ and its control, heat-inactivated PKCγ. The appearance of a second population of events with faster decay kinetics was observed upon application of active PKCγ. **C**: Decay time constant histograms of mEPSCs obtained from PKCγ-injected morpholino (PKCγ-MO) embryos and PKCγ mRNA injected (rescue) embryos at 48 hpf. The arrow indicates the incorporation of a new population of AMPAR with faster decay time constants.

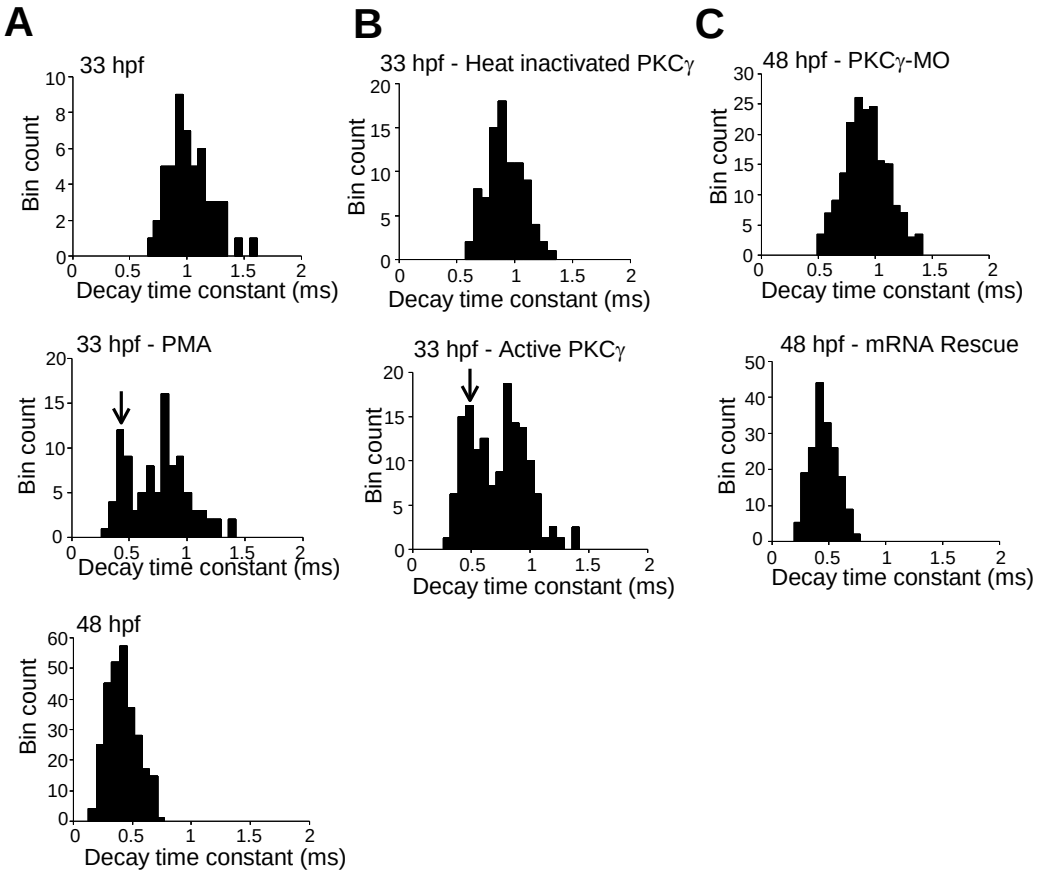
A
33 hpf
Bin count
Decay time constant (ms)
33 hpf - PMA
Bin count
Decay time constant (ms)
48 hpf
Bin count
Decay time constant (ms)
B
33 hpf - Heat inactivated PKCγ
Bin count
Decay time constant (ms)
33 hpf - Active PKCγ
Bin count
Decay time constant (ms)
C
48 hpf - PKCγ-MO
Bin count
Decay time constant (ms)
48 hpf - mRNA Rescue
Bin count
Decay time constant (ms)

Figure 6.12 Activation of PKC induces the trafficking of primarily GluR2-containing AMPARs. Application of the GluR2 blocker, pentobarbital (PB, 100 μM; n=5) in 33 hpf embryos has a significantly greater effect on mEPSC amplitude after 100 nM PMA application (n=5; $p < 0.001$). The non-GluR2 blocker, NASPM (10 μM) had a significantly smaller effect on mEPSC amplitude after administration of PMA (n=5; $p < 0.001$). The data set for the % inhibition of mEPSC amplitude in the presence of PB and NASPM (Chapter 4, Figure 4.7) were used as controls (absence of PMA) in this figure. *** Significantly different, $p < 0.001$.

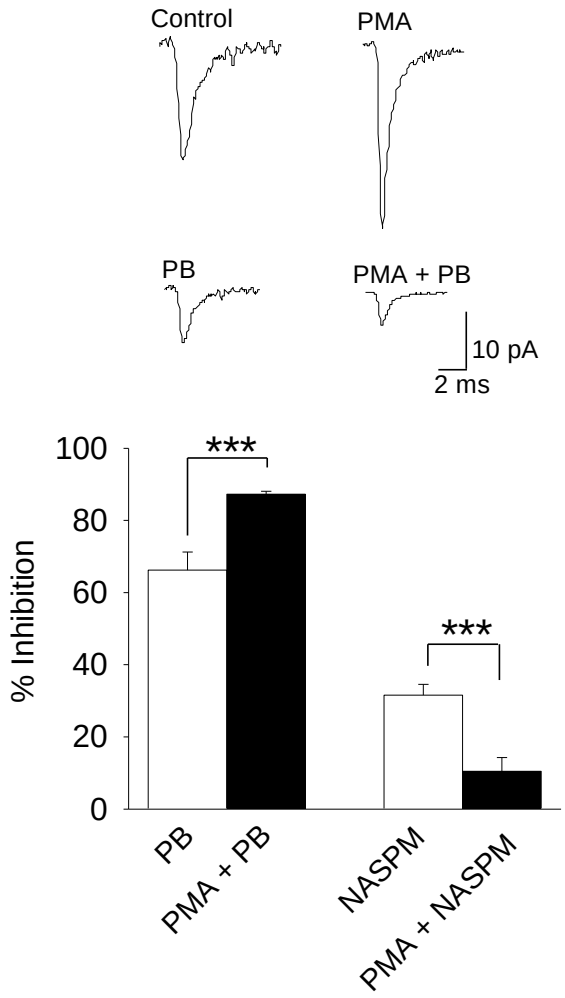
Control
PMA
PB
PMA + PB
10 pA
2 ms
100
80
60
40
20
0
% Inhibition
***
***
PB
PMA + PB
NASPM
PMA + NASPM

Figure 6.13 AMPARs are trafficked to the synaptic membranes in 33 hpf embryos. Latrunculin B (5 μM) blocks the PMA-induced (100 nM) increase in mEPSC amplitude (**A**) and frequency (**B**), and the decrease in the decay time constant (**C**) Intracellular application of the NSF-GluR2 interaction-inhibiting peptide pep2m (200 μM, n=5) blocks the PMA-induced increase in mEPSC amplitude and frequency (**D** and **E**), and the decrease in the decay time constant (**F**). The control peptide, pep4c (200 μM, n=5*)* had no effect (**D-F**). *** Significantly different, $p < 0.001$.

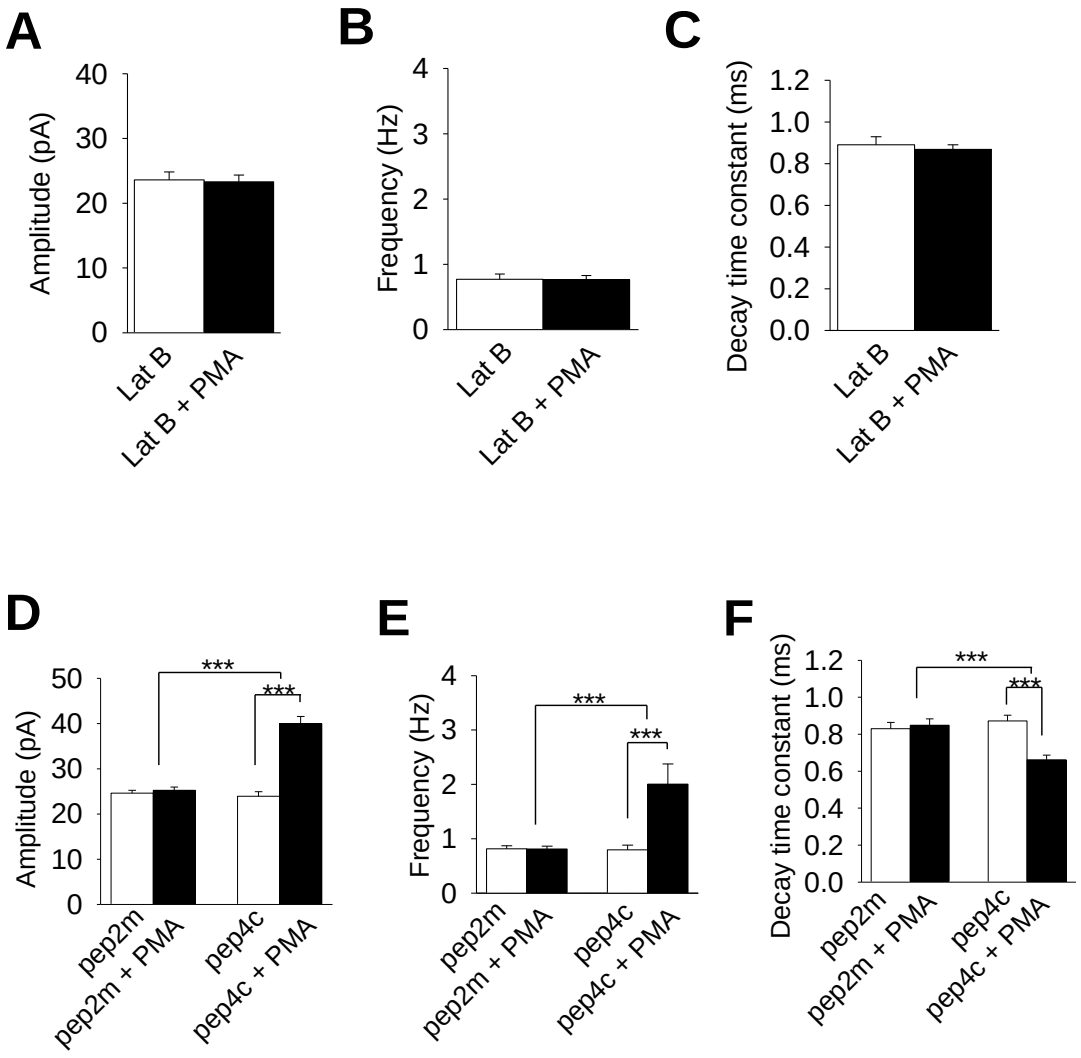
A
Amplitude (pA)
40
30
20
10
0
Lat B
Lat B + PMA
B
Frequency (Hz)
4
3
2
1
0
Lat B
Lat B + PMA
C
Decay time constant (ms)
1.2
1.0
0.8
0.6
0.4
0.2
0.0
Lat B
Lat B + PMA
D
Amplitude (pA)
50
40
30
20
10
0
***
***
pep2m
pep2m + PMA
pep4c
pep4c + PMA
E
Frequency (Hz)
4
3
2
1
0
***
***
pep2m
pep2m + PMA
pep4c
pep4c + PMA
F
Decay time constant (ms)
1.2
1.0
0.8
0.6
0.4
0.2
0.0
***
***
pep2m
pep2m + PMA
pep4c
pep4c + PMA

Figure 6.14 PMA-induced changes in AMPAR properties are Ca^{2+}-dependent. Preventing the rise in intracellular Ca^{2+} by including BAPTA (5 mM) in the patch pipette blocked the PMA-induced (100 nM) increases in mEPSC amplitude and frequency, and decrease in decay time constant ($n=5$; $p < 0.001$).

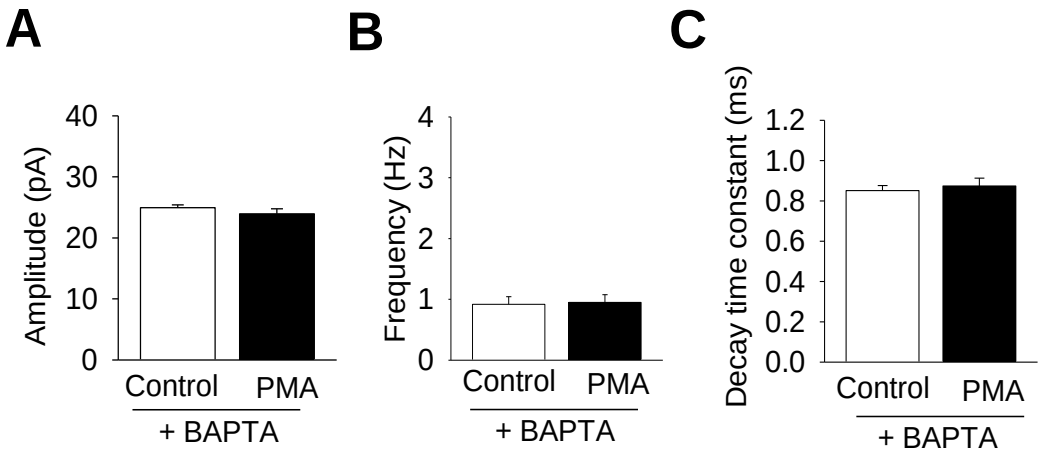
A
B
C
Amplitude (pA)
40
30
20
10
0
Control
PMA
+ BAPTA
Frequency (Hz)
4
3
2
1
0
Control
PMA
+ BAPTA
Decay time constant (ms)
1.2
1.0
0.8
0.6
0.4
0.2
0.0
Control
PMA
+ BAPTA

Figure 6.15 Activity-induced trafficking of AMPARs in 33 hpf embryos. **A**: Representative recordings of mEPSCs recorded in the absence and presence of 5 mM K^+. Application of 5 mM K^+ results in a significant increase in mEPSC amplitude (**B**, n=5; $p < 0.001$) and frequency (**C**, n=5; $p < 0.001$), and a decrease in the decay time constant (**D**, n=5; $p < 0.001$). Bath application of APV (50 μM; n=5) prevented the effects of 5 mM K^+ on amplitude (**E**), frequency (**F**) and decay time constant (**G**). *** Significantly different, $p < 0.001$.

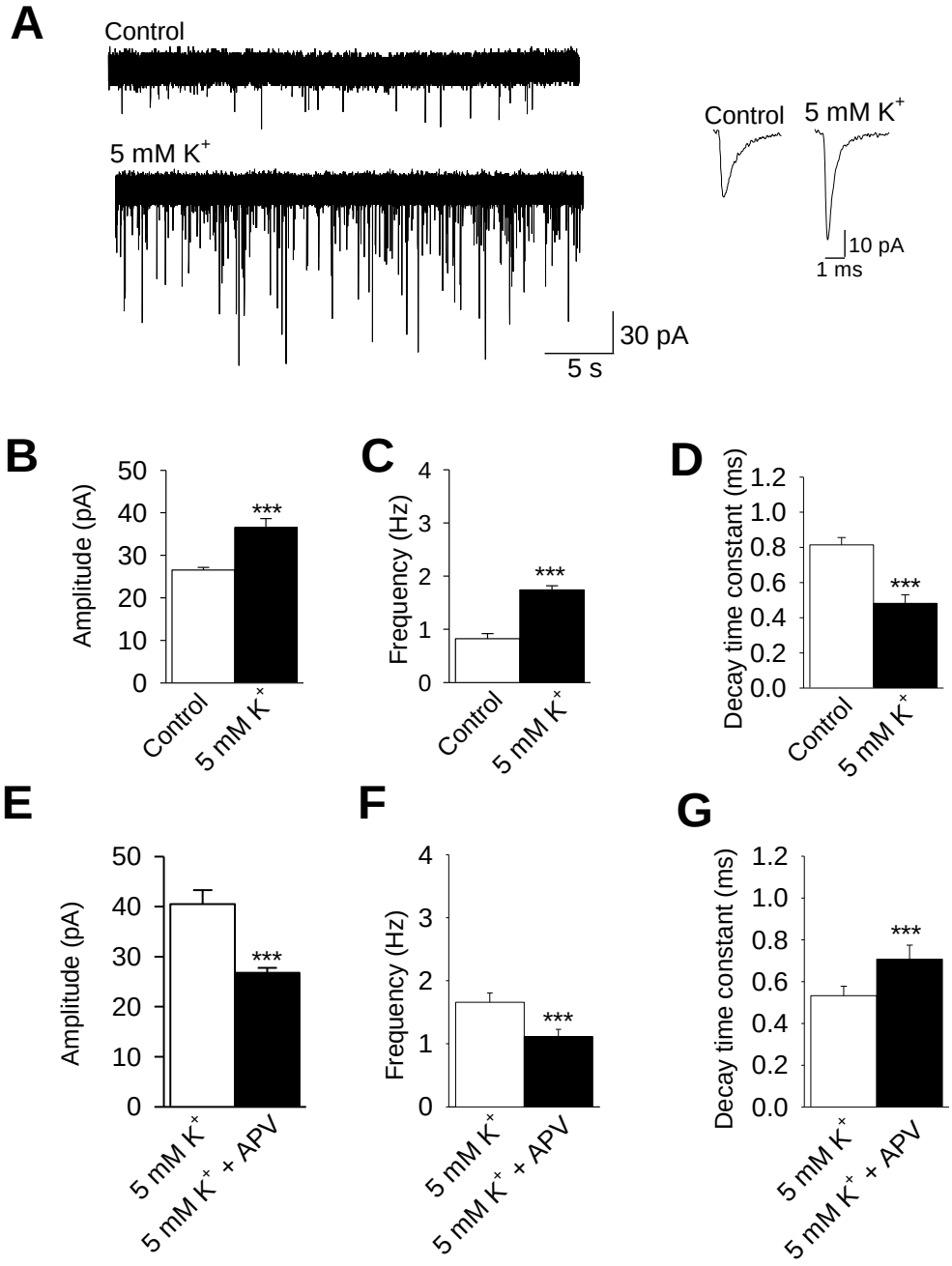
A
Control
5 mM K+
30 pA
5 s
Control
5 mM K+
10 pA
1 ms
B
Amplitude (pA)
***
Control
5 mM K+
C
Frequency (Hz)
***
Control
5 mM K+
D
Decay time constant (ms)
***
Control
5 mM K+
E
Amplitude (pA)
***
5 mM K+
5 mM K+ + APV
F
Frequency (Hz)
***
5 mM K+
5 mM K+ + APV
G
Decay time constant (ms)
***
5 mM K+
5 mM K+ + APV

Figure 6.16 NMDA-induced trafficking of AMPARs is PKCγ-dependent. **A**: Representative recordings of mEPSCs in the presence of NMDA (100 μM) and γV5-3 + NMDA (10 nM + 100 μM, respectively). **B**: Averaged mEPSC traces obtained from 33 hpf embryos on control recordings and after administration of NMDA (n=5), and γV5-3 + NMDA (n=5). Application of NMDA induced a significant increase in mEPSC amplitude (**C**; n=5; $p < 0.001$) and frequency (**D**; n=5; $p < 0.001$), and a decrease in the decay time constant (**E**; n=5; $p < 0.001$), that were all blocked by intracellular administration of γV5-3 (**C-E**; 10nM; n=5; $p < 0.001$). *** Significantly different, $p < 0.001$.

.

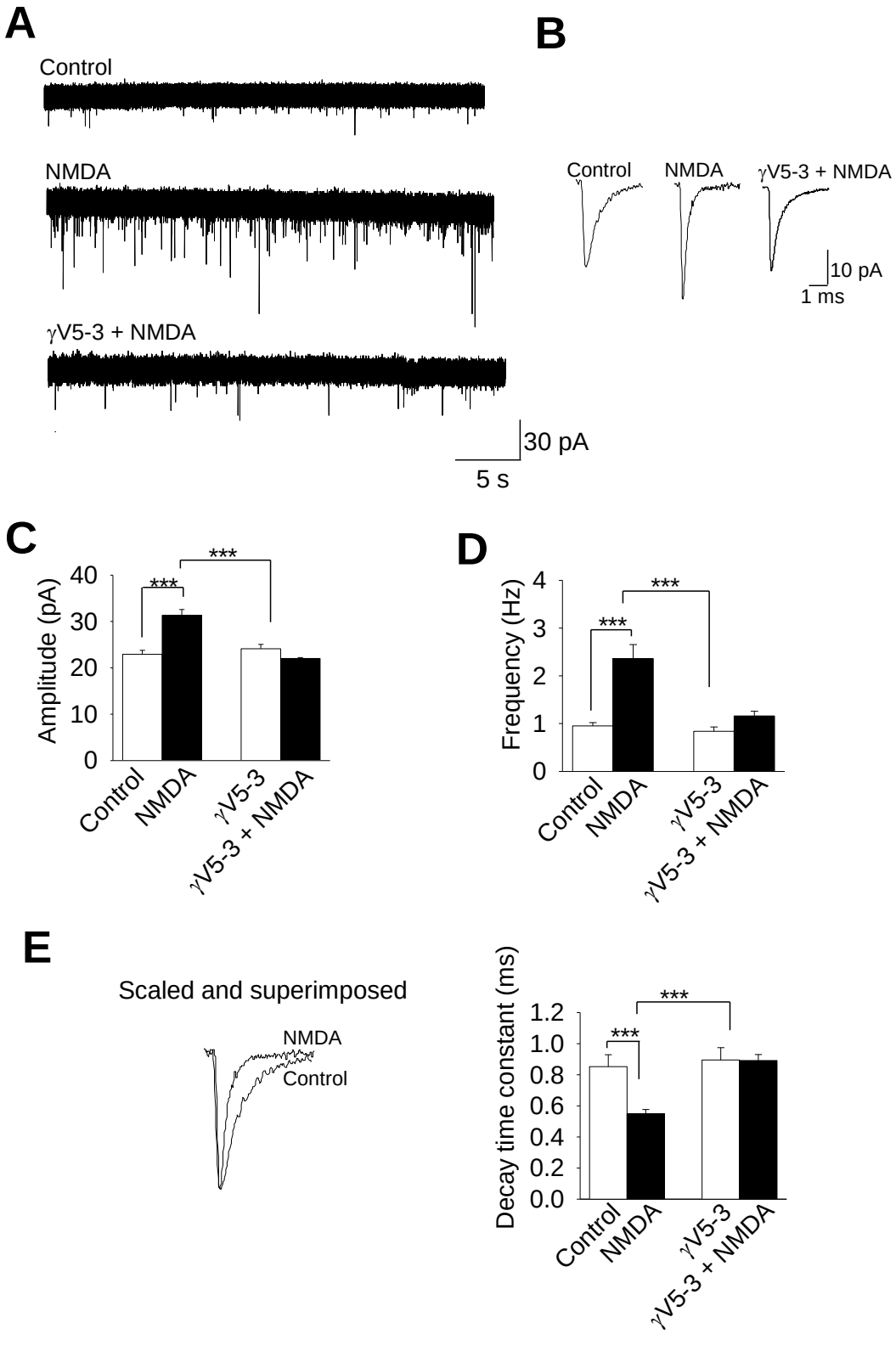
A
Control
NMDA
γV5-3 + NMDA
30 pA
5 s
B
Control
NMDA
γV5-3 + NMDA
10 pA
1 ms
C
Amplitude (pA)
40
30
20
10
0
***
***
Control
NMDA
γV5-3
γV5-3 + NMDA
D
Frequency (Hz)
4
3
2
1
0
***
***
Control
NMDA
γV5-3
γV5-3 + NMDA
E
Scaled and superimposed
NMDA
Control
Decay time constant (ms)
1.2
1.0
0.8
0.6
0.4
0.2
0.0
***
***
Control
NMDA
γV5-3
γV5-3 + NMDA

Chapter 7 Discussion

7.1 Overview of findings

In this thesis, I have described results of experiments designed to characterize the developmental changes in AMPAR-mediated currents in zebrafish M-cells and the mechanisms underlying these changes. In Chapter 3, I showed that there is indeed a developmental change in the AMPAR-mEPSC kinetics in zebrafish M-cells. Recent findings of AMPA-EPSCs in cerebellar granule cells suggested that developmental alterations in the kinetics of AMPAR-mediated currents occur because of changes in synaptic morphology (Cathala et al., 2003) rather than differential subunit assembly, as shown in other systems (Das et al., 1998; Lawrence and Trussell, 2000). In zebrafish, I provided five lines of evidence (Chapter 4) that are consistent with a subunit switching rather than a change in synaptic morphology. First, application of DL-TBOA and KYN did not alter the kinetics of the mEPSC, suggesting that the glutamate concentration in the synaptic cleft did not change during development. The decay time course of AMPAR mEPSCs decreased between 33 and 48 hpf. Second, in 48 hpf fish, the decay time constant was affected by voltage to a much larger degree than it is at 33 hpf. Third, CTZ increased the decay time constant of AMPAR mEPSCs four-fold in 48 hpf fish, but only 1.5-fold at 33 hpf. Fourth, the main single channel conductance of AMPAR at 33 hpf is ~9 pS, but ~15 pS at 48 hpf. Fifth, 48

hpf fish have a higher proportion of GluR2-containing AMPARs than 33 hpf fish. Taken together, these data suggest that the population of AMPARs at 33 hpf is functionally different from that at 48 hpf.

In Chapter 5, I showed that activation of PKCγ enhances AMPAR-mEPSC amplitude in 48 hpf zebrafish by inducing the insertion of GluR2-containing AMPA receptors into synaptic membranes. In addition, the trafficking mechanism requires AMPARs to associate with the scaffolding proteins NSF and PICK1, and occurs through a SNARE-dependent process. To my knowledge this was the first study to report the PKCγ-induced trafficking of AMPARs in an embryonic organism, and one of the few to implicate a combined role for both NSF and PICK1 in the movement and insertion of AMPARs into synaptic membranes. Furthermore, this was the first study to report that PKCγ is necessary for the trafficking of GluR2-containing AMPARs. Several lines of evidence support my conclusions. First, immunohistochemistry suggested that of the conventional PKC isoforms, PKCγ, as opposed to PKCα or PKCβII, is highly expressed in M-cells. Second, application of the active form of PKCγ to the cytosol resulted in an increase in mEPSC amplitude. Third, the PKCγ-blocking peptide γV5-3 completely prevented the effect of PMA. Fourth, peptides that specifically block the association of NSF and PICK1 with the AMPA GluR2 subunit prevented the PMA-induced increase in mEPSC amplitude. Thus, PKCγ is the principal PKC isoform in zebrafish M-cells that is

required for the movement and insertion of AMPAR into synaptic membranes. However, one cannot discount the possibility that other PKC isoforms may be partially involved, but the ability of γV5-3 to completely prevent the 5 mM K^+-induced increase in AMPA mEPSC, indicates that PKCγ is likely to be the principal endogenous PKC isoform involved in this process. These findings indicate that PKCγ is a necessary intermediary in the activity-dependent enhancement of synaptic activity, and that this enhancement primarily occurs via receptor trafficking rather than an up-regulation of channel conductance.

In Chapter 6, I provided strong evidence that PKCγ is necessary for the developmental switch in AMPAR subtypes from slow receptors to fast receptors. This process occurs via trafficking of faster kinetics GluR2-containing AMPARs. The activation of PKC by PMA in 33 hpf zebrafish decreased the decay time constant of AMPAR-mediated miniature EPSCs (Chapter 6). This speeding of mEPSC decay time constant is DAG- and Ca^{2+}-dependent, and occurs upon activation of the conventional PKCγ isoform. Activation of PKCγ led to an increase in synaptic GluR2-containing AMPARs. I showed that the actin-polymerization blocker latrunculin B, and peptide that prevents the association of NSF with the GluR2 subunit, prevented the decrease in mEPSC decay time constant. Increasing synaptic activity in the embryos, via application of an elevated K^+ medium or direct application of NMDA, induced a rapid PKCγ-

dependent trafficking of fast kinetic AMPARs to the synaptic membrane. Finally, targeted knockdown of PKCγ in developing zebrafish reduced the expression of PKCγ and prevented the normal speeding up of AMPAR kinetics. PKCγ knockdown embryos were incapable of trafficking AMPARs after application of PMA or intracellular administration of PKCγ. In addition, embryos lacking PKCγ were incapable of hatching and did not exhibit the C-start escape behaviour. Taken together, our findings reveal the example of a signalling mechanism required for the developmental speeding of AMPARs at excitatory synapses.

During developmental regulation of glutamate synapses, the AMPAR kinetics becomes faster (Das et al., 1998; Brenowitz and Trussell, 2001; Wall et al., 2002). At many central excitatory synapses, the speeding up of AMPAR kinetics occurs via a switch in receptor subtypes (Edmonds et al., 1995; Das et al., 1998; Conti and Weinberg, 1999). However, the mechanisms that underlie the speeding of the AMPAR kinetics still remain controversial (Cathala et al., 2003). This thesis presents the mechanism underlying the developmental speeding of AMPAR kinetics in zebrafish and proposes a model (Figure 7.1) for this process.

Figure 7.1 Model for how activation of PKCγ leads to the speeding of AMPAR kinetics and propably promoting the functional maturation of the glutamate synapse. At 33 hpf, activation of PKCγ recruits AMPARs with faster kinetics to the synaptic membrane via a Ca^{2+}- and NMDA-dependent process. These receptors are then inserted into the membrane upon interaction with the scaffolding protein, NSF. At 48 hpf, there is further trafficking of fast kinetics GluR2-containing AMPARs are inserted into the membrane via NMDA-, PICK1- and NSF- dependent process.

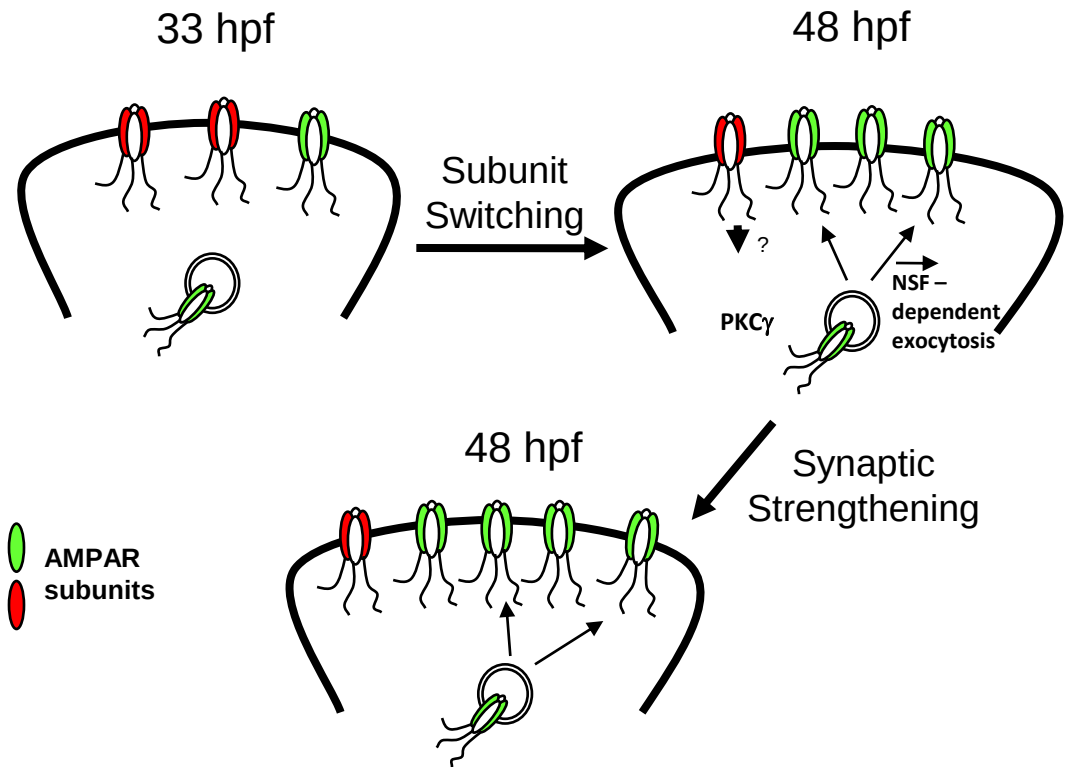
33 hpf
48 hpf
Subunit
Switching
?
PKCγ
NSF –
dependent
exocytosis
48 hpf
Synaptic
Strengthening
AMPAR
subunits

According to this model, the M-cell glutamate synapse is born with slow kinetics AMPARs. Between 33 hpf and 48 hpf, there is an up-regulation of fast kinetics GluR2-containing AMPARs via PKCγ-dependent trafficking mechanisms. By correlated pre- and postsynaptic activity (Chapter 5), GluR2-containing receptors are inserted in the membrane via NSF. At 48 hpf, synaptic maturation is likely complete but there is synaptic strengthening by trafficking of more GluR2-containing AMPARs.

7.2 A developmental switch in AMPAR subunits underlies the changes in AMPAR- mEPSC kinetics

The decay kinetics of AMPAR-mEPSCs can be influenced by a number of factors including the composition of the postsynaptic receptors (Edmonds et al., 1995; Conti and Weinberg, 1999), the rate at which they desensitize (Sucher et al., 1995), the dynamics of glutamate in the synaptic cleft (e.g., release, clearance), and changes in synaptic structure and surrounding neuropil (Cathala et al., 2003). My findings are similar to a number of other studies, which show a developmental speeding of AMPA mEPSC kinetics in preparations such as rat cochlear nucleus (Brenowitz and Trussell, 2001), cerebellar mossy fibre granule cells (Wall et al., 2002), median nucleus trapezoid bodies (Taschenberger and von Gersdorff, 2000) and mammalian neocortical pyramidal neurons (Das et al., 1998). These changes are thought to be brought about by alterations in the composition of the AMPA receptor (Conti and Weinberg, 1999).

Similarly, a switch in receptor subunit composition is thought to underlie the developmental speeding of the decay time course in glycinergic and NMDA receptor-mediated synaptic currents (Hestrin, 1992b; Takahashi et al., 1996; Singer et al., 1998). However, a recent study has shown that the speeding of AMPA EPSC kinetics in mouse cerebellar granule cells occurs via a different mechanism: maturation of synaptic morphology rather than subunit alterations (Cathala et al., 2003). My findings suggest that in zebrafish M-cells, subunit switching is likely to be the main determinant of the accelerated decay of AMPAR-EPSCs.

The decay time constant increased with depolarization at all ages, but it occurred to a greater extent in older animals. A similar voltage-dependent effect on the AMPA mEPSC decay kinetics has been reported (Otis et al., 1996; Glowatzki and Fuchs, 2002; Morkve et al., 2002); however, it is not known which subunit (s) might be responsible for this property (Morkve et al., 2002). I observed a significant difference in the % increase in the decay time constant with depolarization between 33 hpf and 48 hpf animals, suggesting that the receptor gating properties contributing to the EPSC decay kinetics are different at those ages. Since receptor gating properties are dependent on the receptor's subunit composition, it is likely that the AMPARs in M-cells undergo a developmental switch in their subunit composition.

One of the most compelling findings was the differential effect of CTZ at 48 hpf compared with 33 hpf. The dramatic increase in τ at 48 hpf but not at 33 hpf, suggests that the alternatively spliced, flip variant is present in greater quantities in older animals. CTZ blocks desensitization of AMPARs and preferentially has a stronger effect on the flip forms of the subunits (Partin et al., 1994). Thus the differential effects of CTZ at 48 hpf and 33 hpf argue in favour of the flop form associated with M-cells early in development, with the emerging onset of the flip version sometime later. This contrasts with a recent study showing that both forms increase in expression during the zebrafish development, but there is no change in the ratio of the flip and flop splice variants (Rial Verde et al., 2006). However, even though the overall ratio of flip and flop splice variants in the whole animal does not change during development, there might still be changes in the expression levels of the flip and flop variants in the M-cells.

I found that in older animals, the AMPARs exhibited outward rectification while the I-V relationship was linear at 33 hpf. The shape of the I-V curve is dependent on subunit composition (Verdoorn et al., 1991). AMPAR subunits GluR1, GluR3 and GluR4, in homomeric or heteromeric assembly, form strong inward rectifying receptor channels that are highly permeable to Ca^{2+}. However, co-assembly of any of these subunits with the edited GluR2 subunit results in a linear I-V relationship or outward rectification (Verdoorn et al., 1991; Morkve et al., 2002). The mechanisms

that give rise to linear or outwardly rectifying I-V curves are not well understood. However, it is known that assemblages of AMPARs with varying proportions of GluR2 subunits yield I-V curves with different degrees of rectification (Hollmann et al., 1991; Hollmann and Heinemann, 1994). Interestingly, in a study on hippocampal neurons, AMPA currents that exhibited a linear I-V relationship had a substantial permeability to Ca^{2+}, while cells that showed an outward rectification were Ca^{2+} impermeable (Lerma et al., 1994). Therefore, both types of receptor assembly can co-exist in the same cell resulting in a linear I-V relationship (Lerma et al., 1994). Thus, the fact that I detected only a linear I-V relation in young animals, and only outward rectification in older fish, supports the view that the population of AMPARs is different between the two ages. Interestingly, outward rectification of AMPAR currents can be induced by site-directed mutagenesis of single amino acid residues (Dingledine et al., 1992). Hence, a different amino acid identity between mammalian and zebrafish AMPAR subunits may underlie the rectification properties found in my study.

The small but significant developmental increase in mEPSC amplitude (Chapter 3) could be due to a number of factors, including an increase in :1) the number of postsynaptic receptors, 2) single channel conductance, 3) quantal content or 4) a change in synaptic morphology. My findings show that AMPARs on 33 hpf M-cells exhibited a smaller

conductance (~ 9 pS) than those at 48 hpf (~15 pS). My findings are similar to those observed in other systems where values of ~8-10 pS and 15-20 pS have been found (Morkve et al., 2002; Cathala et al., 2003; Momiyama et al., 2003; Bannister et al., 2005). The conductance of AMPARs is critically dependent upon subunit composition (Swanson et al., 1997), suggesting that the different conductances observed at 33 hpf and 48 hpf are due to separate population of AMPARs at these two ages.

Furthermore, I found that the relative proportion of GluR2 subunits in the M-cells increases at 48 hpf. Interestingly, Lin et al., (2006) showed that during zebrafish development and starting 30 hpf onwards, the amount of GluR2 transcripts clearly exceeds the total amount of GluR1, GluR3 and GluR4 transcripts. My findings indicate that the AMPARs at the ages examined here contain at least one GluR2 subunit and that the overall receptor subunit assembly probably changes between 33 hpf and 48 hpf to incorporate more GluR2 subunits. While my results strongly suggest that a subunit switch occurs, they are not conclusive; the precise difference in AMPAR subunit composition between two age groups still needs to be elucidated. Preliminary data using single-cell reverse transcriptase-PCR (RT-PCR) confirmed the expression of GluR2 in 48 hpf M-cells. I have also performed immunohistochemistry experiments to analyze the expression of the GluR subunits in zebrafish. I have used a number of different antibodies generated against mammalian GluR

subunits; however none of them were specific enough to detect zebrafish GluR subunits. Furthermore, it is also possible that unknown developmental mechanisms may account for a number of the changes that I observed.

In the absence of PKCγ (PKCγ-MO-injected embryos), the developmental speeding of AMPAR kinetics does not occur. Results in Chapter 6 are consistent with the presence of different populations of slow and fast mEPSCs at 33 and 48 hpf, respectively. The population of fast events can be rapidly recruited at 33 hpf following activation of PKCγ by PMA or DOG, or by direct application of PKCγ to the M-cell cytosol. Thus, the receptors are probably located close to the synapse and are ready to be trafficked to the membrane upon activation by the appropriate signal. In PKCγ-MO-injected embryos, no treatment (except for bypass with PKCγ mRNA rescue) was capable of inducing either the increase in mEPSC amplitude, or the switch to faster kinetics (Chapter 6), suggesting that PKCγ is absolutely required for AMPAR trafficking over the short term and the long term. I found that the actin polymerization blocker latrunculin B, and a peptide which interferes with the interaction of GluR2 with the trafficking protein NSF, pep2m, are both capable of blocking the effect of PMA. Furthermore, that pentobarbital and NASPM were capable of blocking significantly different proportions of receptors before and after

PKCγ activation suggest that the populations contained different numbers of GluR2-containing receptors.

7.3 Trafficking of AMPARs by PKCγ

AMPAR trafficking upon PKC activation is well known to underlie synaptic plasticity phenomena in LTP and LTD (Chung et al., 2000; Matsuda et al., 2000; Malinow and Malenka, 2002; Rial Verde et al., 2006). For instance, PKC is required to drive the insertion of GluR2-containing receptors to the synapse during 5-HT-induced LTP in dorsal horn neurons (Huang et al., 1987; Kose et al., 1990; Tanaka and Saito, 1992). Similarly, in hippocampal neurons, synaptic incorporation of AMPARs during LTP is also controlled by PKC (Boehm et al., 2006, Ling et al., 2006; Yao et al., 2008). Perez and colleagues (2001) have shown that PKC regulates the trafficking of GluR2-containing AMPAR to spines in hippocampal neurons during LTD, and loss of AMPARs from the synaptic membrane during LTD has been reported in hippocampal and Purkinje cells (Daw et al., 2000; Kim et al., 2001). To my knowledge, my work is the first study to report a role for PKCγ in the trafficking of GluR2-containing AMPARs. The involvement of other PKC isoforms such as PKCα and PKMζ in the trafficking of GluR2 AMPARs has been documented (Ling et al., 2006; Yao et al., 2008; Daw et al., 2000; Perez et al., 2001). At hippocampal synapses, GluR2-GRIP/ABP interactions retain AMPARs in intracellular stores and phosphorylation by PKCα releases these receptors

for insertion into the synaptic membrane (Daw et al., 2000). PKCγ is the most abundant PKC isoform in the cerebral cortex and hippocampus, and in cerebellar Purkinje cells (Herms et al., 1993). It has been implicated in synaptogenesis (Abeliovich et al., 1993b; Abeliovich et al., 1993a; Kano et al., 1995) and synaptic plasticity (Abeliovich et al., 1993b).For instance, PKCγ knockout mice have impaired LTP in the hippocampus (Kano et al., 1995). They exhibited mild deficits in motor coordination tasks (Abeliovich et al., 1993a) and in spatial and contextual learning (Kano et al., 1995). Furthermore, PKCγ activity seems to control the elimination of climbing fibers during cerebellar development because Purkinje cells from PKCγ mutant mice persist with multiple climbing fibers into adulthood (Chavez-Noriega and Stevens, 1994; Tomita et al., 2003). PKCγ expression is highly restricted to the M-cells in embryonic zebrafish and that it plays a key role in trafficking of AMPARs (Chapter 5). Knockdown of PKCγ in zebrafish prevented the proper AMPAR synaptic development and resulted in fish that exhibit major deficits in hatching and escape responses. However, the effects of the loss of PKCγ in the PKCγ-MO cannot be solely attributed to the impairment in AMPAR trafficking.

The amplitude and kinetics of AMPAR mEPSCs were similar in the PKCγ-MO-injected and uninjected embryos. Furthermore, the γV5-3 peptide and peptides that block the interaction of NSF and PICK1 with GluR2 had no effect on properties of basal AMPAR mEPSCs. Thus,

PKCγ-induced AMPAR trafficking via NSF and PICK1 is not part of the signalling mechanism that governs the initial production and placement of receptors into synaptic membranes. In addition, for receptor turnover to proceed, there must be a signal to remove the slow kinetic receptors from synaptic membranes while the mature receptors are trafficked and inserted into synapses. At present, the identity of the signals and the mechanisms involved in these processes are unclear.

7.4 PKCγ-induced trafficking of AMPARs requires PICK1 and NSF

PKCγ-induced trafficking of AMPARs in embryonic zebrafish depends on PICK1 and NSF. PICK1 has been implicated in a number of physiological and pathological situations that involve regulating the surface expression of the GluR2-containing AMPARs. Interestingly, in most of these events, PICK1 decreases GluR2 surface expression in a PKC-dependent mechanism (Lu and Ziff, 2005). In contrast, my findings showed that PICK1 is involved in a PKCγ-driven insertion of AMPARs into the membrane. This role is consistent with the previously proposed idea that PICK1 regulates the recruitment of GluR2-containing AMPARs to hippocampal synapses (Daw et al., 2000). As well as simply regulating the number of AMPARs at the synapse, recent reports suggest that PICK1 is involved in mechanisms that switch the subunit composition of synaptic AMPARs. More specifically, PICK1 appears to regulate the GluR2 content

of synaptic receptors, which in turn determines their Ca^{2+}-permeability. For instance, PICK1 mediates a switch from GluR2-containing to GluR2-lacking AMPARs in dopaminergic neurons in the ventral tegmental area following exposure to cocaine (Bellone and Luscher, 2006). This presumably occurs via PICK1-dependent removal of GluR2-containing receptors from the synapse in conjunction with insertion of GluR2-lacking receptors. In cerebellar stellate cells, Ca^{2+}-permeable AMPARs that do not contain GluR2 subunit are replaced in an activity- and PICK1-dependent manner by Ca^{2+}-impermeable receptors containing GluR2 (Gardner et al., 2005; Liu and Cull-Candy, 2005). In this case, PICK1 appears to be involved in the trafficking of GluR2-containing receptors towards the synaptic plasma membrane. My work indicates that PICK1 is important for the up-regulation of synaptic GluR2-containing AMPARs. I found that the EVKI peptide that specifically blocks the association of PICK1 with AMPA GluR2 subunit prevented the PMA-induced increase in mEPSC amplitude decrease in decay time constant. These results suggest a possible novel role for PICK1 in synaptic development mediating a switch from slow to fast AMPAR kinetics.

As PICK1, NSF is also involved in various receptor trafficking events and has been shown to bind directly to the GluR2 subunit (Nishimune et al., 1998; Osten et al., 1998). The primary role of NSF is to facilitate the rapid incorporation of GluR2-containing AMPA receptors into postsynaptic membranes (Lin and Sheng, 1998; Lee et al., 2002; Gardner

et al., 2005; Huang et al., 2005). Interfering with the GluR2-NSF interaction by using peptides caused a rapid decrease in synaptic strength by reducing the surface expression of AMPARs (Nishimune et al., 1998; Carroll et al., 1999b). In this thesis, I found that blockade of the GluR2–NSF interaction with pep2m (Chapters 5 and 6) prevented the PMA-induced increase in mEPSC amplitude and decrease in the decay time constant, presumably by inhibiting the trafficking of GluR2-containing AMPARs. Recent findings suggest that binding of NSF to GluR2 stabilizes a population of AMPARs in the plasma membrane and makes them resistant to regulated endocytosis. Thus it is not clear whether, in my study, the blocking peptide pep2m leads to impairment in the delivery of AMPARs to the synaptic plasma membrane or to a decrease in the stability of AMPARs in the membrane after they were successfully delivered. Nearly all intracellular membrane fusion events require the association of NSF and SNARE complexes. Therefore, NSF is probably involved in the actual trafficking of GluR2-containing AMPARs in my study since disruption of the SNARE complexes prevented the effects of PKCγ on AMPA mEPSCs. Braithwaite et al., (2002), showed that only regulated but not constitutive cycling of GluR2 is dependent on NSF binding. This finding correlates well with my experimental data, where I found that the complete block of the PKCγ-induced increase in mEPSC amplitude with pep2m is activity-dependent.

Although the direct target of PKCγ cannot be identified through my work and could be one of multiple postsynaptic proteins, biochemical data indicates that the PKC phosphorylation site, S880, on GluR2 is a very likely candidate for this regulation. Several studies have shown that PICK1 also regulates the surface expression of GluR2-containing AMPARs (Perez et al., 2001; Terashima et al., 2004) and this regulation is associated with the PKC phosphorylation of S880 on the C terminal of GluR2 (Perez et al., 2001; Chung et al., 2002). Phosphorylated S880 promotes binding of PICK1 to GluR2 and this interaction leads to either endocytosis of the receptors (Chung et al., 2002, Perez et al., 2001; Terashima et al., 2004; Lu and Ziff, 2004) or trafficking of AMPARs to the plasma membrane (Daw et al., 2000; Hanley et al., 2002; Gardner et al., 2005). Therefore it is likely that a similar mechanism is involved in my study, but further work is required to prove the actual link between PKCγ and PICK1 in the trafficking of AMPARs. Interestingly, my data showed the requirement of both NSF and PICK1 for the trafficking of AMPARs to the synaptic membrane. According to Hanley et al. (2002), NSF functions to dissociate PICK1 from GluR2 subunit; the removal of PICK1 allowing the GluR2 subunit to enter the membrane. Hence, at developing M-cell synapses, activation of PKCγ might lead to phosphorylation of intracellular GluR2-containing AMPARs (probably at the S880 site). Interaction of the phosphorylated GluR2-containing AMPARs and PICK1 then promotes movement of the endosome to the plasma membrane where binding of

NSF dissociates PICK1 and allows insertion of the receptor in the membrane.

7.5 Developmental increases in the mEPSC frequency

Application of PMA and DOG led to large increases in mEPSC frequency (Chapters 5 and 6). The ability of BIS I, pep2m and γV5-3 (applied to the cytosol of the M-cell via the patch pipette) to completely block the PMA-induced increase in mEPSC frequency at 33 hpf (Chapter 6) indicates that the effect on frequency is postsynaptic in origin. This differs markedly from the results on 48 hpf embryos where the effect of PMA on mEPSC frequency was assumed to be presynaptic in origin since addition of the inhibitors in the patch pipette had no effects on the induced changes in mEPSC frequency (Chapter 5). The postsynaptic increase in mEPSC frequency is probably due to the insertion of AMPARs into silent synapses. Therefore, synaptic maturation might follow a paradigm similar to LTP, whereby silent synapses contain primarily (or only) NMDA receptors, and as development proceeds, PKCγ is activated and it starts to traffick GluR2-containing AMPARs into synaptic membranes (Figure 7.2).

Figure 7.2 Proposed model for the postsynaptic increase in mEPSC frequency. Some synapses contain only NMDA receptors, and as NMDARs are activated, it allows and influx of Ca^{2+} in the postsynaptic cell. This leads to the activation of PKCγ which then allows trafficking and insertion of GluR2-containing AMPARs into the plasma membrane. This trafficking process is actin-, PICK1- and NSF-dependent.

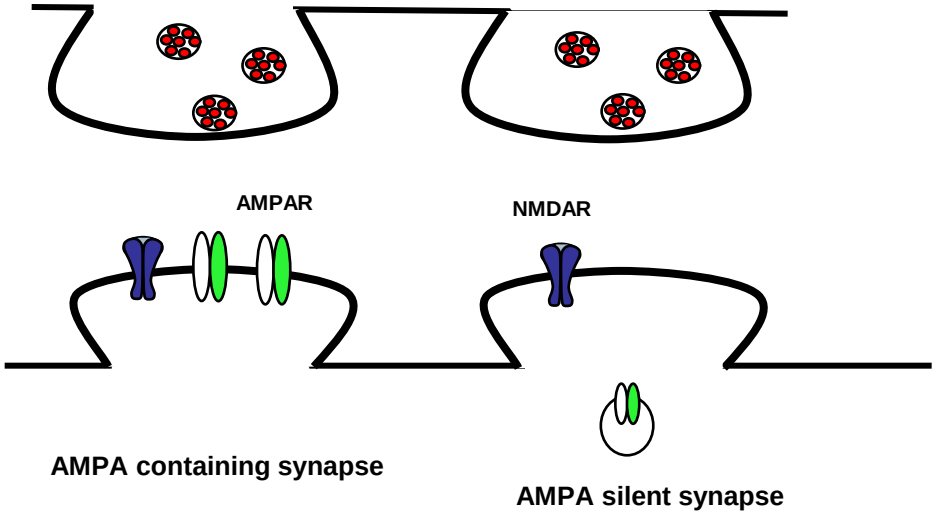

NMDA-dependent
activation of PKCγ

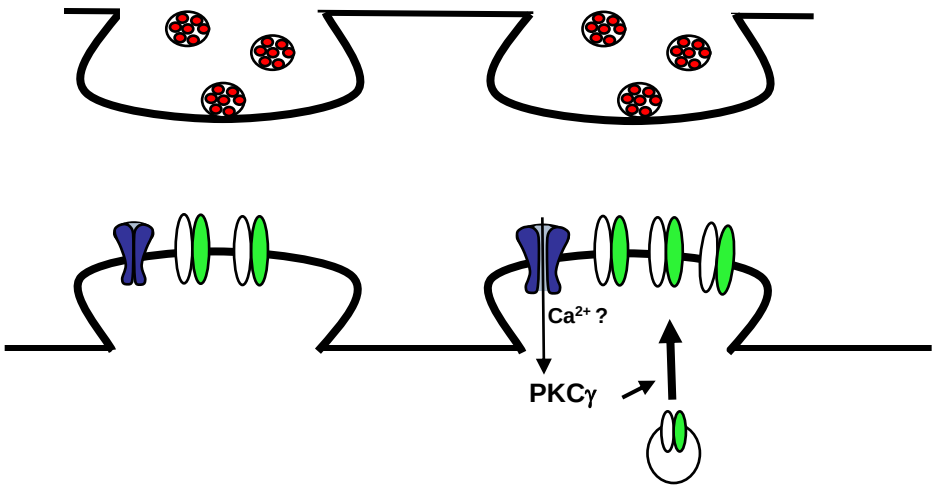

However, the PKCγ-mediated insertion of AMPARs at silent synapses by PKCγ cannot fully account for the observed developmental increase in mEPSC frequency. This is because the mEPSC frequency recorded in 48 hpf PKCγ-knockdown fish is higher than that recorded in normal 33 hpf fish. Experimental data in chapter 4 demonstrated that there is no change in the glutamate concentration in the synaptic cleft between 33 hpf and 48 hpf. Thus, the developmental increase in mEPSC frequency is probably not due to presynaptic mechanisms, but occurs via postsynaptic mechanisms linked to an increase in the number of synaptic AMPARs. Indeed, the basal level of AMPA responses was not affected in PKCγ knockdown fish. Therefore, there must be another mechanism for synaptic insertion of AMPAR for basal activity. The insertion mechanism responsible for basal transmission is probably required for synaptic formation. Synapses are also equipped with the full, functional machinery for PKCγ-dependent AMPAR trafficking which quickly can be utilized once the developing synapses receive the “correct” type of activity pattern. This trafficking mechanism might allow synapses to now become stable and mature.

The presynaptic increase in mEPSC frequency at 48 hpf, after application of PMA, is consistent with other studies and may be due to an increase in the vesicle recycling rate, an increase in the size of the readily releasable pool, an increase in presynaptic Ca^{2+} influx, or the induction of new release sites (Parfitt and Madison, 1993). In hippocampal CA1

pyramidal cells, mEPSC frequency is potentiated by PMA in a PKC-dependent manner (Bouron, 1997). PKC also potentiates transmitter release from *Aplysia* sensory neurons and from cholinergic nerve terminals of autonomic ganglia and neuromuscular junctions (Bachoo et al., 1992; Byrne and Kandel, 1996; Somogyi et al., 1996; Redman et al., 1997). However, phorbol esters have also been shown to increase the frequency of mEPSCs by potentiation of the neurosecretion signalling pathway independent of PKC (Redman et al., 1997; Searl and Silinsky, 1998; Silinsky and Searl, 2003). For example, in a study of mossy fibre terminals in the mouse hippocampus, phorbol esters were found to increase the mEPSC frequency (Honda et al., 2000). However, this increase was not affected by PKC inhibitors but mediated by activation of Munc13-1 which is a non-PKC phorbol ester receptor that plays a crucial role in the process of neurotransmitter release (Augustin et al., 1999; Honda et al., 2000; Silinsky and Searl, 2003). In the zebrafish preparation, PMA increases the mEPSC frequency but whether this increase occurs upon action of PKC or Munc13-1 is unknown.

7.6 Activity-dependent trafficking of AMPARs

How is PKCγ activated during development? This remains to be determined but may simply be due to an increase in synaptic activity. In this thesis, I found that neuronal activity induced by elevating the extracellular K^+ levels led to an increase in mEPSC amplitude and a

decrease in the decay time constant at 33 hpf. These effects were due to the trafficking of AMPARs via activation of endogenous PKCγ since the effects of the 5 mM K^+ solution on mEPSCs were completely occluded by active PKCγ and blocked in the presence of the PKCγ inhibitory peptide, γV5-3. It is well established that neuronal depolarization with elevated K^+ (chemical stimulation) evokes Ca^{2+}-dependent exocytosis of synaptic vesicles and release of endogenous neurotransmitter from presynaptic terminals. My results also suggest that the depolarization of the afferents, by the 5 mM K^+ solution, onto M-cells induces the trafficking of AMPARs by activating PKCγ. Chemical stimulation protocols has been shown to target the same subcellular machinery in the induction of synaptic potentiation as electrical stimulation (Huang and Malenka, 1993; Hanse and Gustafsson, 1994; Hosokawa et al., 1995). However, it is most likely that the major difference between these methods of potentiation lies in the proportion of synapses that are strengthened, rather than in the induction mechanism. It will be interesting to test whether a similar trafficking mechanism occurs upon electrical stimulation of the presynaptic cells in this preparation. One might argue that use of an elevated K^+ is an unphysiological way to induce synaptic potentiation. It is likely that this *in vitro* stimulation protocol is unphysiological in comparison to the *in vivo* situation. But *in vitro* stimulation protocols are widely used to enhance synaptic activity and have had a significant impact on our understanding of synaptic function in aspects of development and plasticity. The DPP

protocol can also induce the potentiation of mEPSC amplitudes. This potentiation is not dependent on NMDAR activation but rather requires an increase in intracellular calcium levels via voltage-gated calcium channels (Baxter and Wyllie, 2006). The potentiation described in my thesis is NMDA-dependent, and thus explains why the DPP protocol had no effect on mEPSC amplitudes in the M-cell. Furthermore, my findings also suggest the voltage-gated calcium channels have virtually little or no role in the trafficking of AMPARs in zebrafish M-cells.

The changes in the properties of AMPA mEPSCs by K^+ were completely blocked in the presence of the NMDA antagonist, APV. Furthermore, when NMDA receptors were directly activated via application of NMDA, there was an increase in PKCγ-dependent trafficking (Chapter 6). Therefore, NMDA receptor activity is capable of inducing the rapid trafficking of AMPARs, but it is still unclear whether NMDA activity is necessary for the developmental switch in AMPARs.

Most forms of synaptic plasticity require intracellular Ca^{2+} signals to trigger appropriate regulated AMPAR trafficking events. I found that postsynaptic Ca^{2+} is required for trafficking of AMPARs. There are several potential Ca^{2+} sources in the postsynaptic neuron, including NMDAR channels, mGluR-activated Ca^{2+} release from internal stores, voltage-gated calcium channels and Ca^{2+} permeable AMPARs. In this thesis, NMDARs are likely to be the major source for Ca^{2+} since AMPAR

trafficking is completely blocked by the addition of APV (Chapters 5 and 6). However, there may exist compensatory mechanisms such that different Ca^{2+} sources which may compensate for each other for the induction of AMPAR trafficking. Thus, it remains to be tested whether combinations of antagonists of NMDARs and blockers of voltage-gated calcium channels and/or mGluRs are effective. Several types of voltage-gated calcium channels (L, N, P/Q, R and T-types) exist postsynaptically. L-type channels are activated at depolarized potentials while the other types are largely inactivated. AMPAR trafficking did not occur when the postsynaptic cell is depolarized by the DPP protocol (Chapter 5), thus L-type channels cannot be responsible for AMPAR trafficking. However, the N-,P/Q-, R- and T- type channels could be involved in providing a certain level of resting Ca^{2+} concentration, that might be necessary for the induction of AMPAR trafficking. The GluR2-lacking Ca^{2+}-permeable AMPAR is also a very good candidate. However, the findings in this thesis do not support an important role for Ca^{2+}-permeable AMPARs. The blocker of Ca^{2+}- permeable AMPARs (NASPM), had no effect on AMPAR trafficking. However, these results may not conclusively rule out the potential role for Ca^{2+}-permeable AMPARs for the induction of AMPAR trafficking. In summary, the inhibition of AMPAR trafficking with intracellular BAPTA shows that postsynaptic Ca^{2+} is somehow necessary for the induction of AMPAR trafficking, but the Ca^{2+} source remains elusive.

7.7 Functional Significance

Spontaneous mEPSCs play a pivotal role in shaping the time course of the action potential during evoked excitatory synaptic transmission (Renger et al., 2001; Cathala et al., 2003). Thus, alterations in the properties of the mEPSCs will impact cell excitability and may have a broad impact on neuronal function. The slow AMPAR-mEPSC associated with 33 hpf zebrafish M-cells could potentially serve to increase the depolarization associated with each quanta, such that the Mg^{2+} block of synaptic NMDAR is more effectively relieved in order to mediate plasticity and Ca^{2+}-dependent neuronal processes early in development. On the other hand, speeding of the mEPSC decay contributes to faster rising EPSPs (Galarreta and Hestrin, 2001; Cathala et al., 2003) and allows synaptic potentials to repolarize quickly, thereby minimizing inactivation of voltage-gated Na^{+} channels (Futai et al., 2001; Takahashi, 2005). Thus, at 48 hpf, AMPAR currents may contribute to a faster rising EPSP, short duration action potential and a reduced spike latency. Indeed, the M-cell spike of zebrafish embryos (24 hpf) is longer in duration and smaller in amplitude than in larvae (48 hpf) (Eaton et al., 1977b; Eaton and Nissanov, 1985).

What might be the physiological significance of this speeding in AMPAR kinetics? Current theory suggests that this phenomenon occurs in order to ensure temporal precision of synaptic transmission and increased efficiency of information transfer (London et al., 2002). This is thought to

contribute to a refinement of motor co-ordination and increases in the precision of sensory perception and cognition (Galarreta and Hestrin, 2001; Cathala et al., 2003; Takahashi, 2005). For example, at the calyx of Held, a brainstem auditory relay synapse, synaptic transmission is unreliable for high frequency inputs at immature synapses and postsynaptic action potentials (APs) follow presynaptic APs only up to a frequency of 10 Hz (Futai et al., 2001). However, as animals mature, the synapse gradually becomes able to follow high frequency input up to 400 Hz. This high-fidelity transmission is acquired via developmental speeding of the time course of EPSCs and permits sound localization on the basis of interaural time differences (Reyes et al., 1996). The M-cell receives sensory inputs and it has to fire to activate motoneurons in the spinal cord to initiate muscle contraction. The developmental speeding of the M-cell AMPA kinetics may make coincidence detection more stringent and shift the optimum frequency range over which this crucial circuit functions. In my thesis, I have shown that AMPARs switch subunits (and exhibit faster kinetics) between 33 and 48 h, immediately before hatching. At 24 hpf, zebrafish embryos acquire a touch/startle response (Saint-Amant and Drapeau, 1998). However, synaptic development continues, and at around 48 hpf, embryos start to hatch out of the egg casing, at which point they can swim away from a stimulus. Thus, the generation of faster currents would likely lead to a more efficient and a stronger startle response once the fish is out of the egg case. The perceived advantage of this would be

to be able to mount an escape response when the fish is free-swimming in a predator rich environment.

Furthermore, embryonic M-cells also fire spontaneously up to the time of hatching. It is believed that this spontaneous activity of the M-cell results in strong tail contractions (similar to those occurring during a startle response) that can rupture the egg case. Thus, the M-cell initiated escape response has been suggested to play an important role in hatching (Eaton and Nissanov, 1985). I have shown that activation of PKCγ is necessary for the developmental speeding of AMPAR kinetics at M-cell synapses, and that PKCγ-MO-injected embryos are unable to hatch out of their egg envelope and exhibit poor touch responses. It is possible that the inability to generate faster AMPA currents in PKCγ-MO fish might have severe consequences on M-cell excitability which, in turn, may prevent hatching and robust escape responses. However, the importance of the speeding of the decay time for normal zebrafish behavioural development remains elusive.

The developmental speeding of the AMPARs is the result of a switch in AMPAR subunits (Chapter 4). Altering the synaptic AMPAR subunit composition is a mechanism for the control of neuronal excitability and development (Takahashi et al., 1996; Pellegrini-Giampietro et al., 1997). During development, there is an up-regulation in synaptic GluR2

content in many systems. For instance, in hippocampal neurons (Pickard et al., 2000) and in neocortical pyramidal neurons (Kumar et al., 2002), the relative abundance of GluR2 at synaptic AMPARs increases with development. These studies along with mine demonstrate an increase in synaptic GluR2 AMPARs during synaptic development, suggesting that the alterations in GluR2 content may be a common feature of neuronal development. The developmental switch in GluR2 expression results in an alteration in the Ca^{2+} permeability of AMPARs (Geiger et al., 1995; Gu et al., 1996; Washburn et al., 1997; Yin et al., 1999). For example, in spinal interneurons of *Xenopus* embryos, there is a transient occurrence of Ca^{2+}-permeable AMPARs early in development. As development proceeds, there is a decrease in the Ca^{2+}-permeability due to an increase in the GluR2-containing AMPARs (Rohrbough and Spitzer, 1999). Ca^{2+} influx through GluR2-lacking AMPAR is thought to play a critical role in synaptogenesis and in the formation of neuronal circuitry during early development (McDonald and Johnston, 1990). In fact, the increase in $[Ca^{2+}]$ is crucial for growth cone movements and experience-dependent modifications of synaptic connection (McDonald and Johnston, 1990). An increase in GluR2-containing AMPAR is thought to modify the efficacy of synaptic transmission (Liu and Cull-Candy, 2000). Furthermore, because the activation of GluR2-lacking AMPAR can lead to Ca^{2+}-mediated excitotoxic neuronal cell death, the switch in AMPAR phenotype could provide a developmental mechanism regulating the Ca^{2+} level in cells.

Indeed, knockdown of GluR2 in rat by antisense oligonucleotides causes Ca^{2+}-mediated death of pyramidal neurons (Oguro et al., 1999). GluR2 and its appropriate regulation is critical not only for AMPAR function but also for normal brain function (Monyer et al., 1992; Brusa et al., 1995; Gerlai et al., 1998; Hartmann et al., 2004; Shimshek et al., 2006a; Shimshek et al., 2006b). For instance, GluR2 -/- mice exhibit a wide variety of profound detrimental phenotypes in synaptic function, development, and behaviour (Jia et al., 1996; Gerlai et al., 1998; Yan et al., 2002; Shimshek et al., 2006a; Shimshek et al., 2006b). Moreover, there is considerable evidence that disruption in GluR2 function is associated with several neurological disorders such as cerebral ischemia, amyotrophic lateral sclerosis, pain, and epilepsy (Cull-Candy et al., 2006). The low GluR2 content at 33 hpf may be important to allow enough influx of Ca^{2+} into the M-cells for proper synaptogenesis and formation of the escape response circuitry. On the other hand, the up-regulation of GluR2 at 48 hpf is likely crucial for normal startle behaviour. Further work is needed to investigate the Ca^{2+}-permeability of AMPARs at 33hpf and 48 hpf.

7.7 Future Research

In my thesis, I have shown that the population of AMPARs at 33 hpf is functionally different from that at 48 hpf (Chapter 4) and there is an increase in GluR2-containing AMPARs. However, the precise composition of the AMPARs at each developmental stage remains to be examined. Further work is required to confirm the developmental switch in AMPAR subunits and to fully characterize the zebrafish M-cell AMPARs. Using single-cell RT-PCR, I confirmed the expression of GluR2 in 48 hpf M-cells but the expression analysis of all of the 4 GluR subunits zebrafish M-cells still needs to be investigated. To accurately identify the AMPAR subunit composition in developing M-cells, quantitative PCR could be performed. In addition, the identity of the AMPAR subunit composition in zebrafish M-cells could be determined using microarray analysis of cDNA from 33 hpf and 48 hpf and immunohistochemical analysis. I have already tested a number of different antibodies generated against mammalian GluR subunits, but none have been specific enough to detect zebrafish GluR subunits. Therefore, antibodies specific to zebrafish GluRs have to be produced before immunohistochemical analysis of the expression of AMPAR subunits in M-cells can be achieved. Lastly, to fully characterize M-cell AMPARs, the Ca^{2+} permeability of these receptors at 33 hpf and 48 hpf needs to be determined.

PKCγ-induced trafficking of AMPARs in zebrafish depends on NSF and PICK1, but the entire cascade of events underlying this process is

unknown. For instance, we still do not know what the substrate for PKCγ is, or how PKCγ recruits PICK1? These questions would need to be answered if we are to fully understand the PKCγ-induced trafficking of AMPARs in zebrafish. Based on the current literature, PKCγ is likely to phosphorylate the S880 site of the GluR2 subunit, which allows it to interact with PICK1 and be inserted into the membrane. Attempts using a commercial antibody generated against rat anti-phospho-GluR2 (S880) to investigate whether this site was phosphorylated upon activation of PKCγ were unsuccessful. A similar experimental design needs to be performed with other commercial or zebrafish specific anti-phospho-GluR2 (S880) antibodies. Furthermore, immuno-coprecipitation studies have to be performed to confirm the interaction between phosphorylated GluR2 and PICK1.

The phosphorylation of AMPARs by PKA and CaMKII is also known to regulate ion channel function during LTP and LTD. For instance, phosphorylation of GluR1 by PKA and CaMKII has been shown to enhance responses in synaptic plasticity (Li et al., 2003; Fang et al., 2003). It remains to be determined if zebrafish AMPAR function can also be modulate by these kinases and if this plays a role during synaptic development. Preliminary data showed that activation of the cAMP/PKA pathway via the application of forskolin and IBMX caused a dramatic increase in mEPSC frequency but no significant change in the amplitude

and kinetics of the mEPSC. These results are consistent with previous studies (Carroll at al., 1998, Chavez-Noriega and Stevens, 1994) and suggest that PKA is not involved in modulating of AMPAR function in zebrafish M-cell.

The M-cells activate a touch-tap escape movement by driving neurons controlling the various muscular contractions associated with the behaviour (Liu and Fetcho, 1999). Hatching appears to be triggered by strong tail contractions following dissolution of the envelope by hatching enzymes (Eaton and Nissanov, 1985). These tail contractions are similar to those known to be driven by the M-cell (Eaton et al., 1977a). Therefore, it is possible that AMPA receptor trafficking is important for proper activity and function of the M-cell. However, these behavioural observations in the PKCγ-MO-injected embryos could also be due to impairment at the level of motoneurons and muscles and thus this needs to be investigated. Preliminary data showed that muscle fibres in the PKCγ-MO-injected zebrafish appear to be normal because they express nicotinic acetylcholine receptors and support miniature end-plate currents and they can produce normal action potentials. Future work is required to examine whether motoneurons can still produce action potential in the PKCγ-MO fish.

Transmembrane AMPAR regulatory proteins (TARPs) are a family of proteins which act as auxiliary subunits of AMPARs. They consist of proteins γ-2 (stargazin), γ-3, γ-4, γ-7 and γ-8, which modulate AMPAR trafficking and function (Tomita et al., 2003; Kato et al., 2007). TARPs are important players in the trafficking of AMPARs to the plasma membrane. For instance, phosphorylation of stargazin by PKC is known to promote synaptic trafficking of AMPA receptors (Tomita et al., 2005b; Tomita et al., 2005a). TARPs also regulate many aspects of AMPA receptor activity such as increases in glutamate affinity, and slow channel deactivation and desensitization (Priel et al., 2005; Kott et al., 2007; Menuz et al., 2008). Recently, Menuz et al. (2008) showed that loss of TARP function in transgenic mice caused a decrease in the AMPAR kinetics, and resulted in mice which express different AMPARs compared with wild-type mice. Preliminary blast search of the zebrafish genome for TARP genes revealed the presence of γ-2 (GenBank accession number: NM_200641) and γ-4 (GenBank accession number: XM_001338049). Therefore, it will be interesting to investigate the role of these TARPs in regulating zebrafish AMPARs and whether (1) PKCγ can promote receptor trafficking via phosphorylation of TARPs and (2) if TARP activity contributes to the developmental changes in AMPAR properties observed in zebrafish M-cell.

NMDARs also play critical roles in fast synaptic transmission and the development and remodelling of central excitatory pathways. They undergo a developmentally regulated shift in their underlying subunit composition. Specifically, the NR2B subunit predominates in receptor complexes at earlier stages of synaptic development, while the NR2A subunit predominates at later stages (Cull-Candy et al., 2001). The expression and properties of NMDAR have been studied at developing zebrafish (Ali et al., 2000b; Cox et al., 2005), but it is still unknown if a developmental subunit switch in NMDAR occurs in zebrafish.

A key step in the maturation of glutamate synapses is the developmental speeding of AMPAR kinetics. My work provides novel insights into the mechanism underlying this process in developing zebrafish. I also provide the first example of a signalling link required for the developmental switch in AMPAR subunits. This might contribute to our understanding of subunit switching in diseased states or abnormal synaptic physiology. My findings also further our understanding of GluR2 AMPAR trafficking in embryonic organisms and have important functional implications for developmental and activity-dependent forms of synaptic plasticity.

Chapter 8 REFERENCES

Abeliovich A, Paylor R, Chen C, Kim JJ, Wehner JM, Tonegawa S (1993a) PKC gamma mutant mice exhibit mild deficits in spatial and contextual learning. Cell 75:1263-1271.

Abeliovich A, Chen C, Goda Y, Silva AJ, Stevens CF, Tonegawa S (1993b) Modified hippocampal long-term potentiation in PKC gamma-mutant mice. Cell 75:1253-1262.

Adesnik H, Nicoll RA, England PM (2005) Photoinactivation of native AMPA receptors reveals their real-time trafficking. Neuron 48:977-985.

Ali DW, Drapeau P, Legendre P (2000a) Development of spontaneous glycinergic currents in the Mauthner neuron of the zebrafish embryo. J Neurophysiol 84:1726-1736.

Ali DW, Buss RR, Drapeau P (2000b) Properties of miniature glutamatergic EPSCs in neurons of the locomotor regions of the developing zebrafish. J Neurophysiol 83:181-191.

Ambros-Ingerson J, Lynch G (1993) Channel gating kinetics and synaptic efficacy: a hypothesis for expression of long-term potentiation. Proc Natl Acad Sci U S A 90:7903-7907.

Ambros-Ingerson J, Xiao P, Larson J, Lynch G (1993) Waveform analysis suggests that LTP alters the kinetics of synaptic receptor channels. Brain Res 620:237-244.

Anwyl R (1999) Metabotropic glutamate receptors: electrophysiological properties and role in plasticity. Brain Res Brain Res Rev 29:83-120.

Ascher P, Nowak L (1988) The role of divalent cations in the N-methyl-D-aspartate responses of mouse central neurones in culture. J Physiol 399:247-266.

Augustin I, Rosenmund C, Sudhof TC, Brose N (1999) Munc13-1 is essential for fusion competence of glutamatergic synaptic vesicles. Nature 400:457-461.

Bachoo M, Heppner T, Fiekers J, Polosa C (1992) A role for protein kinase C in long term potentiation of nicotinic transmission in the superior cervical ganglion of the rat. Brain Res 585:299-302.

Bannister NJ, Benke TA, Mellor J, Scott H, Gurdal E, Crabtree JW, Isaac JT (2005) Developmental changes in AMPA and kainate receptor-mediated quantal transmission at thalamocortical synapses in the barrel cortex. J Neurosci 25:5259-5271.

Barria A, Derkach V, Soderling T (1997) Identification of the Ca2+/calmodulin-dependent protein kinase II regulatory phosphorylation site in the alpha-amino-3-hydroxyl-5-methyl-4-isoxazole-propionate-type glutamate receptor. J Biol Chem 272:32727-32730.

Baxter AW, Wyllie DJ (2006) Phosphatidylinositol 3 kinase activation and AMPA receptor subunit trafficking underlie the potentiation of miniature EPSC amplitudes triggered by the activation of L-type calcium channels. J Neurosci 26:5456-5469.

Bear MF, Cooper LN, Ebner FF (1987) A physiological basis for a theory of synapse modification. Science 237:42-48.
Bellingham MC, Lim R, Walmsley B (1998) Developmental changes in EPSC quantal size and quantal content at a central glutamatergic synapse in rat. J Physiol 511 (Pt 3):861-869.
Bellone C, Luscher C (2006) Cocaine triggered AMPA receptor redistribution is reversed in vivo by mGluR-dependent long-term depression. Nat Neurosci 9:636-641.
Ben-Ari Y (2001) Developing networks play a similar melody. Trends Neurosci 24:353-360.
Benke TA, Luthi A, Isaac JT, Collingridge GL (1998) Modulation of AMPA receptor unitary conductance by synaptic activity. Nature 393:793-797.
Beretta F, Sala C, Saglietti L, Hirling H, Sheng M, Passafaro M (2005) NSF interaction is important for direct insertion of GluR2 at synaptic sites. Mol Cell Neurosci 28:650-660.
Berridge MJ, Irvine RF (1984) Inositol trisphosphate, a novel second messenger in cellular signal transduction. Nature 312:315-321.
Bliss TV, Collingridge GL (1993) A synaptic model of memory: long-term potentiation in the hippocampus. Nature 361:31-39.
Boehm J, Kang MG, Johnson RC, Esteban J, Huganir RL, Malinow R (2006) Synaptic incorporation of AMPA receptors during LTP is controlled by a PKC phosphorylation site on GluR1. Neuron 51:213-225.
Bolshakov VY, Siegelbaum SA (1995) Hippocampal long-term depression: arachidonic acid as a potential retrograde messenger. Neuropharmacology 34:1581-1587.
Bouron A (1997) Colchicine affects protein kinase C-induced modulation of synaptic transmission in cultured hippocampal pyramidal cells. FEBS Lett 404:221-226.
Braithwaite SP, Xia H, Malenka RC (2002) Differential roles for NSF and GRIP/ABP in AMPA receptor cycling. Proc Natl Acad Sci U S A 99:7096-7101.
Bredt DS, Nicoll RA (2003) AMPA receptor trafficking at excitatory synapses. Neuron 40:361-379.
Brenowitz S, Trussell LO (2001) Maturation of synaptic transmission at end-bulb synapses of the cochlear nucleus. J Neurosci 21:9487-9498.
Brusa R, Zimmermann F, Koh DS, Feldmeyer D, Gass P, Seeburg PH, Sprengel R (1995) Early-onset epilepsy and postnatal lethality associated with an editing-deficient GluR-B allele in mice. Science 270:1677-1680.
Byrne JH, Kandel ER (1996) Presynaptic facilitation revisited: state and time dependence. J Neurosci 16:425-435.
Carroll RC, Lissin DV, von Zastrow M, Nicoll RA, Malenka RC (1999a) Rapid redistribution of glutamate receptors contributes to long-term depression in hippocampal cultures. Nat Neurosci 2:454-460.
Carroll RC, Beattie EC, Xia H, Luscher C, Altschuler Y, Nicoll RA, Malenka RC, von Zastrow M (1999b) Dynamin-dependent endocytosis of ionotropic glutamate receptors. Proc Natl Acad Sci U S A 96:14112-14117.

Cathala L, Brickley S, Cull-Candy S, Farrant M (2003) Maturation of EPSCs and intrinsic membrane properties enhances precision at a cerebellar synapse. J Neurosci 23:6074-6085.
Chang YT, Lin JW, Faber DS (1987) Spinal inputs to the ventral dendrite of the teleost Mauthner cell. Brain Res 417:205-213.
Chavez-Noriega LE, Stevens CF (1994) Increased transmitter release at excitatory synapses produced by direct activation of adenylate cyclase in rat hippocampal slices. J Neurosci 14:310-317.
Choi S, Klingauf J, Tsien RW (2000) Postfusional regulation of cleft glutamate concentration during LTP at 'silent synapses'. Nat Neurosci 3:330-336.
Chung HJ, Xia J, Scannevin RH, Zhang X, Huganir RL (2000) Phosphorylation of the AMPA receptor subunit GluR2 differentially regulates its interaction with PDZ domain-containing proteins. J Neurosci 20:7258-7267.
Ciabarra AM, Sullivan JM, Gahn LG, Pecht G, Heinemann S, Sevarino KA (1995) Cloning and characterization of chi-1: a developmentally regulated member of a novel class of the ionotropic glutamate receptor family. J Neurosci 15:6498-6508.
Codazzi F, Di Cesare A, Chiulli N, Albanese A, Meyer T, Zacchetti D, Grohovaz F (2006) Synergistic control of protein kinase Cgamma activity by ionotropic and metabotropic glutamate receptor inputs in hippocampal neurons. J Neurosci 26:3404-3411.
Collingridge GL, Kehl SJ, McLennan H (1983) Excitatory amino acids in synaptic transmission in the Schaffer collateral-commissural pathway of the rat hippocampus. J Physiol 334:33-46.
Colquhoun D, Hawkes AG (1982) On the stochastic properties of bursts of single ion channel openings and of clusters of bursts. Philos Trans R Soc Lond B Biol Sci 300:1-59.
Conti F, Weinberg RJ (1999) Shaping excitation at glutamatergic synapses. Trends Neurosci 22:451-458.
Cotton JL, Partin KM (2000) The contributions of GluR2 to allosteric modulation of AMPA receptors. Neuropharmacology 39:21-31.
Cottrell JR, Borok E, Horvath TL, Nedivi E (2004) CPG2: a brain- and synapse-specific protein that regulates the endocytosis of glutamate receptors. Neuron 44:677-690.
Coussens L, Rhee L, Parker PJ, Ullrich A (1987) Alternative splicing increases the diversity of the human protein kinase C family. DNA 6:389-394.
Cox JA, Kucenas S, Voigt MM (2005) Molecular characterization and embryonic expression of the family of N-methyl-D-aspartate receptor subunit genes in the zebrafish. Dev Dyn 234:756-766.
Crair MC, Malenka RC (1995) A critical period for long-term potentiation at thalamocortical synapses. Nature 375:325-328.
Cull-Candy S, Brickley S, Farrant M (2001) NMDA receptor subunits: diversity, development and disease. Curr Opin Neurobiol 11:327-335.

Cull-Candy S, Kelly L, Farrant M (2006) Regulation of Ca2+-permeable AMPA receptors: synaptic plasticity and beyond. Curr Opin Neurobiol 16:288-297.

Das S, Sasaki YF, Rothe T, Premkumar LS, Takasu M, Crandall JE, Dikkes P, Conner DA, Rayudu PV, Cheung W, Chen HS, Lipton SA, Nakanishi N (1998) Increased NMDA current and spine density in mice lacking the NMDA receptor subunit NR3A. Nature 393:377-381.

Daw MI, Chittajallu R, Bortolotto ZA, Dev KK, Duprat F, Henley JM, Collingridge GL, Isaac JT (2000) PDZ proteins interacting with C-terminal GluR2/3 are involved in a PKC-dependent regulation of AMPA receptors at hippocampal synapses. Neuron 28:873-886.

Dekker LV, Parker PJ (1994) Protein kinase C--a question of specificity. Trends Biochem Sci 19:73-77.

Derkach VA, Oh MC, Guire ES, Soderling TR (2007) Regulatory mechanisms of AMPA receptors in synaptic plasticity. Nat Rev Neurosci 8:101-113.

Diamond JS, Jahr CE (1997) Transporters buffer synaptically released glutamate on a submillisecond time scale. J Neurosci 17:4672-4687.

Dingledine R, Hume RI, Heinemann SF (1992) Structural determinants of barium permeation and rectification in non-NMDA glutamate receptor channels. J Neurosci 12:4080-4087.

Drapeau P, Ali DW, Buss RR, Saint-Amant L (1999) In vivo recording from identifiable neurons of the locomotor network in the developing zebrafish. J Neurosci Methods 88:1-13.

Dudek SM, Bear MF (1993) Bidirectional long-term modification of synaptic effectiveness in the adult and immature hippocampus. J Neurosci 13:2910-2918.

Duffy SN, Craddock KJ, Abel T, Nguyen PV (2001) Environmental enrichment modifies the PKA-dependence of hippocampal LTP and improves hippocampus-dependent memory. Learn Mem 8:26-34.

Durand GM, Bennett MV, Zukin RS (1993) Splice variants of the N-methyl-D-aspartate receptor NR1 identify domains involved in regulation by polyamines and protein kinase C. Proc Natl Acad Sci U S A 90:6731-6735.

Eaton R, Nissanov (1985) A review of Mauthner-initiated escape behavior and its possible role in hatching in the immature zebrafish, *Brachydanio rerio*. Environmental Biology of Fishes 12:265-279.

Eaton RC, Farley RD (1973) Development of the maunther neurons in embryos and larvae of the zebrafish. Copeia 4:673-682.

Eaton RC, Bombardieri RA, Meyer DL (1977a) The Mauthner-initiated startle response in teleost fish. J Exp Biol 66:65-81.

Eaton RC, Lee RK, Foreman MB (2001) The Mauthner cell and other identified neurons of the brainstem escape network of fish. Prog Neurobiol 63:467-485.

Eaton RC, Farley RD, Kimmel CB, Schabtach E (1977b) Functional development in the Mauthner cell system of embryos and larvae of the zebra fish. J Neurobiol 8:151-172.

Edmonds B, Gibb AJ, Colquhoun D (1995) Mechanisms of activation of glutamate receptors and the time course of excitatory synaptic currents. Annu Rev Physiol 57:495-519.
Faber DS, Korn H (1975) Inputs from the posterior lateral line nerves upon the goldfish Mauthner cells. II. Evidence that the inhibitory components are mediated by interneurons of the recurrent collateral network. Brain Res 96:349-356.
Fang L, Wu J, Lin Q, Willis WD (2003) Protein kinases regulate the phosphorylation of the GluR1 subunit of AMPA receptors of spinal cord in rats following noxious stimulation. Brain Res Mol Brain Res 118:160-165.
Fischbach GD, Schuetze SM (1980) A post-natal decrease in acetylcholine channel open time at rat end-plates. J Physiol 303:125-137.
Futai K, Okada M, Matsuyama K, Takahashi T (2001) High-fidelity transmission acquired via a developmental decrease in NMDA receptor expression at an auditory synapse. J Neurosci 21:3342-3349.
Galarreta M, Hestrin S (2001) Spike transmission and synchrony detection in networks of GABAergic interneurons. Science 292:2295-2299.
Gardner SM, Takamiya K, Xia J, Suh JG, Johnson R, Yu S, Huganir RL (2005) Calcium-permeable AMPA receptor plasticity is mediated by subunit-specific interactions with PICK1 and NSF. Neuron 45:903-915.
Garner CC, Zhai RG, Gundelfinger ED, Ziv NE (2002) Molecular mechanisms of CNS synaptogenesis. Trends Neurosci 25:243-251.
Gasparini S, Saviane C, Voronin LL, Cherubini E (2000) Silent synapses in the developing hippocampus: lack of functional AMPA receptors or low probability of glutamate release? Proc Natl Acad Sci U S A 97:9741-9746.
Ge S, Goh EL, Sailor KA, Kitabatake Y, Ming GL, Song H (2006) GABA regulates synaptic integration of newly generated neurons in the adult brain. Nature 439:589-593.
Geiger JR, Melcher T, Koh DS, Sakmann B, Seeburg PH, Jonas P, Monyer H (1995) Relative abundance of subunit mRNAs determines gating and Ca2+ permeability of AMPA receptors in principal neurons and interneurons in rat CNS. Neuron 15:193-204.
Gerlai R, Henderson JT, Roder JC, Jia Z (1998) Multiple behavioral anomalies in GluR2 mutant mice exhibiting enhanced LTP. Behav Brain Res 95:37-45.
Glowatzki E, Fuchs PA (2002) Transmitter release at the hair cell ribbon synapse. Nat Neurosci 5:147-154.
Goldberg M, Steinberg SF (1996) Tissue-specific developmental regulation of protein kinase C isoforms. Biochem Pharmacol 51:1089-1093.
Gomes AR, Correia SS, Esteban JA, Duarte CB, Carvalho AL (2007) PKC anchoring to GluR4 AMPA receptor subunit modulates PKC-driven receptor phosphorylation and surface expression. Traffic 8:259-269.
Groc L, Gustafsson B, Hanse E (2002) Spontaneous unitary synaptic activity in CA1 pyramidal neurons during early postnatal development: constant contribution of AMPA and NMDA receptors. J Neurosci 22:5552-5562.

Grunwald DJ, Kimmel CB, Westerfield M, Walker C, Streisinger G (1988) A neural degeneration mutation that spares primary neurons in the zebrafish. Dev Biol 126:115-128.
Gu JG, Albuquerque C, Lee CJ, MacDermott AB (1996) Synaptic strengthening through activation of Ca2+-permeable AMPA receptors. Nature 381:793-796.
Hall BJ, Ghosh A (2008) Regulation of AMPA receptor recruitment at developing synapses. Trends Neurosci 31:82-89.
Hanley JG, Khatri L, Hanson PI, Ziff EB (2002) NSF ATPase and alpha-/beta-SNAPs disassemble the AMPA receptor-PICK1 complex. Neuron 34:53-67.
Hannun YA, Bell RM (1988) Aminoacridines, potent inhibitors of protein kinase C. J Biol Chem 263:5124-5131.
Hanse E, Gustafsson B (1994) TEA elicits two distinct potentiations of synaptic transmission in the CA1 region of the hippocampal slice. J Neurosci 14:5028-5034.
Hartmann B, Ahmadi S, Heppenstall PA, Lewin GR, Schott C, Borchardt T, Seeburg PH, Zeilhofer HU, Sprengel R, Kuner R (2004) The AMPA receptor subunits GluR-A and GluR-B reciprocally modulate spinal synaptic plasticity and inflammatory pain. Neuron 44:637-650.
Hayashi Y, Shi SH, Esteban JA, Piccini A, Poncer JC, Malinow R (2000) Driving AMPA receptors into synapses by LTP and CaMKII: requirement for GluR1 and PDZ domain interaction. Science 287:2262-2267.
Herms J, Zurmohle U, Schlingensiepen KH, Brysch W (1993) Transient expression of PKC gamma mRNA in cerebellar granule cells during rat brain development. Neuroreport 4:899-902.
Hestrin S (1992a) Activation and desensitization of glutamate-activated channels mediating fast excitatory synaptic currents in the visual cortex. Neuron 9:991-999.
Hestrin S (1992b) Developmental regulation of NMDA receptor-mediated synaptic currents at a central synapse. Nature 357:686-689.
Hestrin S (1993) Different glutamate receptor channels mediate fast excitatory synaptic currents in inhibitory and excitatory cortical neurons. Neuron 11:1083-1091.
Hirai H (2001) Modification of AMPA receptor clustering regulates cerebellar synaptic plasticity. Neurosci Res 39:261-267.
Hirokawa N, Takemura R (2005) Molecular motors and mechanisms of directional transport in neurons. Nat Rev Neurosci 6:201-214.
Hollmann M, Heinemann S (1994) Cloned glutamate receptors. Annu Rev Neurosci 17:31-108.
Hollmann M, Hartley M, Heinemann S (1991) Ca2+ permeability of KA-AMPA--gated glutamate receptor channels depends on subunit composition. Science 252:851-853.
Hollmann M, Boulter J, Maron C, Beasley L, Sullivan J, Pecht G, Heinemann S (1993) Zinc potentiates agonist-induced currents at certain splice variants of the NMDA receptor. Neuron 10:943-954.

Honda I, Kamiya H, Yawo H (2000) Re-evaluation of phorbol ester-induced potentiation of transmitter release from mossy fibre terminals of the mouse hippocampus. J Physiol 529 Pt 3:763-776.
Hoppmann V, Wu JJ, Soviknes AM, Helvik JV, Becker TS (2008) Expression of the eight AMPA receptor subunit genes in the developing central nervous system and sensory organs of zebrafish. Dev Dyn 237:788-799.
Hosokawa T, Rusakov DA, Bliss TV, Fine A (1995) Repeated confocal imaging of individual dendritic spines in the living hippocampal slice: evidence for changes in length and orientation associated with chemically induced LTP. J Neurosci 15:5560-5573.
Hrabetova S, Sacktor TC (1996) Bidirectional regulation of protein kinase M zeta in the maintenance of long-term potentiation and long-term depression. J Neurosci 16:5324-5333.
Hu GY, Hvalby O, Walaas SI, Albert KA, Skjeflo P, Andersen P, Greengard P (1987) Protein kinase C injection into hippocampal pyramidal cells elicits features of long term potentiation. Nature 328:426-429.
Hua SY, Charlton MP (1999) Activity-dependent changes in partial VAMP complexes during neurotransmitter release. Nat Neurosci 2:1078-1083.
Huang FL, Yoshida Y, Nakabayashi H, Knopf JL, Young WS, 3rd, Huang KP (1987) Immunochemical identification of protein kinase C isozymes as products of discrete genes. Biochem Biophys Res Commun 149:946-952.
Huang KP, Huang FL (1986) Immunochemical characterization of rat brain protein kinase C. J Biol Chem 261:14781-14787.
Huang Y, Man HY, Sekine-Aizawa Y, Han Y, Juluri K, Luo H, Cheah J, Lowenstein C, Huganir RL, Snyder SH (2005) S-nitrosylation of N-ethylmaleimide sensitive factor mediates surface expression of AMPA receptors. Neuron 46:533-540.
Huang YY, Malenka RC (1993) Examination of TEA-induced synaptic enhancement in area CA1 of the hippocampus: the role of voltage-dependent Ca2+ channels in the induction of LTP. J Neurosci 13:568-576.
Hug H, Sarre TF (1993) Protein kinase C isoenzymes: divergence in signal transduction? Biochem J 291 (Pt 2):329-343.
Igarashi M, Komiya Y (1991) Subtypes of protein kinase C in isolated nerve growth cones: only type II is associated with the membrane skeleton from growth cones. Biochem Biophys Res Commun 178:751-757.
Isaac JT, Nicoll RA, Malenka RC (1995) Evidence for silent synapses: implications for the expression of LTP. Neuron 15:427-434.
Isaac JT, Ashby M, McBain CJ (2007) The role of the GluR2 subunit in AMPA receptor function and synaptic plasticity. Neuron 54:859-871.
Isaac JT, Crair MC, Nicoll RA, Malenka RC (1997) Silent synapses during development of thalamocortical inputs. Neuron 18:269-280.
Ishii T, Moriyoshi K, Sugihara H, Sakurada K, Kadotani H, Yokoi M, Akazawa C, Shigemoto R, Mizuno N, Masu M, et al. (1993) Molecular characterization of the family of the N-methyl-D-aspartate receptor subunits. J Biol Chem 268:2836-2843.

Iwasaki S, Takahashi T (2001) Developmental regulation of transmitter release at the calyx of Held in rat auditory brainstem. J Physiol 534:861-871.
Jia Z, Agopyan N, Miu P, Xiong Z, Henderson J, Gerlai R, Taverna FA, Velumian A, MacDonald J, Carlen P, Abramow-Newerly W, Roder J (1996) Enhanced LTP in mice deficient in the AMPA receptor GluR2. Neuron 17:945-956.
Jonas P, Sakmann B (1992) Glutamate receptor channels in isolated patches from CA1 and CA3 pyramidal cells of rat hippocampal slices. J Physiol 455:143-171.
Joshi I, Wang LY (2002) Developmental profiles of glutamate receptors and synaptic transmission at a single synapse in the mouse auditory brainstem. J Physiol 540:861-873.
Kano M, Hashimoto K, Chen C, Abeliovich A, Aiba A, Kurihara H, Watanabe M, Inoue Y, Tonegawa S (1995) Impaired synapse elimination during cerebellar development in PKC gamma mutant mice. Cell 83:1223-1231.
Kato AS, Zhou W, Milstein AD, Knierman MD, Siuda ER, Dotzlaf JE, Yu H, Hale JE, Nisenbaum ES, Nicoll RA, Bredt DS (2007) New transmembrane AMPA receptor regulatory protein isoform, gamma-7, differentially regulates AMPA receptors. J Neurosci 27:4969-4977.
Kauer JA, Malenka RC, Nicoll RA (1988) A persistent postsynaptic modification mediates long-term potentiation in the hippocampus. Neuron 1:911-917.
Kemp N, Bashir ZI (2001) Long-term depression: a cascade of induction and expression mechanisms. Prog Neurobiol 65:339-365.
Kim CH, Chung HJ, Lee HK, Huganir RL (2001) Interaction of the AMPA receptor subunit GluR2/3 with PDZ domains regulates hippocampal long-term depression. Proc Natl Acad Sci U S A 98:11725-11730.
Kimmel CB, Patterson J, Kimmel RO (1974) The development and behavioral characteristics of the startle response in the zebra fish. Dev Psychobiol 7:47-60.
Kimmel CB, Sessions SK, Kimmel RJ (1981) Morphogenesis and synaptogenesis of the zebrafish Mauthner neuron. J Comp Neurol 198:101-120.
Kimmel CB, Hatta K, Metcalfe WK (1990) Early axonal contacts during development of an identified dendrite in the brain of the zebrafish. Neuron 4:535-545.
Kimmel CB, Ballard WW, Kimmel SR, Ullmann B, Schilling TF (1995) Stages of embryonic development of the zebrafish. Dev Dyn 203:253-310.
Klann E, Chen SJ, Sweatt JD (1993) Mechanism of protein kinase C activation during the induction and maintenance of long-term potentiation probed using a selective peptide substrate. Proc Natl Acad Sci U S A 90:8337-8341.
Kolarow R, Brigadski T, Lessmann V (2007) Postsynaptic secretion of BDNF and NT-3 from hippocampal neurons depends on calcium calmodulin kinase II signaling and proceeds via delayed fusion pore opening. J Neurosci 27:10350-10364.
Kolleker A, Zhu JJ, Schupp BJ, Qin Y, Mack V, Borchardt T, Kohr G, Malinow R, Seeburg PH, Osten P (2003) Glutamatergic plasticity by synaptic

delivery of GluR-B(long)-containing AMPA receptors. Neuron 40:1199-1212.
Korkotian E, Segal M (2007) Morphological constraints on calcium dependent glutamate receptor trafficking into individual dendritic spine. Cell Calcium 42:41-57.
Korn H, Faber DS (2005) The Mauthner cell half a century later: a neurobiological model for decision-making? Neuron 47:13-28.
Kosaka Y, Ogita K, Ase K, Nomura H, Kikkawa U, Nishizuka Y (1988) The heterogeneity of protein kinase C in various rat tissues. Biochem Biophys Res Commun 151:973-981.
Kose A, Ito A, Saito N, Tanaka C (1990) Electron microscopic localization of gamma- and beta II-subspecies of protein kinase C in rat hippocampus. Brain Res 518:209-217.
Kott S, Werner M, Korber C, Hollmann M (2007) Electrophysiological properties of AMPA receptors are differentially modulated depending on the associated member of the TARP family. J Neurosci 27:3780-3789.
Kung SS, Chen YC, Lin WH, Chen CC, Chow WY (2001) Q/R RNA editing of the AMPA receptor subunit 2 (GRIA2) transcript evolves no later than the appearance of cartilaginous fishes. FEBS Lett 509:277-281.
Kutsuwada T, Kashiwabuchi N, Mori H, Sakimura K, Kushiya E, Araki K, Meguro H, Masaki H, Kumanishi T, Arakawa M, et al. (1992) Molecular diversity of the NMDA receptor channel. Nature 358:36-41.
Lawrence JJ, Trussell LO (2000) Long-term specification of AMPA receptor properties after synapse formation. J Neurosci 20:4864-4870.
Lee HK, Kameyama K, Huganir RL, Bear MF (1998) NMDA induces long-term synaptic depression and dephosphorylation of the GluR1 subunit of AMPA receptors in hippocampus. Neuron 21:1151-1162.
Lee HK, Takamiya K, Han JS, Man H, Kim CH, Rumbaugh G, Yu S, Ding L, He C, Petralia RS, Wenthold RJ, Gallagher M, Huganir RL (2003) Phosphorylation of the AMPA receptor GluR1 subunit is required for synaptic plasticity and retention of spatial memory. Cell 112:631-643.
Lee SH, Sheng M (2000) Development of neuron-neuron synapses. Curr Opin Neurobiol 10:125-131.
Lee SH, Liu L, Wang YT, Sheng M (2002) Clathrin adaptor AP2 and NSF interact with overlapping sites of GluR2 and play distinct roles in AMPA receptor trafficking and hippocampal LTD. Neuron 36:661-674.
Legendre P (1997) Pharmacological evidence for two types of postsynaptic glycinergic receptors on the Mauthner cell of 52-h-old zebrafish larvae. J Neurophysiol 77:2400-2415.
Lerma J, Morales M, Ibarz JM, Somohano F (1994) Rectification properties and Ca2+ permeability of glutamate receptor channels in hippocampal cells. Eur J Neurosci 6:1080-1088.
Lin B, Brucher FA, Colgin LL, Lynch G (2002) Long-term potentiation alters the modulator pharmacology of AMPA-type glutamate receptors. J Neurophysiol 87:2790-2800.

Lin JW, Sheng M (1998) NSF and AMPA receptors get physical. Neuron 21:267-270.
Lin JW, Wyszynski M, Madhavan R, Sealock R, Kim JU, Sheng M (1998) Yotiao, a novel protein of neuromuscular junction and brain that interacts with specific splice variants of NMDA receptor subunit NR1. J Neurosci 18:2017-2027.
Ling DS, Benardo LS, Sacktor TC (2006) Protein kinase Mzeta enhances excitatory synaptic transmission by increasing the number of active postsynaptic AMPA receptors. Hippocampus 16:443-452.
Lise MF, Wong TP, Trinh A, Hines RM, Liu L, Kang R, Hines DJ, Lu J, Goldenring JR, Wang YT, El-Husseini A (2006) Involvement of myosin Vb in glutamate receptor trafficking. J Biol Chem 281:3669-3678.
Liu KS, Fetcho JR (1999) Laser ablations reveal functional relationships of segmental hindbrain neurons in zebrafish. Neuron 23:325-335.
Liu SJ, Cull-Candy SG (2005) Subunit interaction with PICK and GRIP controls Ca2+ permeability of AMPARs at cerebellar synapses. Nat Neurosci 8:768-775.
Liu SQ, Cull-Candy SG (2000) Synaptic activity at calcium-permeable AMPA receptors induces a switch in receptor subtype. Nature 405:454-458.
London M, Schreibman A, Hausser M, Larkum ME, Segev I (2002) The information efficacy of a synapse. Nat Neurosci 5:332-340.
Lu W, Ziff EB (2005) PICK1 interacts with ABP/GRIP to regulate AMPA receptor trafficking. Neuron 47:407-421.
Lu W, Man H, Ju W, Trimble WS, MacDonald JF, Wang YT (2001) Activation of synaptic NMDA receptors induces membrane insertion of new AMPA receptors and LTP in cultured hippocampal neurons. Neuron 29:243-254.
Makhinson M, Chotiner JK, Watson JB, O'Dell TJ (1999) Adenylyl cyclase activation modulates activity-dependent changes in synaptic strength and Ca2+/calmodulin-dependent kinase II autophosphorylation. J Neurosci 19:2500-2510.
Malenka RC, Nicoll RA (1993) NMDA-receptor-dependent synaptic plasticity: multiple forms and mechanisms. Trends Neurosci 16:521-527.
Malenka RC, Kauer JA, Perkel DJ, Mauk MD, Kelly PT, Nicoll RA, Waxham MN (1989) An essential role for postsynaptic calmodulin and protein kinase activity in long-term potentiation. Nature 340:554-557.
Maletic-Savatic M, Malinow R (1998) Calcium-evoked dendritic exocytosis in cultured hippocampal neurons. Part I: trans-Golgi network-derived organelles undergo regulated exocytosis. J Neurosci 18:6803-6813.
Malinow R, Malenka RC (2002) AMPA receptor trafficking and synaptic plasticity. Annu Rev Neurosci 25:103-126.
Malinow R, Madison DV, Tsien RW (1988) Persistent protein kinase activity underlying long-term potentiation. Nature 335:820-824.
Malinow R, Schulman H, Tsien RW (1989) Inhibition of postsynaptic PKC or CaMKII blocks induction but not expression of LTP. Science 245:862-866.

Malinow R, Mainen ZF, Hayashi Y (2000) LTP mechanisms: from silence to four-lane traffic. Curr Opin Neurobiol 10:352-357.
Mammen AL, Kameyama K, Roche KW, Huganir RL (1997) Phosphorylation of the alpha-amino-3-hydroxy-5-methylisoxazole4-propionic acid receptor GluR1 subunit by calcium/calmodulin-dependent kinase II. J Biol Chem 272:32528-32533.
Man HY, Sekine-Aizawa Y, Huganir RL (2007) Regulation of {alpha}-amino-3-hydroxy-5-methyl-4-isoxazolepropionic acid receptor trafficking through PKA phosphorylation of the Glu receptor 1 subunit. Proc Natl Acad Sci U S A 104:3579-3584.
Matsuda S, Mikawa S, Hirai H (1999) Phosphorylation of serine-880 in GluR2 by protein kinase C prevents its C terminus from binding with glutamate receptor-interacting protein. J Neurochem 73:1765-1768.
Matsuda S, Launey T, Mikawa S, Hirai H (2000) Disruption of AMPA receptor GluR2 clusters following long-term depression induction in cerebellar Purkinje neurons. Embo J 19:2765-2774.
McDonald BJ, Chung HJ, Huganir RL (2001) Identification of protein kinase C phosphorylation sites within the AMPA receptor GluR2 subunit. Neuropharmacology 41:672-679.
McDonald JW, Johnston MV (1990) Physiological and pathophysiological roles of excitatory amino acids during central nervous system development. Brain Res Brain Res Rev 15:41-70.
Menuz K, O'Brien JL, Karmizadegan S, Bredt DS, Nicoll RA (2008) TARP redundancy is critical for maintaining AMPA receptor function. J Neurosci 28:8740-8746.
Metcalfe WK, Mendelson B, Kimmel CB (1986) Segmental homologies among reticulospinal neurons in the hindbrain of the zebrafish larva. J Comp Neurol 251:147-159.
Migues PV, Cammarota M, Kavanagh J, Atkinson R, Powis DA, Rostas JA (2007) Maturational changes in the subunit composition of AMPA receptors and the functional consequences of their activation in chicken forebrain. Dev Neurosci 29:232-240.
Mishina M, Takai T, Imoto K, Noda M, Takahashi T, Numa S, Methfessel C, Sakmann B (1986) Molecular distinction between fetal and adult forms of muscle acetylcholine receptor. Nature 321:406-411.
Mochly-Rosen D, Miller KG, Scheller RH, Khaner H, Lopez J, Smith BL (1992) p65 fragments, homologous to the C2 region of protein kinase C, bind to the intracellular receptors for protein kinase C. Biochemistry 31:8120-8124.
Momiyama A, Silver RA, Hausser M, Notomi T, Wu Y, Shigemoto R, Cull-Candy SG (2003) The density of AMPA receptors activated by a transmitter quantum at the climbing fibre-Purkinje cell synapse in immature rats. J Physiol 549:75-92.
Monyer H, Burnashev N, Laurie DJ, Sakmann B, Seeburg PH (1994) Developmental and regional expression in the rat brain and functional properties of four NMDA receptors. Neuron 12:529-540.

Monyer H, Sprengel R, Schoepfer R, Herb A, Higuchi M, Lomeli H, Burnashev N, Sakmann B, Seeburg PH (1992) Heteromeric NMDA receptors: molecular and functional distinction of subtypes. Science 256:1217-1221.
Morkve SH, Veruki ML, Hartveit E (2002) Functional characteristics of non-NMDA-type ionotropic glutamate receptor channels in AII amacrine cells in rat retina. J Physiol 542:147-165.
Mosbacher J, Schoepfer R, Monyer H, Burnashev N, Seeburg PH, Ruppersberg JP (1994) A molecular determinant for submillisecond desensitization in glutamate receptors. Science 266:1059-1062.
Mulkey RM, Malenka RC (1992) Mechanisms underlying induction of homosynaptic long-term depression in area CA1 of the hippocampus. Neuron 9:967-975.
Muslimov IA, Nimmrich V, Hernandez AI, Tcherepanov A, Sacktor TC, Tiedge H (2004) Dendritic transport and localization of protein kinase Mzeta mRNA: implications for molecular memory consolidation. J Biol Chem 279:52613-52622.
Nakanishi S (1992) Molecular diversity of the glutamate receptors. Clin Neuropharmacol 15 Suppl 1 Pt A:4A-5A.
Nasevicius A, Ekker SC (2000) Effective targeted gene 'knockdown' in zebrafish. Nat Genet 26:216-220.
Nishimune A, Isaac JT, Molnar E, Noel J, Nash SR, Tagaya M, Collingridge GL, Nakanishi S, Henley JM (1998) NSF binding to GluR2 regulates synaptic transmission. Neuron 21:87-97.
Nishizuka Y (1992) Intracellular signaling by hydrolysis of phospholipids and activation of protein kinase C. Science 258:607-614.
Nowak L, Bregestovski P, Ascher P, Herbet A, Prochiantz A (1984) Magnesium gates glutamate-activated channels in mouse central neurones. Nature 307:462-465.
Nuriya M, Oh S, Huganir RL (2005) Phosphorylation-dependent interactions of alpha-Actinin-1/IQGAP1 with the AMPA receptor subunit GluR4. J Neurochem 95:544-552.
Oguro K, Oguro N, Kojima T, Grooms SY, Calderone A, Zheng X, Bennett MV, Zukin RS (1999) Knockdown of AMPA receptor GluR2 expression causes delayed neurodegeneration and increases damage by sublethal ischemia in hippocampal CA1 and CA3 neurons. J Neurosci 19:9218-9227.
Ohanian V, Ohanian J, Shaw L, Scarth S, Parker PJ, Heagerty AM (1996) Identification of protein kinase C isoforms in rat mesenteric small arteries and their possible role in agonist-induced contraction. Circ Res 78:806-812.
Ohno S, Nishizuka Y (2002) Protein kinase C isotypes and their specific functions: prologue. J Biochem 132:509-511.
Osada S, Mizuno K, Saido TC, Suzuki K, Kuroki T, Ohno S (1992) A new member of the protein kinase C family, nPKC theta, predominantly expressed in skeletal muscle. Mol Cell Biol 12:3930-3938.

Osborne NN, Wood J, Groome N (1994) The occurrence of three calcium-independent protein kinase C subspecies (delta, epsilon and zeta) in retina of different species. Brain Res 637:156-162.
Osten P, Srivastava S, Inman GJ, Vilim FS, Khatri L, Lee LM, States BA, Einheber S, Milner TA, Hanson PI, Ziff EB (1998) The AMPA receptor GluR2 C terminus can mediate a reversible, ATP-dependent interaction with NSF and alpha- and beta-SNAPs. Neuron 21:99-110.
Oster H, Eichele G, Leitges M (2004) Differential expression of atypical PKCs in the adult mouse brain. Brain Res Mol Brain Res 127:79-88.
Otis T, Zhang S, Trussell LO (1996) Direct measurement of AMPA receptor desensitization induced by glutamatergic synaptic transmission. J Neurosci 16:7496-7504.
Otis TS, Trussell LO (1996) Inhibition of transmitter release shortens the duration of the excitatory synaptic current at a calyceal synapse. J Neurophysiol 76:3584-3588.
Palmer MJ, Isaac JT, Collingridge GL (2004) Multiple, developmentally regulated expression mechanisms of long-term potentiation at CA1 synapses. J Neurosci 24:4903-4911.
Parfitt KD, Madison DV (1993) Phorbol esters enhance synaptic transmission by a presynaptic, calcium-dependent mechanism in rat hippocampus. J Physiol 471:245-268.
Park M, Penick EC, Edwards JG, Kauer JA, Ehlers MD (2004) Recycling endosomes supply AMPA receptors for LTP. Science 305:1972-1975.
Park M, Salgado JM, Ostroff L, Helton TD, Robinson CG, Harris KM, Ehlers MD (2006) Plasticity-induced growth of dendritic spines by exocytic trafficking from recycling endosomes. Neuron 52:817-830.
Parker PJ, Coussens L, Totty N, Rhee L, Young S, Chen E, Stabel S, Waterfield MD, Ullrich A (1986) The complete primary structure of protein kinase C--the major phorbol ester receptor. Science 233:853-859.
Partin KM, Patneau DK, Mayer ML (1994) Cyclothiazide differentially modulates desensitization of alpha-amino-3-hydroxy-5-methyl-4-isoxazolepropionic acid receptor splice variants. Mol Pharmacol 46:129-138.
Partin KM, Patneau DK, Winters CA, Mayer ML, Buonanno A (1993) Selective modulation of desensitization at AMPA versus kainate receptors by cyclothiazide and concanavalin A. Neuron 11:1069-1082.
Passafaro M, Piech V, Sheng M (2001) Subunit-specific temporal and spatial patterns of AMPA receptor exocytosis in hippocampal neurons. Nat Neurosci 4:917-926.
Patten SA, Sihra RK, Dhami KS, Coutts CA, Ali DW (2007) Differential expression of PKC isoforms in developing zebrafish. Int J Dev Neurosci 25:155-164.
Patterson SL, Pittenger C, Morozov A, Martin KC, Scanlin H, Drake C, Kandel ER (2001) Some forms of cAMP-mediated long-lasting potentiation are associated with release of BDNF and nuclear translocation of phospho-MAP kinase. Neuron 32:123-140.

Pellegrini-Giampietro DE, Gorter JA, Bennett MV, Zukin RS (1997) The GluR2 (GluR-B) hypothesis: Ca(2+)-permeable AMPA receptors in neurological disorders. Trends Neurosci 20:464-470.

Perez-Otano I, Schulteis CT, Contractor A, Lipton SA, Trimmer JS, Sucher NJ, Heinemann SF (2001) Assembly with the NR1 subunit is required for surface expression of NR3A-containing NMDA receptors. J Neurosci 21:1228-1237.

Perkel DJ, Petrozzino JJ, Nicoll RA, Connor JA (1993) The role of Ca2+ entry via synaptically activated NMDA receptors in the induction of long-term potentiation. Neuron 11:817-823.

Pickard L, Noel J, Henley JM, Collingridge GL, Molnar E (2000) Developmental changes in synaptic AMPA and NMDA receptor distribution and AMPA receptor subunit composition in living hippocampal neurons. J Neurosci 20:7922-7931.

Plant K, Pelkey KA, Bortolotto ZA, Morita D, Terashima A, McBain CJ, Collingridge GL, Isaac JT (2006) Transient incorporation of native GluR2-lacking AMPA receptors during hippocampal long-term potentiation. Nat Neurosci 9:602-604.

Priel A, Kolleker A, Ayalon G, Gillor M, Osten P, Stern-Bach Y (2005) Stargazin reduces desensitization and slows deactivation of the AMPA-type glutamate receptors. J Neurosci 25:2682-2686.

Rall W (1969) Time constants and electrotonic length of membrane cylinders and neurons. Biophys J 9:1483-1508.

Raman IM, Trussell LO (1992) The kinetics of the response to glutamate and kainate in neurons of the avian cochlear nucleus. Neuron 9:173-186.

Raymond LA, Blackstone CD, Huganir RL (1993) Phosphorylation of amino acid neurotransmitter receptors in synaptic plasticity. Trends Neurosci 16:147-153.

Redman RS, Searl TJ, Hirsh JK, Silinsky EM (1997) Opposing effects of phorbol esters on transmitter release and calcium currents at frog motor nerve endings. J Physiol 501 (Pt 1):41-48.

Renger JJ, Egles C, Liu G (2001) A developmental switch in neurotransmitter flux enhances synaptic efficacy by affecting AMPA receptor activation. Neuron 29:469-484.

Rial Verde EM, Lee-Osbourne J, Worley PF, Malinow R, Cline HT (2006) Increased expression of the immediate-early gene arc/arg3.1 reduces AMPA receptor-mediated synaptic transmission. Neuron 52:461-474.

Roche KW, O'Brien RJ, Mammen AL, Bernhardt J, Huganir RL (1996) Characterization of multiple phosphorylation sites on the AMPA receptor GluR1 subunit. Neuron 16:1179-1188.

Rohrbough J, Spitzer NC (1999) Ca(2+)-permeable AMPA receptors and spontaneous presynaptic transmitter release at developing excitatory spinal synapses. J Neurosci 19:8528-8541.

Ron D, Mochly-Rosen D (1995) An autoregulatory region in protein kinase C: the pseudoanchoring site. Proc Natl Acad Sci U S A 92:492-496.

Rumpel S, Kattenstroth G, Gottmann K (2004) Silent synapses in the immature visual cortex: layer-specific developmental regulation. J Neurophysiol 91:1097-1101.
Rybin VO, Buttrick PM, Steinberg SF (1997) PKC-lambda is the atypical protein kinase C isoform expressed by immature ventricle. Am J Physiol 272:H1636-1642.
Sacktor TC (2008) PKMzeta, LTP maintenance, and the dynamic molecular biology of memory storage. Prog Brain Res 169:27-40.
Sacktor TC, Osten P, Valsamis H, Jiang X, Naik MU, Sublette E (1993) Persistent activation of the zeta isoform of protein kinase C in the maintenance of long-term potentiation. Proc Natl Acad Sci U S A 90:8342-8346.
Sah P, Lopez De Armentia M (2003) Excitatory synaptic transmission in the lateral and central amygdala. Ann N Y Acad Sci 985:67-77.
Saint-Amant L, Drapeau P (1998) Time course of the development of motor behaviors in the zebrafish embryo. J Neurobiol 37:622-632.
Saito N (1994) Immunocytochemicallocalization ofPKC subspecies in the hippocampus. In: Protein kinase C in the CNS focus on neuronal plasticity, pp pp 10-15.
Saito N, Tsujino T, Fukuda K, Tanaka C (1994) Alpha-, beta II- and gamma-subspecies of protein kinase C localized in the monkey hippocampus: pre- and post-synaptic localization of gamma-subspecies. Brain Res 656:245-256.
Sakmann B, Brenner HR (1978) Change in synaptic channel gating during neuromuscular development. Nature 276:401-402.
Schechtman D, Mochly-Rosen D (2001) Adaptor proteins in protein kinase C-mediated signal transduction. Oncogene 20:6339-6347.
Searl TJ, Silinsky EM (1998) Increases in acetylcholine release produced by phorbol esters are not mediated by protein kinase C at motor nerve endings. J Pharmacol Exp Ther 285:247-251.
Seeburg PH (1996) The role of RNA editing in controlling glutamate receptor channel properties. J Neurochem 66:1-5.
Seifert G, Zhou M, Dietrich D, Schumacher TB, Dybek A, Weiser T, Wienrich M, Wilhelm D, Steinhauser C (2000) Developmental regulation of AMPA-receptor properties in CA1 pyramidal neurons of rat hippocampus. Neuropharmacology 39:931-942.
Shearman MS, Naor Z, Sekiguchi K, Kishimoto A, Nishizuka Y (1989) Selective activation of the gamma-subspecies of protein kinase C from bovine cerebellum by arachidonic acid and its lipoxygenase metabolites. FEBS Lett 243:177-182.
Shepherd JD, Huganir RL (2007) The cell biology of synaptic plasticity: AMPA receptor trafficking. Annu Rev Cell Dev Biol 23:613-643.
Shi S, Hayashi Y, Esteban JA, Malinow R (2001) Subunit-specific rules governing AMPA receptor trafficking to synapses in hippocampal pyramidal neurons. Cell 105:331-343.
Shimshek DR, Bus T, Grinevich V, Single FN, Mack V, Sprengel R, Spergel DJ, Seeburg PH (2006a) Impaired reproductive behavior by lack of GluR-B

containing AMPA receptors but not of NMDA receptors in hypothalamic and septal neurons. Mol Endocrinol 20:219-231.
Shimshek DR, Jensen V, Celikel T, Geng Y, Schupp B, Bus T, Mack V, Marx V, Hvalby O, Seeburg PH, Sprengel R (2006b) Forebrain-specific glutamate receptor B deletion impairs spatial memory but not hippocampal field long-term potentiation. J Neurosci 26:8428-8440.
Sigworth FJ (1980) The variance of sodium current fluctuations at the node of Ranvier. J Physiol 307:97-129.
Silinsky EM, Searl TJ (2003) Phorbol esters and neurotransmitter release: more than just protein kinase C? Br J Pharmacol 138:1191-1201.
Silver RA, Cull-Candy SG, Takahashi T (1996a) Non-NMDA glutamate receptor occupancy and open probability at a rat cerebellar synapse with single and multiple release sites. J Physiol 494 (Pt 1):231-250.
Silver RA, Colquhoun D, Cull-Candy SG, Edmonds B (1996b) Deactivation and desensitization of non-NMDA receptors in patches and the time course of EPSCs in rat cerebellar granule cells. J Physiol 493 (Pt 1):167-173.
Singer JH, Talley EM, Bayliss DA, Berger AJ (1998) Development of glycinergic synaptic transmission to rat brain stem motoneurons. J Neurophysiol 80:2608-2620.
Slatter CA, Kanji H, Coutts CA, Ali DW (2005) Expression of PKC in the developing zebrafish, Danio rerio. J Neurobiol 62:425-438.
Smart TG (1997) Regulation of excitatory and inhibitory neurotransmitter-gated ion channels by protein phosphorylation. Curr Opin Neurobiol 7:358-367.
Soderling TR (1990) Protein kinases. Regulation by autoinhibitory domains. J Biol Chem 265:1823-1826.
Soloff RS, Katayama C, Lin MY, Feramisco JR, Hedrick SM (2004) Targeted deletion of protein kinase C lambda reveals a distribution of functions between the two atypical protein kinase C isoforms. J Immunol 173:3250-3260.
Sommer B, Keinanen K, Verdoorn TA, Wisden W, Burnashev N, Herb A, Kohler M, Takagi T, Sakmann B, Seeburg PH (1990) Flip and flop: a cell-specific functional switch in glutamate-operated channels of the CNS. Science 249:1580-1585.
Somogyi GT, Tanowitz M, Zernova G, de Groat WC (1996) M1 muscarinic receptor-induced facilitation of ACh and noradrenaline release in the rat bladder is mediated by protein kinase C. J Physiol 496 (Pt 1):245-254.
Song I, Huganir RL (2002) Regulation of AMPA receptors during synaptic plasticity. Trends Neurosci 25:578-588.
Song I, Kamboj S, Xia J, Dong H, Liao D, Huganir RL (1998) Interaction of the N-ethylmaleimide-sensitive factor with AMPA receptors. Neuron 21:393-400.
Steinberg JP, Huganir RL, Linden DJ (2004) N-ethylmaleimide-sensitive factor is required for the synaptic incorporation and removal of AMPA receptors during cerebellar long-term depression. Proc Natl Acad Sci U S A 101:18212-18216.

Stern P, Behe P, Schoepfer R, Colquhoun D (1992) Single-channel conductances of NMDA receptors expressed from cloned cDNAs: comparison with native receptors. Proc Biol Sci 250:271-277.
Steward O, Worley PF (2001) Selective targeting of newly synthesized Arc mRNA to active synapses requires NMDA receptor activation. Neuron 30:227-240.
Sucher NJ, Akbarian S, Chi CL, Leclerc CL, Awobuluyi M, Deitcher DL, Wu MK, Yuan JP, Jones EG, Lipton SA (1995) Developmental and regional expression pattern of a novel NMDA receptor-like subunit (NMDAR-L) in the rodent brain. J Neurosci 15:6509-6520.
Swanson GT, Kamboj SK, Cull-Candy SG (1997) Single-channel properties of recombinant AMPA receptors depend on RNA editing, splice variation, and subunit composition. J Neurosci 17:58-69.
Takahashi T (2005) Postsynaptic receptor mechanisms underlying developmental speeding of synaptic transmission. Neurosci Res 53:229-240.
Takahashi T, Feldmeyer D, Suzuki N, Onodera K, Cull-Candy SG, Sakimura K, Mishina M (1996) Functional correlation of NMDA receptor epsilon subunits expression with the properties of single-channel and synaptic currents in the developing cerebellum. J Neurosci 16:4376-4382.
Tanaka C, Saito N (1992) Localization of subspecies of protein kinase C in the mammalian central nervous system. Neurochem Int 21:499-512.
Tanaka C, Nishizuka Y (1994) The protein kinase C family for neuronal signaling. Annu Rev Neurosci 17:551-567.
Tanaka S, Tominaga M, Yasuda I, Kishimoto A, Nishizuka Y (1991) Protein kinase C in rat brain synaptosomes. Beta II-subspecies as a major isoform associated with membrane-skeleton elements. FEBS Lett 294:267-270.
Tang CM, Shi QY, Katchman A, Lynch G (1991) Modulation of the time course of fast EPSCs and glutamate channel kinetics by aniracetam. Science 254:288-290.
Taschenberger H, von Gersdorff H (2000) Fine-tuning an auditory synapse for speed and fidelity: developmental changes in presynaptic waveform, EPSC kinetics, and synaptic plasticity. J Neurosci 20:9162-9173.
Tavalin SJ (2008) AKAP79 selectively enhances protein kinase C regulation of GluR1 at a Ca2+-calmodulin-dependent protein kinase II/protein kinase C site. J Biol Chem 283:11445-11452.
Terashima A, Cotton L, Dev KK, Meyer G, Zaman S, Duprat F, Henley JM, Collingridge GL, Isaac JT (2004) Regulation of synaptic strength and AMPA receptor subunit composition by PICK1. J Neurosci 24:5381-5390.
Thiam K, Loing E, Zoukhri D, Rommens C, Hodges R, Dartt D, Verwaerde C, Auriault C, Gras-Masse H, Sergheraert C (1999) Direct evidence of cytoplasmic delivery of PKC-alpha, -epsilon and -zeta pseudosubstrate lipopeptides: study of their implication in the induction of apoptosis. FEBS Lett 459:285-290.
Tingley WG, Roche KW, Thompson AK, Huganir RL (1993) Regulation of NMDA receptor phosphorylation by alternative splicing of the C-terminal domain. Nature 364:70-73.

Tomita S, Stein V, Stocker TJ, Nicoll RA, Bredt DS (2005a) Bidirectional synaptic plasticity regulated by phosphorylation of stargazin-like TARPs. Neuron 45:269-277.
Tomita S, Chen L, Kawasaki Y, Petralia RS, Wenthold RJ, Nicoll RA, Bredt DS (2003) Functional studies and distribution define a family of transmembrane AMPA receptor regulatory proteins. J Cell Biol 161:805-816.
Tomita S, Adesnik H, Sekiguchi M, Zhang W, Wada K, Howe JR, Nicoll RA, Bredt DS (2005b) Stargazin modulates AMPA receptor gating and trafficking by distinct domains. Nature 435:1052-1058.
Traynelis SF, Silver RA, Cull-Candy SG (1993) Estimated conductance of glutamate receptor channels activated during EPSCs at the cerebellar mossy fiber-granule cell synapse. Neuron 11:279-289.
Triller A, Rostaing P, Korn H, Legendre P (1997) Morphofunctional evidence for mature synaptic contacts on the Mauthner cell of 52-hour-old zebrafish larvae. Neuroscience 80:133-145.
Verdoorn TA, Burnashev N, Monyer H, Seeburg PH, Sakmann B (1991) Structural determinants of ion flow through recombinant glutamate receptor channels. Science 252:1715-1718.
Verhage M, Maia AS, Plomp JJ, Brussaard AB, Heeroma JH, Vermeer H, Toonen RF, Hammer RE, van den Berg TK, Missler M, Geuze HJ, Sudhof TC (2000) Synaptic assembly of the brain in the absence of neurotransmitter secretion. Science 287:864-869.
Vincent P, Armstrong CM, Marty A (1992) Inhibitory synaptic currents in rat cerebellar Purkinje cells: modulation by postsynaptic depolarization. J Physiol 456:453-471.
Vyklicky L, Jr., Patneau DK, Mayer ML (1991) Modulation of excitatory synaptic transmission by drugs that reduce desensitization at AMPA/kainate receptors. Neuron 7:971-984.
Wall MJ, Robert A, Howe JR, Usowicz MM (2002) The speeding of EPSC kinetics during maturation of a central synapse. Eur J Neurosci 15:785-797.
Wang JH, Feng DP (1992) Postsynaptic protein kinase C essential to induction and maintenance of long-term potentiation in the hippocampal CA1 region. Proc Natl Acad Sci U S A 89:2576-2580.
Wang YT, Linden DJ (2000) Expression of cerebellar long-term depression requires postsynaptic clathrin-mediated endocytosis. Neuron 25:635-647.
Washburn MS, Numberger M, Zhang S, Dingledine R (1997) Differential dependence on GluR2 expression of three characteristic features of AMPA receptors. J Neurosci 17:9393-9406.
Westerfield M (2000) The zebrafish book. A guide for the laboratory use of zebrafish (*Danio rerio*), 4th Edition. Eugene: University of Oregon Press.
Wetsel WC, Khan WA, Merchenthaler I, Rivera H, Halpern AE, Phung HM, Negro-Vilar A, Hannun YA (1992) Tissue and cellular distribution of the extended family of protein kinase C isoenzymes. J Cell Biol 117:121-133.

Whelan RD, Parker PJ (1998) Loss of protein kinase C function induces an apoptotic response. Oncogene 16:1939-1944.
Wikstrom MA, Matthews P, Roberts D, Collingridge GL, Bortolotto ZA (2003) Parallel kinase cascades are involved in the induction of LTP at hippocampal CA1 synapses. Neuropharmacology 45:828-836.
Wyllie DJ, Cull-Candy SG (1994) A comparison of non-NMDA receptor channels in type-2 astrocytes and granule cells from rat cerebellum. J Physiol 475:95-114.
Yamada KA, Tang CM (1993) Benzothiadiazides inhibit rapid glutamate receptor desensitization and enhance glutamatergic synaptic currents. J Neurosci 13:3904-3915.
Yamashita T, Ishikawa T, Takahashi T (2003) Developmental increase in vesicular glutamate content does not cause saturation of AMPA receptors at the calyx of held synapse. J Neurosci 23:3633-3638.
Yan J, Zhang Y, Jia Z, Taverna FA, McDonald RJ, Muller RU, Roder JC (2002) Place-cell impairment in glutamate receptor 2 mutant mice. J Neurosci 22:RC204.
Yao Y, Kelly MT, Sajikumar S, Serrano P, Tian D, Bergold PJ, Frey JU, Sacktor TC (2008) PKM zeta maintains late long-term potentiation by N-ethylmaleimide-sensitive factor/GluR2-dependent trafficking of postsynaptic AMPA receptors. J Neurosci 28:7820-7827.
Yasuda H, Barth AL, Stellwagen D, Malenka RC (2003) A developmental switch in the signaling cascades for LTP induction. Nat Neurosci 6:15-16.
Ye GL, Song Liu X, Pasternak JF, Trommer BL (2000) Maturation of glutamatergic neurotransmission in dentate gyrus granule cells. Brain Res Dev Brain Res 124:33-42.
Yin HZ, Sensi SL, Carriedo SG, Weiss JH (1999) Dendritic localization of Ca(2+)-permeable AMPA/kainate channels in hippocampal pyramidal neurons. J Comp Neurol 409:250-260.
Zamanillo D, Sprengel R, Hvalby O, Jensen V, Burnashev N, Rozov A, Kaiser KM, Koster HJ, Borchardt T, Worley P, Lubke J, Frotscher M, Kelly PH, Sommer B, Andersen P, Seeburg PH, Sakmann B (1999) Importance of AMPA receptors for hippocampal synaptic plasticity but not for spatial learning. Science 284:1805-1811.
Zheng Z, Keifer J (2008) Protein kinase C-dependent and independent signaling pathways regulate synaptic GluR1 and GluR4 AMPAR subunits during in vitro classical conditioning. Neuroscience 156:872-884.
Zhu JJ, Esteban JA, Hayashi Y, Malinow R (2000) Postnatal synaptic potentiation: delivery of GluR4-containing AMPA receptors by spontaneous activity. Nat Neurosci 3:1098-1106.
Zottoli SJ (1978) Comparison of Mauthner cell size in teleosts. J Comp Neurol 178:741-757.
Zucker RS, Regehr WG (2002) Short-term synaptic plasticity. Annu Rev Physiol 64:355-405.

Cedar Thomas Webpage:
URL:http://www.swarthmore.edu/NatSci/sgilber1/DB_lab/Fish/fish_stage.html.